The University of Nottingham

UNITED KINGDOM · CHINA · MALAYSIA

Navigating the Quantum-Classical Frontier

Thomas R. Bromley

Thesis submitted to the University of Nottingham for the degree of Doctor of Philosophy

July 2017

Abstract

The description of a quantum system follows a fundamentally different paradigm to that of a classical system, leading to unique yet counter-intuitive properties. In this thesis we consider some of these unique properties, here termed simply *the quantum*. We focus on understanding some important types of *the quantum*: quantum coherence and quantum correlations, as well as quantum entanglement as an important subclass of quantum correlations. Our objective is to investigate how to quantify *the quantum*, what it can be used for, and how it can be preserved in the adverse presence of noise. These findings help to clarify the frontier between quantum and classical systems, a crucial endeavour for understanding the applications and advantageous features of the quantum world.

Acknowledgements

I would like to thank all those that have been part of the Quantum Correlations group in Nottingham for making it a wonderful place to study and develop. I have had the pleasure to work with many interesting people and have gained much from my interactions with them. First and foremost I want to convey my gratitude to my supervisor, Professor Gerardo Adesso. Thank you for being my guide, for being patient as I learnt the basics, for giving me confidence in my abilities, and for dedicating your time whenever it was needed. I could not have asked for more from a supervisor. Many thanks also to my friend, Doctor Marco Cianciaruso. We have made a great team over the years and had a lot of fun along the way. You have had a big impact on me both personally and as a researcher. Thanks to all of my collaborators for their hard work, including: Carmine Napoli, Rosanna Nichols, Bartosz Regula, Isabela Almeida Silva, and Doctors Luis Correa, Marco Piani, and Tommaso Tufarelli. I've also had some great discussions with present and past members of the Quantum Correlations group: Pietro Liuzzo Scorpo and Buqing Xu, and Doctors Ioannis Kogias, Sara Di Martino, and Sammy Ragy. Additionally, there is Ben Davis, Matthew Levitt, and Doctor Joel Bradshaw, who together made my office a brilliant place to work in; thanks for all the good times! My family and friends have also played a crucial role during my PhD and I would like to thank all of them. In particular, none of this would have happened without the unconditional support of my parents. This work is dedicated to you.

Contents

Introduction

Quantum mechanics provides a set of laws to understand nature at small length scales. It was developed over the past century in response to the failure of classical mechanics to accurately explain the behaviour of atomic and subatomic particles. Quantum mechanics has proven to be very successful, and is now regularly used in many areas of present day science and technology. This success relies on a foundation of principles that are fundamentally different to those in classical mechanics, necessitated by the counter-intuitive behaviour of nature at microscopic length scales. The objective of this thesis is to investigate the quantum-classical frontier: the transition of a physical system from the domain of classical mechanics to the domain of quantum mechanics. In doing so, we further our understanding of the quantum world and its potential for application. Such an endeavour can be achieved by characterising the properties of a physical system that manifest uniquely from quantum mechanics. Here we refer to these properties collectively as *the quantum*.

There has already been some progress along this path: quantum coherence [1] and quantum entanglement [2] have long been understood as key types of *the quantum*, arising only from the formalism of quantum mechanics. Their study has evolved over the years, from the simple qualitative acknowledgement of their presence within quantum systems to an important discipline in the field of quantum science. Quantum coherence captures the ability of a quantum particle to be in a *coherent superposition*, existing in more than one state at the same time. Such a property can only be described in classical mechanics using the concept of a wave, leading to the idea of a duality between waves and particles in quantum

mechanics [3]. The counter-intuitive nature of quantum coherence was captured by the famous Schrödinger's cat thought experiment [4, 5]. Entanglement represents a portion of the quantum correlations between subsystems of a composite system and has been studied since the dawn of quantum mechanics. It is the resource behind important processes such as quantum teleportation [6, 7] and dense coding [7, 8]. Yet, entanglement does not entirely capture all the non-classical correlations in a composite quantum system [9–11]. Instead, general quantum correlations are also recognised as another relevant type of *the quantum*, being important for a variety of applications including within quantum communication and metrology.

Focussing on quantum coherence, quantum correlations, and quantum entanglement as key types of *the quantum*, we investigate three important questions:

1. How much of *the quantum* is there?

2. What can *the quantum* be used for?

3. Can *the quantum* be preserved in the presence of noise?

Finding an answer to Question 1 allows for a quantification of the departure of a physical system from classical mechanics. Question 2 then investigates whether *the quantum* can be harnessed to perform tasks in a superior way. However, the presence of noise in physical systems tends to destroy *the quantum* and return the system to behaving within the laws of classical mechanics. Question 3 therefore considers whether *the quantum* may be preserved despite the negative effects of noise. These three questions together present a relevant line of investigation to help navigate the quantum-classical frontier, see Fig. I.1 for an illustration as well as Ref. [12].

This text is structured in seven chapters. The following chapter contains a summary of some important concepts describing the mechanics of classical and quantum systems, providing the background for their comparison. Chapter 2 shows how quantum coherence, quantum correlations, and quantum entanglement arise from quantum mechanics as unique properties of a quantum system.

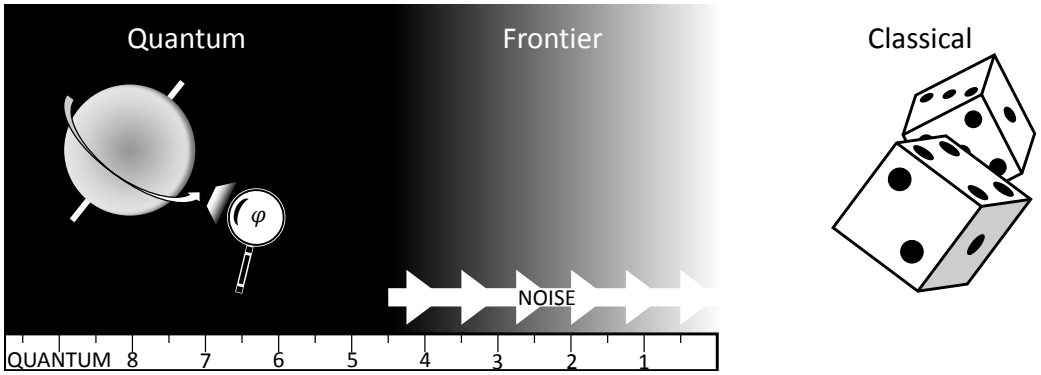

Figure I.1: A schematic of the quantum-classical frontier. The left-hand side represents quantum mechanics and is given by a single quantum spin, while the right-hand side represents classical mechanics and is given by a pair of dice. Our objective is to understand the frontier between quantum and classical mechanics by characterising properties unique to quantum systems: *the quantum*. We investigate how *the quantum* can be quantified (represented here with a ruler extending towards the side of quantum mechanics), what *the quantum* can be used for (represented here with a magnifying glass to estimate a parameter φ, as explained further in Chapter 5), and how *the quantum* can be preserved in the presence of noise (represented here with an arrow transforming from quantum to classical mechanics).

Chapters 3, 4, 5 and 6 then focus on answering the three questions posed. Finally, a discussion of the results found, and their potential implications for further research into quantum science, is given in Chapter 7. The contents of this thesis presents research that has been previously reported in a collection of works contributed to by the author, referenced with the prefix TRB. Figure I.2 displays a roadmap of this thesis. Here, the light blue boxes each correspond to a chapter of this thesis. The dark blue boxes then represent some of the important methods and constructions, described in more detail below, utilised to help elucidate the three questions. Finally, the green ellipses represent the works of the author, whose findings are demarcated by green arrows connecting to the relevant boxes.

Chapter 3 shows how one can quantify *the quantum*. Introducing the framework of quantum resource theories [13–15], we give a set of rigorous requirements

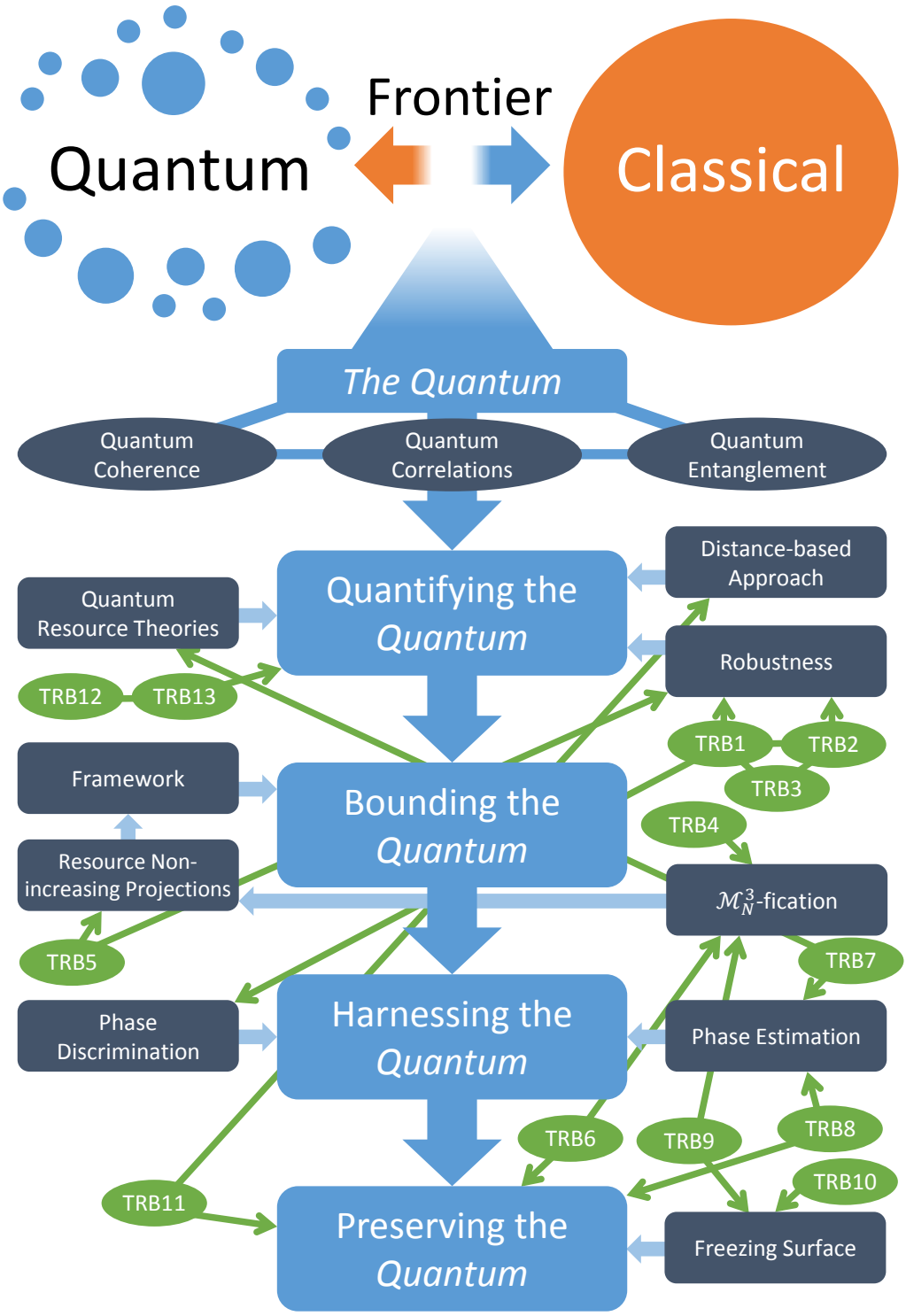

Figure I.2: A roadmap of the structure of this thesis (explained further in the main text). The references [TRB1-TRB13] correspond to the works of the author.

for measures of a quantum resource and highlight how the framework can be specialised to the resources given by our three types of *the quantum*. Two geometric approaches to constructing measures of *the quantum* are then given: the robustness and the distance-based approach. The robustness of a resource quantifies the amount of classical mixing required to recover a resource-free state [16, 17]. Instead, the distance-based approach measures a resource by quantifying the distance to the set of resource-free states [18–20]. Both approaches lead to measures of a resource that satisfy the given requirements. It is shown that the robustness of a resource is observable and may be efficiently evaluated numerically as the solution to a semidefinite program, provided the corresponding framework of the resource theory satisfies certain conditions. Furthermore, the robustness is specialised to the resource of quantum coherence, leading to the robustness of coherence and the robustness of k coherence [TRB1, TRB2, TRB3].

Next, Chapter 4 considers the difficulty of evaluating measures of *the quantum* for generic states of a quantum system. We construct a general multi-step framework to provide lower bounds to these measures, relying on the introduced concept of a resource non-increasing projection [TRB4, TRB5, TRB6]. An example of the application of this framework to provide lower bounds to the distance-based measures of multiqubit entanglement and coherence is then provided with the identification of a simple family of N qubit states, resulting from the action of a particular resource non-increasing projection called $\mathcal{M}_N^3$-fication. The resultant lower bounds are particularly relevant experimentally due to their low overhead in terms of the required local measurement settings. We also identify an alternative resource non-increasing projection to show the wider applicability of our framework.

Chapter 5 looks at how *the quantum* can be harnessed. We focus on the operational tasks of phase discrimination and phase estimation in quantum metrology. Phase discrimination is a type of quantum channel discrimination [21–24] with the objective of using a quantum probe to infer which of a set of phases was applied by a unitary with a fixed Hamiltonian according to a prior probability distribution. We show that quantum coherence in the probe with respect to

the eigenbasis of the Hamiltonian is necessary to improve the probability of successfully inferring the phase beyond simply guessing from the known probability distribution. The robustness of coherence of the quantum probe is then shown to quantify the optimum advantage in the probability of success [TRB1, TRB2]. On the other hand, the objective of phase estimation [25–29] is to precisely measure a phase applied by a unitary. We discuss the roles of the three types of *the quantum* in phase estimation. In particular, both quantum correlations and quantum entanglement can be quantitatively linked to the performance of phase estimation in a type of worst-case scenario quantum interferometer [30, TRB7]. We show that there exists a strict hierarchy between quantum correlations and quantum entanglement, with quantum correlations constituting the most relevant type of *the quantum* in this setting.

Finally, in Chapter 6 we investigate a mechanism to preserve *the quantum* in the presence of certain types of noise. This is an important task given the typical adverse sensitivity of *the quantum* to noise [TRB8]. Using the distance-based approach to measuring a resource, we identify conditions in which quantum coherence and quantum correlations can be preserved, or *frozen*, despite the action of the noise [31–33]. These conditions consist of a certain class of initial states of a two qubit system (known as the freezing surface) subjected to simple qubit bit flip noise, and are universal in the sense that freezing occurs independent of the particular distance used to measure the resource [TRB9, TRB10]. We provide an example of conditions where both the quantum coherence and quantum correlations freeze and compare with the behaviour of quantum entanglement, total correlations, and classical correlations [TRB6, TRB11], which is also observed to freeze [34]. A physical intuition is then suggested to explain the observed freezing phenomenon. Finally, the conditions for frozen multiqubit entanglement are explored [TRB4, 35, 36].

Chapter 1

Classical and Quantum Systems

This chapter provides an outline of some of the important concepts used to describe a physical system in classical and quantum mechanics. Despite their fundamental differences, both a classical and a quantum system can be specified with just a few ingredients: the state, the evolution, and the observables. Here we explain these concepts for finite dimensional systems and give a simple example in each case. We also discuss the description of composite systems, which are composed of a collection of separately accessible subsystems. The chapter is then concluded with a comparison of the two approaches, highlighting both the similarities and differences, which lead to the unique quantum properties that we call *the quantum*. It is important to emphasise that the following does not represent a full exposition of either classical or quantum mechanics, but rather an outline of the relevant topics presented from the perspective of a quantum scientist. The basis for the material presented in this chapter is Refs. [7, 20].

1.1 Classical Systems

We restrict to classical systems that can exist in a finite number of configurations. The number of possible configurations d is called the dimension of the system. This restriction is both for mathematical simplicity and to provide the most suitable comparison to the finite dimensional quantum systems that are the main focus of this thesis. A d-dimensional classical system can be described by a phase

space $\mathcal{P} = \{i\}_{i=1}^{d}$ of d points, with each point in the phase space representing one possible configuration of the system.

1.1.1 State

The state of a classical system represents our current knowledge on the configuration of the system. We do not always have full knowledge of the system, and hence any state is given by a probability distribution $\mathbf{p} = \{p_i\}_{i=1}^{d}$, with $p_i \geq 0$ for all i and $\sum_{i=1}^{d} p_i = 1$. Each probability p_i gives the likelihood that the system is in the i-th configuration of the phase space $\mathcal{P}$. If the system is known to be in configuration $i \in \mathcal{P}$, it is said to be in a pure state $\boldsymbol{\delta}^{(i)} = \{\delta_{ij}\}_{j=1}^{d}$, where δ_{ij} is the Kronecker delta, i.e. $\delta_{ij} = 1$ if $i = j$ and $\delta_{ij} = 0$ if $i \neq j$. A general state $\mathbf{p}$ can be expressed in a unique way as a convex mixture of pure states,

$$\mathbf{p} = \{p_i\}_{i=1}^{d} = \sum_{i=1}^{d} p_i \boldsymbol{\delta}^{(i)}, \tag{1.1}$$

and is hence called a mixed state (unless it is itself a pure state). The set of states can then be thought of as the $(d-1)$-simplex which is the convex hull of the d pure states $\boldsymbol{\delta}^{(i)}$.

The current knowledge on the configuration of the system can be quantified by the Shannon entropy [37]

$$\mathcal{S}(\mathbf{p}) := -\sum_{i=1}^{d} p_i \log p_i, \tag{1.2}$$

which is a function of the state of the system $\mathbf{p}$. This quantity ranges from 0 to $\log d$. It is 0 for pure states, when there is full knowledge on the configuration of the system, and $\log d$ for the uniform distribution state $\mathbf{u} = \{\frac{1}{d}\}_{i=1}^{d}$. The state $\mathbf{u}$ corresponds to having minimum knowledge on the configuration of the system, where it is thought that each configuration is equally likely with probability $\frac{1}{d}$, and is hence called the maximally mixed state. The base of the logarithm in Eq. (1.2) is typically set to d when considering a d-dimensional system, so that the Shannon entropy ranges from 0 to 1. On the other hand, when considering composite d^N-dimensional systems consisting of N subsystems of dimension d

(see the following Section 1.3 for further details), the base of the logarithm is still typically set to d so that the Shannon entropy ranges from 0 to N.

It is also instructive to quantify the difference, or distinguishability, between the state $\mathbf{p}$ and another state $\mathbf{q} = \{q_i\}_{i=1}^d$. A measure of distinguishability can be given by calculating the distance $D_\delta(\mathbf{p}, \mathbf{q})$ between $\mathbf{p}$ and $\mathbf{q}$, where δ denotes the choice of a particular distance function. A distance is a non-negative function obeying three requirements for all $\mathbf{p}$, $\mathbf{q}$ and $\mathbf{r}$:

$$D_\delta(\mathbf{p}, \mathbf{q}) = 0 \quad \Leftrightarrow \quad \mathbf{p} = \mathbf{q}, \tag{1.3}$$

$$D_\delta(\mathbf{p}, \mathbf{q}) = D_\delta(\mathbf{q}, \mathbf{p}), \tag{1.4}$$

$$D_\delta(\mathbf{p}, \mathbf{q}) \leq D_\delta(\mathbf{p}, \mathbf{r}) + D_\delta(\mathbf{r}, \mathbf{q}), \tag{1.5}$$

where $\mathbf{r} = \{r_i\}_{i=1}^d$ is another state. An example of a distance satisfying these requirements is the trace distance, given by

$$D_{Tr}(\mathbf{p}, \mathbf{q}) := \frac{1}{2} \sum_{i=1}^{d} |p_i - q_i| \,. \tag{1.6}$$

The Hellinger distance,

$$D_{He}(\mathbf{p}, \mathbf{q}) := \left(\sum_{i=1}^{d} (\sqrt{p_i} - \sqrt{q_i})^2 \right)^{\frac{1}{2}}, \tag{1.7}$$

is an alternative distance that is a monotonically decreasing function of the classical fidelity,

$$F(\mathbf{p}, \mathbf{q}) := \left(\sum_{i=1}^{d} \sqrt{p_i q_i} \right)^2. \tag{1.8}$$

Finally, the relative entropy (also commonly known as the Kullback–Leibler divergence) is an important distinguishability measure given by

$$D_{RE}(\mathbf{p}, \mathbf{q}) := \sum_{i=1}^{d} p_i \log \frac{p_i}{q_i}. \tag{1.9}$$

However, it is not a distance since it does not obey the requirements in (1.4) and (1.5) [38]. Nevertheless, it will often be referred to as a distance in the rest of this thesis. A further discussion of distinguishability and the physical motivations behind the trace and Hellinger distances, as well as the relative entropy, as measures of distinguishability can be found in Refs. [7, 20]. Figure 1.1 shows

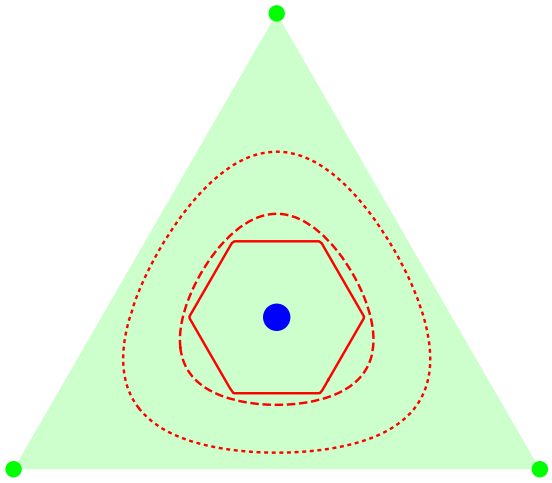

Figure 1.1: The set of states for a 3-dimensional classical system forms the green 2-simplex given by the convex hull of the pure states, shown as the green points. States at a distance of $\frac{1}{4}$ from the maximally mixed state $\mathbf{u}$ (central blue point) are given as lines for D_{Tr} (red solid line), D_{He} (red dashed line), and D_{RE} (red dotted line). To provide a fair comparison as measures of distinguishability, here the distances are normalised such that the distance between any pure state and the maximally mixed state is unity.

the sets of states at a distance of $\frac{1}{4}$ from the maximally mixed state $\mathbf{u}$ according to D_{Tr}, D_{He}, and D_{RE} for a 3-dimensional system, illustrating the dependence of distinguishability upon the choice of distance.

1.1.2 Evolution

Consider the evolution of a classical system in a fixed time interval. If the system is initially described by a state $\mathbf{p}$, then the evolved system can be described by a state $\mathbf{p}' = \{p'_i\}_{i=1}^d$. We focus on stochastic evolutions, so that the evolved state is given by the map $\mathbf{p}' = S\mathbf{p}$, where S is a $d \times d$ stochastic matrix and $\mathbf{p}$ and $\mathbf{p}'$ are taken to be column vectors, which will be the convention adopted in the following. Stochastic matrices are square matrices with elements S_{ij} obeying

$$S_{ij} \geq 0 \qquad \forall i, j \in \{1, 2, \ldots, d\}, \tag{1.10}$$

$$\sum_{i=1}^{d} S_{ij} = 1 \qquad \forall j \in \{1, 2, \ldots, d\}. \tag{1.11}$$

These conditions ensure that $\mathbf{p}'$ is a state, i.e. a valid probability distribution: condition (1.10) means that $p'_i \geq 0$ for all i, while condition (1.11) preserves normalisation, $\sum_{i=1}^{d} p'_i = 1$. The stochastic evolution of a classical system causes the distinguishability between any two states $\mathbf{p}$ and $\mathbf{q}$ to decrease. Hence, a measure of distinguishability must be monotonically non-increasing under the action of stochastic maps. This property is satisfied whenever the corresponding distance $D_\delta(\mathbf{p}, \mathbf{q})$ is *contractive* under any stochastic map S,

$$D_\delta(S\mathbf{p}, S\mathbf{q}) \leq D_\delta(\mathbf{p}, \mathbf{q}) \tag{1.12}$$

for all $\mathbf{p}$, $\mathbf{q}$ and S. All of the distances already discussed here satisfy this property [20].

The action of noise upon a classical system is typically given by a bistochastic map, which transforms the system in an initial state $\mathbf{p}$ to the evolved state $\mathbf{p}' = B\mathbf{p}$, where B is a $d \times d$ bistochastic matrix. Bistochastic matrices are stochastic matrices with elements B_{ij} that obey

$$\sum_{j=1}^{d} B_{ij} = 1 \qquad \forall i \in \{1, 2, \ldots, d\}. \tag{1.13}$$

Such maps are unital, meaning that the maximally mixed state is mapped into itself, $\mathbf{u} = B\mathbf{u}$. Bistochastic maps can be thought of as noise because they always cause a state to become more uniform in terms of its probability distribution, meaning that knowledge on the configuration of the classical system is lost. Uniformity can be measured by turning to the concept of majorisation. A set of d real numbers $\mathbf{x} = \{x_i\}_{i=1}^{d}$ is majorised by another set of d real numbers $\mathbf{y} = \{y_i\}_{i=1}^{d}$, written as $\mathbf{x} \prec \mathbf{y}$, when

$$\begin{aligned} \sum_{i=1}^{k} x_i^{\downarrow} &\leq \sum_{i=1}^{k} y_i^{\downarrow} \qquad \forall \;\; k \in \{1, 2, \ldots, d-1\}, \\ \sum_{i=1}^{d} x_i &= \sum_{i=1}^{d} y_i, \end{aligned} \tag{1.14}$$

where $\{x_i^{\downarrow}\}_{i=1}^{d}$ and $\{y_i^{\downarrow}\}_{i=1}^{d}$ are rearrangements of $\{x_i\}_{i=1}^{d}$ and $\{y_i\}_{i=1}^{d}$, respectively, into non-increasing order. If one state $\mathbf{p}'$ of a classical system is majorised by

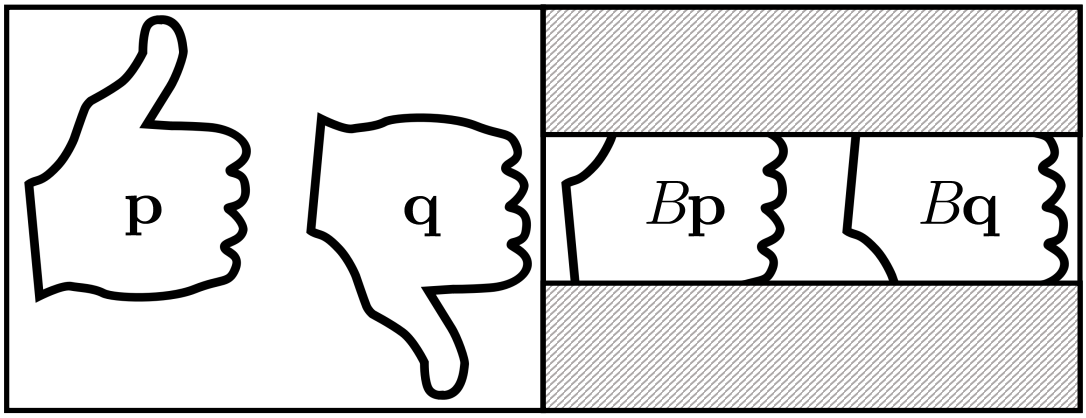

Figure 1.2: States $\mathbf{p}$ and $\mathbf{q}$ (here represented by a "thumbs up" and a "thumbs down") of a classical system become less distinguishable after the application of a bistochastic map B due to loss of information on the configuration of the system (represented by the hatched region) [7].

another state $\mathbf{p}$, i.e. $\mathbf{p}' \prec \mathbf{p}$, then $\mathbf{p}'$ is more uniform than $\mathbf{p}$. In fact, for any state $\mathbf{p}$,

$$\mathbf{u} \prec \mathbf{p} \prec \boldsymbol{\delta}^{(i)} \qquad \forall\, i \in \{1, 2, \ldots, d\}, \tag{1.15}$$

so that the maximally mixed state $\mathbf{u}$ is the most uniform of all states, and the pure states $\boldsymbol{\delta}^{(i)}$ are the least uniform. Majorisation thus imposes an order on the set of states in terms of uniformity. A rigorous connection between the action of bistochastic maps on a classical system and the increase in uniformity of the state is then provided by the statement [39]

$$\mathbf{p}' \prec \mathbf{p} \quad \Leftrightarrow \quad \exists \text{ a bistochastic matrix } B \text{ such that } \mathbf{p}' = B\mathbf{p}. \tag{1.16}$$

The increase in uniformity due to a bistochastic map means that the Shannon entropy increases, i.e. $S(B\mathbf{p}) \geq S(\mathbf{p})$ (this follows from the fact that the Shannon entropy is a Schur concave function). Hence, the evolution due to a bistochastic map always leads to loss of information on the configuration of the classical system. This loss of information provides a very intuitive motivation for why bistochastic maps (as special cases of stochastic maps) cause the distinguishability between states to decrease, see Figure 1.2 for a pictorial representation.

1.1.3 Observables

An observable of a classical system consists of the real numbers $\mathbf{O} = \{o_i\}_{i=1}^{d}$ such that the observable takes the value o_i when the system is in the configuration $i \in \mathcal{P}$. Let $\mathbf{R}$ be the set of possible results of measuring the observable $\mathbf{O}$, i.e. the set containing all the unique values of $\mathbf{O}$ without repetition. If the state describing the system is $\mathbf{p}$, then the probability of the observable taking the value $r \in \mathbf{R}$ is

$$p(r|\mathbf{p}) = \sum_{i:o_i=r} p_i, \tag{1.17}$$

with $\{p(r|\mathbf{p})\}_{r\in\mathbf{R}}$ a probability distribution. The expectation value of the observable is then

$$\langle \mathbf{O} \rangle_{\mathbf{p}} = \sum_{r\in\mathbf{R}} rp(r|\mathbf{p}) = \sum_{i=1}^{d} o_i p_i. \tag{1.18}$$

1.1.4 Example

A ubiquitous problem in classical mechanics is to describe the motion of a group of interacting macroscopic bodies. Such a system has an infinite number of configurations with a continuous phase space of position and momentum, and is hence not immediately explained by the concepts presented here. Nevertheless, there are still some important examples of finite dimensional classical systems that are worthy of further study. The 2-dimensional system is of particular interest in computing and information theory as it can represent the most fundamental unit of information, "on" or "off". This system is given the name bit, a shortened form of binary digit [40]. Systems of N bits are also often considered, with dimension $d = 2^N$. For example, the 8 bit system with a dimension of 256 is called a byte and is very important in computing.

We now show how the rolling of a 6-sided die provides a simple yet informative example of a finite dimensional classical system. In this setting we have a 6-dimensional system with a phase space $\mathcal{P} = \{i\}_{i=1}^{6}$, where $i \in \mathcal{P}$ represents the side of the die facing upwards after a roll. Suppose that the result of the roll is not immediately seen. The state $\mathbf{p} = \{p_i\}_{i=1}^{6}$ represents our current knowledge on the configuration of the system and depends on whether there is any bias in the

die. A fair die is described by the maximally mixed state $\mathbf{u} = \{\frac{1}{6}\}_{i=1}^{6}$, meaning that each result is equally likely. On the other hand, a completely biased die that always rolls the result $i \in \mathcal{P}$ is described by the pure state $\boldsymbol{\delta}^{(i)} = \{\delta_{ij}\}_{j=1}^{6}$. Any die with some intermediate level of bias is described by the general state $\mathbf{p}$. The Shannon entropy of $\mathbf{p}$ is then in the range 0 to 1 (assuming the logarithm is set to base 6), where $\mathcal{S}(\boldsymbol{\delta}^{(i)}) = 0$ for any i and $\mathcal{S}(\mathbf{u}) = 1$.

Consider the scenario where we have two 6-sided dice with different levels of bias, each corresponding to a different realisation of the 6-dimensional system. One die is partially biased and only gives the results $\{1, 2, 3\} \in \mathcal{P}$ randomly, while the other die is fair. The dice are described by the states $\mathbf{p}$ and $\mathbf{q}$, respectively, with $\mathbf{p} = \{\frac{1}{3}, \frac{1}{3}, \frac{1}{3}, 0, 0, 0\}$ and $\mathbf{q} = \mathbf{u}$. The Shannon entropies of these two states are $\mathcal{S}(\mathbf{p}) = \log_6 3 \approx 0.61$ and $\mathcal{S}(\mathbf{q}) = \log_6 6 = 1$, while their distinguishability is $D_{Tr}(\mathbf{p}, \mathbf{q}) = \frac{1}{2}$ according to the trace distance. Now imagine that the results of the rolls of both dice are altered by a friend. If the result of a die roll is odd then the friend replaces the die with a fair die and rolls again. Instead, if the result of a die roll is even, then the friend either does nothing or reduces the value shown on the die by 1, with each event occurring at a 50% probability. This particularly mischievous friend represents a source of noise applied to the system in the form of a bistochastic map with a bistochastic matrix

$$B = \begin{pmatrix} \frac{1}{6} & \frac{1}{2} & \frac{1}{6} & 0 & \frac{1}{6} & 0 \\ \frac{1}{6} & \frac{1}{2} & \frac{1}{6} & 0 & \frac{1}{6} & 0 \\ \frac{1}{6} & 0 & \frac{1}{6} & \frac{1}{2} & \frac{1}{6} & 0 \\ \frac{1}{6} & 0 & \frac{1}{6} & \frac{1}{2} & \frac{1}{6} & 0 \\ \frac{1}{6} & 0 & \frac{1}{6} & 0 & \frac{1}{6} & \frac{1}{2} \\ \frac{1}{6} & 0 & \frac{1}{6} & 0 & \frac{1}{6} & \frac{1}{2} \end{pmatrix}. \tag{1.19}$$

The state of the first die after this map is $\mathbf{p}' = B\mathbf{p} = \{\frac{5}{18}, \frac{5}{18}, \frac{1}{9}, \frac{1}{9}, \frac{1}{9}, \frac{1}{9}\}$, while the state of the second die is unchanged since the map is unital, $\mathbf{q}' = B\mathbf{q} = \mathbf{q}$. The distinguishability between $\mathbf{p}'$ and $\mathbf{q}'$ according to the trace distance is $D_{Tr}(\mathbf{p}', \mathbf{q}') = \frac{2}{9} < D_{Tr}(\mathbf{p}, \mathbf{q}) = \frac{1}{2}$, exhibiting the contractivity of the trace distance from (1.12). Furthermore, it can be found that $\mathbf{p}'$ is more uniform than

$\mathbf{p}$, i.e. $\mathbf{p}' \prec \mathbf{p}$, which is equivalently implied by (1.16) since $\mathbf{p}' = B\mathbf{p}$.

Finally, consider measuring the squared value of the result of a die roll, which is represented by the observable $\mathbf{O} = \{i^2\}_{i=1}^6$. With the first die in the state $\mathbf{p}$, the probability of observing each of the results $\{1, 4, 9\} \subset \mathbf{O}$ of the observable is $\frac{1}{3}$ and the probability of observing any of the results $\{16, 25, 36\} \subset \mathbf{O}$ is 0, with the corresponding expectation value of the observable $\langle \mathbf{O} \rangle_{\mathbf{p}} = \frac{14}{3}$. Instead, for the second die in the state $\mathbf{q}$, the probability of observing any one of the results in $\mathbf{O}$ is $\frac{1}{6}$ and the expectation value is $\langle \mathbf{O} \rangle_{\mathbf{q}} = \frac{91}{6}$.

1.2 Quantum Systems

A finite dimensional quantum system can be described by a d-dimensional complex Hilbert space $\mathcal{H}$, equipped with an inner product $\langle \phi | \psi \rangle \in \mathbb{C}$ defined between any two vectors $|\phi\rangle$ and $|\psi\rangle$ in $\mathcal{H}$. An orthonormal basis (ONB) is any collection of d orthogonal and normalised vectors $\{|e_i\rangle\}_{i=1}^d$ in the Hilbert space, i.e. satisfying $|e_i\rangle \in \mathcal{H}$ and $\langle e_i | e_j \rangle = \delta_{ij}$ for all $i, j \in \{1, 2, \ldots, d\}$. Any vector $|\psi\rangle \in \mathcal{H}$ can be expressed with respect to this orthonormal basis (ONB) as

$$|\psi\rangle = \sum_{i=1}^{d} \psi_i \, |e_i\rangle \, , \tag{1.20}$$

with $\psi_i = \langle e_i | \psi \rangle$. This representation allows $|\psi\rangle$ to be associated with the column vector $\boldsymbol{\psi} = \{\psi_i\}_{i=1}^d \in \mathbb{C}^d$. The inner product can then be written as

$$\langle \phi | \psi \rangle = \boldsymbol{\phi}^\dagger \boldsymbol{\psi} = \sum_{i=1}^{d} \phi_i^* \psi_i, \tag{1.21}$$

where $\boldsymbol{\phi} = \{\phi_i\}_{i=1}^d \in \mathbb{C}^d$ is the column vector corresponding to $|\phi\rangle$ with $\phi_i = \langle e_i | \phi \rangle$, $\dagger$ denotes the conjugate transpose and $*$ denotes the conjugate, which will be the notation adopted henceforth.

The configurations of a quantum system are given by the normalised vectors of $\mathcal{H}$, i.e. the $|\psi\rangle \in \mathcal{H}$ satisfying $\langle \psi | \psi \rangle = 1$. However, any two vectors $|\psi\rangle \in \mathcal{H}$ and $|\psi'\rangle \in \mathcal{H}$ related to each other through a complex phase factor $|\psi'\rangle = e^{i\phi} |\psi\rangle$ for some $\phi \in \mathbb{R}$ correspond to the same configuration of the quantum system. We hence say that the configurations of the quantum system are all the normalised

vectors of $\mathcal{H}$ up to an absolute phase factor. There is an infinite number of such vectors, and hence a finite dimensional quantum system has an infinite number of possible configurations. There is also an infinite number of ONBs of $\mathcal{H}$. For a 2-dimensional quantum system, the most natural ONB is given by the computational basis $\{|0\rangle, |1\rangle\}$, where $|0\rangle$ is associated to the column vector $\mathbf{0} := \{1, 0\}$ and $|1\rangle$ is associated to $\mathbf{1} := \{0, 1\}$. On the other hand, whenever the dimension of a quantum system is larger than 2, the typical ONB is the standard basis $\{|i\rangle\}_{i=1}^{d}$ with each $|i\rangle$ associated to the column vector $\mathbf{i} := \{\delta_{ij}\}_{j=1}^{d}$.

1.2.1 State

The state of a quantum system again represents our knowledge on the configuration of the system. If the configuration of the quantum system is known to be the normalised vector $|\psi\rangle \in \mathcal{H}$ then we describe it with a pure state given by a projection operator (also known as a projector) $|\psi\rangle\langle\psi|$ acting on $\mathcal{H}$, that projects all elements of $\mathcal{H}$ onto the vector $|\psi\rangle$. This pure state can be represented with respect to a chosen ONB as a matrix $\boldsymbol{\psi}\boldsymbol{\psi}^{\dagger}$ when $\boldsymbol{\psi}$ is written as a complex column vector as specified above. In general, a projector is given by any operator P satisfying $P^2 = P$ whose action is to project any $|\psi\rangle \in \mathcal{H}$ onto the subspace given by the range of P. However, not every projector corresponds to a pure state of the quantum system: P is a pure state projector only when $P = |\psi\rangle\langle\psi|$ for some configuration $|\psi\rangle$, or equivalently when P has a rank of one and $\mathrm{Tr}(P) = 1$, where $\mathrm{Tr}(X)$ denotes the trace of an operator X. Note that, after this chapter, we will often refer to the configurations $|\psi\rangle$ as pure states, following the standard language of quantum mechanics.

If we do not have full knowledge of the quantum system then it may be described by any one of a collection of possible configurations $\{|\psi_i\rangle\}_i$ with corresponding probability distribution $\{q_i\}_i$. The system is then said to be in a mixed state represented by a self-adjoint operator ρ written as

$$\rho = \sum_i q_i |\psi_i\rangle\langle\psi_i|, \tag{1.22}$$

which is the convex combination of pure state projectors onto the configurations

$|\psi_i\rangle$, where any operator X acting on $\mathcal{H}$ is self-adjoint if $X = X^\dagger$. An operator ρ can be written as a convex combination of pure state projectors if and only if it satisfies the requirements [7]

$$\begin{aligned} \mathrm{Tr}\,(\rho) &= 1, & (1.23)\\ \rho &\geq 0, & (1.24) \end{aligned}$$

where $X \geq 0$ means that the self-adjoint operator X is positive semidefinite, i.e.

$$\langle\psi|X|\psi\rangle \geq 0 \quad \forall \quad |\psi\rangle \in \mathcal{H}. \tag{1.25}$$

If these conditions hold, ρ is defined to be a *density operator*. The density operators of pure states are the pure state projectors $\rho = |\psi\rangle\langle\psi|$. Hence, the states of a quantum system are given by all the density operators acting on $\mathcal{H}$. We denote the convex set of density operators, or equivalently the set of states, by $\mathcal{D}(\mathcal{H})$. Any density operator can be represented with respect to a given ONB $\{|e_i\rangle\}_{i=1}^d$ as a density matrix on $\mathbb{C}^d$ with elements $\rho_{ij} = \langle e_i|\rho|e_j\rangle$.

It is important to note that the decomposition of a mixed state in Eq. (1.22) is not unique. In fact, there is an infinite number of ways to choose a collection of pure states and a probability distribution so that the corresponding convex combination of pure state projectors is equal to ρ. However, a density operator ρ can always be decomposed as

$$\rho = \sum_{i=1}^{d} p_i\, |p_i\rangle\langle p_i|\,, \tag{1.26}$$

where $\{p_i\}_{i=1}^d$ are the eigenvalues of ρ, which sum to 1, and $\{|p_i\rangle\}_{i=1}^d$ are eigenvectors of ρ, which form an ONB of $\mathcal{H}$ known as the eigenbasis of ρ. This decomposition is called the spectral decomposition of ρ, and is of special importance. It can be seen that any operator written in the form of Eq. (1.26) is a density operator if and only if

$$p_i \geq 0 \quad \forall \ i \in \{1, 2, \ldots, d\}, \qquad \sum_{i=1}^{d} p_i = 1. \tag{1.27}$$

Our ignorance on the configuration of the quantum system described by a

state ρ can be quantified by the von Neumann entropy [41]

$$\mathcal{S}(\rho) := -\mathrm{Tr}\left(\rho \log \rho\right) = -\sum_{i=1}^{d} p_i \log p_i, \tag{1.28}$$

where the second equality uses the eigenvalues $\{p_i\}_{i=1}^{d}$ from the spectral decomposition of ρ in Eq. (1.26). Like the Shannon entropy, this quantity ranges from 0 for pure state projectors $\rho = |\psi\rangle\langle\psi|$ to $\log d$ for the maximally mixed state $\rho = \frac{\mathbb{I}}{d}$, where $\mathbb{I}$ is the identity operator leaving every vector in $\mathcal{H}$ invariant. The maximally mixed state corresponds to a uniform mixture of pure state projectors onto any ONB $\{|e_i\rangle\}_{i=1}^{d}$, i.e.

$$\frac{\mathbb{I}}{d} = \frac{1}{d}\sum_{i=1}^{d} |e_i\rangle\langle e_i| . \tag{1.29}$$

Finally, the distinguishability between two states ρ and σ can be measured by finding the distance between them according to a distance $D_\delta(\rho, \sigma)$ defined on the set of density operators. This distance must obey analogous requirements to those in (1.3), (1.4), and (1.5) for a given choice of function δ. Table 1.1 presents some commonly used distances between density operators. Further information on these distances and their physical justification as distinguishability measures can be found in Refs. [7, 20, 42]. The function

$$F(\rho, \sigma) := \left[\mathrm{Tr}\left(\sqrt{\sqrt{\rho}\sigma\sqrt{\rho}}\right)\right]^2 \tag{1.30}$$

is the quantum fidelity, which is a generalisation of the classical fidelity in Eq. (1.8) to the set of density operators.

1.2.2 Evolution

A quantum system evolves in a fixed time interval according to a quantum operation Λ, which transforms an initial state of the system ρ to an evolved state ρ' according to the map $\rho' = \Lambda(\rho)$. Quantum operations are given by the completely positive and trace preserving (CPTP) linear maps acting on density operators. Complete positivity of a quantum operation Λ ensures that not only $\Lambda(\rho) \geq 0$ for any initial state ρ, but also that any density operator describing a higher

Distance	δ	$D_\delta(\rho,\sigma)$
Trace	Tr	$\frac{1}{2}\mathrm{Tr}\left\|\rho-\sigma\right\|$
Hellinger (squared)	He	$2\left[1-\mathrm{Tr}\left(\sqrt{\rho}\sqrt{\sigma}\right)\right]$
Bures (squared)	Bu	$2\left[1-\sqrt{F(\rho,\sigma)}\right]$
Infidelity	F	$1-F(\rho,\sigma)$
Relative entropy	RE	$\mathrm{Tr}(\rho\log\rho-\rho\log\sigma)$

Table 1.1: Distances $D_\delta(\rho,\sigma)$ between two density operators ρ and σ, where $|\rho-\sigma| := \sqrt{(\rho-\sigma)^2}$. The squared versions of the Hellinger distance and Bures distance are preferred because they have the useful property of joint convexity, which is discussed in more detail in Section 3.2.2.

dimensional quantum system remains positive semidefinite whenever Λ acts on a part it, Ref. [7] provides a formal definition of this property. Trace preservation means that $\mathrm{Tr}(\Lambda(\rho)) = 1$ for all initial states ρ. Hence, the output state $\Lambda(\rho)$ of any quantum operation Λ is always a density operator for any initial state ρ. We note that quantum operations can in general map to an output system of different dimension, but we do not consider such a scenario in this thesis.

A linear map Λ is CPTP if and only if it can be written in the form [43]

$$\Lambda(\rho) = \sum_i K_i \rho K_i^\dagger \tag{1.31}$$

for some set of operators $\{K_i\}_i$ which obey

$$\sum_i K_i^\dagger K_i = \mathbb{I}. \tag{1.32}$$

This is called the operator sum representation of Λ and provides a useful characterisation of quantum operations. The $\{K_i\}_i$ are called Kraus operators, but there is not a unique way to choose them for a given Λ. Quantum operations are also called quantum channels because they can be thought of as a communication channel of quantum information. Furthermore, quantum operations form the quantum analogue of the stochastic maps discussed in Section 1.1.2.

Unital quantum operations are then the quantum analogue of the bistochastic maps. They map the maximally mixed state $\frac{\mathbb{I}}{d}$ to itself and are characterised by

having their Kraus operators obey

$$\sum_i K_i K_i^\dagger = \mathbb{I}. \tag{1.33}$$

Just like for classical systems, there is a rigorous connection between the action of unital quantum operations and increasing uniformity of the state. A state σ of a quantum system can be thought of as more uniform than the state ρ when $\sigma \prec \rho$, which holds when the vector of eigenvalues of σ is majorised by the vector of eigenvalues of ρ using the definition in Eq. (1.14). The link with unital quantum operations is then given by [20]

$$\sigma \prec \rho \quad \Leftrightarrow \quad \exists \text{ a unital quantum operation } \Lambda \text{ such that } \sigma = \Lambda(\rho). \tag{1.34}$$

Quantum operations cause the distinguishability between any two states ρ and σ of a quantum system to decrease. A measure of distinguishability is then monotonically non-increasing under the action of quantum operations when the corresponding distance $D_\delta(\rho, \sigma)$ is contractive under any CPTP map, i.e.

$$D_\delta(\Lambda(\rho), \Lambda(\sigma)) \leq D_\delta(\rho, \sigma) \tag{1.35}$$

for any two states ρ and σ and all CPTP maps Λ. All of the distances defined on the set of density operators listed in Table 1.1 are contractive [20, 44].

We can also account for the situation where a quantum operation is not always applied to a quantum system. A *probabilistic* quantum operation Λ occurs with a probability $\mathrm{Tr}(\Lambda(\rho))$ that is dependent upon the initial state ρ of the system. If Λ does occur, then it transforms the system to the evolved state ρ' according to the map $\rho' = \Lambda(\rho)/\mathrm{Tr}(\Lambda(\rho))$. Here, Λ is a completely positive map, but does not preserve the trace since $0 \leq \mathrm{Tr}(\Lambda(\rho)) \leq 1$. We may write any probabilistic quantum operation in terms of Kraus operators $\{K_i\}_i$ as $\Lambda(\rho) = \sum_i K_i \rho K_i^\dagger$ using the operator sum representation, but now it must hold that

$$\sum_i K_i^\dagger K_i \leq \mathbb{I}. \tag{1.36}$$

Probabilistic quantum operations form an important part of the general description of measurement in quantum mechanics, as will now be discussed in the following section.

1.2.3 Observables

The observables of a quantum system are given by self-adjoint operators acting on $\mathcal{H}$. An observable O can be written in terms of its eigenvalues and eigenvectors as

$$O = \sum_i o_i \left|o_i\right\rangle \left\langle o_i\right|, \tag{1.37}$$

where the eigenvalues $\{o_i\}_{i=1}^d$ are real and the eigenvectors $\{|o_i\rangle\}_{i=1}^d$ form an ONB of $\mathcal{H}$. Measurement of the observable O on a quantum system in configuration $|\psi\rangle$ causes the system to collapse onto one of the configurations $\{|o_i\rangle\}_{i=1}^d$ with probability $|\langle o_i|\psi\rangle|^2$, yielding the corresponding measurement results $\{o_i\}_{i=1}^d$. This is a remarkable difference to the case of classical systems, where an observable measurement does not alter the configuration of the system. On the other hand, to account for the possibility that we do not know the exact configuration of the quantum system, we describe an observable measurement more generally in the following way. Let $\mathbf{R}$ be the set of possible results of measuring O, which is given by the set containing all the unique eigenvalues of O without repetition. This allows O to be rewritten as

$$O = \sum_{r\in\mathbf{R}} rP_r, \tag{1.38}$$

where

$$P_r := \sum_{i:o_i=r} \left|o_i\right\rangle \left\langle o_i\right| \tag{1.39}$$

are projectors onto the eigenspace of O with eigenvalue r. If the quantum system is in state ρ, then measuring the observable O gives result r with probability $p(r|\rho) = \mathrm{Tr}(P_r\rho)$ and leaves the system in the state

$$\theta_r = \frac{P_r\rho P_r}{p(r|\rho)}. \tag{1.40}$$

If the result of measuring the observable is not known then the system will be described by the state

$$\theta = \sum_{r\in\mathbf{R}} p(r|\rho)\theta_r = \sum_{r\in\mathbf{R}} P_r\rho P_r, \tag{1.41}$$

with corresponding expectation value

$$\langle O\rangle_\rho = \sum_{r\in\mathbf{R}} p(r|\rho)r = \mathrm{Tr}(O\rho). \tag{1.42}$$

The result of measuring an observable can tell us the present configuration of the quantum system. If O has a non-degenerate set of eigenvalues, i.e. with each eigenvector $|o_i\rangle$ corresponding to a unique eigenvalue o_i, then the possible results of measuring O are $\mathbf{R} = \{o_i\}_{i=1}^{d}$. Observing the result o_i then tells us that the system is in the configuration $|o_i\rangle$.

The probability of observing the result r and the resultant state of the system do not depend on the exact value of r, and so it is often more useful just to consider *which* of the $r \in \mathbf{R}$ was observed rather than *the value* of the particular $r \in \mathbf{R}$. A quantum instrument is a formalism describing the probabilities of observing a set of measurement outcomes $\{i\}_i$ when measuring a quantum system, as well as the corresponding states $\{\theta_i\}_i$ after the measurement [45, TRB12]. The quantum instrument corresponds to a more general form of measurement of a quantum system and is composed of a set $\{\Lambda_i\}_i$ of probabilistic quantum operations that together sum to a quantum operation Λ. Upon measurement of the quantum system with the quantum instrument, one of the probabilistic quantum operations Λ_i occurs with the state dependent probability $p(\Lambda_i|\rho) = \mathrm{Tr}(\Lambda_i(\rho))$, giving the resultant state

$$\theta_i = \frac{\Lambda_i(\rho)}{p(\Lambda_i|\rho)}. \tag{1.43}$$

This event is associated with the measurement outcome i. If the result of the measurement outcome is not known then the state of the system is

$$\theta = \sum_i p(\Lambda_i|\rho)\Lambda_i = \Lambda(\rho), \tag{1.44}$$

i.e. the result of the quantum operation Λ.

A projective measurement is a special type of quantum instrument whose probabilistic quantum operations are given by $\Lambda_i(\rho) = P_i\rho P_i$, corresponding to a set of projectors $\{P_i\}_i$ that are orthogonal, i.e. $P_iP_j = \delta_{ij}\mathbb{I}$ for any i and j, and sum to the identity, i.e. $\sum_i P_i = \mathbb{I}$. A projective measurement corresponds to an observable measurement when each outcome i is associated with a result r. Another type of quantum instrument is specified by the set of Kraus operators $\{K_i\}_i$ from the operator sum representation of any quantum operation Λ, where

each probabilistic quantum operation is given by the completely positive map $\Lambda_i(\rho) = K_i \rho K_i^\dagger$.

Even more general than a quantum instrument is the concept of a positive operator valued measure (POVM). Here, only the probabilities of each outcome are important and we do not specify the corresponding states of the system. A POVM consists of any set of positive semidefinite operators $\{M_i\}_i$ that sum to the identity, $\sum_i M_i = \mathbb{I}$, so that each outcome i is associated with the probability

$$p(M_i|\rho) = \mathrm{Tr}(M_i \rho). \tag{1.45}$$

Every quantum instrument $\{\Lambda_i\}_i$ has a corresponding set of POVM elements $\{M_i\}_i$ with $M_i = \Lambda_i^\dagger(\mathbb{I})$. The map $\Lambda_i^\dagger$ is the dual of Λ_i, i.e. the map satisfying $\mathrm{Tr}(\Lambda_i^\dagger(\rho)\sigma) = \mathrm{Tr}(\rho\Lambda_i(\sigma))$ for any density operators ρ and σ [20, 46]. The correspondence can then be seen by considering the outcome probabilities,

$$p(\Lambda_i|\rho) = \mathrm{Tr}(\Lambda_i(\rho)) = \mathrm{Tr}(\mathbb{I}\Lambda_i(\rho)) = \mathrm{Tr}(\Lambda_i^\dagger(\mathbb{I})\rho) = \mathrm{Tr}(M_i\rho) = p(M_i|\rho). \tag{1.46}$$

We note that more than one quantum instrument corresponds to the same set of POVM elements, meaning that there is not a unique set of resultant states $\{\theta_i\}_i$ compatible with the probabilities $\{p(M_i|\rho)\}_i$.

1.2.4 Example

We now detail the description of a 2-dimensional quantum system, which has been studied extensively in quantum science. The 2-dimensional system is often thought of as the quantum analogue of a classical bit, and is hence called a qubit. Any state ρ of a qubit can be written as a density operator in the following way

$$\rho = \frac{1}{2}\left(\mathbb{I} + \sum_{i=1}^{3} n_i \sigma_i\right), \tag{1.47}$$

where $n_1^2 + n_2^2 + n_3^2 \leq 1$, $\mathbb{I}$ is the 2-dimensional identity operator and $\{\sigma_i\}_{i=1}^3$ are the Pauli operators, defined by their action on the computational basis $\{|0\rangle, |1\rangle\}$,

$$\begin{aligned} \sigma_1|0\rangle &= |1\rangle & \sigma_1|1\rangle &= |0\rangle, \\ \sigma_2|0\rangle &= i|1\rangle & \sigma_2|1\rangle &= -i|0\rangle, \\ \sigma_3|0\rangle &= |0\rangle & \sigma_3|1\rangle &= -|1\rangle. \end{aligned} \tag{1.48}$$

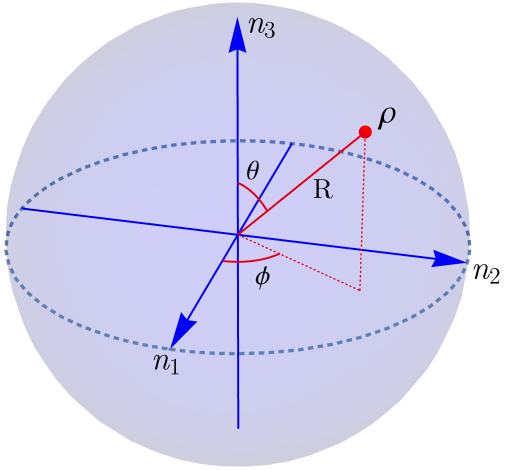

Figure 1.3: The Bloch ball representation of the state ρ of a qubit system.

The state ρ and the Pauli operators can be expressed as matrices with respect to the computational basis, i.e.

$$\rho = \frac{1}{2}\begin{pmatrix} 1+n_3 & n_1 - in_2 \\ n_1 + in_2 & 1-n_3 \end{pmatrix},$$
$$\sigma_1 = \begin{pmatrix} 0 & 1 \\ 1 & 0 \end{pmatrix}, \quad \sigma_2 = \begin{pmatrix} 0 & -i \\ i & 0 \end{pmatrix}, \quad \sigma_3 = \begin{pmatrix} 1 & 0 \\ 0 & -1 \end{pmatrix}. \tag{1.49}$$

The vector $\mathbf{n} := \{n_i\}_{i=1}^3$ lies within the unit ball $\mathcal{B}_1$ in $\mathbb{R}^3$, and can be described in spherical coordinates by a radius $R := \sqrt{n_1^2 + n_2^2 + n_3^2}$ and two angles $\theta \in [0, \pi]$ and $\phi \in [0, 2\pi[$ as $\mathbf{n} = \{R\cos(\phi)\sin(\theta), R\sin(\phi)\sin(\theta), R\cos(\theta)\}$. This is called the Bloch ball representation of a qubit state and is visualised in Figure 1.3. The eigenvalues of ρ are

$$p_1 = \frac{1-R}{2}, \qquad p_2 = \frac{1+R}{2}. \tag{1.50}$$

The von Neumann entropy is then

$$\mathcal{S}(\rho) = -\frac{1-R}{2}\log\left(\frac{1-R}{2}\right) - \frac{1+R}{2}\log\left(\frac{1+R}{2}\right), \tag{1.51}$$

which varies between 0, when $R = 1$, and 1, when $R = 0$. The pure state projectors are given by all ρ with $R = 1$, and hence lie on the surface of the Bloch ball. The corresponding configurations are

$$|\psi\rangle = \cos\left(\frac{\theta}{2}\right)|0\rangle + e^{i\phi}\sin\left(\frac{\theta}{2}\right)|1\rangle. \tag{1.52}$$

It can be seen that the pure state projector $|0\rangle\langle 0|$ onto the computational basis has corresponding coordinates $\mathbf{n} = \{0, 0, 1\}$ in the Bloch ball, while the pure state projector $|1\rangle\langle 1|$ has coordinates $\mathbf{n} = \{0, 0, -1\}$.

1.3 Composite Systems

In this thesis we will also be considering composite systems. Here we briefly outline the description of a bipartite system consisting of either two classical subsystems or two quantum subsystems. We label these subsystems A and B and consider them to be finite dimensional with dimensions d_A and d_B.

Composite Classical Systems

If the two subsystems are classical, then they have phase spaces $\mathcal{P}^A = \{i\}_{i=1}^{d_A}$ and $\mathcal{P}^B = \{j\}_{j=1}^{d_B}$, respectively. The phase space $\mathcal{P}^{AB}$ of the composite system is given by the Cartesian product of $\mathcal{P}^A$ and $\mathcal{P}^B$,

$$\mathcal{P}^{AB} := \mathcal{P}^A \times \mathcal{P}^B = \{(i, j)\}_{i,j=1}^{d_A,d_B}, \tag{1.53}$$

where $\times$ denotes the Cartesian product. The state of the composite system is then given by a joint probability distribution $\mathbf{p}^{AB} = \{p_{ij}^{AB}\}_{i,j=1}^{d_A,d_B}$ defined on $\mathcal{P}^{AB}$, with p_{ij}^{AB} giving the likelihood that subsystem A is in configuration $i \in \mathcal{P}^A$ and subsystem B is in configuration $j \in \mathcal{P}^B$. The overall likelihood that subsystem A is in configuration i (i.e. regardless of the configuration of subsystem B) is given by $p_i^A = \sum_{j=1}^{d_B} p_{ij}^{AB}$, and hence the state of subsystem A is the marginal probability distribution $\mathbf{p}^A = \{p_i^A\}_{i=1}^{d_A}$. Likewise, the state of subsystem B is the marginal probability distribution $\mathbf{p}^B = \{p_j^B\}_{j=1}^{d_B}$, with $p_j^B = \sum_{i=1}^{d_A} p_{ij}^{AB}$. If the configurations of subsystems A and B are known to be $i \in \mathcal{P}^A$ and $j \in \mathcal{P}^B$, then the state of the composite system is given by the pure state $(\boldsymbol{\delta}^{(ij)})^{AB} = \{\delta_{ik}\delta_{jl}\}_{k,l=1}^{d_A,d_B}$. Any state $\mathbf{p}^{AB}$ of the composite system can be expressed in a unique way as a convex mixture of pure states,

$$\mathbf{p}^{AB} = \{p_{ij}^{AB}\}_{i,j=1}^{d_A,d_B} = \sum_{i,j=1}^{d_A,d_B} p_{ij}^{AB} (\boldsymbol{\delta}^{(ij)})^{AB}. \tag{1.54}$$

The composite system may be correlated in such a way that our knowledge on the configuration of one subsystem is affected by our knowledge on the configuration of the other subsystem. If the state of the composite system is $\mathbf{p}^{AB} = \{p_{ij}^{AB}\}_{i,j=1}^{d_A,d_B}$, then the probability that subsystem A is in configuration $i \in \mathcal{P}^A$ given that subsystem B is in configuration $j \in \mathcal{P}^B$ is $p_i^{A|B=j} = p_{ij}^{AB}/p_j^B$. The state of subsystem A is then $\mathbf{p}^{A|B=j} = \{p_i^{A|B=j}\}_{i=1}^{d_A}$ with a corresponding Shannon entropy $\mathcal{S}(\mathbf{p}^{A|B=j})$. Taking the average of this Shannon entropy over all the configurations of subsystem B gives the conditional entropy

$$\mathcal{S}_{A|B}(\mathbf{p}^{AB}) = \sum_{j=1}^{d_B} p_j^B \mathcal{S}(\mathbf{p}^{A|B=j}), \tag{1.55}$$

which measures our average uncertainty on the configuration of subsystem A given knowledge on the configuration of subsystem B. We then say that the subsystems are correlated whenever $\mathcal{S}_{A|B}(\mathbf{p}^{AB})$ is less than $\mathcal{S}(\mathbf{p}^A)$. The difference between these two quantities is a measure of the correlations and is called the mutual information, which can be expressed in three equivalent forms

$$\begin{aligned} \mathcal{I}(\mathbf{p}^{AB}) &= \mathcal{S}(\mathbf{p}^A) - \mathcal{S}_{A|B}(\mathbf{p}^{AB}) \\ &= \mathcal{S}(\mathbf{p}^B) - \mathcal{S}_{B|A}(\mathbf{p}^{AB}) \\ &= \mathcal{S}(\mathbf{p}^A) + \mathcal{S}(\mathbf{p}^B) - \mathcal{S}(\mathbf{p}^{AB}). \end{aligned} \tag{1.56}$$

The mutual information is non-negative and zero only for uncorrelated systems where the state $\mathbf{p}^{AB} = \{p_i^A p_j^B\}_{i,j=1}^{d_A,d_B}$ is the product of subsystem states $\mathbf{p}^A = \{p_i^A\}_{i=1}^{d_A}$ and $\mathbf{p}^B = \{p_j^B\}_{j=1}^{d_B}$.

An observable of the composite system is given by the real numbers $\mathbf{O}^{AB} = \{o_{ij}\}_{i,j=1}^{d_A,d_B}$ so that the observable takes the value o_{ij} when subsystem A is in configuration $i \in \mathcal{P}^A$ and subsystem B is in configuration $j \in \mathcal{P}^B$. Local observables of the subsystems are given by the collections of real numbers $\mathbf{O}^A = \{o_i\}_{i=1}^{d_A}$ and $\mathbf{O}^B = \{o_j\}_{j=1}^{d_B}$, and can be measured jointly on the composite system as the product $\mathbf{O}^{AB} = \mathbf{O}^A \times \mathbf{O}^B = \{o_i o_j\}_{i,j=1}^{d_A,d_B}$. Hence, measurement of the local observable $\mathbf{O}^A$ on the composite system is achieved by jointly measuring with the identity observable $\mathbf{I} = \{1\}_{j=1}^{d_B}$ on subsystem B, i.e. resulting in the product

$\mathbf{O}^{AB} = \mathbf{O}^A \times \mathbf{I} = \{o_i\}_{i,j=1}^{d_A,d_B}$ so that the value o_i is taken whenever subsystem A is in configuration $i \in \mathcal{P}^A$, regardless of the configuration of subsystem B.

Composite Quantum Systems

If the two subsystems are quantum, then they have Hilbert spaces $\mathcal{H}^A$ and $\mathcal{H}^B$, respectively. The composite system is then described by a $(d_A \times d_B)$-dimensional Hilbert space $\mathcal{H}^{AB}$ given by the tensor product of $\mathcal{H}^A$ and $\mathcal{H}^B$,

$$\mathcal{H}^{AB} := \mathcal{H}^A \otimes \mathcal{H}^B, \tag{1.57}$$

where $\otimes$ denotes the tensor product. The state of the composite system is given by a density operator ρ^{AB} acting on $\mathcal{H}^{AB}$, while the states ρ^A and ρ^B of subsystems A and B, respectively, are given by the marginal density operators found by performing the partial trace over the complementary Hilbert space, i.e.

$$\rho^A = \mathrm{Tr}_B(\rho^{AB}) \qquad\qquad \rho^B = \mathrm{Tr}_A(\rho^{AB}), \tag{1.58}$$

where Tr_X indicates the partial trace over subsystem X. If the configuration of the composite system is known, then its density operator is the pure state projector $|\psi^{AB}\rangle\langle\psi^{AB}|$. Any state ρ^{AB} of the composite system can be expressed as a (non-unique) convex combination of pure state projectors, i.e. there always exists a set of pure state projectors $\{|\psi_i^{AB}\rangle\langle\psi_i^{AB}|\}_i$ such that

$$\rho^{AB} = \sum_i q_i \, |\psi_i^{AB}\rangle\langle\psi_i^{AB}| \,, \tag{1.59}$$

for a probability distribution $\{q_i\}_i$.

The correlations of the composite system in state ρ^{AB} are given by the mutual information

$$\mathcal{I}(\rho^{AB}) = \mathcal{S}(\rho^A) + \mathcal{S}(\rho^B) - \mathcal{S}(\rho^{AB}). \tag{1.60}$$

Furthermore, the observables of the composite quantum system are the self-adjoint operators acting on $\mathcal{H}^{AB}$, while observables of the subsystems are the self-adjoint operators acting on $\mathcal{H}^A$ and $\mathcal{H}^B$, respectively. Measurement of the local observable O^A on the composite system is achieved with the tensor product $O^A \otimes \mathbb{I}^B$, where $\mathbb{I}^B$ is the identity operator acting on subsystem B.

As well as bipartite quantum systems, it will also be useful to describe composite quantum systems of N qubits. Here, the 2^N-dimensional Hilbert space is given by the tensor product $\mathcal{H}^{\otimes N}$ of the qubit Hilbert space highlighted in Section 1.2.4. Any state of the N qubit system can be written as

$$\rho = \frac{1}{2^N} \sum_{i_1 i_2 \ldots i_N = 0}^{3} R_{i_1 i_2 \ldots i_N} \sigma_{i_1} \otimes \sigma_{i_2} \otimes \ldots \otimes \sigma_{i_N}, \tag{1.61}$$

where $\sigma_0 := \mathbb{I}$ is the 2-dimensional identity operator. The real correlation tensor $R_{i_1 i_2 \ldots i_N} = \mathrm{Tr}(\rho\, \sigma_{i_1} \otimes \sigma_{i_2} \otimes \ldots \otimes \sigma_{i_N}) \in [-1, 1]$ must obey certain requirements for ρ to be a density matrix. Since the Pauli operators are traceless, $\mathrm{Tr}(\rho) = 1$ when $R_{00\ldots0} = 1$. However, the constraints on $R_{i_1, i_2, \ldots, i_N}$ for ρ to be positive semidefinite for a general N are complicated and not yet fully characterised.

1.4 Comparison

The preceding discussion of classical and quantum systems has highlighted a lot of similarities in their description, Table 1.2 provides a summary. However, there are some differences between classical and quantum systems that lead to very contrasting properties. These properties are what we call *the quantum*, which form the focus of this thesis.

One of the most notable features of a quantum system is that it can exist in an infinite number of possible configurations. Nevertheless, we have seen that an observation of the quantum system through an observable O with non-degenerate eigenvalues allows us to single out a set of d configurations corresponding to the ONB $\{|e_i\rangle\}_{i=1}^d$ of O. We can reconcile the configurations of this ONB with the d possible configurations of a classical system. Indeed, a classical system in state $\mathbf{p} = \{p_i\}_{i=1}^d$ can be associated with the state $\rho = \sum_{i=1}^d p_i \, |e_i\rangle \langle e_i|$ of the quantum system, i.e. so that the eigenbasis of ρ coincides with the ONB $\{|e_i\rangle\}_{i=1}^d$. In this case, we have that the probability $\langle e_i|\rho|e_i\rangle$ of the quantum system being in configuration $|e_i\rangle$ after measuring O is exactly the corresponding p_i from the probability distribution. Nevertheless, there is an infinite number of other possible ONBs of $\mathcal{H}$ that may describe the eigenbasis of ρ, so that ρ does

	Classical systems	Quantum systems
Space	$\mathcal{P}$	$\mathcal{H}$
Configurations	$i \in \mathcal{P}$	$\|\psi\rangle \in \mathcal{H}$
States	$\mathbf{p} = \sum_{i=1}^{d} p_i \boldsymbol{\delta}^{(i)}$ $p_i \geq 0$, $\sum_{i=1}^{d} p_i = 1$	$\rho = \sum_{i=1}^{d} p_i \|p_i\rangle \langle p_i\|$ $p_i \geq 0$, $\sum_{i=1}^{d} p_i = 1$
Entropy	$\mathcal{S}(\mathbf{p}) = -\sum_{i=1}^{d} p_i \log p_i$	$\mathcal{S}(\rho) = -\sum_{i=1}^{d} p_i \log p_i$
Distinguishability	$D_\delta(\mathbf{p}, \mathbf{q})$	$D_\delta(\rho, \sigma)$
Evolution	$S\mathbf{p}$	$\Lambda[\rho]$
Observables	$\mathbf{O} = \sum_{i=1}^{d} o_i \boldsymbol{\delta}^{(i)}$	$O = \sum_{i=1}^{d} o_i \|o_i\rangle \langle o_i\|$
Composition	$\times$	$\otimes$

Table 1.2: A summary of the structures used to describe classical systems and quantum systems.

not generally commute with the observable O (i.e. $[\rho, O] := \rho O - O\rho \neq 0$). This peculiarity of quantum mechanics gives rise to the concept of quantum coherence, as discussed in the next chapter.

Another remarkable feature of quantum mechanics is the formalism used to describe composite quantum systems. In Section 1.3 we saw that composite classical systems use the Cartesian product structure of the phase space, while composite quantum systems rely on the tensor product structure of the Hilbert space. It is this tensor product structure that gives rise to the presence of quantum correlations in a composite quantum system, as we discuss in further detail in the following chapter. Indeed, for a composite classical system the Cartesian product structure implies that whenever the composite system is in a pure state, then its subsystems are also in pure states. On the other hand, the tensor product structure of a composite quantum system means that a pure state of the composite system does not necessarily imply that the states of the subsystems are also pure. This quantum feature is associated with the property of quantum entanglement, a particular type of quantum correlations.

Chapter 2

The Quantum-Classical Frontier

In this chapter we explain the three key types of *the quantum* considered in this thesis: quantum coherence, quantum correlations, and quantum entanglement. Building upon our comparison of classical and quantum systems in the previous chapter, we discuss how each type of *the quantum* arises uniquely from the description of a physical system provided by quantum mechanics. Characterising these types of *the quantum* then sets the stage for an investigation of Questions 1, 2, and 3 in the following chapters.

2.1 Quantum Coherence

Consider a quantum system in the pure state $|\psi\rangle \in \mathcal{H}$ along with the measurement of an observable O on the system with non-degenerate eigenvalues and an associated reference ONB $\{|e_i\rangle\}_{i=1}^{d}$. We can write the vector $|\psi\rangle$ with respect to this ONB as

$$|\psi\rangle = \sum_{i=1}^{d} \psi_i \, |e_i\rangle \, , \tag{2.1}$$

where $\psi_i = \langle e_i|\psi\rangle \in \mathbb{C}$ and $\sum_{i=1}^{d} |\psi_i|^2 = 1$. From Section 1.2.3, we know that, by measuring the observable O, we will observe one of the non-degenerate eigenvalues with probability $|\langle e_i|\psi\rangle|^2 = |\psi_i|^2$ and conclude that the quantum system collapses onto the corresponding configuration $|e_i\rangle$. Hence, unless $|\psi\rangle = |e_i\rangle$ for any i, we will have an uncertainty on the resultant configuration of the quantum system.

This uncertainty does not arise from our lack of knowledge of the system, since we know it is initially in the pure state $|\psi\rangle$, but rather from an intrinsic uncertainty due to the probabilistic nature of quantum mechanics itself. We call quantum coherence the property that characterises this intrinsic uncertainty [1, 47, 48]. Hence, a pure state of the quantum system $|\psi\rangle$ is coherent with respect to the reference ONB if more than one of the ψ_i is non-zero. If this is the case, $|\psi\rangle$ is said to be in a coherent superposition. The pure states that are not in a coherent position are called incoherent, and are given by all the $\{|e_i\rangle\}_{i=1}^d$.

While for pure states any uncertainty on the resultant configuration $\{|e_i\rangle\}_{i=1}^d$ of the system after measuring the observable O is only due to the probabilistic nature of quantum mechanics, for mixed states we have an additional uncertainty due to our lack of knowledge on the configuration of the system. The states with coherence are then defined to be those for which there is always a non-zero probability that the system is described by a coherent pure state. As we have seen in Section 1.2.1, there is not a unique decomposition of a density operator ρ according to Eq. (1.22) into a convex combination of pure state projectors $\{|\psi_i\rangle\langle\psi_i|\}_i$ according to the probability distribution $\{q_i\}_i$. The coherent states are hence those for which every decomposition always has at least one $|\psi_i\rangle$ that is coherent (with $q_i > 0$). Conversely, the incoherent states are those not satisfying this property, such that there exists a decomposition of ρ into only incoherent pure state projectors, i.e. so that each $|\psi_i\rangle$ is equal to one of the $\{|e_i\rangle\}_{i=1}^d$. It can then be said that a state δ is incoherent with respect to the ONB $\{|e_i\rangle\}_{i=1}^d$ if it can be written as

$$\delta = \sum_{i=1}^{d} \delta_i |e_i\rangle\langle e_i| , \tag{2.2}$$

where $\{\delta_i\}_{i=1}^d$ is a probability distribution. We represent the set of incoherent states with $\mathcal{I}$. The incoherent density matrices are given by all the density matrices that are diagonal when represented with respect to the reference ONB.

It can be seen that the eigenbasis of a coherent state ρ does not coincide with the reference ONB $\{|e_i\rangle\}_{i=1}^d$ with respect to which coherence is measured. Hence, coherence arises from the non-uniqueness of the ONBs of $\mathcal{H}$, or alternatively

the non-commutative nature of self-adjoint operators in quantum mechanics. In classical mechanics, there is a unique basis $\{i\}_{i=1}^{d}$ to describe the phase space $\mathcal{P}$ of the system. The configuration of a classical system is left unchanged by the measurement of an observable, and hence there is no intrinsic uncertainty on the resultant configuration. As has already been alluded to in Section 1.4, the incoherent quantum states δ in Eq. (2.2) can thought of as representing a classical system in state $\{\delta_i\}_{i=1}^{d}$ with respect to the reference ONB.

2.1.1 Coherence Number

Instead of characterising just the presence of an intrinsic uncertainty in a quantum system with respect to the configurations of the ONB $\{|e_i\rangle\}_{i=1}^{d}$ corresponding to measuring the observable O, it can also be informative to count how many of the $|e_i\rangle$ there is an uncertainty with respect to. This concept is captured by the coherence number [TRB3, 49–53]. A pure state of the quantum system $|\psi\rangle = \sum_{i=1}^{d} \psi_i |e_i\rangle$ has a coherence number of k with respect to the fixed reference ONB $\{|e_i\rangle\}_{i=1}^{d}$ if exactly k of the ψ_i are non-zero. The coherence number ranges from 1 to d, corresponding to the dimension of the system.

Just like with coherence, the coherence number of a general state ρ depends on the decomposition of ρ into pure state projectors $\{|\psi_i\rangle \langle\psi_i|\}_i$ with probabilities $\{q_i\}_i$. We say that ρ has a coherence number of k if every decomposition has at least one pure state $|\psi_i\rangle$ (and $q_i > 0$) with a coherence number of at least k, and if there exists at least one decomposition where one pure state $|\psi_i\rangle$ (with $q_i > 0$) has a coherence number of k and all the other $|\psi_i\rangle$ have a coherence number less than or equal to k. In such a way, there is always a non-zero probability that the system is described by a pure state with a coherence number of at least k, but it is not always guaranteed that it can be described by a pure state with a coherence number of more than k.

In practice, it will be more useful to define the states with a coherence number of less than k. A density operator ρ has a coherence number of less than k if it can be decomposed as a convex mixture of pure state projectors $\{|\psi_i\rangle \langle\psi_i|\}_i$ such

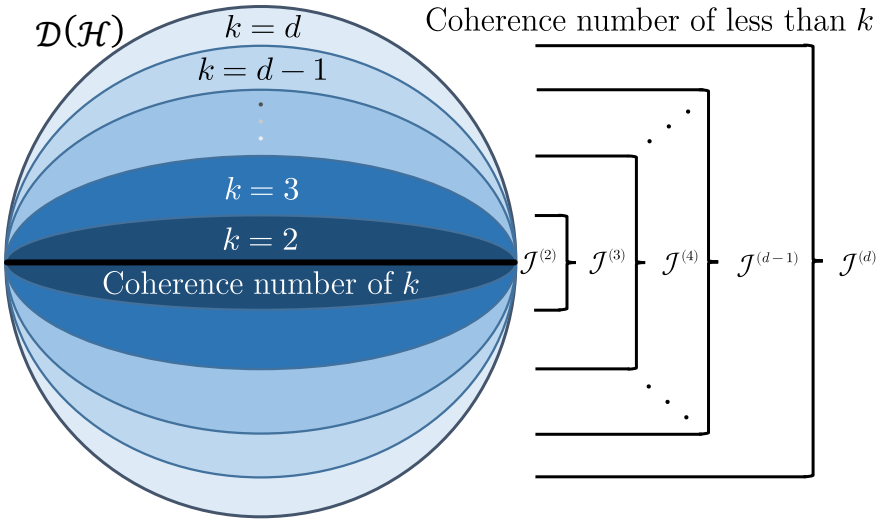

Figure 2.1: The set of states $\mathcal{D}(\mathcal{H})$ of a d-dimensional system (represented here by the circle) can be structured into the convex sets $\mathcal{I}^{(k)}$ of states with a coherence number of less than k (represented as the concentric ellipses), with $\mathcal{I}^{(2)} \subset \mathcal{I}^{(3)} \subset \ldots \subset \mathcal{I}^{(d)} \subset \mathcal{D}(\mathcal{H})$. On the other hand, the (non-convex) sets of states with a coherence number of exactly k are given by the difference between the sets $\mathcal{I}^{(k+1)}$ (or $\mathcal{D}(\mathcal{H})$ when $k = d$) and $\mathcal{I}^{(k)}$. Note that the areas of ellipses are not representative of the volumes of the corresponding sets $\mathcal{I}^{(k)}$, although the set of incoherent states $\mathcal{I}^{(2)}$ is known to be zero measure within $\mathcal{D}(\mathcal{H})$ [1, TRB1], and is hence drawn as a line.

that all of the pure states $|\psi_i\rangle$ have a coherence number of less than k. The convex set of density operators with a coherence number of less than k is given by $\mathcal{I}^{(k)}$ for $k \in \{2, 3, \ldots, d\}$, and it follows that $\mathcal{I}^{(2)} \subset \mathcal{I}^{(3)} \subset \ldots \subset \mathcal{I}^{(d)} \subset \mathcal{D}(\mathcal{H})$. The set of incoherent states is given in particular by $\mathcal{I} = \mathcal{I}^{(2)}$. Figure 2.1 provides a visualisation of the sets $\mathcal{I}^{(k)}$ that have a coherence number of less than k in a d-dimensional system, along with a comparison to the sets of states with a coherence number of exactly k.

2.2 Quantum Correlations

As we have seen in Section 1.3, the description of a composite quantum system is markedly different to that of a composite classical system. Here we focus on the

unique nature of composite quantum systems. This unique nature is captured by the property of quantum correlations in the composite system [9–11, 54–58], one of the key types of *the quantum* discussed in this thesis. To identify these quantum correlations, we first need to be able to compare composite quantum systems and composite classical systems within the same paradigm. This can be achieved by establishing the description of classical subsystems within the quantum formalism, as we now proceed to do for the case of bipartite composite systems using the setting of Section 1.3. The material presented here is derived from the review papers in Refs. [TRB12, TRB13].

Suppose that the state of a bipartite quantum system is given by the density operator

$$\chi_{CC}^{AB} = \sum_{i=1}^{d_A} \sum_{j=1}^{d_B} p_{ij}^{AB} \left|e_i^A\right\rangle \left\langle e_i^A\right| \otimes \left|f_j^B\right\rangle \left\langle f_j^B\right|, \tag{2.3}$$

where $\{p_{ij}^{AB}\}_{i,j=1}^{d_A,d_B}$ is a joint probability distribution and $\{|e_i^A\rangle\}_{i=1}^{d_A}$ and $\{|f_j^B\rangle\}_{j=1}^{d_B}$ are ONBs of $\mathcal{H}^A$ and $\mathcal{H}^B$, respectively. We can associate the ONBs $\{|e_i^A\rangle\}_{i=1}^{d_A}$ and $\{|f_j^B\rangle\}_{j=1}^{d_B}$ with the configurations $\mathcal{P}^A$ and $\mathcal{P}^B$ of two classical subsystems A and B, respectively, so that the probability that subsystem A is in configuration $i \in \mathcal{P}^A$ and subsystem B is in configuration $j \in \mathcal{P}^B$ is

$$\langle e_i^A \otimes f_j^B | \chi_{CC}^{AB} | e_i^A \otimes f_j^B \rangle = p_{ij}^{AB}. \tag{2.4}$$

Furthermore, the states of subsystems A and B are given by Eq. (1.58) as

$$\rho^A = \sum_{i=1}^{d_A} p_i^A \left|e_i^A\right\rangle \left\langle e_i^A\right|, \qquad \rho^B = \sum_{j=1}^{d_B} p_j^B \left|f_j^B\right\rangle \left\langle f_j^B\right|, \tag{2.5}$$

where $p_i^A = \sum_{j=1}^{d_B} p_{ij}^{AB}$ and $p_j^B = \sum_{i=1}^{d_A} p_{ij}^{AB}$. Hence, the probability that subsystem A is in configuration i is p_i^A and the probability that subsystem B is in configuration j is p_j^B. Therefore, the density operator χ_{CC}^{AB} effectively describes a bipartite classical system in state $\mathbf{p}^{AB} = \{p_{ij}^{AB}\}_{i,j=1}^{d_A,d_B}$, provided one chooses to represent the configurations of the classical subsystems A and B with the ONBs $\{|e_i^A\rangle\}_{i=1}^{d_A}$ and $\{|f_j^B\rangle\}_{j=1}^{d_B}$, respectively. Such states are called classical-classical (CC) states because both subsystems A and B are classical with respect to the choices of ONB. Since one is free to choose the local bases used to represent the classical

subsystems, the set of classical-classical states is then

$$\mathcal{C}_{CC}^{AB} := \left\{ \rho^{AB} \quad \middle| \quad \rho^{AB} = \sum_{i=1}^{d_A} \sum_{j=1}^{d_B} p_{ij}^{AB} \left|e_i^A\right\rangle \left\langle e_i^A\right| \otimes \left|f_j^B\right\rangle \left\langle f_j^B\right| \right\} \tag{2.6}$$

for any ONB $\{|e_i^A\rangle\}_{i=1}^{d_A}$ of A and $\{|f_j^B\rangle\}_{j=1}^{d_B}$ of B.

It is also possible to have an intermediate scenario whereby only one subsystem can be described classically. A classical-quantum (CQ) state of a bipartite system is given by

$$\chi_{CQ}^{AB} = \sum_{i=1}^{d_A} p_i^A \left|e_i^A\right\rangle \left\langle e_i^A\right| \otimes \rho_i^B, \tag{2.7}$$

where $\{p_i^A\}_{i=1}^{d_A}$ is a probability distribution, $\{|e_i^A\rangle\}_{i=1}^{d_A}$ is an ONB of A, and $\{\rho_i^B\}_{i=1}^{d_A}$ are arbitrary states of subsystem B. We can see that the marginal states of subsystems A and B are

$$\rho^A = \sum_{i=1}^{d_A} p_i^A \left|e_i^A\right\rangle \left\langle e_i^A\right|, \qquad\qquad \rho^B = \sum_{i=1}^{d_A} p_i^A \rho_i^B. \tag{2.8}$$

If we associate the ONB $\{|e_i^A\rangle\}_{i=1}^{d_A}$ with the configurations $\mathcal{P}^A$ of a classical subsystem, then it is clear that subsystem A can be described classically with respect to this ONB by the state $\mathbf{p}^A = \{p_i^A\}_{i=1}^{d_A}$. Indeed, the probability that subsystem A is in configuration $i \in \mathcal{P}^A$ is $\langle e_i^A|\rho^A|e_i^A\rangle = p_i^A$. On the other hand, in general subsystem B does not correspond to a classical subsystem with respect to any choice of ONB. The set of classical-quantum states is then

$$\mathcal{C}_{CQ}^{AB} := \left\{ \rho^{AB} \quad \middle| \quad \rho^{AB} = \sum_{i=1}^{d_A} p_i^A \left|e_i^A\right\rangle \left\langle e_i^A\right| \otimes \rho_i^B \right\} \tag{2.9}$$

for any ONB $\{|e_i^A\rangle\}_{i=1}^{d_A}$ of A. The quantum-classical (QC) states are justified analogously and are written as

$$\chi_{QC}^{AB} = \sum_{j=1}^{d_B} p_j^B \rho_j^A \otimes \left|f_j^B\right\rangle \left\langle f_j^B\right|, \tag{2.10}$$

where $\{p_j^B\}_{j=1}^{d_B}$ is a probability distribution, $\{|f_j^B\rangle\}_{j=1}^{d_B}$ is an ONB of B, and $\{\rho_j^A\}_{j=1}^{d_B}$ are arbitrary states of subsystem A. The corresponding set is then

$$\mathcal{C}_{QC}^{AB} := \left\{ \rho^{AB} \quad \middle| \quad \rho^{AB} = \sum_{j=1}^{d_B} p_j^B \rho_j^A \otimes \left|f_j^B\right\rangle \left\langle f_j^B\right| \right\}, \tag{2.11}$$

for any ONB $\{|f_j^B\rangle\}_{j=1}^{d_B}$ of B.

The CC, CQ and QC states may be referred to as classically correlated because at least one of the subsystems can be described classically in a certain ONB. In particular, the CC states are classically correlated for both subsystems, the CQ states are classically correlated for subsystem A, while the QC states are classically correlated for subsystem B. The sets $\mathcal{C}_{CC}^{AB}$, $\mathcal{C}_{CQ}^{AB}$, and $\mathcal{C}_{QC}^{AB}$ are not convex, and it also holds that $\mathcal{C}_{CC}^{AB} = \mathcal{C}_{CQ}^{AB} \cap \mathcal{C}_{QC}^{AB}$. Quantumly correlated states are the states that are not classically correlated. Specifically, if $\rho^{AB} \notin \mathcal{C}_{CC}^{AB}$ then ρ^{AB} has quantum correlations originating from at least one of the subsystems, if $\rho^{AB} \notin \mathcal{C}_{CQ}^{AB}$ then ρ^{AB} has quantum correlations from subsystem A, and if $\rho^{AB} \notin \mathcal{C}_{QC}^{AB}$ then ρ^{AB} has quantum correlations from subsystem B.

In Refs. [TRB12, TRB13] we review a number of different justifications for using the term quantum correlations, see also Refs. [11, 54–58] for further details. The original notion of quantum correlations was suggested in Refs. [9, 10], where it was noticed that the so-called classical correlations resulting from local measurements on the subsystems of a bipartite quantum system do not generally account for all of the total correlations according to the mutual information in Eq. (1.60). The difference between the total correlations and the classical correlations then results in a well-known quantity, called the quantum discord, as a measure of quantum correlations. In this thesis, we do not report on the quantum correlations from this perspective, and instead follow a distance-based approach to its quantification, outlined in Chapter 3. The rest of this section on quantum correlations is devoted to highlighting two of the characteristic features of a quantumly correlated composite system: the presence of local coherence, and a sensitivity to local projective measurements. In the following, the quantumly correlated states will be those that are not CQ. Analogous features also exist for CC and QC states.

2.2.1 Local Quantum Coherence

Consider a state $|\psi^A\rangle\langle\psi^A| \otimes \rho^B$ of a bipartite quantum system, where $|\psi^A\rangle \in \mathcal{H}^A$ is a pure state of subsystem A and ρ^B is an arbitrary state of subsystem B. The state of subsystem A can be written with respect to an ONB $\{|e_i^A\rangle\}_{i=1}^{d_A}$ of $\mathcal{H}^A$ as

$$|\psi^A\rangle = \sum_{i=1}^{d_A} \psi_i^A |e_i^A\rangle \tag{2.12}$$

with $\psi_i^A = \langle e_i^A|\psi^A\rangle$. From the discussion in Section 2.1, it is clear that $|\psi^A\rangle$ is coherent in the reference ONB $\{|e_i^A\rangle\}_{i=1}^{d_A}$ if more than one ψ_i^A is non-zero. Hence, the state $|e_i^A\rangle\langle e_i^A| \otimes \rho^B$, for any i, is locally incoherent in subsystem A. In fact, any state that can be written as

$$\delta_{IQ}^{AB} = \sum_{i}^{d_A} p_i^A |e_i^A\rangle\langle e_i^A| \otimes \rho_i^B \tag{2.13}$$

is locally incoherent in subsystem A or incoherent-quantum (IQ), where $\{p_i^A\}_{i=1}^{d_A}$ is a probability distribution and $\{\rho_i^B\}_{i=1}^{d_A}$ are arbitrary states of subsystem B. The set of IQ states in the chosen reference ONB $\{|e_i^A\rangle\}_{i=1}^{d_A}$ is thus defined as

$$\mathcal{I}_{IQ}^{AB} := \left\{ \rho^{AB} \quad \middle| \quad \rho^{AB} = \sum_{i=1}^{d_A} p_i^A |e_i^A\rangle\langle e_i^A| \otimes \rho_i^B \right\}. \tag{2.14}$$

By referring to Eq. (2.7), it can be seen that IQ states are always CQ, i.e. $\mathcal{I}_{IQ}^{AB} \subset \mathcal{C}_{CQ}^{AB}$. Furthermore, $\mathcal{C}_{CQ}^{AB}$ is equal to the union of the sets of IQ states $\mathcal{I}_{IQ}^{AB}$ over all possible choices of ONB of subsystem A. This means that CQ states are exactly the states that are locally incoherent in an ONB of subsystem A. The quantumly correlated states, being those $\rho^{AB} \notin \mathcal{C}_{CQ}^{AB}$, are therefore the states that are locally coherent in all ONBs of subsystem A. This provides an interesting link between quantum coherence and quantum correlations, showing that types of *the quantum* are often interrelated.

2.2.2 Sensitivity to Local Measurements

Suppose a local observable measurement is carried out on our bipartite system in state ρ^{AB}, where the observable is applied to subsystem A and given by $O^A =$

$\sum_{i=1}^{d_A} e_i^A \left|e_i^A\right\rangle \left\langle e_i^A\right|$, with $\{|e_i\rangle\}_{i=1}^{d_A}$ an ONB of $\mathcal{H}^A$ and $\{e_i^A\}_{i=1}^{d_A}$ the corresponding eigenvalues that are fixed to be non-degenerate. From Section 1.2.3, the state of subsystem A is $|e_i^A\rangle$ if result e_i^A is observed. Additionally, the state of subsystem B after result e_i^A is

$$\rho_i^B = \frac{\langle e_i^A|\rho^{AB}|e_i^A\rangle}{\mathrm{Tr}\left(\langle e_i^A|\rho^{AB}|e_i^A\rangle\right)}, \tag{2.15}$$

so that the state of the bipartite system becomes $|e_i^A\rangle \langle e_i^A| \otimes \rho_i^B$. If the result of the observable is not recorded, then the system is described by a density operator

$$\theta_A^{AB} = \sum_{i=1}^{d_A} p_i^A \left|e_i^A\right\rangle \left\langle e_i^A\right| \otimes \rho_i^B, \tag{2.16}$$

where $\{p_i^A\}_{i=1}^{d_A}$ is a probability distribution given by $p_i^A = \langle e_i^A|\rho^A|e_i^A\rangle$, with $\rho^A = \mathrm{Tr}_B(\rho^{AB})$ the state of subsystem A.

It is then clear that the state of the quantum system after any local observable measurement (with the result unknown) is CQ, i.e. $\theta_A^{AB} \in \mathcal{C}_{CQ}^{AB}$. Hence, if the system in the initial state ρ^{AB} is unchanged by this measurement then it must be classically correlated, $\rho^{AB} = \theta_A^{AB} \Rightarrow \rho^{AB} \in \mathcal{C}_{CQ}^{AB}$. Conversely, if $\rho^{AB} \in \mathcal{C}_{CQ}^{AB}$ then it can be seen that there exists an observable with non-degenerate eigenvalues and an ONB $\{|e_i\rangle\}_{i=1}^{d_A}$ such that $\rho^{AB} = \theta_A^{AB}$. This provides a characterisation of the CQ states as

$$\rho^{AB} \in \mathcal{C}_{CQ}^{AB} \quad \Leftrightarrow \quad \exists\, O^A \text{ with distinct } \{e_i\}_{i=1}^{d} \text{ such that } \rho^{AB} = \theta_A^{AB}.$$

The quantumly correlated states, i.e. those $\rho^{AB} \notin \mathcal{C}_{QC}^{AB}$, are therefore sensitive to all local observable measurements on subsystem A with non-degenerate spectrum so that $\rho^{AB} \neq \theta_A^{AB}$. We have hence highlighted another unique feature of a bipartite quantum system arising from quantum correlations as a type of *the quantum*.

2.3 Quantum Entanglement

An intuitive feature of a composite classical system is that its configuration is completely specified by the configurations of its constituent subsystems, meaning

that full knowledge of the whole system is equivalent to full knowledge of the subsystems. Indeed, when we have full knowledge of a bipartite classical system it is described by the pure state $(\boldsymbol{\delta}^{(ij)})^{AB} = \{\delta_{ik}\delta_{jl}\}_{k,l=1}^{d_A,d_B}$. The corresponding states of the subsystems $(\boldsymbol{\delta}^{(i)})^{A} = \{\delta_{ik}\}_{k=1}^{d_A}$ and $(\boldsymbol{\delta}^{(j)})^{B} = \{\delta_{jl}\}_{l=1}^{d_B}$ are also pure, meaning that we have full knowledge of the subsystems.

Instead, composite quantum systems cannot generally be specified by their subsystems. Consider when we have maximum possible knowledge of a bipartite quantum system so that it is described by the pure state $|\psi^{AB}\rangle$. The states of the subsystems are $\rho^A = \mathrm{Tr}_B(|\psi^{AB}\rangle\langle\psi^{AB}|)$ and $\rho^B = \mathrm{Tr}_A(|\psi^{AB}\rangle\langle\psi^{AB}|)$ and are generally mixed. On the other hand, we have maximum possible knowledge of the subsystems when they are described by the pure states $|\psi^A\rangle$ of subsystem A and $|\psi^B\rangle$ of subsystem B. Hence, only when the state of the composite system is $|\psi^{AB}\rangle = |\psi^A\rangle\otimes|\psi^B\rangle$ is maximum possible knowledge of the subsystems equivalent to maximum possible knowledge of the composite system. Any bipartite quantum system described by a pure state that cannot be written as a tensor product, i.e. $|\psi^{AB}\rangle \neq |\psi^A\rangle \otimes |\psi^B\rangle$, exhibits quantum correlations between its subsystems. On the other hand, if $|\psi^{AB}\rangle = |\psi^A\rangle \otimes |\psi^B\rangle$ then the subsystems are completely uncorrelated. This means that a quantum system in a pure state can either be completely uncorrelated or quantumly correlated.

Hence, for pure states there is a unique notion of quantum correlations. This is not the case for mixed states. We have already discussed in the previous section one approach to extend the definition of quantum correlations to bipartite mixed states by considering the embedding of classical subsystems into the bipartite quantum system. However, quantum correlations can also be associated with quantum entanglement, steering, and Bell nonlocality, which result from different approaches to extending the same notion of quantum correlations for pure states onto the set of mixed states. These different types of quantum correlations form a strict hierarchy, indicating an increasingly strong presence of *the quantum* in mixed states of a composite system: from the most general quantum correlations (i.e. those discussed in the previous section), to entanglement, steering, and then Bell nonlocality as the strongest type of quantum correlations. Entanglement [2,

20] is explained in more detail in the following, while steering and Bell nonlocality are not discussed in the rest of this thesis. Refs. [59, 60] provide in depth accounts of steering and Bell nonlocality.

Consider a state of a bipartite quantum system with density operator ς^{AB} that is a convex combination of product pure state projectors,

$$\varsigma^{AB} = \sum_i p_i \left|\psi_i^A\right\rangle \left\langle\psi_i^A\right| \otimes \left|\phi_i^B\right\rangle \left\langle\phi_i^B\right|, \tag{2.17}$$

where $\{p_i\}_i$ is a probability distribution and $\{|\psi_i^A\rangle\}_i$ and $\{|\phi_i^B\rangle\}_i$ are arbitrary pure states of subsystems A and B, respectively. These states are called separable states and can describe a system that is in an uncorrelated pure state. The set of separable states is

$$\mathcal{S}^{AB} := \left\{ \rho^{AB} \quad \middle| \quad \rho^{AB} = \sum_i p_i \left|\psi_i^A\right\rangle \left\langle\psi_i^A\right| \otimes \left|\phi_i^B\right\rangle \left\langle\phi_i^B\right| \right\}, \tag{2.18}$$

which is associated with the entanglement-free states. Hence, any state $\rho \notin \mathcal{S}^{AB}$ is said to be entangled (or inseparable). A hierarchy of types of correlations can be seen as

$$\mathcal{P}^{AB} \subset \mathcal{C}_{CC}^{AB} \subset \mathcal{C}_{CQ}^{AB} \subset \mathcal{S}^{AB}, \tag{2.19}$$

where $\mathcal{P}^{AB}$ are the uncorrelated states

$$\mathcal{P}^{AB} := \left\{ \rho^{AB} \quad \middle| \quad \rho^{AB} = \rho^A \otimes \rho^B \right\}, \tag{2.20}$$

for any state ρ^A of subsystem A and ρ^B of subsystem B.

2.3.1 Multipartite Entanglement

We have so far used bipartite systems to investigate quantum correlations. However, quantum correlations can of course exist in quantum systems composed of more than two subsystems. This thesis focusses in particular on multipartite entanglement in systems of $N \geq 2$ qubits, also called multiqubit entanglement [2, 61]. The following notation can be used to properly account for the various distributions of qubits into different subsystems:

- the sequence $\{1, 2, \ldots, N\}$ labelling the individual qubits;

- the sequence $\{1, 2, \ldots, M\}$ labelling the subsystems, where the positive integer M represents the number of subsystems, with $1 < M \leq N$;

- the sequence of positive integers $\{K_\alpha\}_{\alpha=1}^{M}$, where K_α represents the number of qubits in subsystem $\alpha \in \{1, 2, \ldots, M\}$, where $\sum_{\alpha=1}^{M} K_\alpha = N$;

- the sequence of sequences of positive integers $\{Q_\alpha\}_{\alpha=1}^{M}$ with the sequence $Q_\alpha = \{i_1^{(\alpha)}, i_2^{(\alpha)}, \ldots, i_{K_\alpha}^{(\alpha)}\}$, where $i_j^{(\alpha)} \in \{1, 2, \ldots, N\}$, $Q_\alpha \cap Q_{\alpha'} = \emptyset$ for $\alpha \neq \alpha'$, and $\bigcup_{\alpha=1}^{M} Q_\alpha = \{1, 2, \ldots, N\}$, represents with Q_α the labelled qubits belonging to subsystem $\alpha \in \{1, 2, \ldots, M\}$.

A partition of the N qubit system into M subsystems is specified by $\{Q_\alpha\}_{\alpha=1}^{M}$. We note that the number of possible partitions grows rapidly with the number of qubits [62, 63].

The set of N qubit separable states with respect to an M-partition $\{Q_\alpha\}_{\alpha=1}^{M}$ is

$$\mathcal{S}_{\{Q_\alpha\}_{\alpha=1}^{M}} := \left\{ \rho \quad \middle| \quad \rho = \sum_i p_i \rho_i^{(1)} \otimes \rho_i^{(2)} \otimes \ldots \otimes \rho_i^{(M)} \right\}, \tag{2.21}$$

where $\{p_i\}_i$ is a probability distribution and $\{\rho_i^{(\alpha)}\}_i$ are arbitrary states of subsystem α. Note that this representation of separable states as a convex mixture of product *mixed* states is equivalent to the previously discussed representation in terms of product *pure* state projectors, which means that the bipartite separable states $\mathcal{S}^{AB}$ given in Eq. (2.18) coincide with the separable states given above when $N = 2$ and $M = 2$. Any N qubit system with state $\rho \notin \mathcal{S}_{\{Q_\alpha\}_{\alpha=1}^{M}}$ is entangled (or inseparable) with respect to the M-partition $\{Q_\alpha\}_{\alpha=1}^{M}$.

One partition $\mathbf{P}^{(1)} = \{Q_\alpha^{(1)}\}_{\alpha=1}^{M^{(1)}}$ of the quantum system into $M^{(1)}$ subsystems is said to contain another partition $\mathbf{P}^{(2)} = \{Q_\beta^{(2)}\}_{\beta=1}^{M^{(2)}}$ of the system into $M^{(2)}$ subsystems if $M^{(1)} < M^{(2)}$ and for all $Q_\alpha^{(1)} \in \mathbf{P}^{(1)}$

$$Q_\alpha^{(1)} = \bigcup_{\beta(\alpha)} Q_\beta^{(2)}, \tag{2.22}$$

where $\beta(\alpha) \subset \{1, 2, \ldots, M^{(2)}\}$, $\bigcup_\alpha \beta(\alpha) = \{1, 2, \ldots, M^{(2)}\}$, and $\beta(\alpha) \cap \beta(\alpha') = \emptyset$ for all $\alpha \neq \alpha'$ [62]. Simply, partition $\mathbf{P}^{(1)}$ contains partition $\mathbf{P}^{(2)}$ if it can be formed by joining together some of the subsystems of $\mathbf{P}^{(2)}$. A given partition can

generally contain more than one partition, and can generally be contained within more than one partition. The partition of qubits into individual subsystems, i.e. with $M = N$, contains no partitions but is contained within all other partitions. On the other end of the scale, any bipartition, i.e. with $M = 2$, is never contained within another partition. By considering Eq. (2.21), it can be seen that

$$\mathcal{S}_{\{Q_\alpha^{(1)}\}_{\alpha=1}^{M^{(1)}}} \supset \mathcal{S}_{\{Q_\beta^{(2)}\}_{\beta=1}^{M^{(2)}}} \quad \Leftrightarrow \quad \mathbf{P}^{(1)} \text{ contains } \mathbf{P}^{(2)}. \tag{2.23}$$

Hence, if an N qubit system is separable with respect to the partition $\{Q_\beta^{(2)}\}_{\beta=1}^{M^{(2)}}$, then it is separable with respect to all containing partitions $\{Q_\alpha^{(1)}\}_{\alpha=1}^{M^{(1)}}$. Conversely, if the system is entangled with respect to the partition $\{Q_\alpha^{(1)}\}_{\alpha=1}^{M^{(1)}}$, then it is entangled with respect to all contained partitions $\{Q_\beta^{(2)}\}_{\beta=1}^{M^{(2)}}$. This provides a hierarchy of the multiqubit entanglement present in the N qubit system in terms of its partitions.

An alternative partition independent approach also exists to characterise multiqubit entanglement. An N qubit system in state ρ is M-separable if ρ can be written as a convex combination of states that are each separable with respect to any (possibly different) M-partition $\{Q_\alpha\}_{\alpha=1}^{M}$. The set of M-separable states is consequently all possible convex combinations of states taken from any $\mathcal{S}_{\{Q_\alpha\}_{\alpha=1}^{M}}$ for a given M, which is the convex hull of all $\mathcal{S}_{\{Q_\alpha\}_{\alpha=1}^{M}}$:

$$\mathcal{S}_M := conv \left\{ \bigcup_{\{Q_\alpha\}_{\alpha=1}^{M}} \mathcal{S}_{\{Q_\alpha\}_{\alpha=1}^{M}} \right\}. \tag{2.24}$$

A state $\rho \notin \mathcal{S}_M$ is said to be M-inseparable. The M-separable states form a hierarchy in terms of M,

$$\mathcal{S}_2 \supset \mathcal{S}_3 \supset \ldots \supset \mathcal{S}_N. \tag{2.25}$$

Figure 2.2 illustrates this hierarchy and compares the partition independent and partition dependent approaches to characterising the multiqubit entanglement for the particular case of $N = 3$.

The concept of M-inseparability can be viewed in the following way. In general, the N qubit system can have entanglement between various numbers of qubits. Consider the largest block of entangled qubits. If the system is M-inseparable then we can think of this block as having size at least $N - M + 2$.

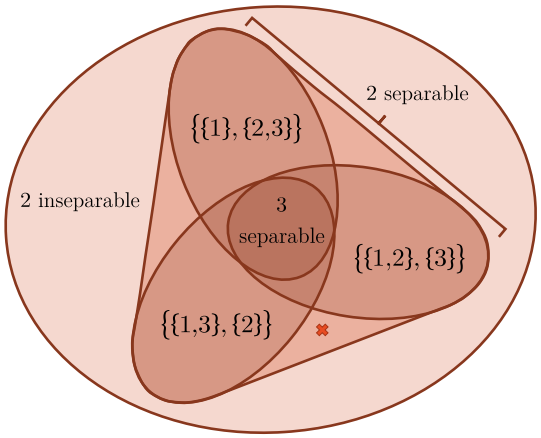

Figure 2.2: States of the 3 qubit quantum system can be characterised in terms of their multiqubit entanglement. The 2-separable states are the convex hull of the separable states with respect to the 2-partitions $\{\{1\},\{2,3\}\}$, $\{\{1,2\},\{3\}\}$, and $\{\{1,3\},\{2\}\}$. The 3-separable states are separable with respect to the only 3-partition $\{\{1\},\{2\},\{3\}\}$, which is contained within each of the 2-partitions such that the 3-separable states are the intersection of the separable states with respect to all the 2-partitions. Note that a state may be 2-separable yet inseparable individually with respect to each of the 2-partitions (shown for example by the cross).

Indeed, an M-inseparable system can always be described with a non-zero probability by a pure state that is inseparable with respect to every possible M-partition $\{Q_\alpha\}_{\alpha=1}^{M}$. Out of all these M-partitions, the largest possible subsystem is of size $N-M+1$, which is achieved by treating $M-1$ of the qubits individually and the remaining $N-(M-1)$ qubits in a block together. Hence, there is always a non-zero probability that an M-inseparable system has entanglement shared between at least $N-M+2$ qubits. We note here an alternative nomenclature also in use [64, 65]: the k-producible states are the states with entanglement shared between a block of at most k qubits, with $k \in \{1,2,\ldots,N\}$. It is then clear that the k producible states are given by $\mathcal{S}_{N-k+1}$ for $k \in \{1,2,\ldots,N-1\}$ and $\mathcal{D}(\mathcal{H})$ for $k=N$.

Some more terminology is now in order. When $M=N$ the only partition is the one given by partitioning each qubit individually. Hence, the partition

dependent and independent approaches coincide. If the N qubit system is N-separable, or fully separable, then it has no entanglement. Instead, if the system is N-inseparable then there is some global multiqubit entanglement [61, 66] and the largest entangled block is of at least 2 qubits in size. When $M = 2$ then the system can be 2-separable (also called biseparable) or 2-inseparable. If the system is 2-inseparable then it is said to have genuine multiqubit entanglement [67–69] since all of the N qubits are entangled together. Any entanglement for an intermediate $2 < M < N$ is called partial multiqubit entanglement [70].

Chapter 3

Quantifying *the Quantum*

So far we have discussed the similarities and differences between the description of classical and quantum systems and highlighted some of the unique properties of a quantum system by identifying three key types of *the quantum*: quantum coherence, quantum correlations, and quantum entanglement. The purpose of this chapter is to go beyond just the identification of *the quantum* by showing how it can be quantified. Quantification of *the quantum* is relevant both from a fundamental and a technological perspective. Fundamentally, it is natural to want to quantify the departure of a quantum system from a classical description. On the other hand, if *the quantum* is to be comprehensively utilised as a resource in quantum technologies [71], then it will be desirable to benchmark the performance of different quantum systems by quantifying the amount of useful resource.

This chapter begins by outlining the concept of a resource theory, which provides a rigorous framework for the quantification of a quantum resource. We give some general requirements that a measure of a quantum resource should satisfy and then describe two geometric approaches to quantifying *the quantum*. The first approach gives the *robustness* measures by considering the minimum amount of classical mixing required for a quantum system to lose all of its resource [16, 17, TRB1, TRB2, TRB3], while the second approach gives the *distance-based* measures by quantifying the distinguishability between resource and resource-free states [18, 19].

3.1 Quantum Resources

A resource theory provides the formal framework required to impose a hierarchy on the set of states of a physical system in terms of a given resource. The framework of a resource theory is specified by three concepts [14, 15]: (i) the resource under consideration; (ii) the free states $\mathcal{F}$, which are all the states of the system without any resource; and (iii) the free operations $\mathcal{O}$, which are the operations that can be carried out by a restricted agent on the physical system without consuming any resource [72]. These concepts are interlinked, since a free operation must not be able to create a resource state from a free state. This means that the free operations must be a subset of the set of operations that cannot create the resource. The set of free operations is said to be maximal if it is equal to this set.

While the free operations cannot transform from a free state to a resource state, they can allow some transformations between resource states. This can be used to impose a hierarchy on the resource states, whereby a resource state ρ is said to be more resourceful than another resource state σ if there is a free operation that can convert ρ to σ. Since it is not generally possible to convert between arbitrary resource states using the free operations, the hierarchy can assume a complicated multi-branch structure. At the top of each branch is a maximally resourceful state from which every state within the branch can be created by using only free operations [73].

Rather than considering a qualitative hierarchy of the resource states, one may instead resort to a measure that quantifies the amount of resource present in a resource state. This condenses the complicated hierarchy into a total ordering of resource states which preserves the hierarchy within a given branch but also places an ordering on states that are not linked through a free operation (e.g. those in different branches). Since there is not a unique way to create such an ordering from a non-trivial hierarchy, there is not a corresponding unique quantitative measure of a resource. Instead, any function satisfying a number of rigorous requirements, arising from the resource theory, represents a resource

measure. Such functions may be chosen based on geometric considerations, as will be shown in Section 3.2, as well as information theoretic considerations. The physical significance of a resource measure is conferred by its quantitative representation of the figure of merit in the performance of an operational task that consumes the resource. However, the operational significance of a resource measure is not always immediate. This is considered further in Chapter 5.

3.1.1 Requirements of a Measure of *the Quantum*

We now discuss some requirements, arising from the resource theoretic framework, that are imposed on measures of a quantum resource. A real and non-negative function $R(\rho)$ of a density operator ρ must satisfy the following requirements for it to be a measure of the quantum resources present in a quantum system described by the state ρ. Firstly, $R(\rho)$ must vanish when ρ is a free state,

Requirement (i): $R(\rho) = 0$ if $\rho \in \mathcal{F}$.

It can further be imposed that $R(\rho) = 0$ only for $\rho \in \mathcal{F}$, a property known as *faithfulness*, which will be the case for all measures of *the quantum* discussed in the rest of this thesis. The second requirement is that $R(\rho)$ cannot increase under the action of the free operations,

Requirement (ii): $R(\Lambda(\rho)) \leq R(\rho)$ for all $\Lambda \in \mathcal{O}$ and any state ρ.

This requirement is called monotonicity and can be understood as a conservation law, since it imposes that it is not possible to generate resource by using operations that cost no resource to implement.

Together these two requirements represent the minimum constraints on a resource measure. However, supplemental requirements can also be imposed that depend upon the structure of the underlying resource theory. We now introduce two supplemental requirements. If the set of free states is convex, then classical mixing of free states cannot create a resource state. It can then be imposed that classical mixing of generally resource states cannot increase resources, which is expressed mathematically as a convexity requirement:

Requirement (iii): $R(p\rho_1+(1-p)\rho_2) \leq pR(\rho_1)+(1-p)R(\rho_2)$ for any probability $p \in [0,1]$ and any two states ρ_1 and ρ_2.

The second supplemental requirement is given in the following way. Whenever the set of free operations is such that any free operation Λ admits an operator sum representation with Kraus operators $\{K_i\}_i$ where $\sum_i K_i^\dagger K_i = \mathbb{I}$, such that for any i

$$\frac{K_i \rho K_i^\dagger}{\mathrm{Tr}\left(K_i \rho K_i^\dagger\right)} \in \mathcal{F} \qquad \forall \ \ \rho \in \mathcal{F}, \tag{3.1}$$

then we can associate any free operation with a certain free quantum instrument. This free quantum instrument is composed of the probabilistic quantum operations $\{\Lambda_i\}_i$ where $\Lambda_i(\rho) = K_i \rho K_i^\dagger$ occurs with probability $\mathrm{Tr}(K_i \rho K_i^\dagger)$ when the system is in state ρ (see Section 1.2.3 for further details). In this setup, the quantum instrument cannot create a resource state from a free state even when one knows which of the operations Λ_i was applied by the quantum instrument. It can then be imposed that the quantum instrument should not be able to increase the resources in the quantum system when averaged over the resultant states of the system. Hence, we have the following requirement for a resource measure,

Requirement (iv):

$$\sum_i \mathrm{Tr}(K_i \rho K_i^\dagger) R\left(\frac{K_i \rho K_i^\dagger}{\mathrm{Tr}\left(K_i \rho K_i^\dagger\right)}\right) \leq R(\rho) \tag{3.2}$$

for any state ρ and any set of operators $\{K_i\}_i$ obeying (3.1) with $\sum_i K_i^\dagger K_i = \mathbb{I}$ and $\Lambda(\rho) = \sum_i K_i \rho K_i^\dagger$ corresponding to a free operation $\Lambda \in \mathcal{O}$ on ρ.

This requirement is called strong monotonicity. Indeed, any measure of a resource satisfying Requirement (iii) and Requirement (iv) will necessarily satisfy Requirement (ii), i.e. monotonicity. This follows since for any ρ

$$R(\Lambda(\rho)) \leq \sum_i \mathrm{Tr}(K_i \rho K_i^\dagger) R\left(\frac{K_i \rho K_i^\dagger}{\mathrm{Tr}\left(K_i \rho K_i^\dagger\right)}\right) \leq R(\rho), \tag{3.3}$$

where the first inequality is due to the convexity since $\Lambda(\rho)$ is a convex combination of states $\frac{K_i \rho K_i^\dagger}{\mathrm{Tr}(K_i \rho K_i^\dagger)}$ according to the probability distribution $\{\mathrm{Tr}(K_i \rho K_i^\dagger)\}_i$, while the second inequality is due to strong monotonicity.

3.1.2 Resource Theories of *the Quantum*

The framework of resource theories has been used extensively to characterise various resources in a quantum system [13–15, 74–83]. In particular, quantum coherence, quantum correlations and quantum entanglement have been analysed using the resource theoretic framework. We now provide details of the treatment of these types of *the quantum* as a resource, including any additional requirements that are typically imposed on measures of a particular resource. The notation $C(\rho)$, $Q(\rho)$, and $E(\rho)$ is here used to refer to resource measures $R(\rho)$ specified to the resources of quantum coherence, quantum correlations, and quantum entanglement, respectively.

Quantum Coherence

The resource theoretic treatment of quantum coherence was initiated in Ref. [47] with identification of the free states as the set $\mathcal{I}$ whose elements are given by Eq. (2.2) with respect to the reference ONB $\{|e_i\rangle\}_{i=1}^{d}$ [1]. However, the free operations of coherence have been the subject of much discussion, with a number of possible options suggested [47, 48, 84–89]. The maximal set of *incoherence preserving operations* have been given as the free operations in Ref. [48], i.e. all the Λ for which $\Lambda(\delta) \in \mathcal{I}$ for any $\delta \in \mathcal{I}$. Reference [47] proposed instead that the free operations are all the incoherence preserving operations admitting an operator sum representation with incoherent Kraus operators satisfying (3.1). These are called the *incoherent operations*. Another suggested set of free operations is given by the strictly incoherent operations [84, 85], which are motivated as the incoherent operations whose incoherent Kraus operators $\{K_i\}_i$ lead to measurement probabilities in the reference ONB that do not depend on the coherence of any initial state ρ, i.e. for all i and j

$$\langle e_j|K_i\rho K_i^\dagger|e_j\rangle = \langle e_j|K_i\Delta(\rho)K_i^\dagger|e_j\rangle\,, \tag{3.4}$$

where we use the complete dephasing operation

$$\Delta(\rho) := \sum_{i=1}^{d} |e_i\rangle\langle e_i|\rho|e_i\rangle\langle e_i|\,, \tag{3.5}$$

which destroys all of the coherence of ρ. Interestingly, the action of a strictly incoherent operation Λ on any incoherent state $\delta = \sum_{i=1}^{d} \delta_i |e_i\rangle \langle e_i|$ is to transform to another incoherent state $\Lambda(\delta) = \sum_{i=1}^{d} \delta_i' |e_i\rangle \langle e_i|$ such that the vectors $\boldsymbol{\delta} = \{\delta_i\}_{i=1}^{d}$ and $\boldsymbol{\delta'} = \{\delta_i'\}_{i=1}^{d}$ are related through a stochastic map S, i.e. $\boldsymbol{\delta'} = S\boldsymbol{\delta}$, and hence representing the stochastic evolution of a classical system in initial state $\boldsymbol{\delta}$ with respect to the reference ONB [84]. Furthermore, a number of additional requirements may be imposed on a measure of coherence, which are outlined in Ref. [1].

On the other hand, it can be informative to quantify the amount of coherence present in a quantum system that is distributed between at least k configurations of the ONB by using the concept of the coherence number discussed in Section 2.1.1. This resource is called k coherence. Here, the free states are the convex set $\mathfrak{I}^{(k)}$ of states with coherence number less than k, while the free operations have been suggested as the strictly incoherent operations [1, 49].

Quantum coherence can also be viewed within the context of asymmetry [1, 79, 86, 90–95], as has been discussed in [TRB2, 86, 88]. A quantum system is symmetric with respect to a symmetry group G if the state of the system ρ is left unchanged by all elements of the group, i.e.

$$\rho = U_g \rho U_g^\dagger, \tag{3.6}$$

for all $g \in \mathsf{G}$, where U_g is the corresponding unitary representation of g [TRB2, 93, 94] (an operator is unitary if it obeys $U^\dagger U = U U^\dagger = \mathbb{I}$). Instead, a quantum system is asymmetric with respect to G if there exists at least one $g \in \mathsf{G}$ such that Eq. (3.6) does not hold. If one considers the symmetry group given by the d-dimensional representation of $\mathsf{U}(1)$, with elements

$$U(\theta) := \sum_{j=1}^{d} e^{i\theta(j-1)} |e_j\rangle \langle e_j| \tag{3.7}$$

for all $\theta \in [0, 2\pi]$, then the set of symmetric states coincides exactly with the set of incoherent states with respect to the ONB $\{|e_j\rangle\}_{j=1}^{d}$. Hence, the presence of coherence in a quantum system is a type of asymmetry [TRB2, 86, 94]. The

free operations Λ of asymmetry specialised to coherence are a subset of the incoherent operations that commute with any unitary generated by the Hamiltonian $H = \sum_{j=1}^{d}(j-1)\left|e_j\right\rangle\left\langle e_j\right|$, i.e. for any real t and any ρ, the free operations Λ satisfy [TRB1, 86, 94]

$$e^{-iHt}\Lambda(\rho)e^{iHt} = \Lambda(e^{-iHt}\rho e^{iHt}). \tag{3.8}$$

Quantum Entanglement

In a break from the standard order of this thesis, we first explain the well-established resource theory of quantum entanglement [2, 18, 19, 96] and then use this framework to inform us on the resource theory of quantum correlations. Focussing first on entanglement in N qubit systems, the resource theoretic framework may be applied both to the partition dependent and partition independent approaches. In the partition dependent setting, the free states are the set $\mathcal{S}_{\{Q_\alpha\}_{\alpha=1}^{M}}$ given in Eq. (2.21) of separable states with respect to the M-partition $\{Q_\alpha\}_{\alpha=1}^{M}$. The free operations are the physically motivated set of so-called *local operations and classical communication* (LOCC) with respect to the M-partition [TRB4, 97]. This consists of all the possible local operations that each of the subsystems α can perform on their qubits Q_α, combined with classical communication between the subsystems. The set of LOCC is a strict subset of the *separability preserving operations* [98], which are the maximal set of operations that cannot create entanglement. Instead, the *separable operations* are an intermediate subset of the separability preserving operations that additionally satisfy (3.1), i.e. for which there exists an operator sum representation with a set of Kraus operators $\{K_i\}_i$ that can be written as a tensor product of operators acting on the M subsystems so that for all i

$$K_i = K_i^{(1)} \otimes K_i^{(2)} \otimes \ldots \otimes K_i^{(M)}. \tag{3.9}$$

The separable operations have been considered in Refs. [18, 19, 99]. Every LOCC operation is separable, but not every separable operation corresponds to LOCC [100]. Furthermore, the representation of LOCC is much more complicated than the representation of separable operations [101], and hence separable

operations are often utilised when studying entanglement measures [2]. For example, a measure of entanglement $E_{\{Q_\alpha\}_{\alpha=1}^M}(\rho)$ of an N qubit system with respect to the partition $\{Q_\alpha\}_{\alpha=1}^M$ that is monotonically non-increasing under separable operations, i.e. $E_{\{Q_\alpha\}_{\alpha=1}^M}(\Lambda(\rho)) \leq E_{\{Q_\alpha\}_{\alpha=1}^M}(\rho)$ for any separable operation Λ and state ρ, must be monotonically non-increasing under the contained set of LOCC, which means that $E_{\{Q_\alpha\}_{\alpha=1}^M}(\rho)$ satisfies Requirement (ii). On the other hand, Requirement (iv) can be considered for any subset of the separable operations (such as LOCC), since the separable operations are of the necessary form in (3.1). A function satisfying Requirement (i) and Requirement (iv) has historically been referred to as an entanglement monotone [2, 19, 20, 96, 102–104]. We note that, while Requirement (iii) is imposed in this thesis for entanglement, this is not always the case and one can find an example of a well established entanglement monotone that is not convex, see Ref. [103]. A discussion of additional requirements that may be imposed on $E_{\{Q_\alpha\}_{\alpha=1}^M}(\rho)$ can be found in Ref. [20].

In the partition independent approach to characterising the multiqubit entanglement of an N qubit system, the resource is identified as the amount of entanglement shared between at least $N-M+2$ qubits and is called the M-inseparable multiqubit entanglement. The resource theory is constructed by identifying the free states as the set of M-separable states $\mathcal{S}_M$ given in Eq. (2.24). The set of free operations is identified with local operations on each of the N qubits and classical communication between them, i.e. LOCC with respect to the partition of the qubits into individual subsystems [TRB4]. This prevents any pair of qubits being able to create entanglement between themselves and thus potentially increasing the number of qubits sharing entanglement. We then use $E_M(\rho)$ to denote a measure of the M-inseparable multiqubit entanglement of an N qubit system in state ρ. As discussed in Section 2.3.1, $E_N(\rho)$ measures the global multiqubit entanglement and $E_2(\rho)$ measures the genuine multiqubit entanglement, while $E_M(\rho)$ for intermediate M can be said to measure partial multiqubit entanglement.

We have so far specialised to the resource of entanglement in N qubit systems, but one can similarly consider the entanglement of arbitrary dimensional bipartite systems in state ρ^{AB}, consisting of two subsystems A and B. For this resource,

we associate the free states with the bipartite separable states given in Eq. (2.18) and the free operations with bipartite LOCC. Then, for a measure of bipartite entanglement $E(\rho^{AB})$ we can establish the analogous Requirements (i), (ii), (iii) and (iv).

Quantum Correlations

There are three relevant types of resource to characterise in a bipartite quantum system composed of subsystems A and B: the quantum correlations from subsystem A, the quantum correlations from subsystem B, and the quantum correlations from either subsystem. These resources together constitute the quantum correlations of the quantum system, which may be quantified by the resource measures $Q_A(\rho^{AB})$, $Q_B(\rho^{AB})$, and $Q_{AB}(\rho^{AB})$ when the system is in the state ρ^{AB}, with the subscript indicating which subsystem the quantum correlations are measured with respect to. The resource theory of quantum correlations is not fully established [TRB13]. While the free states are identified as the sets $\mathcal{C}_{CQ}^{AB}$, $\mathcal{C}_{QC}^{AB}$, and $\mathcal{C}_{CC}^{AB}$ of CQ, QC, and CC states discussed in Section 2.2, the free operations, which are normally found based upon physical arguments, have not yet been identified.

Instead, what is known is the set of local operations Λ^A acting on subsystem A and Λ^B acting on subsystem B that are unable to create quantum correlations from a classically correlated state. Consider a classically correlated CQ state $\chi_{CQ}^{AB} \in \mathcal{C}_{CQ}^{AB}$. By referring to Eq. (2.7), it is clear that any possible local operation Λ^B on subsystem B is unable to transform χ_{CQ}^{AB} outside of $\mathcal{C}_{CQ}^{AB}$ since Λ^B can only change the arbitrary states $\{\rho_i^B\}_i$ of subsystem B. However, there are local operations acting on subsystem A that are able to create quantum correlations from χ_{CQ}^{AB} [105, 106], i.e. so that $\Lambda^A \otimes \mathbb{I}^B(\chi_{CQ}^{AB}) \notin \mathcal{C}_{CQ}^{AB}$, where $\mathbb{I}^B$ is the quantum operation that leaves all states of subsystem B invariant. The set of all local operations on subsystem A so that $\Lambda^A \otimes \mathbb{I}^B(\chi_{CQ}^{AB}) \in \mathcal{C}_{CQ}^{AB}$ has been identified as the *local commutativity preserving operations* (LCPO) [107]. A quantum operation Λ_{CPO} is a commutativity preserving operation (CPO) if

$$[\Lambda_{CPO}(\rho), \Lambda_{CPO}(\sigma)] = 0 \quad \forall \quad \rho \text{ and } \sigma \text{ such that } [\rho, \sigma] = 0. \tag{3.10}$$

It has then been shown that [107]

$$\Lambda^A \otimes \mathbb{I}^B(\chi^{AB}_{CQ}) \in \mathcal{C}^{AB}_{CQ} \ \ \forall \ \ \chi^{AB}_{CQ} \in \mathcal{C}^{AB}_{CQ} \quad \Leftrightarrow \quad \Lambda^A \text{ is an LCPO.}$$

The situation is analogous for any classically correlated QC state $\chi^{AB}_{QC} \in \mathcal{C}^{AB}_{QC}$, i.e. for any local operation Λ^A on subsystem A it holds that $\Lambda^A \otimes \mathbb{I}^B(\chi^{AB}_{QC}) \in \mathcal{C}^{AB}_{QC}$, and for subsystem B

$$\mathbb{I}^A \otimes \Lambda^B(\chi^{AB}_{QC}) \in \mathcal{C}^{AB}_{QC} \ \ \forall \ \ \chi^{AB}_{QC} \in \mathcal{C}^{AB}_{QC} \quad \Leftrightarrow \quad \Lambda^B \text{ is an LCPO.}$$

For a classically correlated CC state $\chi^{AB}_{CC} \in \mathcal{C}^{AB}_{CC}$, both local operations must be commutativity preserving for quantum correlations not to be generated, i.e.

$$\Lambda^B \otimes \Lambda^B(\chi^{AB}_{CC}) \in \mathcal{C}^{AB}_{CC} \ \ \forall \ \ \chi^{AB}_{CC} \in \mathcal{C}^{AB}_{CC} \quad \Leftrightarrow \quad \Lambda^A \text{ and } \Lambda^B \text{ are LCPOs.}$$

The CPOs have been characterised in Refs. [106–108]. When acting on a qubit, the CPOs are of two types, completely decohering and unital [106]. The completely decohering operations map any state ρ of a d-dimensional quantum system to a state diagonal in a fixed ONB $\{|e_i\rangle\}_{i=1}^d$, $\Lambda(\rho) = \sum_{i=1}^d p_i(\rho) |e_i\rangle \langle e_i|$ with $\{p_i(\rho)\}_{i=1}^d$ a probability distribution dependent upon ρ. Unital operations have been discussed in Section 1.2.2 and map the identity onto itself, $\Lambda(\mathbb{I}) = \mathbb{I}$. Instead, the commutativity preserving operations acting on a d-dimensional quantum system with $d > 2$ are either completely decohering or isotropic [107, 108]. An isotropic operation acting on the state ρ is written as

$$\Lambda(\rho) = t\Phi(\rho) + (1-t)\frac{\mathbb{I}}{d}, \tag{3.11}$$

where $\Phi(\rho)$ is either a unitary operation, $\Phi(\rho) = U\rho U^\dagger$ for any unitary U, or an antiunitary operation, $\Phi(\rho) = U\rho^\intercal U^\dagger$ with $\rho^\intercal$ the transpose of ρ with respect to the standard basis. For an isotropic operation to be completely positive, t must be in the region $[\frac{-1}{d^2-1}, 1]$ when Φ is unitary, while t must be in the region $[\frac{-1}{d-1}, \frac{1}{d+1}]$ when Φ is antiunitary [TRB7, 107]. An operator sum representation of the isotropic operations was found in [TRB7] and is provided in Appendix A.

Although the set of local operations unable to create the resource of quantum correlations has been identified, it is not clear whether there exist non-local operations that are unable to create quantum correlations. However, it seems reasonable to expect that the so far unidentified free operations of quantum correlations

are local since quantum correlations are defined with respect to local subsystems. The convention adopted so far has thus been that the free operations are a subset of all the local operations that are commutativity preserving on the subsystems under consideration [TRB12]. While there is no consensus on the form of the free operations, there have been some attempts at identifying a physically motivated subset of LCPO by considering the free operations of coherence and the link between quantum correlations and local quantum coherence discussed in Section 2.2.1 [84].

Nevertheless, one may impose the requirement that a measure of quantum correlations should be non-increasing under LCPO on the subsystem under consideration and general local operations on any other subsystem [TRB10, TRB12, 109],

Requirement Q(ii): For any state ρ^{AB}

$$\begin{aligned} Q_A(\Lambda^A_{CPO} \otimes \Lambda^B(\rho^{AB})) &\leq Q_A(\rho^{AB}), \\ Q_B(\Lambda^A \otimes \Lambda^B_{CPO}(\rho^{AB})) &\leq Q_B(\rho^{AB}), \\ Q_{AB}(\Lambda^A_{CPO} \otimes \Lambda^B_{CPO}(\rho^{AB})) &\leq Q_{AB}(\rho^{AB}), \end{aligned} \tag{3.12}$$

where Λ^A_{CPO} and Λ^B_{CPO} are any LCPO on subsystems A and B, while Λ^A and Λ^B are arbitrary quantum operations on subsystems A and B.

If the free operations of quantum correlations are eventually identified to coincide exactly with the set of local quantum operations unable to create quantum correlations, then Requirement Q(ii) becomes equivalent to Requirement (ii). Instead, if the free operations are identified as a strict subset of the local operations unable to create quantum correlations, then Requirement Q(ii) is too strong in the sense that it implies Requirement (ii) but there may be proper measures of quantum correlations satisfying Requirement (ii) but not Requirement Q(ii) [TRB7].

When investigating Requirement Q(ii) it can be useful to consider the two types of LCPO: either completely decohering, or unital/isotropic (depending on the dimension of the subsystem). It can be shown that local completely decohering operations always destroy quantum correlations [108], i.e. when Λ^A_{CPO} and

Λ^B_{CPO} are local completely decohering operations

$$\begin{aligned} \Lambda^A_{CPO} \otimes \mathbb{I}^B(\rho^{AB}) &\in \mathcal{C}^{AB}_{CQ}, \\ \mathbb{I}^A \otimes \Lambda^B_{CPO}(\rho^{AB}) &\in \mathcal{C}^{AB}_{QC}, \\ \Lambda^A_{CPO} \otimes \Lambda^B_{CPO}(\rho^{AB}) &\in \mathcal{C}^{AB}_{CC}, \end{aligned} \tag{3.13}$$

for any ρ^{AB}. This means that any non-negative function satisfying Requirement (i) is monotonically non-increasing under the action of local completely decohering operations, since the left-hand side of Eq. (3.12) is always zero. Hence, it is sufficient to consider only LCPO that are unital (for a 2-dimensional subsystem) or isotropic (for a subsystem with dimension larger than 2) when checking Requirement Q(ii).

Since the sets $\mathcal{C}^{AB}_{CQ}$, $\mathcal{C}^{AB}_{QC}$, and $\mathcal{C}^{AB}_{CC}$ are not convex [TRB12], measures of quantum correlations should not satisfy Requirement (iii). Indeed, convex combination of classically correlated states generally creates quantum correlations: while the resultant state is always separable, it typically cannot be expressed in terms of a local ONB on the relevant subsystems. In this case, any measure of quantum correlations will generally violate Requirement (iii). This means that we expect the convex combination of quantumly correlated states to potentially increase quantum correlations. Furthermore, given the lack of clarity on the set of free operations, Requirement (iv) has not been considered for measures of quantum correlations. However, it has been suggested that any measure of quantum correlations in a bipartite quantum system should coincide with a measure of bipartite entanglement $E(\rho^{AB})$ when the state of the system ρ^{AB} is pure [33, TRB10, 56, 110–114]. As has been discussed in Section 2.3, the concepts of entanglement and quantum correlations coincide for pure states of a bipartite system, and hence it might be expected that their measures coincide on pure states [TRB12]. This expectation is perhaps historically motivated, since the study of quantum entanglement has been established for much longer than the study of more general quantum correlations, and it is seen here as a desirable feature of a measure of quantum correlations and not a requirement. A summary of the potential requirements for a measure of quantum correlations, including

some not given here, can be found in Refs. [11, TRB12, 56, 110, 115].

3.2 Geometric Quantification of *the Quantum*

We now explain two geometric approaches to the quantification of a quantum resource and show that these approaches lead to measures that satisfy the given requirements. Details are also provided on the application of these approaches to types of *the quantum* considered as resources in this thesis. The contents of this section is based upon Refs. [TRB1, TRB2, TRB3].

3.2.1 Robustness

Consider the convex mixture of a resource state $\rho \notin \mathcal{F}$ with a free state $\tau \in \mathcal{F}$, which results in another state

$$\sigma = (1-p)\rho + p\tau \tag{3.14}$$

for some probability $p \in [0,1]$. One may consider the range of p for which $\sigma \in \mathcal{F}$, i.e. so that the resultant mixture has no resources. It is always possible to ensure that $\sigma \in \mathcal{F}$ by picking $p = 1$, but we want to consider the lower end of the range. Intuitively, the smallest value of p for which $\sigma \in \mathcal{F}$ provides gauge of the resources present in ρ. Indeed, if the value of p is small, we only need to mix ρ a little bit with a free state τ for us to lose all resources. Building on this intuition, one may consider mixing ρ with *any* free state and finding the smallest p for which $\sigma \in \mathcal{F}$, arriving at the quantity $\inf_{\tau\in\mathcal{F}} \{p \geq 0 | (1-p)\rho + p\tau = \sigma \in \mathcal{F}\}$ as an estimate of the resources present in ρ. If the mixing parameter p is substituted for $p = \frac{s}{1+s}$ so that the mixture is given by

$$\sigma = \frac{\rho + s\tau}{1+s} \tag{3.15}$$

with $s \in [0, \infty]$, we arrive at a similar quantity

$$R^{SR}(\rho) := \inf_{\tau\in\mathcal{F}} \left\{ s \geq 0 \,\middle|\, \frac{\rho + s\tau}{1+s} = \sigma \in \mathcal{F} \right\}. \tag{3.16}$$

This quantity is called the standard robustness of a resource, and measures the resources of ρ by quantifying the minimum amount of mixing needed with a free state to lose all resources, i.e. its *robustness*. Clearly its range of possible values is inherited from the range of s, and it can be seen that $R^{SR}(\rho) = 0$ if and only if $\rho \in \mathcal{F}$. As shall be seen in the following, the justification for changing from the mixing parameter p to s is mathematical simplicity.

The standard robustness has been introduced as a resource measure of entanglement [16] and was shown to obey the four given requirements. However, the standard robustness is not an informative measure of a resource when one considers resources with a set of free states that is zero measure within the set of all states, as is the case for quantum coherence [1, TRB1] and quantum correlations [116]. Indeed, in this case the standard robustness is typically infinite, $R^{SR}(\rho) = \infty$ for $\rho \notin \mathcal{F}$. For example, consider the coherence of a qubit system with respect to the computational basis $\{|0\rangle, |1\rangle\}$. The set of free states $\mathcal{I}$ are the states with density matrix diagonal with respect to the standard basis, which can be written using the Bloch ball representation (see Section 1.2.4) as

$$\delta = \frac{1}{2}\left(\mathbb{I} + d\sigma_3\right) = \frac{1}{2}\begin{pmatrix} 1+d & 0 \\ 0 & 1-d \end{pmatrix} \tag{3.17}$$

for all $d \in [-1, 1]$. Consider a coherent state ρ written as

$$\rho = \frac{1}{2}\left(\mathbb{I} + \sum_{i=1}^{3} n_i \sigma_i\right) = \frac{1}{2}\begin{pmatrix} 1+n_3 & n_1 - in_2 \\ n_1 + in_2 & 1-n_3 \end{pmatrix}, \tag{3.18}$$

where $n_1^2 + n_2^2 + n_3^2 \leq 1$ with $n_1 \neq 0$ and/or $n_2 \neq 0$ so that $\rho \notin \mathcal{I}$. If we want to quantify the quantum coherence using the standard robustness, we must consider the convex combination of ρ and δ,

$$\sigma = \frac{\rho + s\delta}{1+s} = \frac{1}{2(1+s)}\begin{pmatrix} 1+n_3+s(1+d) & n_1 - in_2 \\ n_1 + in_2 & 1-n_3+s(1-d) \end{pmatrix}. \tag{3.19}$$

It is clear that $\sigma \in \mathcal{I}$ only when $s \to \infty$, otherwise σ is not diagonal. Hence, the standard robustness in Eq. (3.16), with the free states identified as the incoherent states $\mathcal{I}$ so as to measure the resource of coherence, is necessarily infinite for any $\rho \notin \mathcal{I}$.

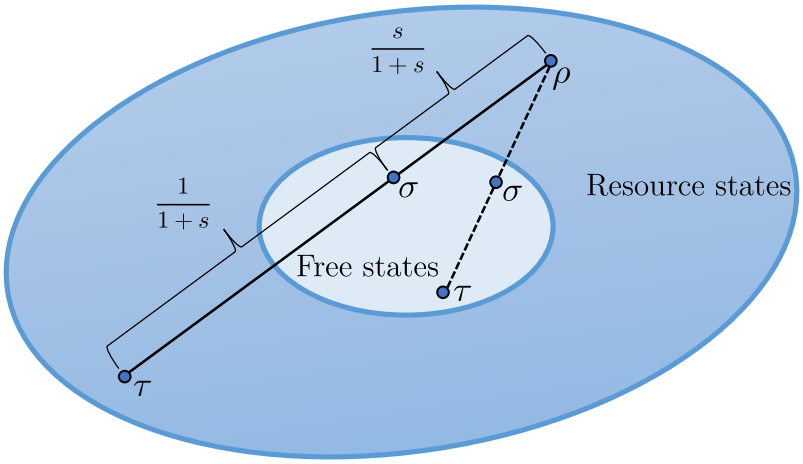

Figure 3.1: Convex combination according to Eq. (3.15) of ρ with any state $\tau \in \mathcal{D}(\mathcal{H})$ (solid line) and with any free state $\tau \in \mathcal{F}$ (dashed line) results in another state σ. The smallest s such that $\sigma \in \mathcal{F}$ is the generalised robustness (solid line) or the standard robustness (dashed line). It is clear that the standard robustness presents an upper bound to the generalised robustness.

The generalised robustness of a resource quantifies the minimum amount of mixing needed with any other state (not necessarily free) to lose all resources. It is an another measure of the resources in the state ρ and is defined as

$$R^R(\rho) := \inf_{\tau \in \mathcal{D}(\mathcal{H})} \left\{ s \geq 0 \,\middle|\, \frac{\rho + s\tau}{1+s} = \sigma \in \mathcal{F} \right\}. \tag{3.20}$$

Figure 3.1 provides a pictorial comparison of the standard and generalised robustness. The generalised robustness is never greater than the standard robustness and does not suffer the same problem discussed above. Hence, we focus herein on the generalised robustness and now omit the "generalised" from its name.

The robustness of a resource satisfies Requirements (i) - (iv) for a resource measure. Before showing that this is the case, we first need to discuss some terminology and an alternative formulation of robustness. The convex mixture in Eq. (3.15) may be rearranged in terms of ρ

$$\rho = (1+s)\sigma - s\tau, \tag{3.21}$$

which is called a pseudomixture of σ and τ. Clearly not every pseudomixture of two states is another state. In evaluating the robustness, we are finding the

smallest possible s so that the pseudomixture between a general state τ and a free state σ is equal to ρ. If $s^\star$ is the minimum such value of s with corresponding states $\tau^\star$ and $\sigma^\star$ then $R^R(\rho) = s^\star$ and

$$\rho = \left(1 + R^R(\rho)\right)\sigma^\star - R^R(\rho)\tau^\star \tag{3.22}$$

is an optimal pseudomixture of ρ. An alternative definition of the robustness may then be given as

$$R^R(\rho) = \inf_{\sigma\in\mathcal{F}} \left\{ s \geq 0 \,|\rho \leq (1+s)\sigma \right\}. \tag{3.23}$$

This may be seen by showing that the right-hand side of this equation $\tilde{s}^\star$ is both an upper and lower bound to $R^R(\rho)$. Indeed, the pseudomixture in Eq. (3.21) implies that $\rho \leq (1+s)\,\sigma$, which means from the equation above that $\tilde{s}^\star \leq s$. This holds for any pseudomixture, including the optimal one in Eq. (3.22), so that $\tilde{s}^\star \leq R^R(\rho)$. On the other hand, if the infimum in Eq. (3.23) is realised by $\rho \leq (1+\tilde{s}^\star)\,\tilde{\sigma}^\star$ for some $\tilde{\sigma}^\star \in \mathcal{F}$, we can always write

$$\tilde{\sigma}^\star = \frac{\rho + \tilde{s}^\star\tau}{1+\tilde{s}^\star} \tag{3.24}$$

for $\tau = \frac{(1+\tilde{s}^\star)\tilde{\sigma}^\star - \rho}{\tilde{s}^\star}$. It can be seen that τ is a state, since it has unit trace and also $\rho \leq (1+\tilde{s}^\star)\,\tilde{\sigma}^\star$ and Eq. (3.24) together imply that $\tau \geq 0$. Hence, we know from Eq. (3.24) and the definition of robustness in Eq. (3.20) that $R^R(\rho) \leq \tilde{s}^\star$. We therefore conclude that $R^R(\rho) = \tilde{s}^\star$.

It is clear that $R^R(\rho)$ is a non-negative function by construction, and that $R^R(\rho) = 0$ for all $\rho \in \mathcal{F}$ since one does not need to mix ρ at all (which corresponds to $s = 0$) with another state to lose all the resource. Hence R^R satisfies Requirement (i). Furthermore, it can be seen that $R^R(\rho) = 0$ only for $\rho \in \mathcal{F}$, since it is always necessary to perform some mixing on a resource state $\rho \notin \mathcal{F}$ to lose the resource. To show that $R^R(\rho)$ satisfies Requirement (ii) and Requirement (iv) we provide the following theorem.

Theorem 1 *Let $\{\Lambda_i\}_i$ be a quantum instrument such that $\Lambda_i(\rho)/\mathrm{Tr}(\Lambda_i(\rho)) \in \mathcal{F}$ for all i and every $\rho \in \mathcal{F}$. Any such quantum instrument acting on any state ρ is not able to increase the robustness of a resource by averaging over the resultant*

states, i.e.

$$\sum_i \mathrm{Tr}\left(\Lambda_i(\rho)\right) R^R\left(\frac{\Lambda_i(\rho)}{\mathrm{Tr}\left(\Lambda_i(\rho)\right)}\right) \leq R^R(\rho) \tag{3.25}$$

for any state ρ [16, 17, TRB2].

Proof. Consider the optimal pseudomixture of ρ in Eq. (3.22) with the optimal states $\tau^\star \in \mathcal{D}(\mathcal{H})$ and $\sigma^\star \in \mathcal{F}$. Applying the probabilistic quantum operation Λ_i to both sides gives

$$\Lambda_i(\rho) = \Big(1 + R^R(\rho)\Big)\, \Lambda_i(\sigma^\star) - R^R(\rho)\Lambda_i(\tau^\star), \tag{3.26}$$

and then performing the trace gives

$$\mathrm{Tr}(\Lambda_i(\rho)) = \Big(1 + R^R(\rho)\Big)\, \mathrm{Tr}(\Lambda_i(\sigma^\star)) - R^R(\rho)\mathrm{Tr}(\Lambda_i(\tau^\star)). \tag{3.27}$$

By using Eq. (3.27), Eq. (3.26) may be rearranged as a pseudomixture

$$\rho_i = (1 + s_i)\, \sigma_i - s_i \tau_i \tag{3.28}$$

with states

$$\rho_i = \frac{\Lambda_i(\rho)}{\mathrm{Tr}(\Lambda_i(\rho))}, \qquad \tau_i = \frac{\Lambda_i(\tau^\star)}{\mathrm{Tr}(\Lambda_i(\tau^\star))}, \qquad \sigma_i = \frac{\Lambda_i(\sigma^\star)}{\mathrm{Tr}(\Lambda_i(\sigma^\star))}, \tag{3.29}$$

and

$$s_i = R^R(\rho)\frac{\mathrm{Tr}(\Lambda_i(\tau^\star))}{\mathrm{Tr}(\Lambda_i(\rho))}. \tag{3.30}$$

Since $\sigma^\star \in \mathcal{F}$ it holds that $\sigma_i \in \mathcal{F}$ and we therefore have a valid pseudomixture of ρ_i in terms of a free state σ_i and any state τ_i. This is not necessarily the optimal pseudomixture of ρ_i needed to satisfy Eq. (3.23), so it holds that

$$R^R(\rho_i) \leq s_i. \tag{3.31}$$

Taking the weighted average over the probabilistic quantum operations with probability $\mathrm{Tr}(\Lambda_i(\rho))$, we have the required inequality

$$\begin{aligned} \sum_i \mathrm{Tr}(\Lambda_i(\rho)) R^R(\rho_i) &\leq \sum_i \mathrm{Tr}(\Lambda_i(\rho)) s_i \\ &= \sum_i \mathrm{Tr}(\Lambda_i(\rho)) R^R(\rho) \frac{\mathrm{Tr}(\Lambda_i(\tau^\star))}{\mathrm{Tr}(\Lambda_i(\rho))} \\ &= R^R(\rho), \end{aligned} \tag{3.32}$$

where in the last equality we use the linearity of the trace and the fact that $\mathrm{Tr}(\sum_i \Lambda_i(\tau^\star)) = 1$ since $\sum_i \Lambda_i(\tau^\star)$ is a trace preserving quantum operation acting on the state $\tau^\star$. □

Consider a quantum instrument composed of a single quantum operation Λ that cannot create resources, i.e. so that $\Lambda(\rho) \in \mathcal{F}$ for any $\rho \in \mathcal{F}$. Theorem 1 implies that $R^R(\Lambda(\rho)) \leq R^R(\rho)$ for any such Λ and any ρ. Since the free operations for any resource must be a subset of the set of operations that cannot create resources, the robustness satisfies Requirement (ii). Furthermore, it is clear that the robustness satisfies Requirement (iv) by setting $\Lambda_i(\rho) = K_i \rho K_i^\dagger$ for any choice of free operations that can be expressed with a set of Kraus operators $\{K_i\}_i$ satisfying (3.1).

We finally show that the robustness of a resource satisfies Requirement (iii), provided that the set of free states is convex.

Theorem 2 *For all resources with a convex set of free states $\mathcal{F}$, the robustness of the resource is a convex function on the set of states, i.e.*

$$R^R(p\rho_1 + (1-p)\rho_2) \leq pR^R(\rho_1) + (1-p)R^R(\rho_2) \tag{3.33}$$

for any probability $p \in [0,1]$ and any two states ρ_1 and ρ_2 [16, 17, TRB2].

Proof. Consider the optimal pseudomixtures corresponding to ρ_1 and ρ_2,

$$\rho_i = \left(1 + R^R(\rho_i)\right)\sigma_i^\star - R^R(\rho_i)\tau_i^\star, \tag{3.34}$$

with $\sigma_i^\star \in \mathcal{F}$ and $\tau_i^\star \in \mathcal{D}(\mathcal{H})$, for $i \in \{1,2\}$. The convex combination $\rho = p\rho_1 + (1-p)\rho_2$ can be rewritten as a pseudomixture $\rho = (1+s)\sigma - s\tau$ with

$$\begin{aligned}
\sigma &= \frac{1}{1+s}\left(p\left(1 + R^R(\rho_1)\right)\sigma_1^\star + (1-p)\left(1 + R^R(\rho_2)\right)\sigma_2^\star\right), \\
\tau &= \frac{1}{s}\left(pR^R(\rho_1)\tau_1^\star + (1-p)R^R(\rho_2)\tau_2^\star\right), \\
s &= pR^R(\rho_1) + (1-p)R^R(\rho_2).
\end{aligned} \tag{3.35}$$

It can be seen that $\sigma \in \mathcal{F}$ because the set of free states is convex and σ can be written as a convex combination of two free states: $\sigma_1^\star \in \mathcal{F}$ with weighting

$p_\sigma = \frac{p(1+R^R(\rho_1))}{1+s}$ and $\sigma_2^\star \in \mathcal{F}$ with weighting $1 - p_\sigma = \frac{(1-p)(1+R^R(\rho_2))}{1+s}$. Note that $p_\sigma \in [0,1]$ as required. Furthermore, we also know that τ is a state because it is a convex combination of two states: $\tau_1^\star$ with weighting $p_\tau = \frac{pR^R(\rho_1)}{s}$ and $\tau_2^\star$ with weighting $1 - p_\tau = \frac{(1-p)R^R(\rho_2)}{s}$, where $p_\tau \in [0,1]$. Since $\rho = (1+s)\sigma - s\tau$ may not be the optimal pseudomixture of ρ to satisfy Eq. (3.23), we know that $R^R(\rho) \leq s$. □

These theorems show that the robustness is a good measure of a resource by satisfying the given requirements. The robustness has been specialised to many types of quantum resource, including entanglement, coherence, asymmetry, steering, and Bell nonlocality [16, 17, TRB1, TRB2, TRB3, 117–122], as well as having been considered generally as a relevant quantity for the asymptotic conversion of resources in a maximal resource theory [15]. The original concept of robustness was given in Refs. [16, 17] by specialising to the resource of entanglement. There they showed that the standard and generalised robustness satisfy the requirements to be a good measure of entanglement. Instead, this thesis provides a very general description of robustness that is applicable to any resource using the resource theoretic framework.

We now discuss the computability of the robustness of a resource, which can be quantitatively linked to the expectation value of a resource witness. A resource witness is a self-adjoint operator W that always has a non-negative expectation value with respect to a free state, i.e.

$$\mathrm{Tr}(W\rho) \geq 0 \qquad \forall \rho \in \mathcal{F}. \tag{3.36}$$

Hence, a negative expectation value of W implies that $\rho \notin \mathcal{F}$. However, the expectation value is not necessarily negative for all resource states, meaning that

$$\begin{aligned} \mathrm{Tr}(W\rho) &< 0 \quad \Rightarrow \quad \rho \notin \mathcal{F}, \\ \mathrm{Tr}(W\rho) &\geq 0 \quad \Leftarrow \quad \rho \in \mathcal{F}, \end{aligned} \tag{3.37}$$

see Fig. 3.2. Resource witnesses are very appealing experimentally since their expectation value is an observable quantity, which when negative gives a sufficient

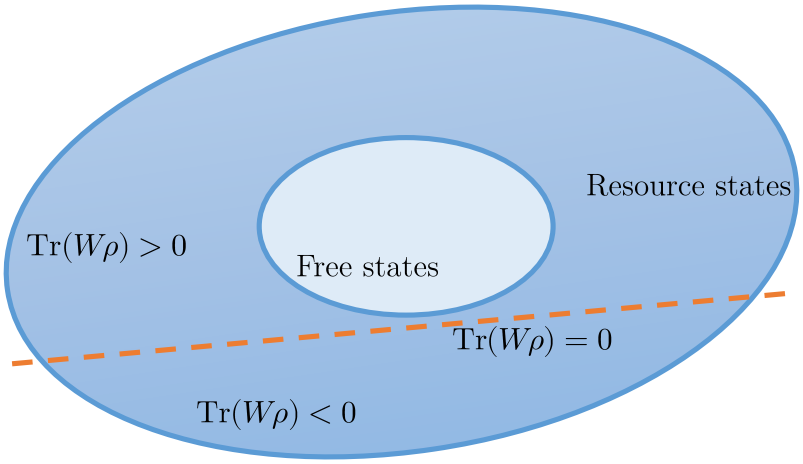

Figure 3.2: A resource witness W is a self-adoint operator whose expectation value is always non-negative with respect to the free states, such that a negative expectation value witnesses a resource state. The witness may be understood pictorially within the set of states as the orange dashed line given by ths states ρ satisfying $\mathrm{Tr}(W\rho) = 0$, which separates a subset of resource states from all the other states.

condition on having a resource state. They have been used extensively for the resource of entanglement [2, 123, 124]. The existence of W is implied by the Hahn–Banach theorem [20, 121, 123, 124], which relies on $\mathcal{F}$ being convex and compact (we assume compactness of $\mathcal{F}$ herein). We can then define the set of resource witnesses as

$$\mathcal{W} := \left\{ W \;:\; W = W^\dagger, \mathrm{Tr}(W\rho) \geq 0 \,\forall\, \rho \in \mathcal{F} \right\}. \tag{3.38}$$

Here we show that the optimisation problem given by computing the robustness of a resource may be written as a simple semidefinite program (SDP) under certain conditions on the framework of the corresponding resource theory. An SDP is a type of convex optimisation problem involving optimisation of a linear function over the positive semidefinite operators subject to a finite set of constraints that can be written as an inequality between self-adjoint operators [125–127]. Casting an optimisation problem as an SDP is particularly useful, since SDPs may be solved efficiently using a variety of algorithms [126]. By rewriting Eq. (3.23), the robustness of a resource can be seen as the solution to the

optimisation of a linear function over the set of free states

$$\begin{aligned} R^R(\rho) \;=\; & \text{minimise} && \mathrm{Tr}(\tilde{\sigma}) - 1 \\ & \text{subject to} && \frac{\tilde{\sigma}}{\mathrm{Tr}(\tilde{\sigma})} \in \mathcal{F}, \\ & && \rho \leq \tilde{\sigma}, \end{aligned} \tag{3.39}$$

where we have set $\tilde{\sigma} = (1+s)\sigma$. Here we show that this optimisation problem corresponds to an SDP when considering a resource theory with a convex set of free states which can be described by a resource destroying quantum operation Φ. A resource destroying operation is a quantum operation that satisfies [81]

$$\begin{aligned} \Phi(\rho) &\in \mathcal{F} \qquad \forall \;\; \rho \in \mathcal{D}(\mathcal{H}) \\ \Phi(\rho) &= \rho \qquad \forall \;\; \rho \in \mathcal{F}, \end{aligned} \tag{3.40}$$

see Fig. 3.3. Such an operation does not always exist for a given resource theory, and necessary and sufficient conditions for its existence have been provided in Ref. [128]. Furthermore, when one does exist, the choice of operation is not unique, i.e. there can be many quantum operations that satisfy (3.40). An example of a resource destroying quantum operation can be found for coherence as the complete dephasing operation Δ given in Eq. (3.5). Resource destroying operations allow the corresponding set of free states to be identified with one simple condition

$$\mathcal{F} := \{\rho \in \mathcal{D}(\mathcal{H}) \;:\; \Phi(\rho) = \rho\}\,. \tag{3.41}$$

Given a resource theory with a convex set of free states and a resource destroying quantum operation Φ, the robustness is given by

$$\begin{aligned} R^R(\rho) \;=\; & \text{minimise} && \mathrm{Tr}(\tilde{\sigma}) - 1 \\ & \text{subject to} && \Phi(\tilde{\sigma}) = \tilde{\sigma}, \\ & && \rho \leq \tilde{\sigma}. \end{aligned} \tag{3.42}$$

In this form, the robustness corresponds to the solution of an SDP. We demonstrate this in Appendix B by showing that (3.42) can be rewritten in a standard

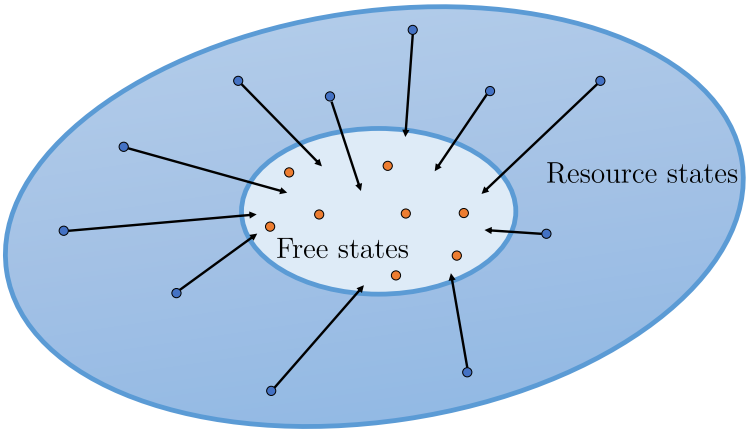

Figure 3.3: A resource destroying quantum operation (black arrows) maps any resource state (blue circles) to a free state while leaving the set of free states (orange circles) invariant. The set of states invariant under a resource destroying operation is hence an alternative characterisation of the set of free states for the corresponding resource.

form for SDPs [TRB2, 117, 125]. Furthermore, provided the resource destroying quantum operation is self-dual, i.e. $\Phi = \Phi^\star$ (see Appendix B) [20, 46], the robustness is also given by the dual problem of the above SDP

$$\begin{aligned} R^R(\rho) \;=\; & \text{maximise} && -\mathrm{Tr}(W\rho) \\ & \text{subject to} && \Phi(W) \geq 0, \\ & && W \leq \mathbb{I}. \end{aligned} \tag{3.43}$$

This is also shown in Appendix B. It can be seen that the dual problem is a constrained optimisation over resource witnesses. Indeed, by using the resource destroying map Φ, the set of resource witnesses is given by

$$\mathcal{W} = \left\{ W \;:\; W = W^\dagger,\, \mathrm{Tr}(W\rho) \geq 0 \,\forall\, \rho \;:\; \Phi(\rho) = \rho \right\}. \tag{3.44}$$

From the self-duality of Φ, it can be shown that

$$\begin{aligned} \mathrm{Tr}(W\rho) \geq 0 \,\forall\, \rho \;:\; \Phi(\rho) = \rho \quad & \Leftrightarrow \quad \mathrm{Tr}(W\Phi(\rho)) \geq 0 \,\forall\, \rho \\ & \Leftrightarrow \quad \mathrm{Tr}(\Phi(W)\rho) \geq 0 \,\forall\, \rho \\ & \Leftrightarrow \quad \Phi(W) \geq 0, \end{aligned} \tag{3.45}$$

so that the set of resource witnesses is equivalently given by

$$\mathcal{W} = \left\{ W \ : \ W = W^\dagger, \, \Phi(W) \geq 0 \right\}, \tag{3.46}$$

which means that the dual problem in Eq. (3.43) is an optimisation over all resource witnesses satisfying $W \leq \mathbb{I}$. This is particularly appealing experimentally, since measuring the expectation value of any $W \in \mathcal{W}$ with $W \leq \mathbb{I}$ can not only witness the presence of a resource but also provide a lower bound to the quantity of resource in terms of robustness.

These results complement previous works on posing the robustness of a resource as an optimisation problem. In particular, it has been shown that the robustness of entanglement is the solution of a convex optimisation problem whose dual is given by an optimisation over all entanglement witnesses satisfying $W \leq \mathbb{I}$ [120, 129]. Such a result could be extended to any resource theory with a convex and compact set of free states. However, this does not necessarily mean that the robustness of a resource is the solution of an SDP. Indeed, it is well known that for entanglement this is not the case [120]. We show that the robustness is the solution to an SDP when the resource satisfies certain constraints, as can be seen by our reformulation of the robustness into Eq. (3.42) and Eq. (3.43), and then in Appendix B into the standard form for an SDP.

Quantum Coherence

Following Refs. [TRB1, TRB2], we now focus on the robustness of coherence, which is given by

$$C^R(\rho) := \inf_{\tau \in \mathcal{D}(\mathcal{H})} \left\{ s \geq 0 \left| \frac{\rho + s\tau}{1+s} = \delta \in \mathcal{I} \right. \right\}, \tag{3.47}$$

where $\mathcal{I}$ is the convex set of incoherent states with respect to the reference ONB $\{|e_i\rangle\}_{i=1}^d$ (see Section 2.1). While $C^R(\rho)$ may be efficiently computed numerically for any ρ using an algorithm to solve the SDP give in Appendix B, we can also investigate an analytical characterisation of $C^R(\rho)$. In doing so, we find that the robustness of coherence is intimately related to the l_1 norm of coherence, which is an intuitive measure of coherence given by summing the absolute values of all

off-diagonal elements of the density matrix of ρ expressed with respect to the reference ONB, i.e.

$$C^{l_1}(\rho) := \sum_{i=1}^{d}\sum_{j=1}^{d} |\rho_{ij}| - 1, \tag{3.48}$$

with $\rho_{ij} = \langle e_i|\rho|e_j\rangle$. The l_1 norm of coherence was introduced in Ref. [47] and was shown to obey Requirements (i)-(iv) when the free operations are identified as the incoherent operations. Furthermore, it can be shown that $0 \leq C^{l_1}(\rho) \leq d-1$, with $C^{l_1}(\rho) = d-1$ only for the maximally coherent state

$$|\Psi_d\rangle := \frac{1}{\sqrt{d}}\sum_{i=1}^{d} |e_i\rangle\,. \tag{3.49}$$

The maximally coherent state is given its name since every quantum state may be generated from it through incoherent operations [47], and it could be argued that any measure of coherence should be maximal only on $|\Psi_d\rangle$ [130]. Note that not every resource theory has a unique maximally resourceful state [1, 73].

The robustness of coherence coincides with the l_1 norm of coherence for all states of a 2-dimensional system. For higher dimensional systems, the two measures are generally different and coincide only under a restricted class of states [TRB2]. This class includes pure states, so that

$$C^R(|\psi\rangle\langle\psi|) = C^{l_1}(|\psi\rangle\langle\psi|) = \left(\sum_{i=1}^{d} |\psi_i|\right)^2 - 1 \tag{3.50}$$

for any pure state $|\psi\rangle = \sum_{i=1}^{d} \psi_i |e_i\rangle$ with $\sum_{i=1}^{d} |\psi_i|^2 = 1$. For a general state ρ it holds that [TRB2]

$$\frac{C^{l_1}(\rho)}{d-1} \leq C^R(\rho) \leq C^{l_1}(\rho). \tag{3.51}$$

We have already discussed saturation of the upper bound of this inequality, and the lower bound can be achieved for the family of states given by

$$\rho = (1+p)\frac{\mathbb{I}}{d} - p\,|\Psi_d\rangle\langle\Psi_d|\,, \tag{3.52}$$

where $p \in [0, \frac{1}{d-1}]$. Considering the range of $C^{l_1}(\rho)$, (3.51) implies that for any ρ, $0 \leq C^R(\rho) \leq d-1$. Furthermore, it can be found that $C^R(\rho) = d-1$ only when ρ is the maximally coherent state [TRB2]. Figure 3.4 provides a comparison

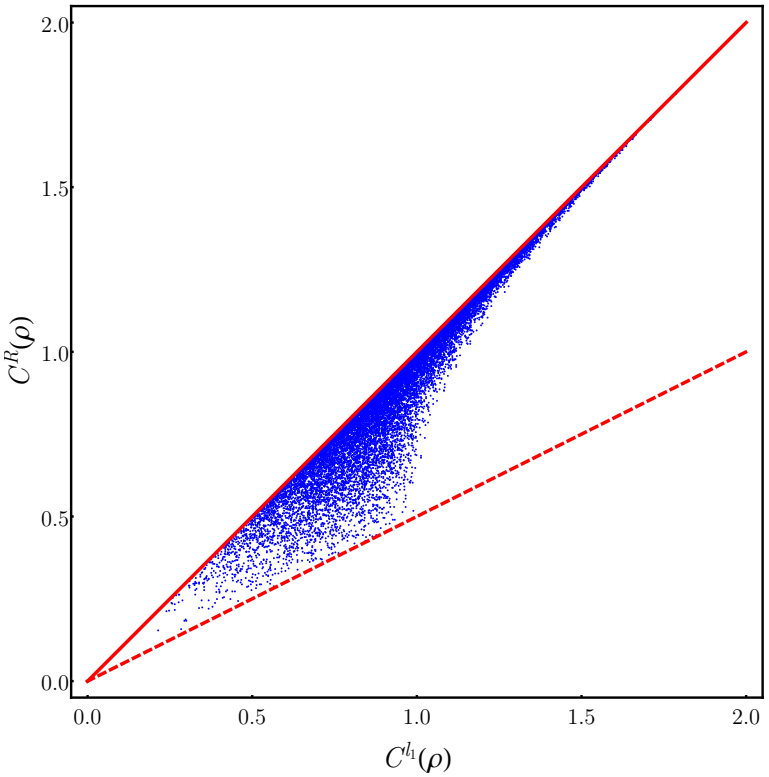

Figure 3.4: A comparison between the robustness of coherence (vertical axis) and the l_1 norm of coherence (horizontal axis) for a 3-dimensional system with 2×10^4 states (blue points) randomly drawn from the uniform distribution according to the Hilbert-Schmidt measure [20, 131]. The solid red line and the dashed red line represent the upper and lower bounds given by (3.51). The robustness of coherence was computed with respect to the standard basis using a numerical algorithm [TRB1] to solve the SDP problem described in Appendix B.

of $C^R(\rho)$ and $C^{l_1}(\rho)$ with respect to the standard basis for 2×10^4 randomly generated states ρ of a 3-dimensional quantum system.

We can also define the robustness of k coherence as

$$C_k^R(\rho) := \inf_{\tau \in \mathcal{D}(\mathcal{H})} \left\{ s \geq 0 \middle| \frac{\rho + s\tau}{1+s} = \sigma \in \mathcal{I}^{(k)} \right\}, \tag{3.53}$$

for $k \in \{2, 3, \ldots, d\}$, with the free states identified as the convex set $\mathcal{I}^{(k)}$ of states with coherence number less than k with respect to the reference ONB $\{|e_i\rangle\}_{i=1}^d$ [TRB3]. The existence of a resource destroying quantum operation for k coherence has not yet been considered. Nevertheless, the robustness of k coherence can still be written as an SDP optimisation problem for any k as

given in Appendix B, and can thus be computed efficiently for general ρ. In the particular case of $k = 2$, the robustness of k coherence becomes equivalent to the robustness of coherence since $\mathcal{I}^{(2)} = \mathcal{I}$, as we have discussed in Section 2.1.1. More generally, for a given state ρ

$$C_2^R(\rho) \geq C_3^R(\rho) \geq \ldots \geq C_d^R(\rho) \geq 0 \tag{3.54}$$

since $\mathcal{I}^{(2)} \subset \mathcal{I}^{(3)} \subset \ldots \subset \mathcal{I}^{(d)}$. However, unlike the robustness of coherence, the robustness of k coherence is not generally equal to the l_1 norm of coherence for pure states. Instead, for any pure state we have that the robustness of k coherence is lower bounded by a function of the l_1 norm of coherence.

Theorem 3 *For any pure state* $|\psi\rangle = \sum_{i=1}^{d} \psi_i |e_i\rangle$ *with* $\sum_{i=1}^{d} |\psi_i|^2 = 1$*, it holds that* [TRB3]

$$C_k^R(|\psi\rangle\langle\psi|) \geq \max\left\{\frac{C^{l_1}(|\psi\rangle\langle\psi|) + 1}{k-1} - 1\,,\, 0\right\}. \tag{3.55}$$

The proof of this theorem is provided in Appendix C. Note that the lower bound can be zero even for a pure state with a coherence number of k or more. Figure 3.5 compares $C_k^R(\rho)$ and $C^{l_1}(\rho)$ with respect to the standard basis for 2×10^4 randomly generated pure states $\rho = |\psi\rangle\langle\psi|$ of a 5-dimensional quantum system with $k = 4$.

We now show that the lower bound provided in Theorem 3 is saturated for the family of d-dimensional pure states given by

$$|\psi(x,j)\rangle := x\sum_{i=1}^{j-1} |e_i\rangle + \sqrt{1-(j-1)x^2}\,|e_j\rangle\,, \tag{3.56}$$

with $x \in \left[0, \frac{1}{\sqrt{j-1}}\right]$ and $j \in \{2,3,\ldots,d\}$.

Theorem 4 *For any* $x \in \left[\frac{1}{\sqrt{j}}, \frac{1}{\sqrt{j-1}}\right]$ *and* $j \in \{2,3,\ldots,d\}$ [TRB3]*,*

$$C_k^R(|\psi(x,j)\rangle\langle\psi(x,j)|) = \max\left\{\frac{C^{l_1}(|\psi(x,j)\rangle\langle\psi(x,j)|) + 1}{k-1} - 1, 0\right\}. \tag{3.57}$$

The proof of this theorem is also provided in Appendix C. For a given j, the pure states $|\psi(x,j)\rangle$ with $x \in \left[\frac{1}{\sqrt{j}}, \frac{1}{\sqrt{j-1}}\right]$ have an l_1 norm of coherence in the

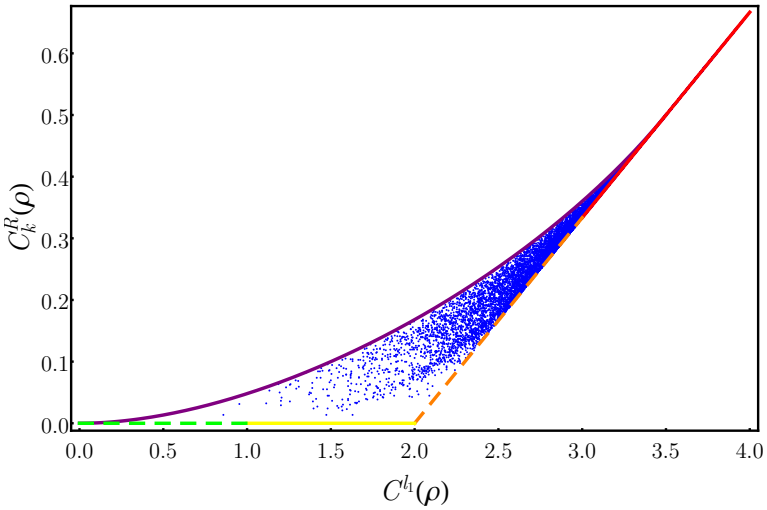

Figure 3.5: A comparison between the robustness of k coherence (vertical axis) and the l_1 norm of coherence (horizontal axis) for a 5-dimensional system with $k = 4$ for 2×10^4 pure states (blue points) randomly drawn from the uniform distribution according to the Haar measure [20]. The lower bound provided by Theorem 3 is shown by plotting $C_k^R(|\psi(x,j)\rangle\langle\psi(x,j)|)$ against $C^{l_1}(|\psi(x,j)\rangle\langle\psi(x,j)|)$ for the pure states $|\psi(x,j)\rangle$ given in Eq. (3.56) with $x \in \left[\frac{1}{\sqrt{j}}, \frac{1}{\sqrt{j-1}}\right]$ for $j = 2$ (green dashed line), $j = 3$ (yellow line), $j = 4$ (orange dashed line), and $j = 5$ (red line). A conjectured upper bound (purple line) is given by $C_k^R(|\psi(x,5)\rangle\langle\psi(x,5)|)$ for $x \in \left[0, \frac{1}{\sqrt{5}}\right]$. The robustness of k coherence was computed with respect to the standard basis using a numerical algorithm to solve the SDP problem described in Appendix B.

range $[j-2, j-1]$, so that one can span the whole range of the l_1 norm of coherence by varying $j \in \{2, 3, \ldots, d\}$. We plot $C_k^R(|\psi(x,j)\rangle\langle\psi(x,j)|)$ against $C^{l_1}(|\psi(x,j)\rangle\langle\psi(x,j)|)$ in Fig. 3.5 with $d = 5$, $j \in \{2,3,4,5\}$, and $x \in \left[\frac{1}{\sqrt{j}}, \frac{1}{\sqrt{j-1}}\right]$, hence saturating the lower bound provided by Theorem 3. It is conjectured, based on numerics, that the pure states $|\psi(x,j)\rangle$, with $j = d$ and $x \in \left[0, \frac{1}{\sqrt{d}}\right]$, furthermore have the *highest* robustness of k coherence among all pure states with a fixed l_1 norm of coherence. Such states are shown by the purple line for $d = 5$ in Fig. 3.5. The maximally coherent state is given by $|\Psi_d\rangle = |\psi(1/\sqrt{d}, d)\rangle$ so that

$$C_k^R(|\Psi_d\rangle\langle\Psi_d|) = \frac{d}{k-1} - 1. \tag{3.58}$$

In summary, the robustness of coherence and the robustness of k coherence

are efficiently computable numerically for any state as well as there being some analytical results for certain types of state. They are furthermore good measures of the resource of coherence, which follows from our earlier discussion on the robustness of a resource in general. In Chapter 5, we discuss how the robustness of coherence and the robustness of k coherence can be quantitatively linked to the performance of a phase discrimination task.

3.2.2 Distance-based Approach

The distance-based measures of a resource in a quantum system provide an alternative geometric quantification of resources by turning to the concept of distinguishability discussed in Chapter 1. They are given by considering the distance-based distinguishability between the state ρ of the system and the set of free states $\mathcal{F}$, i.e.

$$R^{D_\delta}(\rho) := \inf_{\sigma\in\mathcal{F}} D_\delta(\rho,\sigma), \tag{3.59}$$

where D_δ is a distance between quantum states. In this way, we can see that the more ρ is distinguishable from the free states, the more resource is present in the system. Instead, if ρ is indistinguishable from a free state then the system has no resources. The $\tilde{\sigma} \in \mathcal{F}$ satisfying the infimum in Eq. (3.59) form the set $\tilde{\mathcal{F}}$ of closest free states to ρ. While this set can in general be composed of more than one free state, in most cases there is a unique closest free state. Since it is often only necessary to identify an arbitrary element of $\tilde{\mathcal{F}}$ rather than distinguish between them, in the following we often only refer to *the* closest free state.

It is clear that each choice of distance D_δ gives rise to a corresponding distance-based measure $R^{D_\delta}(\rho)$. For D_δ to be a good measure of distinguishability it is imposed that D_δ is contractive, i.e. that the distance between two states never increases under the action of a quantum operation, as defined in Eq. (1.35). Furthermore, it is often imposed that D_δ is jointly convex [20],

$$D(p\rho_1 + (1-p)\rho_2, p\sigma_1 + (1-p)\sigma_2) \leq pD(\rho_1,\sigma_1) + (1-p)D(\rho_2,\sigma_2), \tag{3.60}$$

for any probability $p \in [0,1]$ and any quantum states ρ_1, ρ_2, σ_1, and σ_2. All of the distances listed in Table 1.1 are contractive and jointly convex [20, 44]. We

now see that contractivity and joint convexity of D_δ mean that the corresponding $R^{D_\delta}(\rho)$ is a good measure of a resource. It is clear that $R^{D_\delta}(\rho)$ is a real and non-negative function and is zero only for $\rho \in \mathcal{F}$, which is given from the first property of any distance D_δ in (1.3). Hence, $R^{D_\delta}(\rho)$ satisfies Requirement (i). We now prove that $R^{D_\delta}(\rho)$ satisfies Requirement (ii).

Theorem 5 *For any contractive D_δ it holds that*

$$R^{D_\delta}(\Lambda(\rho)) \leq R^{D_\delta}(\rho) \tag{3.61}$$

for all $\Lambda \in \mathcal{O}$ and any state ρ [18].

Proof.

$$\begin{aligned} R^{D_\delta}(\rho) &= \inf_{\sigma\in\mathcal{F}} D_\delta(\rho,\sigma) \\ &\geq \inf_{\sigma\in\mathcal{F}} D_\delta(\Lambda(\rho),\Lambda(\sigma)) \\ &\geq \inf_{\sigma\in\mathcal{F}} D_\delta(\Lambda(\rho),\sigma) \\ &= R^{D_\delta}(\Lambda(\sigma)), \end{aligned} \tag{3.62}$$

where in the first inequality we use the contractivity of D_δ from (1.35) and in the second inequality we use the fact that for any $\Lambda \in \mathcal{O}$ it holds that $\{\Lambda(\sigma) \,|\, \sigma \in \mathcal{F}\} \subseteq \mathcal{F}$, since $\Lambda(\sigma) \in \mathcal{F}$ for all $\sigma \in \mathcal{F}$. □

Usefully, this theorem implies that $R^{D_\delta}(\rho)$ satisfies Requirement (ii) for any choice of free operations, including the maximal set of operations unable to create the resource, which follows from the fact that in the proof we only require $\Lambda(\sigma) \in \mathcal{F}$ for all $\sigma \in \mathcal{F}$. Finally, $R^{D_\delta}(\rho)$ satisfies Requirement (iii) if $\mathcal{F}$ is convex.

Theorem 6 *For any jointly convex D_δ and resource theory with a convex set of free states $\mathcal{F}$, it holds that*

$$R^{D_\delta}(p\rho_1 + (1-p)\rho_2) \leq pR^{D_\delta}(\rho_1) + (1-p)R^{D_\delta}(\rho_2) \tag{3.63}$$

for any probability $p \in [0,1]$ and any two states ρ_1 and ρ_2 [19].

Proof.

$$\begin{aligned} R^{D_\delta}(p\rho_1 + (1-p)\rho_2) &= \inf_{\sigma\in\mathcal{F}} D_\delta(p\rho_1 + (1-p)\rho_2, \sigma) \\ &= \inf_{\substack{\sigma_1\in\mathcal{F} \\ \sigma_2\in\mathcal{F}}} D_\delta(p\rho_1 + (1-p)\rho_2, p\sigma_1 + (1-p)\sigma_2) \\ &\leq p \inf_{\sigma_1\in\mathcal{F}} D(\rho_1, \sigma_1) + (1-p) \inf_{\sigma_2\in\mathcal{F}} D(\rho_2, \sigma_2) \\ &= pR^{D_\delta}(\rho_1) + (1-p)R^{D_\delta}(\rho_2), \end{aligned} \tag{3.64}$$

where we use the joint convexity of D_δ in the inequality. In the second equality we use the fact that $\{p\sigma_1 + (1-p)\sigma_2 \,|\, \sigma_1 \in \mathcal{F}\,,\, \sigma_2 \in \mathcal{F}\} = \mathcal{F}$. Indeed, it is clear from the convexity of $\mathcal{F}$ that $p\sigma_1 + (1-p)\sigma_2 \in \mathcal{F}$ for any $p \in [0,1]$, $\sigma_1 \in \mathcal{F}$ and $\sigma_2 \in \mathcal{F}$. On the other hand, for any $\sigma \in \mathcal{F}$ we may write $\sigma = p\sigma_1 + (1-p)\sigma_2$ with $\sigma_1 = \sigma_2 = \sigma$ so that $\sigma \in \{p\sigma_1 + (1-p)\sigma_2 \,|\, \sigma_1 \in \mathcal{F}\,,\, \sigma_2 \in \mathcal{F}\}$. □

We can therefore see that the distance-based measures of a resource satisfy the first three requirements. This type of measure was introduced in Refs. [18, 19] for the resource of entanglement, and the distances listed in Table 1.1 have been subsequently used to measure entanglement [2, 20, TRB4, 44, 132–135]. The distance-based approach has also been applied to quantum coherence [1, TRB9, 47, 85, 136, 137], and quantum correlations, for which a comprehensive review can be found in Ref. [TRB12]. Note that it is simple to see from Theorem 5 that Requirement Q(ii) for quantum correlations is also satisfied whenever D_δ is contractive. On the other hand, Requirement (iv) is typically checked on a case-by-case basis for each D_δ, although a sufficient condition on D_δ has been provided in Ref. [19, 47] for the induced resource measure to satisfy this strong monotonicity. The relative entropy and the infidelity are two examples of distances that induce a distance-based resource measure that is strongly monotone [2, 19, 47, 109, 137].

It is a natural question to ask which of the distances D_δ is the most appropriate to use to quantify a resource using $R^{D_\delta}(\rho)$. There is not a clear answer to this. One may choose D_δ because it has appealing features as a measure of distinguishability [7, 20, 42]. However, this does not immediately furnish $R^{D_\delta}(\rho)$ with a physical relevance aside from the more abstract notion of quantifying the

distinguishability between ρ and the set of free states. The physical relevance of $R^{D_\delta}(\rho)$ in terms of being the figure of merit in an operational task must be investigated for each D_δ and each resource, see Refs. [1, 2, 11, TRB12] for further details. In practice, the choice of D_δ is often dictated by the pragmatic motivation of being able to solve the infimum in $R^{D_\delta}(\rho)$. Indeed, $R^{D_\delta}(\rho)$ can be difficult to evaluate both analytically and numerically [138] for arbitrary ρ. To help solve this problem, in the next chapter we give a framework for providing lower bounds on $R^{D_\delta}(\rho)$ that are simpler to evaluate. Furthermore, in this thesis we often prefer not fix a particular distance but instead work generally with distance-based measures of a resource for any contractive and jointly convex distance.

Comparing *the Quantum* within the Distance-based Approach

The geometric nature of the distance-based approach allows for a unified perspective when quantifying the resources in a composite quantum system [139, 140]. This permits a natural comparison between resources and can lead to physical insights into their behaviour and interaction, as will be discussed further in Section 6.1.5. Consider a bipartite system in state ρ^{AB} consisting of subsystem A and B. The quantum coherence, quantum correlations, and quantum entanglement may be quantified in the distance-based approach as

$$C^{D_\delta}(\rho^{AB}) := \inf_{\delta^{AB}\in\mathcal{I}^{AB}} D_\delta(\rho^{AB},\delta^{AB}), \tag{3.65}$$

$$Q^{D_\delta}_{AB}(\rho^{AB}) := \inf_{\chi^{AB}_{CC}\in\mathcal{C}^{AB}_{CC}} D_\delta(\rho^{AB},\chi^{AB}_{CC}), \tag{3.66}$$

$$E^{D_\delta}(\rho^{AB}) := \inf_{\varsigma^{AB}\in\mathcal{S}^{AB}} D_\delta(\rho^{AB},\varsigma^{AB}), \tag{3.67}$$

where we define coherence with respect to a reference ONB $\{|e^A_i\rangle\otimes|f^B_j\rangle\}^{d_A,d_B}_{i,j=1}$ of product pure states of both subsystems and $\mathcal{I}^{AB}$ is the set of incoherent states in such an ONB [TRB9, 137], while we also restrict to considering quantum correlations with respect to both subsystems. It is clear that $\mathcal{I}^{AB}\subset\mathcal{C}^{AB}_{CC}\subset\mathcal{S}^{AB}$, so that $C^{D_\delta}(\rho^{AB})\geq Q^{D_\delta}_{AB}(\rho^{AB})\geq E^{D_\delta}(\rho^{AB})$. In fact, it can be found that $Q^{D_\delta}_{AB}(\rho^{AB})$ is the result of minimising the coherence $C^{D_\delta}(\rho^{AB})$ over all product

ONBs [TRB9, TRB12, 84, 141, 142]. Figure 3.6 illustrates these resources from a geometric perspective. We can also measure the total correlations [10, 139, 140] between the two subsystems as the distance from the uncorrelated states

$$T^{D_\delta}(\rho^{AB}) := \inf_{\omega^{AB}\in\mathcal{P}^{AB}} D_\delta(\rho^{AB},\omega^{AB}), \tag{3.68}$$

with $\mathcal{P}^{AB}$ the product states given in Eq. (2.20). Since $\mathcal{P}^{AB} \subset \mathcal{C}^{AB}_{CC}$ it holds that $T^{D_\delta}(\rho^{AB}) \geq Q^{D_\delta}_{AB}(\rho^{AB})$. As discussed in Section 2.2, the classical correlations can be thought of as the portion of the total correlations that are not quantum. There is not a clear way to define a measure of classical correlations in the distance-based approach (the conventional approach is through an entropic measure [9, 10]). One method is to quantify the classical correlations as the distance between the set $\tilde{\mathcal{C}}^{AB}_{CC} \subset \mathcal{C}^{AB}_{CC}$ of closest classical states to ρ and the set of uncorrelated states [TRB11, 139, 140, 143, 144],

$$CC^{D_\delta}_{AB}(\rho^{AB}) := \inf_{\tilde{\chi}^{AB}_{CC}\in\tilde{\mathcal{C}}^{AB}_{CC}} \inf_{\omega^{AB}\in\mathcal{P}^{AB}} D_\delta(\tilde{\chi}^{AB}_{CC},\omega^{AB}). \tag{3.69}$$

This method was introduced in Ref. [139], but did not include an infimum over all closest classical states to ρ^{AB}. The infimum was then introduced in Ref. [TRB11] to prevent any ambiguities in the definition of classical correlations. However, as can be seen in Fig. 3.6, by using this method in general it holds that $T^{D_\delta}(\rho^{AB}) \neq CC^{D_\delta}_{AB}(\rho^{AB}) + Q^{D_\delta}_{AB}(\rho^{AB})$.

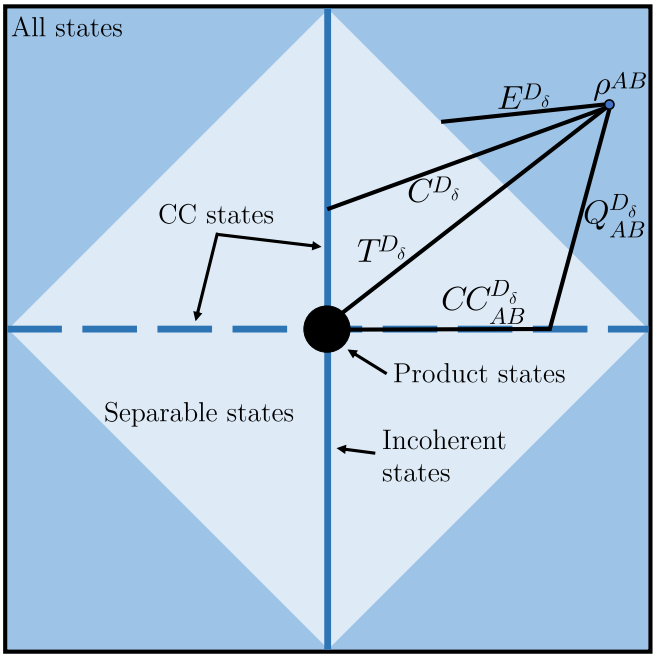

Figure 3.6: Quantification of quantum coherence C^{D_δ}, quantum correlations $Q^{D_\delta}_{AB}$, quantum entanglement E^{D_δ}, total correlations T^{D_δ}, and classical correlations $CC^{D_\delta}_{AB}$ in a bipartite system using the distance-based approach given in Eqs. (3.65)–(3.69). The outer square represents all bipartite states, the inner diamond represents separable states, the solid and dashed blue lines and black inner circle represent the CC states, the solid blue line represents the incoherent states, while finally the black inner circle represents the product states. Note that in general the contractive and jointly convex distances on quantum states do not behave like the Euclidean distance, and so the resource measures are not given by simply finding the distance to the Euclidean orthogonal projection onto the free states.

Chapter 4

Bounding *the Quantum*

In the previous chapter we discussed some general requirements for measures of a quantum resource and presented two geometric approaches to measuring a resource. Having identified these measures, the next step is to evaluate them for a given state either numerically or analytically. We have shown that the robustness of a resource can be evaluated numerically using an SDP, provided the resource theory satisfies some constraints. However, the robustness is not simple to evaluate analytically in general. Furthermore, the distance-based measure is difficult to evaluate both numerically and analytically. In this chapter we outline a general framework to provide lower bounds to measures of a resource, following from the works of Refs. [TRB4, TRB5, TRB6]. After introducing this general framework, we provide an example of its application to the resources of multiqubit entanglement and coherence.

4.1 Framework

Our framework is constructed on the concept of resource non-increasing projections. A resource non-increasing projection Π, is a free quantum operation $\Pi \in \mathcal{O}$ that satisfies $\Pi(\Pi(\rho)) = \Pi(\rho)$ for any state ρ. Each resource non-increasing projection Π identifies a set of resource guarantor states $\mathcal{G} \subset \mathcal{D}(\mathcal{H})$ given by all the states left invariant by Π, i.e. $\mathcal{G} := \{\rho \in \mathcal{D}(\mathcal{H}) \mid \rho = \Pi(\rho)\}$. The action of a resource non-increasing projection is to project any state ρ into the corresponding

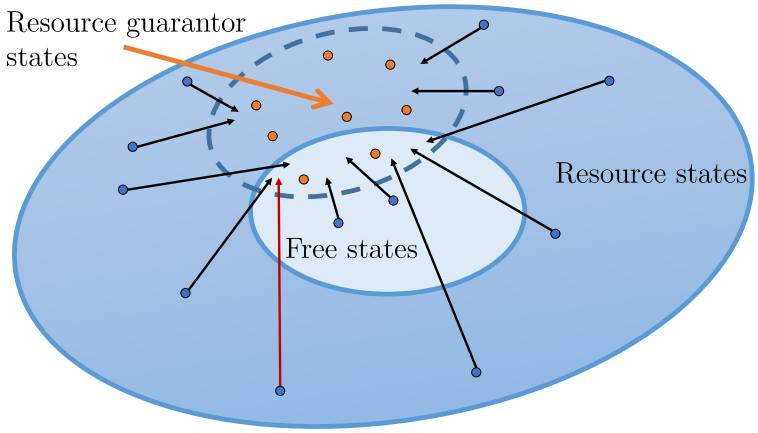

Figure 4.1: A resource non-increasing projection (black arrows) is a free operation that maps any state (blue circles) to a set of resource guarantor states (orange circles). The set of resource guarantor states are all the states left invariant under the action of the resource non-increasing projection, and cannot have more resource than the states they guarantee. Since the resource non-increasing projection is a free operation, the free states are mapped onto a subset of themselves. We note that it is possible for a resource state to be mapped to a free state due to the resource non-increasing projection (as shown for example by the red arrow).

set of resource guarantor states, such that

$$\begin{aligned} \Pi(\rho) &\in \mathcal{G} \qquad \forall \ \rho \in \mathcal{D}(\mathcal{H}), \\ \Pi(\rho) &= \rho \qquad \forall \ \rho \in \mathcal{G}. \end{aligned} \tag{4.1}$$

Any state ρ has a corresponding resource guarantor state $\Pi(\rho) \in \mathcal{G}$ that cannot have more resource than ρ, i.e. $R(\rho) \geq R(\Pi(\rho))$, which follows from Requirement (ii) of R since $\Pi \in \mathcal{O}$. Hence, the resource guarantor state $\Pi(\rho) \in \mathcal{G}$ provides a quantitative guarantee on the resource of ρ in terms of a lower bound arising due to the resource non-increasing projection Π, thus motivating our nomenclature. Note that there are in general many states ρ with the same corresponding resource guarantor state. Figure 4.1 exhibits the action of a resource non-increasing projection on the set of states.

The general framework to provide lower bounds to measures of a resource is then structured into four steps:

Step One: Find a resource non-increasing projection Π and identify the cor-

responding set of resource guarantor states $\mathcal{G}$.

Step Two: Identify the set of free resource guarantor states $\mathcal{F}_{\mathcal{G}}$, i.e. the intersection between the free states $\mathcal{F}$ and the resource guarantor states $\mathcal{G}$.

Step Three: Evaluate a resource measure $R(\varpi)$ on every resource guarantor state $\varpi \in \mathcal{G}$.

Step Four: Find lower bounds to the resource of a general state ρ by varying ρ over free unitaries Υ and finding the corresponding resource guarantor state $\Pi(\Upsilon(\rho)) \in \mathcal{G}$ with the largest amount of resource.

Figure 4.2 summarises the four steps of our framework, which results in a lower bound on a measure of the resources of a system in the state ρ. The first and final steps of this framework have been studied specialised to quantum entanglement in Refs. [145–148], while the second and third steps have been introduced in Refs. [TRB4, TRB5]. We also remark on the experimental applicability of this framework. Indeed, experimentalists often want to quantify the resource (such as entanglement) of a quantum system prepared in a laboratory. This can be done by performing full quantum state tomography [7, 149, 150] to reconstruct the density matrix of the state and then evaluating a resource measure on the density matrix. However, full state tomography is experimentally demanding and evaluation of a resource measure for an arbitrary reconstructed density matrix can be computationally intensive. Instead, finding lower bounds on resource measures using our framework bypasses some of the experimental and numerical difficulty. This is achieved through our restriction to a family of resource guarantor states $\mathcal{G}$ that are necessarily easier to reconstruct experimentally and simpler to evaluate numerically. We now motivate and explain each of the steps in greater detail.

4.1.1 Step One

The first step of this framework is to identify a resource non-increasing projection Π and the corresponding set of resource guarantor states $\mathcal{G}$. The general idea is to pick a Π so that the resource guarantor states $\mathcal{G}$ are a simple family of states

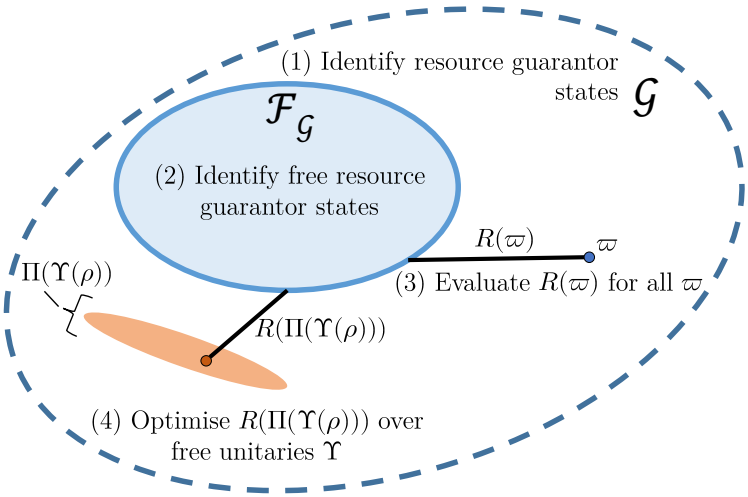

Figure 4.2: The four steps of the framework to provide lower bounds on a resource measure for a system in state ρ. The first two steps consist of (1) finding a resource non-increasing projection Π and identifying the corresponding set of resource guarantor states $\mathcal{G}$, and then (2) identifying the contained set of free states $\mathcal{F}_G = \mathcal{F} \cap \mathcal{G}$. The final two steps consist of (3) evaluating a resource measure R for all $\varpi \in \mathcal{G}$ (shown pictorially using the distance-based approach), and (4) optimising ρ over free unitaries Υ so that the corresponding resource guarantor state $\Pi(\Upsilon(\rho)) \in \mathcal{G}$ has the most resource (the orange ellipse here illustrates the set of resource guarantor states corresponding to $\Upsilon(\rho)$ for each Υ).

with resource measures that can be evaluated on them either analytically or numerically. However, broadly speaking, the simpler the $\mathcal{G}$, the more resource is lost by projecting with Π onto $\mathcal{G}$. This means that the lower bounds provided by $\mathcal{G}$ become smaller and hence less informative. In fact, it is possible that $\Pi(\rho) \in \mathcal{F}$ even if $\rho \notin \mathcal{F}$, as can be seen by the red arrow in Fig. 4.1, so that the lower bound provided by $\Pi(\rho)$ is zero and hence trivial. An extreme example of this can be given by a resource destroying quantum operation, which is a special type of resource non-increasing projection that projects every state onto the free states. We thus have to find a balance between the simplicity of $\mathcal{G}$ and the usefulness of the lower bounds provided by $\mathcal{G}$.

4.1.2 Step Two

The next step of the framework is to identify the set $\mathcal{F}_\mathcal{G}$ of resource guarantor states that are also resource-free, i.e. the intersection $\mathcal{F} \cap \mathcal{G}$. It can be seen that $\mathcal{F}_\mathcal{G}$ is given by applying the resource non-increasing projection onto the set of free states,

$$\mathcal{F}_\mathcal{G} := \mathcal{F} \cap \mathcal{G} = \{\Pi(\rho) \mid \rho \in \mathcal{F}\}\,. \tag{4.2}$$

To see this, it is first clear that for any $\rho \in \mathcal{F}_\mathcal{G}$ we know $\rho \in \mathcal{F}$ and $\rho \in \mathcal{G}$ so that $\rho = \Pi(\rho) \in \{\Pi(\rho) \mid \rho \in \mathcal{F}\}$. On the other hand, for any $\Pi(\rho) \in \{\Pi(\rho) \mid \rho \in \mathcal{F}\}$ then $\Pi(\rho) \in \mathcal{G}$ and $\Pi(\rho) \in \mathcal{F}$ since Π is a free operation and cannot create resource, so that $\Pi(\rho) \in \mathcal{F}_\mathcal{G}$. This proves the equivalence of the two sets. Hence, we can use Eq. (4.2) to characterise $\mathcal{F}_\mathcal{G}$. As we shall see in the next step, characterisation of $\mathcal{F}_\mathcal{G}$ is useful to help evaluate resource measures on the resource guarantor states.

4.1.3 Step Three

In this step of the framework we aim to measure the amount of resources in each resource guarantor state. For general resource measures R, the projection given by Π onto the resource guarantor states $\mathcal{G}$ allows for a variety of tricks to be used to simplify the evaluation of $R(\varpi)$ for any $\varpi \in \mathcal{G}$ when compared to the evaluation of $R(\rho)$ for a general state ρ. This can be seen more concretely by focussing on the two geometric approaches to measuring a resource discussed in Section 3.2. For the robustness, the infimum in Eq. (3.23) over all free states $\mathcal{F}$ can be instead replaced by the infimum over all $\mathcal{F}_\mathcal{G} \subseteq \mathcal{F}$. Indeed, for any $\varpi \in \mathcal{G}$ consider

$$R^R(\varpi) = \inf_{\sigma\in\mathcal{F}} \{s \geq 0 \,|\varpi \leq (1+s)\sigma\}\,, \tag{4.3}$$

$$\tilde{R}^R(\varpi) := \inf_{\tilde{\sigma}\in\mathcal{F}_\mathcal{G}} \{s \geq 0 \,|\varpi \leq (1+s)\tilde{\sigma}\}\,, \tag{4.4}$$

where the first line is the robustness in Eq. (3.23) and the second line is the same optimisation but over the contained set $\mathcal{F}_\mathcal{G}$. It is clear that $R^R(\varpi) \leq \tilde{R}^R(\varpi)$ since $\mathcal{F}_\mathcal{G} \subseteq \mathcal{F}$, but it can also be shown that $R^R(\varpi) \geq \tilde{R}^R(\varpi)$. Take any $\sigma \in \mathcal{F}$ such

that $\varpi \leq (1+s)\sigma$. Since Π preserves positivity and $\Pi(\varpi) = \varpi$ because $\varpi \in \mathcal{G}$,

$$\begin{aligned} \Pi(\varpi) &\leq (1+s)\Pi(\sigma), \\ \varpi &\leq (1+s)\Pi(\sigma). \end{aligned} \tag{4.5}$$

Hence, for any σ in the infimum of Eq. (4.3) with corresponding value s there is a $\tilde{\sigma} = \Pi(\sigma)$ in the infimum of Eq. (4.4) with the same corresponding s so that $\tilde{R}^R(\varpi) \leq R^R(\varpi)$. Putting everything together, we have that

$$R^R(\varpi) = \tilde{R}^R(\varpi). \tag{4.6}$$

This is a particularly appealing result from the perspective of evaluating the robustness numerically, since $\tilde{R}^R(\varpi)$ may be posed as the solution to an SDP when the set $\mathcal{F}_\mathcal{G}$ can be characterised with a finite number of conditions, as will be discussed in the example in the following section.

A similar simplification holds for the distance-based approach to measuring a resource. Here it turns out that minimisation of the distance over all free states in Eq. (3.59) can be simplified to a minimisation over all $\mathcal{F}_\mathcal{G}$. Indeed, for any $\varpi \in \mathcal{G}$, consider

$$R^{D_\delta}(\varpi) = \inf_{\sigma \in \mathcal{F}} D_\delta(\varpi, \sigma), \tag{4.7}$$

$$\tilde{R}^{D_\delta}(\varpi) := \inf_{\tilde{\sigma} \in \mathcal{F}_\mathcal{G}} D_\delta(\varpi, \tilde{\sigma}), \tag{4.8}$$

where the first line is the distance-based measure in Eq. (3.59) and the second line is the same optimisation but over the smaller set $\mathcal{F}_\mathcal{G}$. Again, it is clear that $R^{D_\delta}(\varpi) \leq \tilde{R}^{D_\delta}(\varpi)$ since $\mathcal{F}_\mathcal{G} \subseteq \mathcal{F}$, but it also holds that $R^{D_\delta}(\varpi) \geq \tilde{R}^{D_\delta}(\varpi)$. This can be seen from

$$\begin{aligned} R^{D_\delta}(\varpi) &= \inf_{\sigma \in \mathcal{F}} D_\delta(\varpi, \sigma) \\ &\geq \inf_{\sigma \in \mathcal{F}} D_\delta(\Pi(\varpi), \Pi(\sigma)) \\ &= \inf_{\sigma \in \mathcal{F}} D_\delta(\varpi, \Pi(\sigma)) \\ &= \inf_{\tilde{\sigma} \in \mathcal{F}_\mathcal{G}} D_\delta(\varpi, \tilde{\sigma}) \\ &= \tilde{R}^{D_\delta}(\varpi), \end{aligned} \tag{4.9}$$

where the contractivity of D_δ is used in the inequality, $\Pi(\varpi) = \varpi$ since $\varpi \in \mathcal{G}$ is used in the second equality, and the characterisation of $\mathcal{F}_\mathcal{G}$ in Eq. (4.2) is used in the third equality. Hence we have that

$$R^{D_\delta}(\varpi) = \tilde{R}^{D_\delta}(\varpi). \tag{4.10}$$

This result is appealing from a geometric perspective, since it allows us to focus only on evaluating the distance between states of the same family $\mathcal{G}$. Further details can be found in the forthcoming example.

4.1.4 Step Four

The final step of the framework consists of optimising the lower bound to the resource of ρ over free unitary operations. A free unitary operation $\Upsilon \in \mathcal{O}$ acts on any state ρ as $\Upsilon(\rho) = U\rho U^\dagger$ where U is a unitary operator. The free unitary operations are invertible with inverse given by $\Upsilon^\dagger \in \mathcal{O}$ such that $\Upsilon^\dagger(\Upsilon(\rho)) = \Upsilon(\Upsilon^\dagger(\rho)) = \rho$ where $\Upsilon^\dagger(\rho) = U^\dagger\rho U$. This means that $R(\Upsilon(\rho)) = R(\rho)$ for any Υ because

$$\begin{aligned} R(\rho) &\geq R(\Upsilon(\rho)) \\ R(\Upsilon(\rho)) &\geq R(\Upsilon^\dagger(\Upsilon(\rho))) = R(\rho), \end{aligned} \tag{4.11}$$

which holds for all ρ due to Requirement (ii) and the fact that $\Upsilon \in \mathcal{O}$ and $\Upsilon^\dagger \in \mathcal{O}$. Hence, all states given by $\Upsilon(\rho)$ have the same resource as ρ. We can then consider the resource guarantor states $\Pi(\Upsilon(\rho))$ and note that

$$R(\Pi(\Upsilon(\rho))) \leq R(\Upsilon(\rho)) = R(\rho). \tag{4.12}$$

Since generally $\Pi(\Upsilon(\rho)) \neq \Upsilon(\Pi(\rho))$, the resources of $\Pi(\Upsilon(\rho))$ depend on Υ and we can optimise over free unitaries Υ to provide an improved lower bound to the resources of ρ, i.e.

$$\sup_\Upsilon R(\Pi(\Upsilon(\rho))) = R(\Pi(\Upsilon^\star(\rho))) \leq R(\Upsilon^\star(\rho)) = R(\rho), \tag{4.13}$$

where $\Upsilon^\star$ is the free unitary that provides the optimal lower bound to $R(\rho)$. However, this optimisation can increase the difficulty of providing a lower bound,

and so it may be necessary to restrict the optimisation to a subset of the free unitaries. For the resources of quantum correlations and entanglement, the free unitaries are all the local unitaries acting on each subsystem, while for the resource of coherence the free unitaries depend on the set of free operations identified [1].

4.2 Applying the Framework to Multiqubit Entanglement

So far our framework has been described in very abstract terms. Here we clarify each step of the framework by providing an example of a resource non-increasing projection for multiqubit entanglement. This entanglement non-increasing projection is used to find lower bounds on the distance-based M-inseparable multiqubit entanglement

$$E_M^{D_\delta}(\rho) := \inf_{\varsigma \in \mathcal{S}_M} D_\delta(\rho, \varsigma) \tag{4.14}$$

of an $N \geq 2$ qubit system in the state ρ. The reader is referred to Section 2.3.1 for an explanation of the terminology used here for multiqubit entanglement.

4.2.1 Steps of the Framework

Step One

To define our entanglement non-increasing projection $\Pi(\rho)$, we introduce a set consisting of $2(N-1)$ local unitaries composed of tensor products of unitaries acting on each qubit

$$\begin{aligned}\{U_j\}_{j=1}^{2(N-1)} = \{&(\sigma_1 \otimes \sigma_1 \otimes \mathbb{I}^{\otimes N-2}), (\mathbb{I} \otimes \sigma_1 \otimes \sigma_1 \otimes \mathbb{I}^{\otimes N-3}), \\ &\ldots (\mathbb{I}^{\otimes N-3} \otimes \sigma_1 \otimes \sigma_1 \otimes \mathbb{I}), (\mathbb{I}^{\otimes N-2} \otimes \sigma_1 \otimes \sigma_1) \\ &, (\sigma_2 \otimes \sigma_2 \otimes \mathbb{I}^{\otimes N-2}), (\mathbb{I} \otimes \sigma_2 \otimes \sigma_2 \otimes \mathbb{I}^{\otimes N-3}), \\ &\ldots (\mathbb{I}^{\otimes N-3} \otimes \sigma_2 \otimes \sigma_2 \otimes \mathbb{I}), (\mathbb{I}^{\otimes N-2} \otimes \sigma_2 \otimes \sigma_2)\},\end{aligned} \tag{4.15}$$

with $\{\sigma_i\}_{i=1}^3$ the 2-dimensional Pauli matrices given in Eq. (1.48) and $\mathbb{I}$ the 2-dimensional identity matrix. The entanglement non-increasing projection is given by

$$\Pi(\rho) = \frac{1}{2^{2(N-1)}} \sum_{i=1}^{2^{2(N-1)}} U_i' \varrho U_i'^{\dagger}, \tag{4.16}$$

where U_i' are the following local unitaries

$$\{U_i'\}_{i=1}^{2^{2(N-1)}} = \left\{ \begin{array}{c} \mathbb{I}^{\otimes N} \\ \{U_{i_1}\}_{i_1=1}^{2(N-1)} \\ \{U_{i_2}U_{i_1}\}_{i_2>i_1=1}^{2(N-1)} \\ \cdots \\ \{U_{i_{2(N-1)}} \ldots U_{i_2}U_{i_1}\}_{i_{2(N-1)}>\ldots>i_2>i_1=1}^{2(N-1)} \end{array} \right\}. \tag{4.17}$$

We now see that $\Pi \in \mathcal{O}$. Recall that the free operations for any level of M-inseparable multiqubit entanglement are LOCC where each qubit is treated as an individual subsystem. It can be seen that each U_i' is a local unitary composed of tensor products of unitaries acting on each qubit, so that $\Pi(\rho)$ is a convex combination of such single qubit local unitaries. This can be realised physically by allowing one of the single qubit subsystems to randomly select an $i \in \{1, 2, \ldots, 2^{2(N-1)}\}$ according to the uniform distribution and then communicate the result to all the other qubits, so that together they each perform their local unitary corresponding to U_i'. This is a type of one way single qubit LOCC and so $\Pi \in \mathcal{O}$.

The action of Π on any N qubit state ρ is given by the following theorem.

Theorem 7 *For any N qubit state ρ and $\Pi(\rho)$ as in Eq. (4.16),*

$$\Pi(\rho) = \frac{1}{2^N}\left(\mathbb{I}^{\otimes N} + \sum_{i=1}^{3} c_i \sigma_i^{\otimes N}\right) \tag{4.18}$$

where $c_i = \mathrm{Tr}(\rho\sigma_i^{\otimes N}) \in [-1, 1]$ [TRB4].

The proof of this theorem is provided in Appendix C. Since $\Pi(\Pi(\rho))$ is described by $\tilde{c}_i = \mathrm{Tr}(\Pi(\rho)\sigma_i^{\otimes N}) = c_i$, it is then clear that $\Pi(\Pi(\rho)) = \Pi(\rho)$ so that Π is a projection. The set of resource guarantor states defined by Π, i.e. all those left

invariant under the action of Π, is given by

$$\mathcal{G} = \left\{ \varpi \quad \middle| \quad \varpi = \frac{1}{2^N} \left(\mathbb{I}^{\otimes N} + \sum_{i=1}^{3} c_i \sigma_i^{\otimes N} \right) \right\}, \tag{4.19}$$

where $c_i = \mathrm{Tr}(\varpi \sigma_i^{\otimes N}) \in [-1, 1]$, so that we can describe any $\varpi \in \mathcal{G}$ by the triple of real numbers $\{c_1, c_2, c_3\}$. Every ϖ has a maximally mixed marginal state with respect to any combination of qubits into a subsystem,

$$\begin{aligned} \mathrm{Tr}_{\backslash Q_\alpha}(\varpi) &= \mathrm{Tr}_{\backslash Q_\alpha} \left(\frac{1}{2^N} \left(\mathbb{I}^{\otimes N} + \sum_{i=1}^{3} c_i \sigma_i^{\otimes N} \right) \right) \\ &= \frac{1}{2^N} \left(\mathrm{Tr}_{\backslash Q_\alpha} \left(\mathbb{I}^{\otimes N} \right) + \sum_{i=1}^{3} c_i \mathrm{Tr}_{\backslash Q_\alpha} \left(\sigma_i^{\otimes N} \right) \right) \\ &= \frac{2^{N-K_\alpha}}{2^N} \mathbb{I}^{\otimes K_\alpha} = \frac{1}{2^{K_\alpha}} \mathbb{I}^{\otimes K_\alpha}, \end{aligned} \tag{4.20}$$

since the Pauli matrices are traceless, where $\mathrm{Tr}_{\backslash Q_\alpha}(\varpi)$ is the partial trace over all but subsystem Q_α, for any subsystem Q_α consisting of K_α qubits. It is then said that the ϖ are N qubit states with maximally mixed marginals and are called $\mathcal{M}_N^3$ states, where we associate $\mathcal{G} = \mathcal{M}_N^3$. The resource non-increasing projection $\Pi(\rho) \in \mathcal{G}$ is then called the $\mathcal{M}_N^3$-fication of ρ. Note that the $\mathcal{M}_N^3$ states have been investigated independently in Ref. [151].

The characterisation of the $\mathcal{M}_N^3$ states depends on whether N is even or odd. For even N all the $\mathcal{M}_N^3$ states commute with each other, i.e. $[\varpi_1, \varpi_2] = 0$ for any $\varpi_1 \in \mathcal{M}_N^3$ and $\varpi_2 \in \mathcal{M}_N^3$. This means that the N even $\mathcal{M}_N^3$ states share a common eigenbasis, which is given in Ref. [TRB4]. The eigenvalues of such a $\varpi \in \mathcal{M}_N^3$ are the following:

$$\begin{aligned} &\left\{ \frac{1}{2^N} \left[1 + c_1 + (-1)^{N/2} c_2 + c_3 \right], \frac{1}{2^N} \left[1 + c_1 - (-1)^{N/2} c_2 - c_3 \right], \right. \\ &\left. \frac{1}{2^N} \left[1 - c_1 + (-1)^{N/2} c_2 - c_3 \right], \frac{1}{2^N} \left[1 - c_1 - (-1)^{N/2} c_2 + c_3 \right] \right\}, \end{aligned}$$

where each eigenvalue is $\frac{2^N}{4}$ level degenerate, i.e. with $\frac{2^N}{4}$ eigenvectors corresponding to the same eigenvalue. Hence, every ϖ is a mixed state for even $N > 2$. By imposing that every ϖ with triple $\{c_1, c_2, c_3\}$ is positive semidefinite, i.e. that the above eigenvalues are non-negative, it can be seen that the triple $\{c_1, c_2, c_3\}$ must lie within the tetrahedron $\mathcal{T}_{(-1)^{N/2}}$ with vertices

$$\left\{ \{1, (-1)^{N/2}, 1\}, \{1, -(-1)^{N/2}, -1\}, \{-1, (-1)^{N/2}, -1\}, \{-1, -(-1)^{N/2}, 1\} \right\}.$$

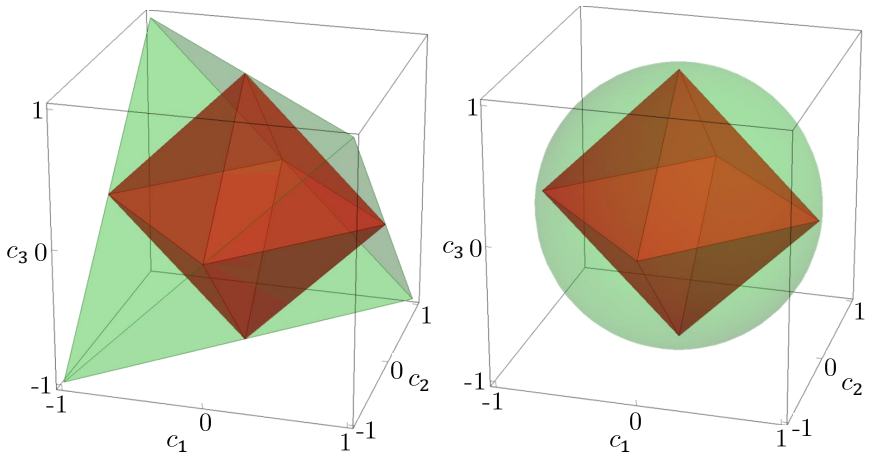

Figure 4.3: The $\mathcal{M}_N^3$ states in the $\{c_1, c_2, c_3\}$ space (shown in green) are contained within the tetrahedron $\mathcal{T}_{(-1)^{N/2}}$ for even N (left, for odd $N/2$) and the unit ball $\mathcal{B}_1$ for odd N (right). The M-separable $\mathcal{M}_N^3$ states for $M > \lceil N/2 \rceil$ are contained within the unit octahedron $\mathcal{O}_1$ with vertices $\{\pm 1, 0, 0\}$, $\{0, \pm 1, 0\}$ and $\{0, 0, \pm 1\}$ (shown in red), while all $\mathcal{M}_N^3$ states are M-separable for $M \leq \lceil N/2 \rceil$. The $\mathcal{M}_N^3$ states are an example of resource guarantor states given by the resource non-increasing projection of Eq. (4.16).

When $N = 2$, the $\mathcal{M}_N^3$ states coincide with the well known Bell-diagonal states, consisting of mixtures of the four maximally entangled pure Bell states [2, 152].

On the other hand, when N is odd, the $\mathcal{M}_N^3$ states do not commute since they no longer share a common eigenbasis. The eigenvalues of the N odd $\mathcal{M}_N^3$ states are $\frac{1}{2^N}(1 \pm r)$ where $r := \sqrt{c_1^2 + c_2^2 + c_3^2}$, with each eigenvalue $\frac{2^N}{2}$ level degenerate. Hence, for odd $N > 1$, every ϖ is a mixed state (for $N = 1$, the $\mathcal{M}_N^3$ states coincide with the set of all qubit states). It can be seen that the $\mathcal{M}_N^3$ states for odd N lie in the unit ball $\mathcal{B}_1$ in the $\{c_1, c_2, c_3\}$ space, an extension of the Bloch ball representation of a qubit discussed in Section 1.2.4. Figure 4.3 shows the $\mathcal{M}_N^3$ states in the $\{c_1, c_2, c_3\}$ space for even and odd N.

Step Two

In this step we identify the M-separable $\mathcal{M}_N^3$ states, $\mathcal{S}_M^{\mathcal{M}_N^3}$. This is done analytically by finding the $\mathcal{M}_N^3$-fication of all the M-separable states, as is shown in the proof of the following theorem.

Theorem 8 *For any N, the set of M-separable $\mathcal{M}_N^3$ states $\mathcal{S}_M^{\mathcal{M}_N^3}$ is either* [TRB4]*:*

- *the set of all $\mathcal{M}_N^3$ states, for any $M \leq \lceil N/2 \rceil$;*
- *the set of $\mathcal{M}_N^3$ states represented in the $\{c_1, c_2, c_3\}$ space by the unit octahedron $\mathcal{O}_1$ with vertices $\{\pm 1, 0, 0\}$, $\{0, \pm 1, 0\}$ and $\{0, 0, \pm 1\}$, for any $M > \lceil N/2 \rceil$.*

The proof of this theorem is also provided in Appendix C. It tells us that the $\mathcal{M}_N^3$ states are always M-separable for any $M \leq \lceil N/2 \rceil$ so that in this case $E_M^{D_\delta}(\varpi) = 0$ for all $\varpi \in \mathcal{M}_N^3$, which means in particular that $E_M^{D_\delta}(\Pi(\rho)) = 0$ and our lower bound on the multiqubit entanglement of a general state ρ is trivial. However, when $M > \lceil N/2 \rceil$ the $\mathcal{M}_N^3$ states are not always M-separable. Figure 4.3 shows the M-separable $\mathcal{M}_N^3$ states for $M > \lceil N/2 \rceil$ in the $\{c_1, c_2, c_3\}$ space. Indeed, if the triple $\{c_1, c_2, c_3\}$ of ϖ does not lie within the unit octahedron $\mathcal{O}_1$, or equivalently if $|c_1| + |c_2| + |c_3| > 1$, then ϖ is M-inseparable. In such a way, if the triple of $\Pi(\rho)$ for an arbitrary state ρ lies outside of the unit octahedron $\mathcal{O}_1$, then we can find nontrivial lower bounds on $E_M^{D_\delta}(\rho)$. Hence, the next step focusses on calculating $E_M^{D_\delta}(\varpi)$ for any $\varpi \in \mathcal{M}_N^3$ and $M > \lceil N/2 \rceil$.

Step Three

Now we calculate $E_M^{D_\delta}(\varpi)$ for any $\varpi \in \mathcal{M}_N^3$ and $M > \lceil N/2 \rceil$ by making use of the simplification from Eq. (4.10), i.e. that

$$E_M^{D_\delta}(\varpi) = \inf_{\varsigma \in \mathcal{S}_M^{\mathcal{M}_N^3}} D_\delta(\varpi, \varsigma). \tag{4.21}$$

From Theorem 8, if ϖ has a triple $\{c_1, c_2, c_3\}$ such that $|c_1| + |c_2| + |c_3| \leq 1$ then $\varpi \in \mathcal{S}_M^{\mathcal{M}_N^3}$ and $E_M^{D_\delta}(\varpi) = 0$. The case of $|c_1| + |c_2| + |c_3| > 1$ is dealt separately for even and odd N.

For even N, the M-inseparable $\mathcal{M}_N^3$ states can be found in the $\{c_1, c_2, c_3\}$ space by the four corners of the tetrahedron $\mathcal{T}_{(-1)^{N/2}}$, which are all local unitarily equivalent so that it is only necessary to focus on one of them. We make use of the universal properties of contractivity and joint convexity of the distance D_δ

to evaluate $E_M^{D_\delta}(\varpi)$ for any D_δ. This is achieved by finding one of the closest M-separable $\mathcal{M}_N^3$ states $\varsigma_\varpi \in \mathcal{S}_M^{\mathcal{M}_N^3}$ to ϖ that universally satisfies the infimum in Eq. (4.21) for any D_δ. Figure 4.4 shows a zoomed in diagram of one of the four corners of the tetrahedron $\mathcal{T}_{(-1)^{N/2}}$. The closest M-separable $\mathcal{M}_N^3$ state ς_ϖ to an $\mathcal{M}_N^3$ state ϖ can be found in the $\{c_1, c_2, c_3\}$ space by extending the line, which connects the corresponding corner of the tetrahedron $\mathcal{T}_{(-1)^{N/2}}$ with ϖ, onto the plane given by the face of the M-separable octahedron $\mathcal{O}_1$. One can then evaluate the distance between ϖ and ς_ϖ and find that for any D_δ it is always a monotonically increasing function f_{D_δ} of the height $h_\varpi := \frac{1}{2}\left(\sum_{i=1}^3 |c_i| - 1\right)$ above the M-separable plane. The plane height h_ϖ is non-positive for all M-separable $\mathcal{M}_N^3$ states within the octahedron $\mathcal{O}_1$, while $0 < h_\varpi \leq 1$ for the M-inseparable $\mathcal{M}_N^3$ states. This then gives a closed formula for the M-inseparable multiqubit entanglement of ϖ,

$$E_M^{D_\delta}(\varpi) = \begin{cases} 0\,, & h_\varpi \leq 0 \text{ (or } M \leq N/2); \\ f_{D_\delta}(h_\varpi)\,, & \text{otherwise.} \end{cases} \tag{4.22}$$

Particular instances of $f_{D_\delta}(h_\varpi)$, for each distance D_δ given in Table 1.1, are shown in Table 4.1. We sketch the details of the derivation of this result in the following, which follows from Appendix E of Ref. [TRB4].

For odd N and $M > \lceil N/2 \rceil$, there is not a universal closest M-separable $\mathcal{M}_N^3$ state for every distance D_δ, although the closest separable state is still independent of the choice of M and N. We focus in particular on evaluating $E_M^{D_{Tr}}(\varpi)$ for the trace distance D_{Tr}. The trace distance between any two N-odd $\mathcal{M}_N^3$ states has the useful property of being equivalent to (half) the Euclidean distance between their two vectors in the $\{c_1, c_2, c_3\}$ space, so that the closest M-separable $\mathcal{M}_N^3$ state ς_ϖ to any M-inseparable $\mathcal{M}_N^3$ state ϖ is simply, in the $\{c_1, c_2, c_3\}$ space, the Euclidean orthogonal projection onto the unit octahedron $\mathcal{O}_1$. We then have that

$$E_M^{D_{\mathrm{Tr}}}(\varpi) = \begin{cases} 0\,, & h_\varpi \leq 0 \text{ (or } M \leq \lceil N/2 \rceil); \\ \frac{h_\varpi}{\sqrt{3}}\,, & 0 < h_\varpi \leq 3|c_j|/2 \ \forall j; \\ \min\limits_j \frac{1}{2}\sqrt{|c_j|^2 + \frac{1}{2}(2h_\varpi - |c_j|)^2}\,, & \text{otherwise,} \end{cases} \tag{4.23}$$

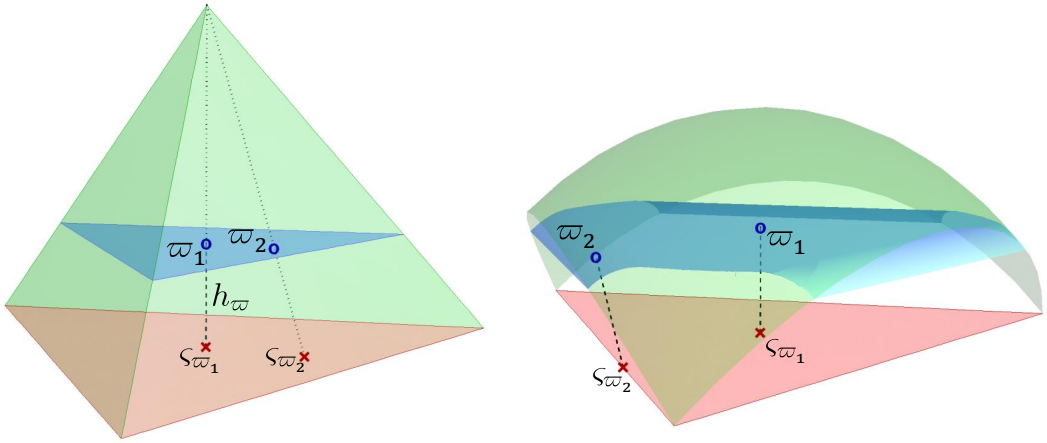

Figure 4.4: An enlargement of the tetrahedron $\mathcal{T}_{(-1)^{N/2}}$ of N even $\mathcal{M}_N^3$ states in the $\{c_1, c_2, c_3\}$ space onto one of the corners given by the M-inseparable $\mathcal{M}_N^3$ states for $M > N/2$ (left), and an enlargement of the unit ball $\mathcal{B}_1$ of $N > 1$ odd $\mathcal{M}_N^3$ states in the $\{c_1, c_2, c_3\}$ space into one of the octants given by the M-inseparable $\mathcal{M}_N^3$ states for $M > \lceil N/2 \rceil$ (right). The red planes represent the border of the unit octahedron $\mathcal{O}_1$ of M-separable $\mathcal{M}_N^3$ states. For even N, the closest M-separable $\mathcal{M}_N^3$ state ς_ϖ to any ϖ is given by extending the line connecting the corner of the tetrahedron $\mathcal{T}_{(-1)^{N/2}}$ through ϖ onto the M-separable plane, with the corresponding distance $D_\delta(\varpi, \varsigma_\varpi)$ a function of only the plane height h_ϖ above the M-separable plane. Instead, for odd N, the closest M-separable $\mathcal{M}_N^3$ state according to the trace distance is given by the Euclidean orthogonal projection onto the M-separable plane. The blue surfaces represent surfaces of constant entanglement.

see Fig. 4.4. The second line of Eq. (4.23) represents the case when the M-inseparable $\mathcal{M}_N^3$ state is orthogonally above one of faces of the M-separable octahedron $\mathcal{O}_1$ (represented by ϖ_1 in the figure, with ς_{ϖ_1} the closest M-separable $\mathcal{M}_N^3$ state), while the third line of Eq. (4.23) represents the case when the M-inseparable $\mathcal{M}_N^3$ state is closest to one of the edges of the octahedron $\mathcal{O}_1$ (represented by ϖ_2 in the figure, with ς_{ϖ_2} the closest M-separable $\mathcal{M}_N^3$ state).

We return now to the even N and $M > N/2$ case and sketch the mathematical proof of the result of Eq. (4.22), following Ref. [TRB4], i.e. that $E_M^{D_\delta}(\varpi)$ is simply a monotonic function of the plane height h_ϖ for any D_δ. First, it is clear from the joint convexity of D_δ that the closest M-separable $\mathcal{M}_N^3$ state to any M-inseparable

D_δ	$f_{D_\delta}(h_\varpi)$
Trace	$\frac{1}{2}h_\varpi$
Hellinger (squared)	$2-\sqrt{1-h_\varpi}-\sqrt{1+h_\varpi}$
Bures (squared)	$2-\sqrt{1-h_\varpi}-\sqrt{1+h_\varpi}$
Infidelity	$\frac{1}{2}\left(1-\sqrt{1-h_\varpi^2}\right)$
Relative entropy	$\frac{1}{2}\Big[(1-h_\varpi)\log_2(1-h_\varpi) + (1+h_\varpi)\log_2(1+h_\varpi)\Big]$

Table 4.1: The M-inseparable multiqubit entanglement $E_M^{D_\delta}(\varpi)$ of an $\mathcal{M}_N^3$ state with even N and $M > N/2$, as given by Eq. (4.22), is a monotonic function $f_{D_\delta}(h_\varpi)$ of the plane height h_ϖ whenever $h_\varpi > 0$.

$\mathcal{M}_N^3$ state ϖ must lie on the corresponding surface of the M-separable octahedron $\mathcal{O}_1$. Now, consider the two M-inseparable $\mathcal{M}_N^3$ states ϖ_1 and ϖ_2 shown in Fig. 4.4 sitting on the same plane with height h_ϖ, along with the two corresponding M-separable $\mathcal{M}_N^3$ states ς_{ϖ_1} and ς_{ϖ_2} given by extending the line connecting the corner of the tetrahedron $\mathcal{T}_{(-1)^{N/2}}$ through ϖ_1 and ϖ_2, respectively, onto the M-separable plane. We think of ϖ_2 as a general $\mathcal{M}_N^3$ state on this plane while ϖ_1 is the particular $\mathcal{M}_N^3$ state at the centre of the plane. It can be shown that

$$D_\delta(\varpi_1, \varsigma_{\varpi_1}) = D_\delta(\varpi_2, \varsigma_{\varpi_2}). \tag{4.24}$$

This is done by identifying two quantum operations Λ_{in} and Λ_{out} such that

$$\begin{aligned} \Lambda_{\text{in}}(\varpi_2) &= \varpi_1 \qquad & \Lambda_{\text{out}}(\varpi_1) &= \varpi_2 \\ \Lambda_{\text{in}}(\varsigma_{\varpi_2}) &= \varsigma_{\varpi_1} \qquad & \Lambda_{\text{out}}(\varsigma_{\varpi_1}) &= \varsigma_{\varpi_2}, \end{aligned}$$

so that from contractivity of D_δ

$$\begin{aligned} D_\delta(\varpi_2, \varsigma_{\varpi_2}) &\geq D_\delta(\Lambda_{\text{in}}(\varpi_2), \Lambda_{\text{in}}(\varsigma_{\varpi_2})) = D_\delta(\varpi_1, \varsigma_{\varpi_1}) \\ D_\delta(\varpi_1, \varsigma_{\varpi_1}) &\geq D_\delta(\Lambda_{\text{out}}(\varpi_1), \Lambda_{\text{out}}(\varsigma_{\varpi_1})) = D_\delta(\varpi_2, \varsigma_{\varpi_2}). \end{aligned} \tag{4.25}$$

These two quantum operations are given in Ref. [TRB4]. Now consider the distance between ϖ_2 and an arbitrary M-separable $\mathcal{M}_N^3$ state ς on the M-separable plane. It can be found that $\Lambda_{\text{in}}(\varsigma) = \varsigma_{\varpi_1}$ so that

$$D_\delta(\varpi_2, \varsigma) \geq D_\delta(\Lambda_{\text{in}}(\varpi_2), \Lambda_{\text{in}}(\varsigma)) = D_\delta(\varpi_1, \varsigma_{\varpi_1}) = D_\delta(\varpi_2, \varsigma_{\varpi_2}), \tag{4.26}$$

which tells us that ς_{ϖ_2} is the closest M-separable $\mathcal{M}_N^3$ state to ϖ_2, i.e.

$$E_M^{D_{\text{Tr}}}(\varpi_2) = D_\delta(\varpi_2, \varsigma_{\varpi_2}) \tag{4.27}$$

for any ϖ_2. This is the main result of Appendix E of Ref. [TRB4]. It can further be shown that $E_M^{D_{\text{Tr}}}(\varpi_2)$ is a monotonic function f_{D_δ} of the plane height h_ϖ, which relies on the fact that $D_\delta(\varpi_2, \varsigma_{\varpi_2}) = D_\delta(\varpi_1, \varsigma_{\varpi_1})$, with $D_\delta(\varpi_1, \varsigma_{\varpi_1})$ a function only of the plane height, and also joint convexity of D_δ, which then imposes that the distance to the M-separable plane must increase with the plane height.

Before proceeding to discuss the final step, we note that the set of M-separable $\mathcal{M}_N^3$ states can be expressed in a general way as any operator $\varpi \geq 0$ with $\text{Tr}(\varpi) = 1$ satisfying the following finite number of conditions

$$\begin{aligned}
\text{Tr}\left(\varpi\sigma_{i_1} \otimes \sigma_{i_2} \ldots \otimes \sigma_{i_N}\right) = 0 \quad \forall \quad \{i_1, i_2, \ldots, i_N\} \quad &\neq \quad \{i, i, \ldots i\},\ i \in \{0,1,2,3\}, \\
\text{Tr}\left(\varpi\sigma_1^{\otimes N}\right) + (-1)^{N/2}\text{Tr}\left(\varpi\sigma_2^{\otimes N}\right) \quad &+ \quad \text{Tr}\left(\varpi\sigma_3^{\otimes N}\right) \leq 1, \\
\text{Tr}\left(\varpi\sigma_1^{\otimes N}\right) - (-1)^{N/2}\text{Tr}\left(\varpi\sigma_2^{\otimes N}\right) \quad &- \quad \text{Tr}\left(\varpi\sigma_3^{\otimes N}\right) \leq 1, \\
-\text{Tr}\left(\varpi\sigma_1^{\otimes N}\right) - (-1)^{N/2}\text{Tr}\left(\varpi\sigma_2^{\otimes N}\right) \quad &+ \quad \text{Tr}\left(\varpi\sigma_3^{\otimes N}\right) \leq 1, \\
-\text{Tr}\left(\varpi\sigma_1^{\otimes N}\right) + (-1)^{N/2}\text{Tr}\left(\varpi\sigma_2^{\otimes N}\right) \quad &- \quad \text{Tr}\left(\varpi\sigma_3^{\otimes N}\right) \leq 1.
\end{aligned} \tag{4.28}$$

This equation, combined with Eq. (4.6), tells us that the robustness of M-inseparable multiqubit entanglement for $\mathcal{M}_N^3$ states is the solution of an SDP and can therefore be evaluated numerically. Nevertheless, we focus here on the analytical results found for the distance-based approach.

Step Four

As we have seen, every N qubit state ρ is transformed into a corresponding $\mathcal{M}_N^3$ state $\varpi = \Pi(\rho)$ with $E_M^{D_\delta}(\varpi) \leq E_M^{D_\delta}(\rho)$. This lower bound may be improved

by varying ρ over the unitaries that are local with respect to each qubit, which are the free unitaries of M-inseparable multiqubit entanglement. For any unitary $U_\otimes$ acting locally on the qubits such that $U_\otimes = \bigotimes_{\alpha=1}^{N} U^{(\alpha)}$ for the single qubit unitaries $U^{(\alpha)}$, we have $E_M^{D_\delta}(U_\otimes \rho U_\otimes^\dagger) = E_M^{D_\delta}(\rho)$. Furthermore,

$$E_M^{D_\delta}(\tilde{\varpi}) \leq E_M^{D_\delta}(U_\otimes \rho U_\otimes^\dagger) = E_M^{D_\delta}(\rho) \tag{4.29}$$

where $\tilde{\varpi} = \Pi(U_\otimes \rho U_\otimes^\dagger)$ is an $\mathcal{M}_N^3$ state with $\tilde{c}_i = \mathrm{Tr}(U_\otimes \rho U_\otimes^\dagger \sigma_i^{\otimes N})$. Hence, we aim to perform the optimisation

$$\sup_{U_\otimes} E_M^{D_\delta}(\tilde{\varpi}) \leq E_M^{D_\delta}(\rho), \tag{4.30}$$

giving the best lower bound on the M-inseparable multiqubit entanglement of ρ by using $\mathcal{M}_N^3$-fication. To understand this optimisation, we turn to the correlation tensor $R_{i_1 i_2 \ldots i_N} = \mathrm{Tr}(\rho\, \sigma_{i_1} \otimes \sigma_{i_2} \otimes \ldots \otimes \sigma_{i_N}) \in [-1, 1]$ used to describe any N qubit state in Eq. (1.61), with $i_j \in \{0, 1, 2, 3\}$ for $j \in \{1, 2, \ldots, N\}$. The correspondence between the special unitary group $\mathsf{SU}(2)$ and special orthogonal group $\mathsf{SO}(3)$ [20] says that for any qubit unitary $U^{(\alpha)}$ there is a corresponding orthogonal 3×3 matrix $O^{(\alpha)}$ such that $U^{(\alpha)} \vec{n} \cdot \vec{\sigma} U^{(\alpha)\dagger} = (O^{(\alpha)} \vec{n}) \cdot \vec{\sigma}$, where $\vec{n} = \{n_1, n_3, n_3\} \in \mathbb{R}^3$ and $\vec{\sigma} = \{\sigma_1, \sigma_2, \sigma_3\}$ is the vector of Pauli matrices. Then, the correlation tensor of $U_\otimes \rho U_\otimes^\dagger$ is

$$\tilde{R}_{i_1 i_2 \cdots i_N} = \sum_{j_1 j_2 \cdots j_N = 0}^{3} R_{j_1 j_2 \cdots j_N} O^{(1)}_{i_1 j_1} O^{(2)}_{i_2 j_2} \cdots O^{(N)}_{i_N j_N}. \tag{4.31}$$

For even N, the optimisation in Eq. (4.30) may be achieved by finding a local unitary $U_\otimes$ so that the plane height $h_{\tilde{\varpi}} = \frac{1}{2}(\sum_{i=1}^{3} |\tilde{c}_i| - 1)$ is largest, or equivalently by solving

$$\sup_{U_\otimes} \left(|\tilde{c}_1| + |\tilde{c}_2| + |\tilde{c}_3|\right) = \sup_{\{O^{(\alpha)}\}} \left(|\tilde{R}_{11\cdots 1}| + |\tilde{R}_{22\cdots 2}| + |\tilde{R}_{33\cdots 3}|\right). \tag{4.32}$$

This optimisation can be solved analytically for $N = 2$ and is given by the orthogonal matrices that diagonalise the correlation matrix $\tilde{R}_{i_1 i_2}$ due to the singular value decomposition [153]. For $N > 2$ this optimisation can be carried out numerically, and can be greatly simplified if ρ is invariant under all permutations of the N qubits. If so, the correlation tensor is fully symmetric, i.e.

$R_{i_1 i_2 \cdots i_N} = R_{\vartheta(i_1 i_2 \cdots i_N)}$ for any permutation ϑ of the indices. When this is the case, it is known that Eq. (4.32) may be solved by restricting the optimisation to identical orthogonal matrices $O^{(1)} = O^{(2)} = \cdots = O^{(N)}$ [153]. A 3×3 orthogonal matrix O can be fully described by three real angles $\{\theta, \psi, \phi\}$ which correspond to the qubit unitary

$$U = \begin{pmatrix} \cos\frac{\theta}{2} e^{-i\frac{\psi+\phi}{2}} & -i\sin\frac{\theta}{2} e^{-i\frac{\phi-\psi}{2}} \\ -i\sin\frac{\theta}{2} e^{i\frac{\phi-\psi}{2}} & \cos\frac{\theta}{2} e^{i\frac{\psi+\phi}{2}} \end{pmatrix}. \tag{4.33}$$

Hence, if ρ is invariant under all permutations of the N qubits, then one only needs to optimise over three angles to solve Eq. (4.32).

4.2.2 Application and Comparison

The lower bounds to the M-inseparable multiqubit entanglement provided by $\mathcal{M}_N^3$ states can be evaluated for important instances of N qubit states. The Greenberger-Horne-Zeilinger (GHZ) [154] and W states [73] are well established examples of N qubit states that are of importance both theoretically and experimentally [20, 73, 155–161] and are given by, respectively,

$$\begin{aligned} |GHZ^{(N)}\rangle &:= \frac{1}{\sqrt{2}}\left(|00\ldots00\rangle + |11\ldots11\rangle\right), \\ |W^{(N)}\rangle &:= \frac{1}{\sqrt{N}}\left(|00\ldots01\rangle + |00\ldots10\rangle + \ldots + |01\ldots00\rangle + |10\ldots00\rangle\right), \end{aligned} \tag{4.34}$$

where $|b_1 b_2 \ldots b_{N-1} b_N\rangle := |b_1\rangle \otimes |b_2\rangle \otimes \ldots \otimes |b_{N-1}\rangle \otimes |b_N\rangle$ with $b_j \in \{0, 1\}$ for all $j \in \{1, 2, \ldots, N\}$. Table 4.2 gives the lower bound to the M-inseparable multiqubit entanglement of these states for any $M > \lceil N/2 \rceil$ provided by optimising $E_M^{D_\delta}(\tilde{\varpi})$ of the corresponding $\mathcal{M}_N^3$ states $\tilde{\varpi} = \Pi(U_\otimes |GHZ^{(N)}\rangle \langle GHZ^{(N)}| U_\otimes^\dagger)$ and $\tilde{\varpi} = \Pi(U_\otimes |W^{(N)}\rangle \langle W^{(N)}| U_\otimes^\dagger)$ over local unitaries $U_\otimes$ for various N. Since both the GHZ and W states are permutationally invariant with respect to permutations of any of the N qubits, we can use the already discussed simplification of restricting to identical qubit unitaries, i.e. $U_\otimes = U^{\otimes N}$ for the qubit unitary U given in Eq. (4.33), and hence only optimising $E_M^{D_\delta}(\tilde{\varpi})$ over three angles $\{\theta, \psi, \phi\}$, which are also given in the table.

N	State	$\{\tilde{c}_1, \tilde{c}_2, \tilde{c}_3\}$	$\sum_{j=1}^{3} \lvert\tilde{c}_j\rvert$	$\{\theta, \psi, \phi\}$
$N=3$	$\lvert\mathrm{GHZ}^{(3)}\rangle$	$\left\{-\sqrt{\frac{8}{27}}, \sqrt{\frac{8}{27}}, -\sqrt{\frac{8}{27}}\right\}$	$2\sqrt{\frac{2}{3}}$	$\left\{\cos^{-1}(\frac{1}{\sqrt{3}}), \frac{5\pi}{30}, \frac{\pi}{4}\right\}$
$N=3$	$\lvert\mathrm{W}^{(3)}\rangle$	$\left\{\frac{1}{\sqrt{3}}, -\frac{1}{\sqrt{3}}, \frac{1}{\sqrt{3}}\right\}$	$\sqrt{3}$	$\left\{\cos^{-1}(\frac{1}{\sqrt{3}}), 0, \frac{\pi}{4}\right\}$
$N=4$	$\lvert\mathrm{GHZ}^{(4)}\rangle$	$\{1, 1, 1\}$	3	$\{0, 0, 0\}$
$N=4$	$\lvert\mathrm{W}^{(4)}\rangle$	$\left\{\frac{5}{9}, \frac{5}{9}, \frac{5}{9}\right\}$	$\frac{5}{3}$	$\left\{\cos^{-1}(\frac{1}{\sqrt{3}}), 0, \frac{\pi}{4}\right\}$
$N=5$	$\lvert\mathrm{GHZ}^{(5)}\rangle$	$\left\{\frac{1}{\sqrt{2}}, \frac{1}{\sqrt{2}}, 0\right\}$	$\sqrt{2}$	$\left\{0, \frac{\pi}{40}, \frac{\pi}{40}\right\}$
$N=5$	$\lvert\mathrm{W}^{(5)}\rangle$	$\left\{\frac{7}{9\sqrt{3}}, -\frac{7}{9\sqrt{3}}, \frac{7}{9\sqrt{3}}\right\}$	$\frac{7}{3\sqrt{3}}$	$\left\{\cos^{-1}(\frac{1}{\sqrt{3}}), 0, \frac{\pi}{4}\right\}$
$N=6$	$\lvert\mathrm{GHZ}^{(6)}\rangle$	$\{1, -1, 1\}$	3	$\{0, 0, 0\}$
$N=6$	$\lvert\mathrm{W}^{(6)}\rangle$	$\{0, 0, -1\}$	1	$\{0, 0, 0\}$

Table 4.2: Lower bounds to the M-inseparable multiqubit entanglement for any $M > \lceil N/2 \rceil$ of N qubit GHZ and W states for various N. The lower bounds are given by the $\mathcal{M}_N^3$ states $\tilde{\varpi} = \Pi(U_\otimes \lvert GHZ^{(N)}\rangle \langle GHZ^{(N)}\rvert U_\otimes^\dagger)$ and $\tilde{\varpi} = \Pi(U_\otimes \lvert W^{(N)}\rangle \langle W^{(N)}\rvert U_\otimes^\dagger)$ satisfying the optimisation in Eq. (4.30) with triple $\{\tilde{c}_1, \tilde{c}_2, \tilde{c}_3\}$ and plane height $h_{\tilde{\varpi}} = \frac{1}{2}(\sum_{i=1}^{3} \lvert\tilde{c}_i\rvert - 1)$, so that the lower bound $E_M^{D_\delta}(\tilde{\varpi})$ may be evaluated by using Eq. (4.22) for even N and Eq. (4.23) for odd N. Due to the permutation invariance of the GHZ and W states, the optimisation need only be performed over the three angles $\{\theta, \psi, \phi\}$ describing the unitary in Eq. (4.33). Note that $h_{\tilde{\varpi}} > 0$ only when $\sum_{i=1}^{3} \lvert\tilde{c}_i\rvert > 1$. For a more comprehensive application of our lower bounds found through $\mathcal{M}_N^3$-fication to a collection of important N qubit states, see Ref. [TRB4].

For even N the lower bound to the M-inseparable multiqubit entanglement provided for the GHZ state is maximum at $h_{\tilde{\varpi}} = 1$. In particular, for the relative entropy distance we have $E_M^{D_{RE}}(\tilde{\varpi}) = 1$ for $M > N/2$, which can be compared to the exact value for the multiqubit entanglement of $E_M^{D_{RE}}(\lvert GHZ^{(N)}\rangle \langle GHZ^{(N)}\rvert) = 1$ calculated in Refs. [TRB4, 162–164] for any M. Our lower bound is then tight for any even N when $M > N/2$. On the other hand, the lower bound to the M-inseparable multiqubit entanglement for W states decreases with increasing N and eventually becomes trivial beyond $N = 5$. This suggests that the lower bounds provided by performing $\mathcal{M}_N^3$-fication are more suited to GHZ-like states than W-like states, which is perhaps expected intuitively since the GHZ state

is actually an eigenstate of any $\mathcal{M}_N^3$ state. Improved lower bounds to the M-inseparable multiqubit entanglement for W states may be found by tailoring the entanglement non-increasing projection Π to project onto a different family of entanglement guarantor states.

Our lower bounds further apply to noisy versions of the GHZ and W states, e.g. by mixing the GHZ state with white noise

$$\rho_{GHZ}^{(N)}(q) := q\left|GHZ^{(N)}\right\rangle\left\langle GHZ^{(N)}\right| + \frac{1-q}{2^N}\mathbb{I}^{\otimes N}, \tag{4.35}$$

the corresponding local unitary optimised $\mathcal{M}_N^3$ state is given by $q\tilde{\varpi} + \frac{1-q}{2^N}\mathbb{I}^{\otimes N}$ with plane height $qh_{\tilde{\varpi}} - \frac{1-q}{2}$, where $\tilde{\varpi} = \Pi(U_\otimes \left|GHZ^{(N)}\right\rangle\left\langle GHZ^{(N)}\right| U_\otimes^\dagger)$. Hence, for the N even GHZ state with $h_{\tilde{\varpi}} = 1$, the lower bound to the M-inseparable multiqubit entanglement of $\rho_{GHZ}^{(N)}(q)$ for $M > N/2$ is non-trivial for $q > \frac{1}{3}$. This can be compared to the established separability threshold for $\rho_{GHZ}^{(N)}(q)$ of $q > 1/(1 + 2^{N-1})$ [62] when $M = N$. This separability threshold tends to zero with increasing N, while our threshold of $q > \frac{1}{3}$ for a non-trivial lower bound remains constant with N, so that we are unable to detect global multiqubit entanglement in an increasingly large region of q. However, our framework focuses on *quantification* of multiqubit entanglement in terms of lower bounds rather than the verification of multiqubit entanglement, which is itself an important topic [62, 68, 70, 165–170].

Furthermore, our results for $\mathcal{M}_N^3$ states are particularly appealing experimentally. Any $\mathcal{M}_N^3$ state $\varpi \in \mathcal{M}_N^3$ is specified by the three real coefficients $\{c_1, c_2, c_3\} \in [-1, 1]$ which may be measured in an experiment by finding the expectation values $\langle\sigma_i^{\otimes N}\rangle_\varpi = \mathrm{Tr}(\varpi\sigma_i^{\otimes N})$ for $i \in \{1, 2, 3\}$. Hence, to provide a lower bound on the M-inseparable multiqubit entanglement for any N qubit state ρ by finding the optimised $\mathcal{M}_N^3$ state $\tilde{\varpi} = \Pi(U_\otimes \rho U_\otimes^\dagger)$, one need only measure the triple $\{\tilde{c_1}, \tilde{c_2}, \tilde{c_2}\}$ given by three expectation values

$$\langle\sigma_i^{\otimes N}\rangle_{\tilde{\varpi}} = \mathrm{Tr}(\tilde{\varpi}\sigma_i^{\otimes N}) = \mathrm{Tr}(U_\otimes \rho U_\otimes^\dagger \sigma_i^{\otimes N}) = \mathrm{Tr}(\rho U_\otimes^\dagger \sigma_i^{\otimes N} U_\otimes) = \left\langle \bigotimes_{\alpha=1}^{N} \tilde{\sigma}_i^{(\alpha)} \right\rangle_\rho,$$

where $\bigotimes_{\alpha=1}^N \tilde{\sigma}_i^{(\alpha)} := U_\otimes^\dagger \sigma_i^{\otimes N} U_\otimes$ is an observable corresponding to a local unitary rotation of the tensor product of Pauli matrices. The three expectation values

of $\bigotimes_{\alpha=1}^{N} \tilde{\sigma}_i^{(\alpha)}$ for $i \in \{1,2,3\}$ may be found experimentally by each qubit subsystem performing a local measurement in a rotated Pauli basis $\{\tilde{\sigma}_i^{(\alpha)}\}_{i=1}^{3}$ and then communicating the results. Since the state ρ of the experimental system may not be known (i.e. if full state tomography has not been carried out), the choice of locally rotated Pauli basis may be given by assuming that ρ is the target state of the experiment and finding the solution of Eq. (4.30). It can thus be said that our lower bound is provided with three local measurement settings. This compares well to other results aimed at providing experimentally friendly lower bounds to multiqubit entanglement [129, 145–148, 171–176], which typically require at least on the order of N local measurement settings. Furthermore, a strength of our result is that it provides lower bounds for all distance-based measures of multiqubit entanglement and for any $M > \lceil N/2 \rceil$. A detailed comparison of our result to other works is given in Ref. [TRB4].

To demonstrate the relevance of our lower bound on M-inseparable multiqubit entanglement to experiments, we apply our findings to some real experimental data. Previous experiments have created and analysed Smolin, Dicke, GHZ and W states, as detailed in the following. Table 4.3 provides lower bounds on the M-inseparable multiqubit entanglement of these experimental states for $M > \lceil N/2 \rceil$ in terms of the trace distance. In each case, our lower bounds are non-trivial. We now provide further details on the reported experimental states. Generalised Smolin states $\rho_S^{(N)}$ of even $N \geq 4$ qubits [151, 177, 178] are special instances of $\mathcal{M}_N^3$ states with correlation triple $\{(-1)^{N/2}, (-1)^{N/2}, (-1)^{N/2}\}$ occupying one of the corners of the tetrahedron $\mathcal{T}_{(-1)^{N/2}}$ in the $\{c_1, c_2, c_3\}$ space, so that we have exactly quantified their entanglement through our approach. A noisy Smolin state $\rho_S^{(N)}(q)$ can be formed in an analogous way to Eq. (4.35) by mixing with white noise, and is also an $\mathcal{M}_N^3$ state sitting on the line connecting the $\{(-1)^{N/2}, (-1)^{N/2}, (-1)^{N/2}\}$ vertex with the origin in the $\{c_1, c_2, c_3\}$ space. A noisy Smolin state of 4 qubits has been generated in Ref. [179] using a quantum optics setup. Symmetric N qubit Dicke states [180, 181]

$$|\mathrm{D}_k^{(N)}\rangle := \frac{1}{\sqrt{Z}} \sum_i \Pi_i (|0\rangle^{\otimes N-k} \otimes |1\rangle^{\otimes k}) \tag{4.36}$$

are superpositions of states with k qubits in the excited state $|1\rangle$ and $N-k$ qubits in the ground state $|0\rangle$, with $\{\Pi_i(\cdot)\}_{i=1}^{Z}$ denoting all the $Z := \binom{N}{k}$ distinct permutations of k tensor products of $|1\rangle$ and $N-k$ tensor products of $|0\rangle$ (where $\binom{N}{k}$ is the binomial coefficient). The even N half excited Dicke states, i.e. with $k = N/2$, are particularly relevant in many-body physics [181] and have a corresponding $\mathcal{M}_N^3$ state with triple $\{1,1,1\}$, hence giving the maximum plane height of $h_\varpi = 1$ and the optimum lower bound to M-inseparable multiqubit entanglement possible through $\mathcal{M}_N^3$-fication. Noisy versions of these half excited Dicke states have been generated for six qubits in two separate quantum optics experiments [182, 183]. Finally, noisy GHZ and W states have been generated in a series of trapped ion experiments [184, 185].

4.2.3 Alternative Projections

As we have seen, the $\mathcal{M}_N^3$ states are M-separable for any $M \leq \lceil N/2 \rceil$. In particular, the $\mathcal{M}_N^3$ states are always 2-separable and hence do not exhibit the strongest form of entanglement with all of the N qubits entangled together. Even if one were to pick a 2-inseparable state ρ, the projection onto the $\mathcal{M}_N^3$ states $\Pi(\rho)$ would be 2-separable. Hence, it could be argued that in this respect the $\mathcal{M}_N^3$-fication projection is too strong since it always destroys the genuine N qubit entanglement. To remedy this, we can choose an alternative entanglement non-increasing projection with a different corresponding set of resource guarantor states.

Consider an ONB of GHZ-like states

$$|\beta_i^{\pm}\rangle := \frac{1}{\sqrt{2}}\left(\mathbb{I}^{\otimes N} \pm \sigma_1^{\otimes N}\right)|i\rangle \tag{4.37}$$

where $i \in \{1, 2, \ldots, 2^{N-1}\}$ and $\{|i\rangle\}_{i=1}^{2^N}$ is the N qubit computational basis in binary order. The standard GHZ state of Eq. (4.34) is given in particular by $|\beta_1^+\rangle$. Any state with its eigenbasis given by this ONB can be written in terms of its eigenvalues and eigenvectors as

$$\xi = \sum_{i=1}^{2^{N-1}} \sum_{\pm} p_i^{\pm} |\beta_i^{\pm}\rangle \langle\beta_i^{\pm}| \tag{4.38}$$

Target State	Ref.	Fidelity (%)	$\sum_{j=1}^{3} \lvert\tilde{c}_j\rvert$	$E_M^{D_{\mathrm{Tr}}}$
$\varrho_{\mathrm{S}}^{(4)}(0.51)$	[179]	96.83 ± 0.05	1.16 ± 0.01	0.040 ± 0.002
$\lvert \mathrm{D}_3^{(6)} \rangle$	[182]	56 ± 2	1.6 ± 0.3	0.15 ± 0.08
$\lvert \mathrm{D}_3^{(6)} \rangle$	[183]	65 ± 2	1.69 ± 0.04	0.17 ± 0.01
$\lvert GHZ^{(4)} \rangle$	[185]	80.3	2.25	0.312
$\lvert W^{(4)} \rangle_A$	[185]	19.4	1.24	0.0589
$\lvert W^{(4)} \rangle_B$	[185]	31.4	1.39	0.0963

Table 4.3: Lower bounds to the M-inseparable multiqubit entanglement for $M > \lceil N/2 \rceil$ of N qubit noisy Smolin, Dicke, GHZ and W states generated in the laboratory for $N = 4$ and $N = 6$. The lower bounds are given by the corresponding $\mathcal{M}_N^3$ state $\tilde{\varpi}$ with triple $\{\tilde{c}_1, \tilde{c}_2, \tilde{c}_3\}$ and plane height $h_{\tilde{\varpi}} = \frac{1}{2}(\sum_{i=1}^{3} |\tilde{c}_i| - 1)$, with the lower bound $E_M^{D_\delta}(\tilde{\varpi})$ evaluated using Eq. (4.22) in particular for the trace distance. The experimental data for the Smolin and Dicke states directly provided the corresponding $\mathcal{M}_N^3$ state $\tilde{\varpi}$ through measurement of the observables $\sigma_i^{\otimes N}$, without allowing for optimisation over local unitaries. Instead, full state tomography was provided for the GHZ state and W states (consisting of two data sets A and B), allowing for a numerical optimisation of the plane height $h_{\tilde{\varpi}}$ over local unitaries. The fidelities according to Eq. (1.30) of the experimentally generated state with the target state are also reported, showing that in some cases the generated state is particularly noisy. However, note that we do not need to assume that the experimentally generated states are of a particular class to provide our lower bounds.

with the eigenvalues $\{p_i^{\pm}\}_{i,\pm}$ forming a probability distribution. Such states are called GHZ-diagonal and are denoted by the set $\mathcal{G}_N$. The GHZ-diagonal states are particularly relevant to study genuine multiqubit entanglement and it has been shown that their biseparable states are all and only those for which we have $p_{\max} := \max_{i,\pm} p_i^{\pm} \leq 1/2$ [68]. Furthermore, the so-called genuine multiparticle negativity and genuinely multipartite concurrence, which are two other measures of 2-inseparable multiqubit entanglement not discussed here, have been evaluated for GHZ-diagonal states [146, 172] and can be seen to coincide up to a factor of 2 (more details are provided in the following). However, the distance-based

measures of 2-inseparable multiqubit entanglement have been evaluated for GHZ-diagonal states only when using the relative entropy distance when restricted to three qubits [164]. It therefore seems fitting to see if our framework may be applied to the GHZ-diagonal states, focussing on 2-inseparability and the distance-based measures.

Actually, the first two steps of our framework have been established. It is well known that there exists a 2-inseparable multiqubit entanglement non-increasing projection Π which projects any N qubit state ρ onto the set of GHZ-diagonal states so that $\Pi(\rho) \in \mathcal{G}_N$ with eigenvalues given by [146]

$$p_i^{\pm} = \langle \beta_i^{\pm} | \rho | \beta_i^{\pm} \rangle \, . \tag{4.39}$$

We call such an entanglement non-increasing projection GHZ-diagonalisation, with the GHZ state $\Pi(\rho) \in \mathcal{G}_N$ an entanglement guarantor for ρ so that we have $E_2(\Pi(\rho)) \leq E_2(\rho)$. The second step of our framework has already been discussed, with the set of 2-separable GHZ-diagonal states given by [68]

$$\mathcal{S}_2^{\mathcal{G}_N} := \left\{ \xi \in \mathcal{G}_N \;\middle|\; p_{\max} := \max_{i,\pm} p_i^{\pm} \leq 1/2 \right\} \subset \mathcal{G}_N. \tag{4.40}$$

The primary contribution of our framework is in the simplification provided in the third step to calculate the distance-based 2-inseparable multiqubit entanglement of any GHZ-diagonal state $\xi \in \mathcal{G}_N$: Eq. (4.10) means that one of the closest 2-separable states ς_ξ to a GHZ-diagonal state is itself GHZ-diagonal, i.e. $\varsigma_\xi \in \mathcal{S}_2^{\mathcal{G}_N}$. Furthermore, we can use joint convexity of the distance to see that ς_ξ is on the border of $\mathcal{S}_2^{\mathcal{G}_N}$ with maximum eigenvalue exactly equal to $\frac{1}{2}$. With this simplification, the infimum in Eq. (4.14) may be evaluated analytically for each of the distances given in Table 1.1. The result is that for any $\xi \in \mathcal{G}_N$ with maximum eigenvalue $p_{\max}$,

$$E_2^{D_\delta}(\xi) = \begin{cases} 0 \, , & p_{\max} \leq 1/2; \\ g_{D_\delta}(p_{\max}) \, , & \text{otherwise}, \end{cases} \tag{4.41}$$

where g_{D_δ} is a monotonically increasing function of $p_{\max}$ for each D_δ, whose explicit form is given in Table 4.4.

D_δ	$g_{D_\delta}(p_{\max})$
Trace	$p_{\max} - \frac{1}{2}$
Hellinger (squared)	$2 - \sqrt{2}\left(\sqrt{1-p_{\max}} + \sqrt{p_{\max}}\right)$
Bures (squared)	$2 - \sqrt{2}\left(\sqrt{1-p_{\max}} + \sqrt{p_{\max}}\right)$
Infidelity	$\frac{1}{2} - \sqrt{p_{\max}(1-p_{\max})}$
Relative entropy	$1 + p_{\max}\log_2 p_{\max} + (1-p_{\max})\log_2(1-p_{\max})$

Table 4.4: The 2-inseparable multiqubit entanglement $E_2^{D_\delta}(\xi)$ of a GHZ-diagonal state $\xi \in \mathcal{G}_N$, as given by Eq. (4.41), is a monotonic function $g_{D_\delta}(p_{\max})$ of only the maximum eigenvalue $p_{\max}$ of ξ whenever $p_{\max} > 1/2$.

Analysing our results, it can be seen that Table 4.4 allows for an exact quantification of the genuine multiqubit entanglement of any N qubit GHZ state since $|GHZ^{(N)}\rangle\langle GHZ^{(N)}| \in \mathcal{G}_N$ with $p_{\max} = 1$. It can also be found that the genuine multiqubit entanglement of the GHZ-diagonal states according to the trace distance coincides with the genuine multiparticle negativity and half the genuinely multipartite concurrence, thus furnishing these measures with a geometric interpretation within this class of states. Furthermore, it is interesting to see that the distance-based measures of genuine multiqubit entanglement shown in Table 4.4 are only functions of the maximum eigenvalue $p_{\max}$ of the GHZ-diagonal state, so that $p_{\max}$ not only characterises the presence of genuine multiqubit entanglement in the GHZ-diagonal state but can also be used to measure the amount – as had already been acknowledged for the genuine multiparticle negativity and genuinely multipartite concurrence.

To provide lower bounds on the distance-based genuine multiqubit entanglement of any state ρ, one therefore only needs the maximum probability from Eq. (4.39) given by the maximum eigenvalue of the corresponding GHZ-diagonal state $\Pi(\rho)$. The final step of our framework is then to optimise the lower bound to the genuine multiqubit entanglement of ρ over local unitaries $U_\otimes$, which in this

case just means optimising $p_{\max} = \max_{i,\pm} \langle \beta_i^{\pm} | U_{\otimes} \rho U_{\otimes}^{\dagger} | \beta_i^{\pm} \rangle$ over $U_{\otimes}$, i.e.

$$\max_{U_{\otimes}} p_{\max} = \max_{U_{\otimes}} \max_{i,\pm} \langle \beta_i^{\pm} | U_{\otimes} \rho U_{\otimes}^{\dagger} | \beta_i^{\pm} \rangle = \max_{U_{\otimes}} \langle GHZ^{(N)} | U_{\otimes} \rho U_{\otimes}^{\dagger} | GHZ^{(N)} \rangle \,, \tag{4.42}$$

where in the second equality we use the fact that the $|\beta_i^{\pm}\rangle$ are local unitarily equivalent to the GHZ state $|GHZ^{(N)}\rangle = |\beta_1^{+}\rangle$. This quantity is the maximum fidelity, according to Eq. (1.30), of the GHZ state with ρ rotated in some local basis. As before, the local basis may be found experimentally with prior knowledge of the target state of the experimental system. It is then known that the fidelity with the GHZ state may be measured with $N + 1$ local measurement settings [186]. Hence, $N + 1$ local measurement settings can provide a lower bound on the 2-inseparable multiqubit entanglement. This can be compared to the 3 local measurement settings needed to provided lower bounds on the M-inseparable multiqubit entanglement for $M > \lceil N/2 \rceil$. Indeed, it may be expected that an increased number of local measurement settings is needed to detect the strongest form of entanglement. It is also clear from Eq. (2.25) that $E_2(\Pi(\rho)) \leq E_2(\rho) \leq E_M(\rho)$ for any M, i.e. that the lower bound $E_2(\Pi(\rho))$ on 2-inseparable multiqubit entanglement through GHZ-diagonalisation gives lower bounds on M-inseparable multiqubit entanglement of the state ρ. However, the lower bounds on M-inseparable multiqubit entanglement provided through $\mathcal{M}_N^3$-fication are still preferred for $M > \lceil N/2 \rceil$ since fewer lower measurement settings are required and the lower bounds can be nontrivial even for biseparable states.

4.3 Applying the Framework to Multiqubit Coherence

The projection of N qubit states onto the $\mathcal{M}_N^3$ states has not only been used to provide lower bounds to the resource of multiqubit entanglement. It has been shown in Ref. [TRB6] that $\mathcal{M}_N^3$-fication is also a coherence non-increasing projection (when the free operations are chosen to be the *incoherent operations*) for any N if one considers multiqubit coherence with respect to the computational

basis of each qubit, i.e. the product ONB $\{|i_1 i_2 \dots i_N\rangle\}_{i_1,i_2,\dots,i_N=0}^{1}$, as specified by the following theorem.

Theorem 9 *The projection* Π *of* $\mathcal{M}_N^3$*-fication in Eq.* (4.16) *is an incoherent operation with respect to the reference ONB* $\{|i_1 i_2 \dots i_N\rangle\}_{i_1,i_2,\dots,i_N=0}^{1}$*, i.e. there exists an operator sum representation of* Π *with Kraus operators* $\{K_i\}_i$ *such that* (3.1) *holds* [TRB6].

The proof of this theorem is provided in Appendix C. This theorem completes the first step of applying our framework to the resource of multiqubit coherence.

The second step of the framework is immediate since the incoherent $\mathcal{M}_N^3$ states are given by

$$\mathcal{I}_{\mathcal{M}_N^3} := \left\{ \varpi \;\middle|\; \varpi = \frac{1}{2^N}\left(\mathbb{I}^{\otimes N} + \alpha \sigma_3^{\otimes N}\right) \right\} \subset \mathcal{M}_N^3 \tag{4.43}$$

for any $\alpha \in [-1, 1]$, i.e. the states on the c_3 axis in the $\{c_1, c_2, c_3\}$ space. For the third step of the framework we can calculate the distance-based measures of coherence $C^{D_\delta}(\varpi)$ for any $\varpi \in \mathcal{M}_N^3$. To do this, the result in Eq. (4.10) can be used to see that one only needs to minimise the distance from ϖ to the set $\mathcal{I}_{\mathcal{M}_N^3}$ of incoherent $\mathcal{M}_N^3$ states to evaluate $C^{D_\delta}(\varpi)$. In general, there is no universally closest incoherent $\mathcal{M}_N^3$ state to ϖ for any D_δ. However, $C^{D_{Tr}}(\varpi)$ for the trace distance D_{Tr} and $\varpi \in \mathcal{M}_N^3$ can be evaluated simply and found to coincide with (half) the l_1 norm of coherence [TRB9] (note that this coincidence does not hold for states in general). Furthermore, it was shown in Ref [TRB2] that the robustness of coherence is equal to the l_1 norm of coherence for $\varpi \in \mathcal{M}_N^3$, i.e. so that

$$C^R(\varpi) = C^{l_1}(\varpi) = 2C^{D_{Tr}}(\varpi) = \begin{cases} \sqrt{c_1^2 + c_2^2} & N \text{ odd} \\ \max\{|c_1|, |c_2|\} & N \text{ even,} \end{cases} \tag{4.44}$$

where ϖ has the triple $\{c_1, c_2, c_3\}$.

In the final step of our framework, we know that $C(\Pi(\rho)) \leq C(\rho)$ for any measure of coherence that is monotonically non-increasing under the action of incoherent operations (since the $\mathcal{M}_N^3$-fication Π is an *incoherent operation*), i.e.

for measures that satisfy Requirement (ii) with the free operations $\mathcal{O}$ as the incoherent operations. The distance-based measures of coherence and the robustness of coherence satisfy this monotonicity property for the incoherent operations, and so $\mathcal{M}_N^3$-fication can be used to give lower bounds on the coherence of a state ρ according to these measures. One can then optimise the lower bound given by $C(\Pi(\Upsilon(\rho))) \leq C(\rho)$ with $\Pi(\Upsilon(\rho)) \in \mathcal{M}_N^3$ over the unitary *incoherent operations* $\Upsilon \in \mathcal{O}$ [1].

Chapter 5

Harnessing *the Quantum*

From a practical perspective, the ultimate goal in the study of quantum systems is the development of technologies that use the resources of *the quantum* to perform tasks in a way that is measurably superior to the performance of presently available technologies. However, it can be a contentious subject to certify whether a given quantum technology can truly outperform its existing counterparts. In this chapter we concentrate on the identification of operational tasks for which quantum resources are known to quantitatively represent the figure of merit, i.e. such that the performance of the task is necessarily improved with the presence of the resource than without. The subsequent objective of manufacturing a quantum technology to carry out such an operational task and the question of its relevance and superiority over existing technologies (which typically use only classical resources) is left for future study [187].

We show how *the quantum* plays a role in two different operational tasks within quantum metrology. Metrology is the science of measurement, and one of the objectives is to work out how to perform measurements to the highest possible precision [188]. In quantum metrology, a quantum system is used to perform such a measurement [189–191]. We focus on the metrological tasks of phase discrimination, a type of quantum channel discrimination [21–24], and phase estimation as a type of quantum parameter estimation [25–29]. In particular, the robustness of coherence is shown to represent the figure of merit in a phase dis-

crimination game where a quantum probe is passed through a black box that encodes a set of possible phases according to a particular unitary with a fixed reference eigenbasis [TRB1, TRB2]. Conversely, it is then shown that the performance of this task can place quantitative lower bounds on the robustness of k coherence [TRB3]. The respective roles of quantum coherence and entanglement in parameter estimation are then discussed. We proceed to study the estimation of a phase imprinted on a bipartite quantum probe by an interferometer according to a least informative unitary generated by a family of Hamiltonians with fixed spectrum but variable eigenbasis, where it is seen that both the quantum correlations and quantum entanglement can represent the figure of merit under different scenarios [30, TRB7]. It is then shown that the corresponding quantum entanglement can never exceed the quantum correlations [TRB7], establishing the expected hierarchy between two types of non-classical correlations.

5.1 Phase Discrimination

Following Refs. [TRB1, TRB2], we begin by describing the setup of a phase discrimination (PD) game. Consider a d-dimensional quantum system described by the state ρ and a unitary transformation that acts on the system by imprinting a phase ϕ as $\Upsilon_\phi(\rho) = U_\phi \rho U_\phi^\dagger$ where $U_\phi = e^{i\phi H}$ with $H := \sum_{j=1}^{d} j \left|e_j\right\rangle \left\langle e_j\right|$ defined with respect to an ONB $\{|e_j\rangle\}_{j=1}^{d}$. Suppose that we have a black box which imprints one of m different phases $\{\phi_k\}_{k=1}^{m}$ according to a known probability distribution $\{p_k\}_{k=1}^{m}$ and the objective is to work out which of the phases was applied, i.e. to find the value of k, see Fig. 5.1. We call this a PD game, which is defined by the set of pairs $\Theta := \{(p_k, \phi_k)\}_{k=1}^{m}$ corresponding to each realisation of the black box. Since the probability distribution $\{p_k\}_{k=1}^{m}$ is known, one option to play the PD game is simply to guess that the phase applied was $k^{\max}$ given by the maximum probability $p_{k^{\max}} := \max\{p_k\}_{k=1}^{m}$.

However, this does not make any use of the state of the quantum system after

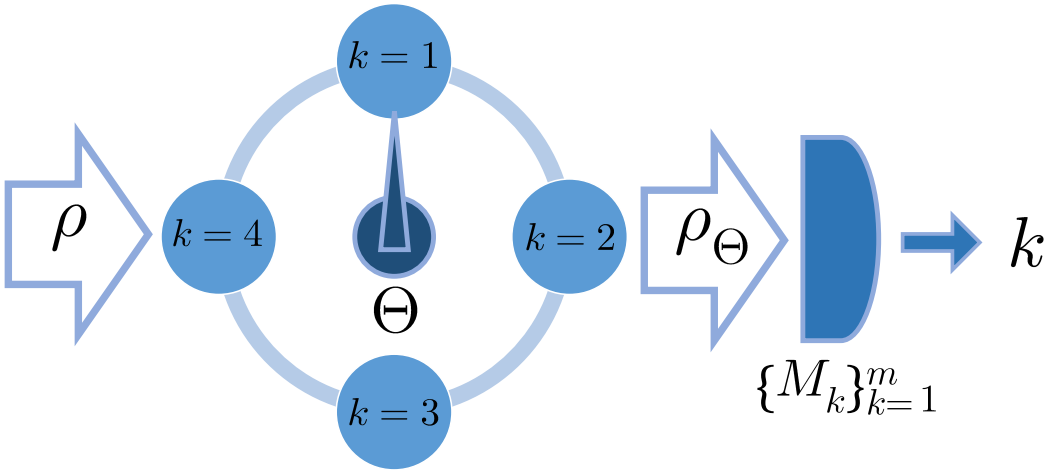

Figure 5.1: A PD game is set by the pairs $\Theta = \{(p_k, \phi_k)\}_{k=1}^m$ describing a black box (represented here by the dial with four settings) which applies one of a set of phases $\{\phi_k\}_{k=1}^m$ with probability distribution $\{p_k\}_{k=1}^m$ according to the unitary Υ_{ϕ_k}. The objective of the PD game is to guess which phase k was applied. To do this, a quantum system in state ρ is used to probe the black box and a POVM $\{M_k\}_{k=1}^m$ is applied to the output state ρ_Θ with the aim of inferring k. It has been shown that coherence in the probe system is needed for the maximum probability of successfully guessing k to exceed $p_{k^{\max}}$, which is given by simply guessing the phase applied corresponding to the maximum value of the known probability distribution $\{p_k\}_{k=1}^m$. Furthermore, the maximum possible advantage of using a coherent probe over an incoherent one is quantified by the robustness of coherence according to Eq. (5.8) [TRB1, TRB2].

interacting with the black box

$$\rho_\Theta = \sum_{k=1}^{m} p_k \Upsilon_{\phi_k}(\rho). \tag{5.1}$$

Instead, we can use the quantum system as a probe of the black box and guess the value of k from the output state ρ_Θ. To this end, we define a POVM $\{M_k\}_{k=1}^m$, with $M_k \geq 0$ for all k and $\sum_{k=1}^m M_k = \mathbb{I}$ (see Section 1.2.3), and associate each M_k with the phase ϕ_k. The probability of observing the outcome k from the POVM

$\{M_k\}_{k=1}^m$ is then

$$\begin{aligned}\mathrm{Tr}(M_k\rho_\Theta) &= \sum_{j=1}^m p_j \mathrm{Tr}(M_k \Upsilon_{\phi_j}(\rho)) \\ &= p_k \mathrm{Tr}(M_k \Upsilon_{\phi_k}(\rho)) + \sum_{j\neq k} p_j \mathrm{Tr}(M_k \Upsilon_{\phi_j}(\rho)) \\ &= p^{\mathrm{succ}}_{\Theta,M_k}(\rho) + p^{\mathrm{fail}}_{\Theta,M_k}(\rho), \end{aligned} \tag{5.2}$$

where we separate the success probability $p^{\mathrm{succ}}_{\Theta,M_k}(\rho)$ of observing k when the phase k was applied from the failure probability $p^{\mathrm{fail}}_{\Theta,M_k}(\rho)$ of observing k when the phase k was not applied. Then, to find the overall probability of successfully guessing the phase from the POVM $\{M_k\}_{k=1}^m$ we sum $p^{\mathrm{succ}}_{\Theta,M_k}(\rho)$ over all k, i.e.

$$p^{\mathrm{succ}}_{\Theta,\{M_k\}_{k=1}^m}(\rho) = \sum_{k=1}^m p^{\mathrm{succ}}_{\Theta,M_k}(\rho) = \sum_{k=1}^m p_k \mathrm{Tr}(M_k \Upsilon_{\phi_k}(\rho)). \tag{5.3}$$

This success probability is dependent upon the choice of POVM $\{M_k\}_{k=1}^m$, and so the maximum success probability is given by

$$p^{\mathrm{succ}}_{\Theta}(\rho) = \max_{\{M_k\}_{k=1}^m} p^{\mathrm{succ}}_{\Theta,\{M_k\}_{k=1}^m}(\rho). \tag{5.4}$$

The right-hand side of the above equation may be written as an SDP in the standard form reported in Ref. [125], so that the maximum probability of success can be efficiently evaluated numerically.

Now suppose that our probe system is initially in an incoherent state $\delta \in \mathcal{I}$ with respect to the reference ONB $\{|e_j\rangle\}_{j=1}^d$ given by the eigenbasis of the Hamiltonian H generating the unitary. It holds for any choice of POVM $\{M_k\}_{k=1}^m$ that

$$\begin{aligned} p^{\mathrm{succ}}_{\Theta,\{M_k\}_{k=1}^m}(\delta) &= \sum_{k=1}^m p_k \mathrm{Tr}(M_k \Upsilon_{\phi_k}(\delta)) \\ &= \sum_{k=1}^m p_k \mathrm{Tr}(M_k \delta) \\ &\leq p_{k^{\max}} \mathrm{Tr}\left(\sum_{k=1}^m M_k \delta\right) = p_{k^{\max}}, \end{aligned} \tag{5.5}$$

which follows since, for any ϕ_k,

$$\Upsilon_{\phi_k}(\delta) = U_{\phi_k} \delta U^\dagger_{\phi_k} = \delta U_{\phi_k} U^\dagger_{\phi_k} = \delta, \tag{5.6}$$

because δ and U_{ϕ_k} commute due to sharing a common eigenbasis given by the reference ONB. Hence, one finds $p_\Theta^{\text{succ}}(\delta) = p_{k^{\max}}$ for any δ, which may be achieved with the trivial POVM $\{M_k\}_{k=1}^m$ consisting of $M_{k^{\max}} = \mathbb{I}$ and $M_k = 0$ for $k \neq k^{\max}$. This means that incoherent states do not help in the PD game because using them gives a probability of success that is never greater than what is achieved from simply guessing that the phase $k^{\max}$ was applied. We then define for any $\delta \in \mathcal{I}$

$$p_\Theta^{\text{succ}}(\mathcal{I}) := \sup_{\delta \in \mathcal{I}} p_\Theta^{\text{succ}}(\delta) = p_{k^{\max}}. \tag{5.7}$$

On the other hand, for any coherent state $\rho \notin \mathcal{I}$ with respect to the reference ONB $\{|e_i\rangle\}_{i=1}^d$, one might intuitively expect that the sensitivity of the probe system to any of the phase imprinting unitary transformations Υ_{ϕ_k}, i.e. $\Upsilon_{\phi_k}(\rho) \neq \rho$ for any k, can be used to increase the maximum probability of success beyond $p_{k^{\max}}$. This expectation was put on a firmer footing in Refs. [TRB1, TRB2] where it was shown that the maximum possible advantage over all PD games Θ of using a coherent state $\rho \notin \mathcal{I}$ over any incoherent state is given by the robustness of coherence, i.e.

$$\max_\Theta \frac{p_\Theta^{\text{succ}}(\rho)}{p_\Theta^{\text{succ}}(\mathcal{I})} = 1 + C^R(\rho). \tag{5.8}$$

The maximum advantage is achieved for the PD game $\Theta^\star := \left\{\left(\frac{1}{d}, \frac{2\pi k}{d}\right)\right\}_{k=1}^d$. Hence, we have identified quantum coherence in the ONB $\{|e_i\rangle\}_{i=1}^d$ set by the Hamiltonian H generating the unitary as the necessary resource to improve the performance of the PD game, with the robustness of coherence exactly quantifying figure of merit as the optimum advantage in performance.

5.1.1 Lower bounding the Robustness of k Coherence

We have seen that if the probability of success in the PD game exceeds $p_{k^{\max}}$ then the probe system must have coherence. This fact may be used to provide a lower bound on the robustness of k coherence for any $k \in \{2, 3, \ldots, d\}$ [TRB2, TRB3], i.e.

$$\max\left\{\frac{p_\Theta^{\text{succ}}(\rho)}{(k-1)p_\Theta^{\text{succ}}(\mathcal{I})} - 1, 0\right\} \leq C_k^R(\rho). \tag{5.9}$$

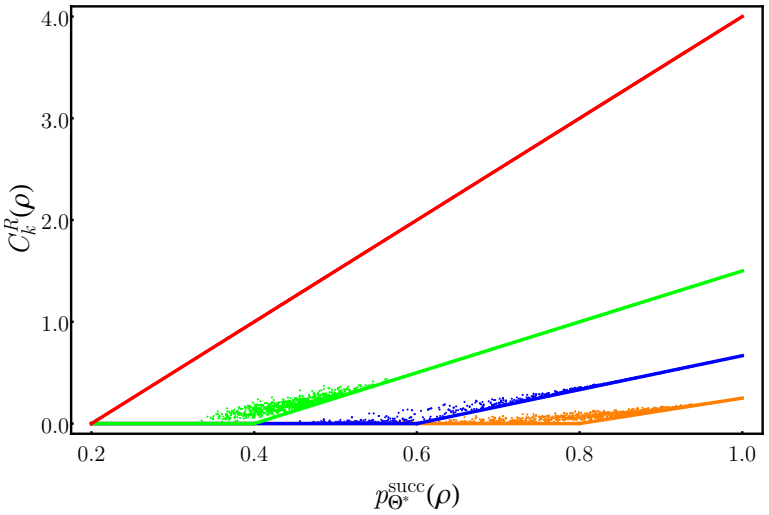

Figure 5.2: The robustness of k coherence $C_k^R(\rho)$ (vertical axis) for a 5-dimensional quantum system in terms of the maximum probability of success $p_{\Theta^\star}^{\text{succ}}(\rho)$ (horizontal axis) given by using the quantum system as a probe for the optimal PD game $\Theta^\star := \left\{\left(\frac{1}{d}, \frac{2\pi k}{d}\right)\right\}_{k=1}^{d}$. The points correspond to 10^3 pure states randomly drawn from the uniform distribution according to the Haar measure [20] and 10^3 mixed states randomly drawn from the uniform distribution according to the Hilbert-Schmidt measure [20, 131], with both $C_k^R(\rho)$ and $p_{\Theta^\star}^{\text{succ}}(\rho)$ evaluated as the solution to an SDP. Lower bounds according to (5.9) are also plotted as the solid lines. We show $C_k^R(\rho)$ and the corresponding lower bound in particular for $k = 2$ (red), $k = 3$ (green), $k = 4$ (blue), and $k = 5$ (orange). Note that since we consider the optimal PD game, for the case $k = 2$ equality holds in (5.9) so that the lower bound is saturated.

This lower bound is particularly interesting because it quantitatively links the robustness of k coherence with an operational task: one needs only to play the PD game and find the corresponding proportion of correct guesses of the phase to get a lower bound on $C_k^R(\rho)$. Figure 5.2 illustrates the lower bound by comparing the robustness of k coherence $C_k^R(\rho)$ for $k \in \{2, 3, 4, 5\}$ with the maximum probability of success $p_{\Theta^\star}^{\text{succ}}(\rho)$ in the optimal PD game $\Theta^\star$ using a 5-dimensional probe system for 10^3 pure states as well as 10^3 mixed states (which ensures the plot is well distributed amongst all values of $p_{\Theta^\star}^{\text{succ}}(\rho)$).

5.2 Parameter Estimation

Now we focus on the role of *the quantum* in another important area of quantum metrology: parameter estimation [25–29]. In parameter estimation the goal is to estimate a parameter associated with a given system, which can be achieved when the following standard set of steps are performed: (1) a probe is prepared, (2) the probe is allowed to interact with the system so that the parameter becomes imprinted on the state of the probe, (3) the probe system is measured. The output of many repetitions of such a scheme is a sequence of data points upon which one then constructs an estimator which gives a value for the estimate of the parameter with a corresponding precision.

In quantum parameter estimation, both the probe and the system whose parameter is to be estimated are quantum systems. Consider a quantum probe initially in the state ρ that interacts with the system of interest according to the quantum operation Λ_φ, which imprints the parameter to be estimated $\varphi \in \mathbb{R}$ onto the probe and resulting in the output state $\Lambda_\varphi(\rho)$. The probe is then measured by a POVM $\{M_i\}_i$, with $M_i \geq 0$ for all i and $\sum_i M_i = \mathbb{I}$, where the probability of outcome i is given by $p_{\Lambda_\varphi, M_i}(\rho) = \mathrm{Tr}(M_i \Lambda_\varphi(\rho))$. After ν repetitions of this procedure, an estimate of φ is then found from an estimator $\tilde{\varphi}$. There exists a wealth of literature addressing the technical points of constructing an estimator of the parameter [28, 189, 190, 192–194]. Here we restrict to unbiased estimators, which have an expectation value that is equal to the actual value of the parameter to be estimated. In this case, it is known that the precision of an unbiased estimator is limited in the conventional frequentist approach by the Fisher information [28, 192]

$$F_{\Lambda_\varphi, \{M_i\}_i}(\rho) = \sum_i \frac{1}{p_{\Lambda_\varphi, M_i}(\rho)} \left(\frac{\partial p_{\Lambda_\varphi, M_i}(\rho)}{\partial \varphi} \right)^2 . \tag{5.10}$$

In particular, the Cramér-Rao bound says that

$$\Delta^2 \tilde{\varphi} \geq \frac{1}{\nu F_{\Lambda_\varphi, \{M_i\}_i}(\rho)}, \tag{5.11}$$

where $\Delta^2 \tilde{\varphi}$ is the variance on the estimator $\tilde{\varphi}$. Hence, there is a lower bound on the variance of the estimator $\tilde{\varphi}$ so that we cannot perform parameter estimation

to arbitrary precision. The Cramér-Rao bound can be saturated in the limit of asymptotically large repetitions of ν by the maximum likelihood estimator [28, 192].

However, this procedure depends on a choice of POVM $\{M_i\}_i$. We may instead define the quantum Fisher information as the maximum Fisher information over all choices of POVM [189, 190, 194], i.e.

$$F_{\Lambda_\varphi}(\rho) = \max_{\{M_i\}_i} F_{\Lambda_\varphi,\{M_i\}_i}(\rho). \tag{5.12}$$

The quantum Fisher information gives the ultimate limit on the precision of the estimator $\tilde{\varphi}$ independent of the choice of measurement strategy used in the estimation procedure. It can be evaluated as

$$F_{\Lambda_\varphi}(\rho) = \mathrm{Tr}(\Lambda_\varphi(\rho)L^2_{\Lambda_\varphi}(\rho)), \tag{5.13}$$

where $L_{\Lambda_\varphi}(\rho)$ is the symmetric logarithmic derivative given by the operator satisfying

$$\frac{L_{\Lambda_\varphi}(\rho)\Lambda_\varphi(\rho) + \Lambda_\varphi(\rho)L_{\Lambda_\varphi}(\rho)}{2} = \frac{\partial\Lambda_\varphi(\rho)}{\partial\varphi}, \tag{5.14}$$

which can be given by [28]

$$L_{\Lambda_\varphi}(\rho) = 2\sum_{\substack{i,j \\ p_i+p_j\neq 0}} \frac{\langle p_i|\partial_\varphi\Lambda_\varphi(\rho)|p_j\rangle}{p_i+p_j} |p_i\rangle\langle p_j| \tag{5.15}$$

with $\Lambda_\varphi(\rho) = \sum_i p_i |p_i\rangle\langle p_i|$ the spectral decomposition of the output state $\Lambda_\varphi(\rho)$ according to Eq. (1.26). Furthermore, the set of pure state projectors onto the eigenbasis of $L_{\Lambda_\varphi}(\rho)$ provides the optimal POVM satisfying the maximisation in Eq. (5.12) over POVMs for the quantum Fisher information.

5.2.1 Quantum Coherence and Quantum Entanglement

Here we discuss how quantum coherence and entanglement in the probe system can play a role in parameter estimation in terms of the quantum Fisher information. Phase estimation is a particularly well studied type of parameter estimation given when the probe interacts unitarily with the system, i.e. according to the transformation $\Lambda_\phi(\rho) := \Upsilon_\phi(\rho) = U_\phi\rho U_\phi^\dagger$ so that a phase ϕ is imprinted upon the

probe, where $U_\phi = e^{i\phi H}$ for some self-adjoint Hamiltonian operator H [26, 27]. The corresponding quantum Fisher information is given by $F_H(\rho)$ and is independent of the value of the phase ϕ. The necessity of quantum coherence here is immediate, if ρ is not coherent with respect to the ONB given by the eigenbasis of the Hamiltonian H then ρ and U_ϕ commute so that $\Upsilon_\phi(\rho) = \rho$. Hence, the phase is not imprinted upon the probe and cannot be estimated. In fact, the quantum Fisher information $F_H(\rho)$ is understood to be a measure of asymmetry with respect to transformations of U_ϕ [1, 86, 195–197], refer to Section 3.1.2 for a discussion of the link to quantum coherence.

To see the role of entanglement, we suppose that we want to estimate the phase of a qubit unitary U_ϕ by using an N qubit probe and applying this unitary in parallel to each of the qubits, resulting in the combined Hamiltonian $H^{(N)}$ [26, 27]. The resultant quantum Fisher information is then $F_{H^{(N)}}(\rho)$ for the N qubit state ρ. This may be compared to the alternative strategy of using a qubit probe in the optimal state $\rho^\star_{qubit}$ to carry out the estimation of ϕ after one application of the unitary, and repeating this process N times with corresponding quantum Fisher information $NF_H(\rho^\star_{qubit})$. What is relevant here is how the quantum Fisher information scales with N. The linear scaling with N given by the second strategy is called the standard quantum limit and represents the ultimate precision on the scaling of an estimator when repeatedly using a single qubit probe for parameter estimation by applying a single interaction of the unitary. We can then investigate whether the first strategy of using an N qubit probe can surpass the standard quantum limit. Whenever the N qubit probe has no entanglement, so that its state $\varsigma \in \mathcal{S}_N$ is fully separable, it can be shown that [198, 199]

$$F_{H^{(N)}}(\varsigma) \leq NF_H(\rho^\star_{qubit}). \tag{5.16}$$

Hence, entanglement is necessary to surpass the standard quantum limit. In fact, the quantum Fisher information $F_{H^{(N)}}(\rho)$ has a quadratic scaling with N for some entangled N qubit probes ρ (see for example the GHZ state in Eq. (4.34)) [199–201]. This scaling is known as the Heisenberg limit and represents the ultimate scaling on the precision of an estimator when using an N qubit probe for

parameter estimation [26, 27]. The necessity of various levels of M-inseparable multiqubit entanglement in the probe for an improved quantum Fisher information have been investigated in Refs. [199–202]. On the other hand, it has also been found that entanglement in the N qubit probe is not sufficient to always surpass the standard quantum limit [203].

5.2.2 Quantum Interferometry

Interferometry is a useful testbed for the study of phase estimation in quantum metrology. Consider a quantum interferometer consisting of two arms A and B, along with a bipartite $(d_A \times d_B)$-dimensional probe in state ρ^{AB} whose subsystems are sent down the corresponding arms of the interferometer. By passing through the interferometer, a phase ϕ is imprinted onto subsystem A of the bipartite probe according to the unitary transformation $U_\phi^A = e^{i\phi H^A}$ generated by the Hamiltonian H^A. The output state of the interacted probe is then $\Lambda_\phi(\rho^{AB}) := \Upsilon_\phi(\rho^{AB}) = (U_\phi^A \otimes \mathbb{I}^B)\rho^{AB}(U_\phi^A \otimes \mathbb{I}^B)^\dagger$ and the objective is to estimate the phase ϕ. As already discussed, an estimate of the phase can be found by performing suitable measurements on the interacted bipartite probe, repeating the process many times, and finding the corresponding value of an estimator $\tilde{\phi}$. The quantum Fisher information $F_{H^A}(\rho^{AB})$ then provides the ultimate limit on the precision of this estimator. We now see that this scenario provides the perfect setting to investigate the role of the quantum correlations and entanglement in the bipartite probe for phase estimation in terms of the quantum Fisher information $F_{H^A}(\rho^{AB})$.

Indeed, it can be informative to consider the suitability of a bipartite probe ρ^{AB} for estimating the phase imprinted by the interferometer. Instead of fixing the local Hamiltonian H^A generating the imprinted phase ϕ, we can consider the suitability of ρ^{AB} when the phase is imprinted by any unitary with a Hamiltonian from a chosen family. One possible family of Hamiltonians is given by $\{H_\Gamma^A\}$, corresponding to all the Hamiltonians with a fixed spectrum of eigenvalues Γ but with a variable eigenbasis, i.e.

$$\{H_\Gamma^A\} := \left\{ H_\Gamma^A \;\middle|\; H_\Gamma^A = U \mathrm{diag}(\Gamma) U^\dagger \right\}, \tag{5.17}$$

for any unitary matrix U, with diag(Γ) a diagonal matrix given by the fixed d_A-dimensional spectrum Γ. Such a family arises when the choice of eigenbasis of the Hamiltonian generating the phase is not certain, as may be the case when the interferometer is subjected to environmental fluctuations or operated by an adversarial third party [30]. Following a series of works in Refs. [30, TRB7, 114, 204, 205], we can then consider the suitability of ρ^{AB} for estimating the phase imprinted when the unitary is generated by any of the Hamiltonians $\{H_\Gamma^A\}$ with spectrum Γ. The suitability can be gauged by the worst-case scenario quantum Fisher information, given by

$$P_A^\Gamma(\rho^{AB}) := \frac{1}{4} \inf_{\{H_\Gamma^A\}} F_{H_\Gamma^A}(\rho^{AB}), \tag{5.18}$$

which represents the ultimate precision on the estimator of the phase imprinted by a least informative Hamiltonian amongst the family $\{H_\Gamma^A\}$. This quantity is called the interferometric power of ρ^{AB} [30]. Note that a convenient normalisation factor of $\frac{1}{4}$ is included.

Quantum Correlations

In this setting, when the interferometric power of a bipartite probe is zero we know that it is not always suitable to estimate the phase imprinted by the interferometer. It has been shown that when the spectrum Γ is non-degenerate, then the interferometric power is zero for all and only the classically correlated CQ states given in Eq. (2.9) [30, 114]. Hence, quantum correlations with respect to subsystem A of the bipartite probe are necessary and sufficient to guarantee that the probe is suitable for phase estimation amongst the family of unitaries generated by $\{H_\Gamma^A\}$. The interferometric power has then been suggested as a measure of quantum correlations [30]. It is clear that $P_A^\Gamma(\rho^{AB})$ is a real and non-negative function satisfying Requirement (i), being zero on the free states for the resource of quantum correlations. However, it has not yet been fully established whether $P_A^\Gamma(\rho^{AB})$ satisfies Requirement Q(ii). It was shown in Ref. [30] that the interferometric power is monotonically non-increasing under all local quantum operations on subsystem B and invariant under local unitaries on subsystem A.

Hence, to fully establish Eq. (3.12) from Requirement Q(ii), it is necessary to see that the interferometric power is monotonically non-increasing under all LCPOs on subsystem A. We show that this is true whenever subsystem A is a qubit.

Theorem 10 *For a $(2 \times d_B)$-dimensional bipartite system it holds for all LCPO Λ^A_{CPO} acting on subsystem A that*

$$P^{\Gamma}_A(\Lambda^A_{CPO} \otimes \mathbb{I}^B(\rho^{AB})) \leq P^{\Gamma}_A(\rho^{AB}) \tag{5.19}$$

for any state ρ^{AB} and any d_B [TRB7].

The proof of this theorem is provided in Appendix C.

On the other hand, whenever subsystem A has a dimension larger than 2, the LCPOs acting on A are either completely decohering or isotropic [107, 108], see Section 3.1.2. As we have already discussed, the local completely decohering operations destroy all quantum correlations, which means that $P^{\Gamma}_A(\Lambda^A_{CPO} \otimes \mathbb{I}^B(\rho^{AB})) = 0$. It is then necessary only to consider the local isotropic operations (see Eq. (3.11)) on subsystem A to test Requirement Q(ii) for the interferometric power when $d_A > 2$. We now see that the interferometric power is monotonically non-increasing under local isotropic operations $\Lambda^A_{CPO}(\rho^A) = t\Phi^A(\rho^A) + (1-t)\frac{\mathbb{I}^A}{d_A}$ whenever $t \in [0,1]$ and $\Phi^A(\rho^A)$ is a unitary transformation on subsystem A in state ρ^A, which results simply from the convexity of the quantum Fisher information.

Theorem 11 *For a $(d_A \times d_B)$-dimensional bipartite system, it holds for all LCPO Λ^A_{CPO} acting on subsystem A of the form $\Lambda^A_{CPO}(\rho^A) = t\Phi^A(\rho^A) + (1-t)\frac{\mathbb{I}^A}{d_A}$, with $t \in [0,1]$ and $\Phi^A(\rho^A)$ a unitary transformation acting on any state ρ^A of subsystem A, that*

$$P^{\Gamma}_A(\Lambda^A_{CPO} \otimes \mathbb{I}^B(\rho^{AB})) \leq P^{\Gamma}_A(\rho^{AB}) \tag{5.20}$$

for any state ρ^{AB} of the bipartite system and any d_A and d_B [TRB7].

The proof of this theorem is also provided in Appendix C. It is not yet clear whether monotonicity of the interferometric power holds also for local isotropic operations when Φ^A is unitary but $t \in [\frac{-1}{d^2-1}, 0[$, or when Φ^A is antiunitary for

any $t \in [\frac{-1}{d-1}, \frac{1}{d+1}]$. Our results therefore go part of the way towards proving that the interferometric power satisfies Requirement Q(ii).

Quantum Entanglement

We now discuss the role of quantum entanglement for estimating the phase in our worst-case scenario quantum interferometer. Consider the variance of the Hamiltonian H_Γ^A with respect to the bipartite probe in state ρ^{AB}

$$V_{H_\Gamma^A}(\rho^{AB}) = \mathrm{Tr}\left((H_\Gamma^A)^2 \otimes \mathbb{I}^B \rho^{AB}\right) - \left(\mathrm{Tr}\left(H_\Gamma^A \otimes \mathbb{I}^B \rho^{AB}\right)\right)^2. \tag{5.21}$$

If the probe is in a pure state $|\psi^{AB}\rangle$ then it is known that the variance is equivalent (up to a factor) to the quantum Fisher information [199], i.e.

$$V_{H_\Gamma^A}(|\psi^{AB}\rangle\langle\psi^{AB}|) = \frac{1}{4} F_{H_\Gamma^A}(|\psi^{AB}\rangle\langle\psi^{AB}|). \tag{5.22}$$

Suppose that we define the following quantity for pure states $|\psi^{AB}\rangle$ as

$$E^\Gamma(|\psi^{AB}\rangle\langle\psi^{AB}|) := \inf_{\{H_\Gamma^A\}} V_{H_\Gamma^A}(|\psi^{AB}\rangle\langle\psi^{AB}|). \tag{5.23}$$

Due to Eq. (5.22), it is clear that this quantity coincides with the interferometric power, i.e. $E^\Gamma(|\psi^{AB}\rangle\langle\psi^{AB}|) = P_A^\Gamma(|\psi^{AB}\rangle\langle\psi^{AB}|)$, so that $E^\Gamma(|\psi^{AB}\rangle\langle\psi^{AB}|)$ gives the ultimate precision on an estimator of the phase imprinted onto a bipartite probe in the pure state $|\psi^{AB}\rangle$ by the least informative Hamiltonian from the family of Hamiltonians $\{H_\Gamma^A\}$. It has been shown in Refs. [30, 114] that $E^\Gamma(|\psi^{AB}\rangle\langle\psi^{AB}|)$ behaves like an entanglement monotone for pure states [2], i.e. $E^\Gamma(|\psi^{AB}\rangle\langle\psi^{AB}|) = 0$ for any pure product state $|\psi^{AB}\rangle = |\psi^A\rangle \otimes |\phi^B\rangle$ and

$$\sum_i \langle\psi^{AB}|(K_i^{AB})^\dagger K_i^{AB}|\psi^{AB}\rangle\, E^\Gamma\left(\frac{K_i^{AB}|\psi^{AB}\rangle\langle\psi^{AB}|(K_i^{AB})^\dagger}{\langle\psi^{AB}|(K_i^{AB})^\dagger K_i^{AB}|\psi^{AB}\rangle}\right) \leq E^\Gamma(|\psi^{AB}\rangle\langle\psi^{AB}|)$$

for any pure state $|\psi^{AB}\rangle$ and any set of product operators $\{K_i^{AB}\}_i$ such that $K_i^{AB} = K_i^A \otimes \mathbb{I}^B$ with $\sum_i (K_i^A)^\dagger K_i^A = \mathbb{I}^A$ or $K_i^{AB} = \mathbb{I}^A \otimes K_i^B$ with $\sum_i (K_i^B)^\dagger K_i^B = \mathbb{I}^B$.

We can then extend the definition of E^Γ to mixed states ρ^{AB} by using the convex roof construction [20, 206–208]. Consider all decompositions of ρ^{AB} into

a convex combination of pure state projectors $\{|\psi_i^{AB}\rangle\langle\psi_i^{AB}|\}_i$, i.e.

$$\rho^{AB} = \sum_i q_i |\psi_i^{AB}\rangle\langle\psi_i^{AB}| \tag{5.24}$$

for some probability distribution $\{q_i\}_i$ as in Eq. (1.22). The convex roof extension of E^Γ considers the decomposition of ρ^{AB} into pure state projectors with the minimum average E^Γ, i.e.

$$E^\Gamma(\rho^{AB}) := \inf_{\substack{\{q_i\}_i,\{|\psi_i^{AB}\rangle\langle\psi_i^{AB}|\}_i \\ \rho^{AB}=\sum_i q_i|\psi_i^{AB}\rangle\langle\psi_i^{AB}|}} \sum_i q_i E^\Gamma(|\psi_i^{AB}\rangle\langle\psi_i^{AB}|). \tag{5.25}$$

It can be shown that this quantity is a measure of entanglement, which we call the interferometric entanglement. Indeed, the interferometric entanglement is a real and non-negative function that satisfies Requirement (i), since for any $\rho^{AB} \in \mathcal{S}^{AB}$ we simply consider the decomposition of ρ^{AB} into product pure state projectors according to Eq. (2.18) to give $E^\Gamma(\rho^{AB}) = 0$. Furthermore, it was shown in Refs. [2, 102] that the convex roof extension of any function that behaves like an entanglement monotone for pure states, such as the interferometric entanglement, satisfies Requirement (iv). Since the convex roof extension is by definition a convex function [208], the interferometric entanglement also satisfies Requirements (ii) and (iii). Hence, the interferometric entanglement satisfies all the given requirements to be a measure of entanglement. Furthermore, we consequently see that the interferometric power satisfies the desirable feature of a measure of quantum correlations discussed in Section 3.1.2 of coinciding with an entanglement measure for pure states.

The interferometric entanglement of a bipartite probe in state ρ^{AB} can be seen to represent one of the roles of entanglement in quantum interferometry. It can be understood to quantify the smallest average precision of optimal estimators of the phase corresponding to imprinting onto the pure states $\{|\psi_i^{AB}\rangle\}_i$ by least informative Hamiltonians H_Γ^A with spectrum Γ, where the average is taken over the probabilities $\{q_i\}_i$ such that $\rho^{AB} = \sum_i q_i |\psi_i^{AB}\rangle\langle\psi_i^{AB}|$. On the other hand, as we have seen, the interferometric power quantifies the precision on an optimal estimator of the phase imprinted through a least informative Hamiltonian H_Γ^A

with spectrum Γ onto the bipartite probe in the mixed state ρ^{AB}. We may then compare the two quantities and find that the interferometric entanglement can never exceed the interferometric power, which is shown to be true in the following theorem.

Theorem 12 *For any state ρ^{AB} of any $(d_A \times d_B)$-dimensional bipartite system* [TRB7]*,*

$$E^{\Gamma}(\rho^{AB}) \leq P_A^{\Gamma}(\rho^{AB}). \tag{5.26}$$

The proof of this theorem is provided in Appendix C, and relies on the recently found property that the quantum Fisher information is (four times) the convex roof of the variance [209, 210]. We hence have a hierarchy between quantum correlations and quantum entanglement, as measured by the interferometric power and interferometric entanglement, respectively. Such a hierarchy between two measures motivated from the same operational perspective is very appealing since it allows for a comparison between the two resources and lends further credence to the idea that quantum correlations beyond entanglement are the relevant resource in worst-case scenario quantum interferometry.

Figure 5.3 shows a comparison between the interferometric power and the interferometric entanglement for 10^5 randomly generated states of a two qubit probe. Whenever the subsystem A is a qubit, both the interferometric power and interferometric entanglement have a simplified form. The interferometric power has been calculated in Ref. [30] and is given by Eq. (C.67) in Appendix C. Instead, the interferometric entanglement coincides (up to a factor) with another established measure of entanglement called the I-tangle [TRB7, 211, 212], which is defined for pure bipartite states $|\psi^{AB}\rangle$ as two times the local linear entropy $2\left(1 - \mathrm{Tr}\left((\rho^A)^2\right)\right)$ of the marginal state $\rho^A = \mathrm{Tr}_B(|\psi^{AB}\rangle\langle\psi^{AB}|)$ and for mixed bipartite states through the convex roof extension. The factor governing the coincidence between the interferometric entanglement and I-tangle depends upon the choice of spectrum Γ, of which the typical choice for a 2-dimensional subsystem is $\Gamma = \{-1, 1\}$ so that the factor is unity. In this case, when subsystem B is

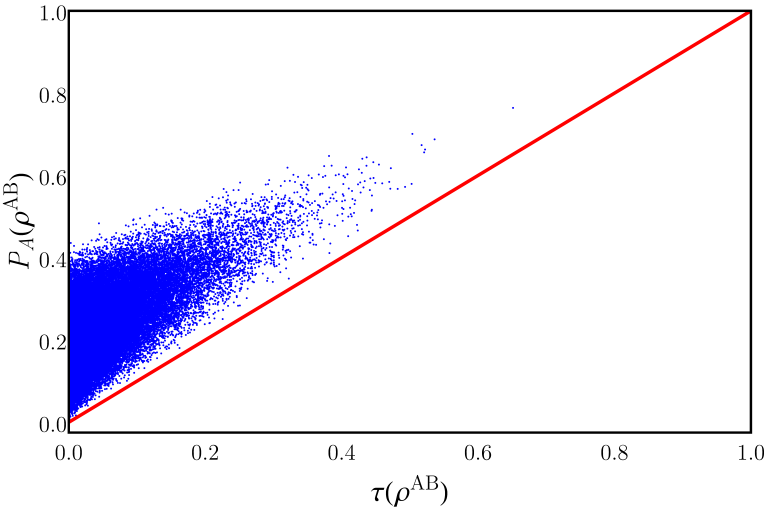

Figure 5.3: A comparison between the interferometric power (vertical axis) and the interferometric entanglement (horizontal axis) for 10^5 states (blue points) of a two qubit probe randomly drawn from the uniform distribution according to the Hilbert-Schmidt measure [20, 131]. With the spectrum set to $\Gamma = \{-1, 1\}$, the interferometric power was calculated according to Eq. (C.67) while the interferometric entanglement reduces to the two qubit tangle $\tau(\rho^{AB})$ in Eq. (5.27). The lower bound provided by Theorem 12 is shown as the red line and is saturated for any pure state. For example, the pure states $|\psi^{AB}\rangle = (|00\rangle + a\,|11\rangle)/\sqrt{1+a^2}$ for $a \in [0, \infty]$ have $P_A(|\psi^{AB}\rangle\langle\psi^{AB}|) = \tau(|\psi^{AB}\rangle\langle\psi^{AB}|) = \frac{4a^2}{(1+a^2)^2} \in [0, 1]$ and so span the full range of the lower bound.

a qubit, the interferometric entanglement and I-tangle reduce to the tangle (or squared concurrence) [20, 213, 214]

$$\tau(\rho^{AB}) := \max\{0, \lambda_1 - \lambda_2 - \lambda_3 - \lambda_4\}^2 \tag{5.27}$$

where $\lambda_1 \geq \lambda_2 \geq \lambda_3 \geq \lambda_4$ are the eigenvalues of $\sqrt{\sqrt{\rho^{AB}}\tilde{\rho}^{AB}\sqrt{\rho^{AB}}}$ with $\tilde{\rho}^{AB} := (\sigma_2 \otimes \sigma_2)(\rho^{AB})^*(\sigma_2 \otimes \sigma_2)$, σ_2 the second Pauli matrix and $(\rho^{AB})^\star$ complex conjugation of ρ^{AB} in the standard basis.

Chapter 6

Preserving *the Quantum*

The effects of noise in a quantum system have long been studied: from decoherence [12, 215] (i.e. the loss of coherence) to the sudden death of entanglement at finite timescales [216, 217], types of *the quantum* are typically sensitive to the presence of noise. Even operational aspects of *the quantum* are known to deteriorate with noise: Fig. 6.1 shows an example of how the ultimate precision in phase estimation in terms of the quantum Fisher information can transfer from the Heisenberg limit to the standard quantum limit with the presence of noise [TRB8, 218–226]. Of course, if we are ever to harness *the quantum* then it will be necessary to develop methods to preserve and protect it from detrimental noise. A number of such methods have already been devised [227–231].

In this chapter we study a mechanism to preserve *the quantum* by preparing the noisy quantum system in a particular family of initial states. The quantum resources of this system are then constant, or *frozen*, despite the presence of noise. We describe the dynamical conditions for the so-called *freezing* of quantum coherence [TRB9], quantum correlations [TRB10], and quantum entanglement [TRB4, 35, 36], focussing in particular on the distance-based approach to quantifying the quantum resources discussed in Section 3.2.2. The dynamical conditions for freezing are specified by two components: (i) the noise acting on the system, and (ii) the initial states of the system. These conditions are universal in the sense that they do not depend upon the distance D_δ chosen to quantify the resource.

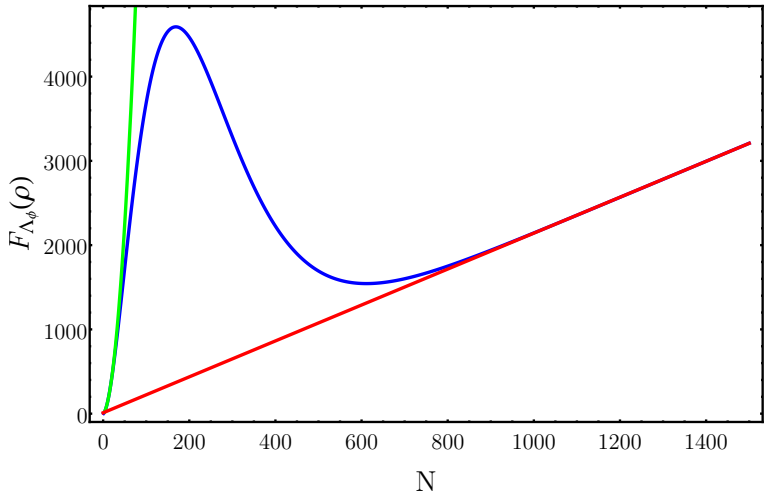

Figure 6.1: The quantum Fisher information $F_{\Lambda_\phi}(\rho)$ (blue line) given by using an N qubit probe in an initial state ρ to estimate a phase ϕ imprinted by a noisy qubit unitary acting on each of the qubits [TRB8]. With the initial probe set as the genuinely entangled GHZ state $\rho = |GHZ^{(N)}\rangle \langle GHZ^{(N)}|$, the expectation is for the quantum Fisher information to scale with the Heisenberg limit as N^2 (see Section 5.2.1). However, the presence of noise in the imprinting unitaries causes a transition from the Heisenberg limit scaling (green line) to the standard quantum limit scaling linear with N (red line). The phase imprinting operation Λ_ϕ is given by a noisy qubit unitary imprinting $\phi = 0.1$ with a Hamiltonian that has an eigenbasis given by an ONB randomly chosen from the von Mises-Fisher distribution [232] on the Bloch sphere centred on the n_3 axis with noise parameter $\kappa = 2$ (see Ref. [TRB8] for further details). Numerous investigations have been carried out on how to maintain a scaling with N of the quantum Fisher information for an N qubit probe that is superior to the standard quantum limit despite the presence of noise [TRB8, 218–226].

6.1 Quantum Coherence and Quantum Correlations

Here we restrict to two qubit systems composed of subsystem A and B in state ρ^{AB} and use the distance-based approach discussed in Section 3.2.2 to measure the resources, see also Fig. 3.6. Quantum coherence is measured relative to the computational basis given by $\{|00\rangle, |01\rangle, |10\rangle, |11\rangle\}$ according to the distance-based approach in Eq. (3.65) as $C^{D_\delta}(\rho^{AB})$. Quantum correlations are measured

with respect to both subsystems using the distance-based approach in Eq. (3.66) as $Q^{D_\delta}_{AB}(\rho^{AB})$, although the following analysis can apply as well to $Q^{D_\delta}_{A}(\rho^{AB})$ and $Q^{D_\delta}_{B}(\rho^{AB})$. The dynamical conditions that lead to freezing are the same for quantum coherence and quantum correlations. We now provide these conditions and show that freezing occurs for any choice of D_δ satisfying the required properties of contractivity and joint convexity. An example of the freezing effect is then provided using the squared Bures distance D_{Bu} to quantify the resources, and we then conclude this section by giving a physically motivated explanation of freezing as well as a comparison of our findings to other established results [31–33, TRB11, 34, 144, 233–241].

6.1.1 Noise

We suppose that each qubit is subjected to bit flip noise, a type of noise analogous to what is typically experienced by a classical bit [7]. Here, the bit flip noise causes a qubit in state $|0\rangle$ to "flip" into the state $|1\rangle$ (and vice versa) with a probability of q, with $q \in [0, 1]$. Now, since each type of noise corresponds to a quantum operation, the bit flip noise transforms the qubit in state ρ according to the operator sum representation $\Lambda(\rho) = \sum_{i=1}^{2} K_i \rho K_i^\dagger$ with Kraus operators $\{K_i\}_{i=1}^{2}$ given by [7]

$$K_1 = \sqrt{1-q}\mathbb{I}\,, \qquad\qquad K_2 = \sqrt{q}\sigma_1\,. \tag{6.1}$$

The bit flip noise can be understood from the perspective of open quantum systems [242] as a time dependent interaction of the qubit with an environment [243]. The environment causes the qubit to bit flip with a probability $q = \frac{1-e^{-\gamma t}}{2}$, where $\gamma \in [0, \infty]$ is the strength of the noise and $t \in [0, \infty]$ is the time of interaction. We then denote the action of bit flip noise after a time t with Λ_t. Considering now bit flip noise applied to both qubits of our two qubit system in state ρ^{AB}, and assuming that the bit flip noise is of identical strength for each qubit and independent of the other qubit, the action of the bit flip noise is

$$\Lambda_t^{AB}(\rho^{AB}) := \Lambda_t \otimes \Lambda_t(\rho^{AB}) = \sum_{i=1}^{2}\sum_{j=1}^{2} K_i \otimes K_j \rho^{AB} K_i^\dagger \otimes K_j^\dagger. \tag{6.2}$$

It can be seen that Λ_t^{AB} is an incoherent operation with respect to the two qubit computational basis and is also an LCPO, so that in general for any t

$$C^{D_\delta}(\Lambda_t^{AB}(\rho^{AB})) \leq C^{D_\delta}(\rho^{AB}) \qquad Q_{AB}^{D_\delta}(\Lambda_t^{AB}(\rho^{AB})) \leq Q_{AB}^{D_\delta}(\rho^{AB}), \quad (6.3)$$

i.e. the bit flip noise can never increase the quantum resources. We now give conditions in terms of initial states ρ^{AB} for which $C^{D_\delta}(\Lambda_t^{AB}(\rho^{AB})) = C^{D_\delta}(\rho^{AB})$ for all t and $Q_{AB}^{D_\delta}(\Lambda_t^{AB}(\rho^{AB})) = Q_{AB}^{D_\delta}(\rho^{AB})$ until a fixed t, for any choice of distance D_δ.

6.1.2 Initial States

The initial states that manifest freezing are given by a subclass of the two qubit Bell-diagonal (BD) states, which consist of mixtures of the four pure Bell states [2, 152]. The BD states coincide with the set of $\mathcal{M}_N^3$ states given in Eq. (4.19) for $N = 2$. Hence, we consider the BD states $\varpi^{AB} \in \mathcal{BD} := \mathcal{M}_2^3$ in terms of the triple $\{c_1, c_2, c_3\}$ with $c_i = \mathrm{Tr}(\varpi^{AB}\sigma_i^A \otimes \sigma_i^B) \in [-1, 1]$, which is contained within a tetrahedron $\mathcal{T}_{-1}$ with vertices $\{1, -1, 1\}$, $\{-1, 1, 1\}$, $\{1, 1, -1\}$, and $\{-1, -1, -1\}$.

When each qubit of the two qubit system in an initial BD state is subjected to bit flip noise, the state of the evolved system remains BD [31, 34]. If the initial BD state has triple $\{c_1(0), c_2(0), c_3(0)\}$, then the evolved BD state has triple

$$\{c_1(t), c_2(t), c_3(t)\} = \{c_1(0), e^{-2\gamma t}c_2(0), e^{-2\gamma t}c_3(0)\}. \quad (6.4)$$

Hence, the action of bit flip noise in the $\{c_1, c_2, c_3\}$ space is to evolve the BD state along a line connecting the initial triple $\{c_1(0), c_2(0), c_3(0)\}$ with the point $\{c_1(0), 0, 0\}$ on the c_1 axis, which is reached at an asymptotically large time.

The subclass of initial BD states that can have frozen coherence or quantum correlations are referred to as the freezing states. The freezing states are given by the initial triple

$$\{c_1(0), c_2(0), c_3(0)\} = \{c_1(0), -c_1(0)c_3(0), c_3(0)\} \quad (6.5)$$

for any $c_1(0) \in [-1, 1]$ and $c_3(0) \in [-1, 1]$, and evolve under bit flip noise according to

$$\{c_1(t), c_2(t), c_3(t)\} = \{c_1(0), -e^{-2\gamma t}c_1(0)c_3(0), e^{-2\gamma t}c_3(0)\}. \quad (6.6)$$

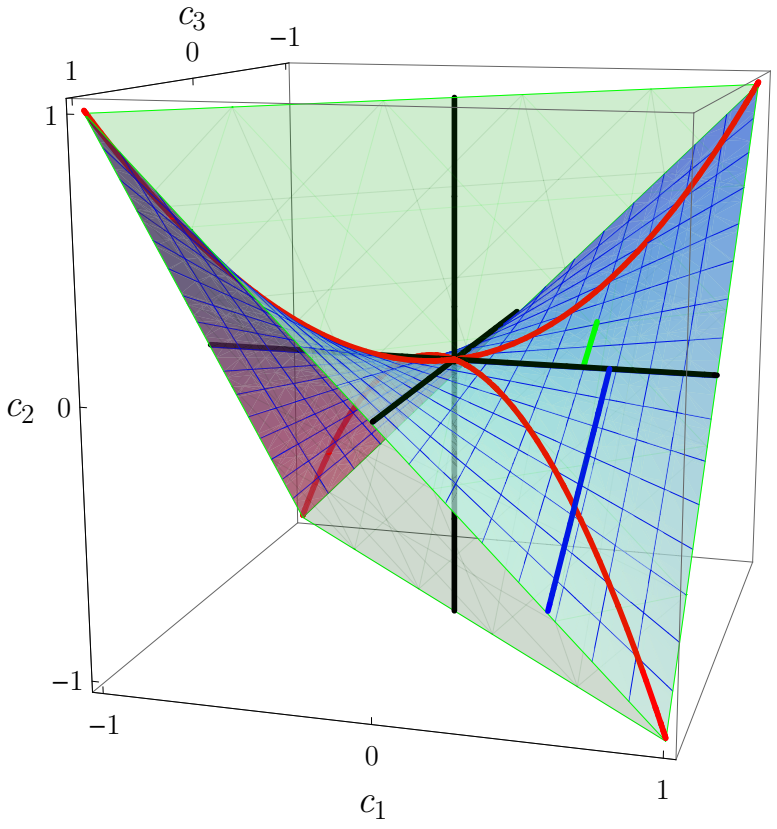

Figure 6.2: The freezing surface (blue meshed surface) in the $\{c_1, c_2, c_3\}$ space of BD states (green tetrahedron corresponding to $\mathcal{T}_{-1}$). The blue and green lines show the time evolution according to Eq. (6.6) of two initial BD states with triple $\{\frac{3}{5}, -\frac{3}{5}, 1\}$ and $\{\frac{1}{2}, \frac{1}{8}, -\frac{1}{4}\}$, respectively, on the freezing surface, which both evolve towards the c_1 axis while remaining on the freezing surface. Both initial BD states have frozen quantum coherence for all time, while only the BD state corresponding to the blue line has frozen quantum correlations, which are frozen for $0 \leq t \leq -\frac{1}{2\gamma} \ln \frac{3}{5}$ according to Eq. (6.7). More generally, every initial BD state on the freezing surface has frozen quantum coherence for all time, while only initial BD states on the freezing surface with a trajectory of evolution crossing the red curves (i.e. so that $|c_3(0)| > |c_1(0)|$) will have frozen quantum correlations until the threshold time $t^\star$.

The freezing states form a so-called freezing surface within the tetrahedron $\mathcal{T}_{-1}$ in the $\{c_1, c_2, c_3\}$ space, as shown by Fig. 6.2. Note that the evolved state of an initial BD state (with triple) on the freezing surface, according to the qubit bit flip noise, is itself a BD state on the freezing surface. We see in the following

that any BD state on the freezing surface has frozen quantum coherence for all time [TRB9], while BD states on the freezing surface where $|c_3(0)| > |c_1(0)|$ have frozen quantum correlations until a threshold time [31, TRB10, 34]

$$t^\star := -\frac{1}{2\gamma} \ln \frac{|c_1(0)|}{|c_3(0)|}, \tag{6.7}$$

after which the quantum correlations generally decay exponentially with time.

6.1.3 Frozen Quantum Coherence

We now evaluate $C^{D_\delta}(\Lambda_t^{AB}(\varpi^{AB}))$ for any time t and any state $\varpi^{AB} \in \mathcal{BD}$ on the freezing surface, with the intention of showing that $C^{D_\delta}(\Lambda_t^{AB}(\varpi^{AB})) = C^{D_\delta}(\varpi^{AB})$. It is clear from Eq. (6.6) that the triple of $\Lambda_t^{AB}(\varpi^{AB})$ is for any t given by $\{c_1, -c_1c_3, c_3\}$ for some $c_1 \in [-1,1]$ and $c_3 \in [-1,1]$, i.e. on the freezing surface. Hence, evaluating $C^{D_\delta}(\Lambda_t^{AB}(\varpi^{AB}))$ is given by the evaluation of $C^{D_\delta}(\varpi^{AB})$ for any BD state ϖ^{AB} on the freezing surface. To simplify notation, we herein adopt the convention of referring to a BD state directly by its triple. The objective is then to calculate $C^{D_\delta}(\{c_1, -c_1c_3, c_3\})$.

Following the discussion in Section 4.3, we know that one of the closest incoherent states to a given BD state is itself a BD state. Furthermore, the incoherent BD states with respect to computational basis given by $\{|00\rangle, |01\rangle, |10\rangle, |11\rangle\}$ are described by $\{0, 0, \alpha\}$ for $\alpha \in [-1, 1]$. Hence, we have for a general BD state (not necessarily on the freezing surface)

$$C^{D_\delta}(\{c_1, c_2, c_3\}) = \inf_{\alpha \in [-1,1]} D_\delta(\{c_1, c_2, c_3\}, \{0, 0, \alpha\}). \tag{6.8}$$

For the trace distance D_{Tr} and the relative entropy distance D_{RE} [47], it can be shown that one of the closest incoherent BD states to the BD state $\{c_1, c_2, c_3\}$ has the triple $\{0, 0, c_3\}$. However, this does not hold for all choices of D_δ. For example, Fig. 6.3 shows a plot of the trace distance, squared Bures distance, and relative entropy distance between a BD state $\left\{-\frac{1}{2}, -\frac{1}{2}, -\frac{1}{2}\right\}$ and the incoherent BD state $\{0, 0, \alpha\}$ as a function of α. Here it can be seen that the closest incoherent BD state according to the squared Bures distance does not have triple $\{0, 0, -\frac{1}{2}\}$.

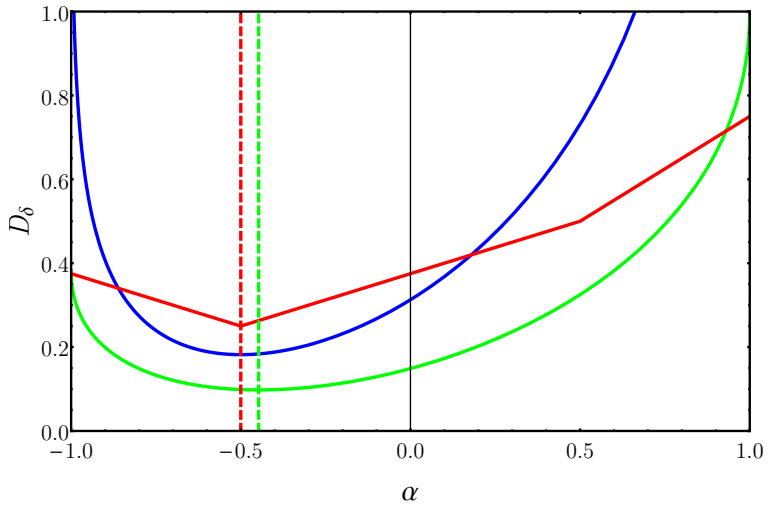

Figure 6.3: The distance D_δ between the BD state $\{-\frac{1}{2}, -\frac{1}{2}, -\frac{1}{2}\}$ and the incoherent BD states $\{0, 0, \alpha\}$ for $\alpha \in [-1, 1]$. The solid lines correspond to the trace distance D_{Tr} (red), squared Bures distance D_{Bu} (green), and relative entropy distance D_{RE} (blue). Instead, the vertical dashed lines locate the minima of the distances and hence give the value of α for the closest incoherent BD state. While the trace distance and relative entropy have the closest incoherent BD state with triple $\{0, 0, -\frac{1}{2}\}$, the closest incoherent BD state according to the squared Bures distance has triple $\left\{0, 0, -\frac{1}{\sqrt{5}}\right\}$.

Remarkably, by restricting to BD states $\{c_1, -c_1c_3, c_3\}$ on the freezing surface, one can prove for *any* contractive distance D_δ that the closest incoherent BD state is always $\{0, 0, c_3\}$, i.e.

$$D_\delta(\{c_1, -c_1c_3, c_3\}, \{0, 0, \alpha\}) \geq D_\delta(\{c_1, -c_1c_3, c_3\}, \{0, 0, c_3\}) \tag{6.9}$$

for any $\alpha \in [-1, 1]$ [TRB9]. We now sketch the proof of this result, which uses similar methods to those discussed in the third step of Section 4.2.1. Fig. 6.4 also illustrates the arguments pictorially. First, we have $D_\delta(\{c_1, -c_1c_3, c_3\}, \{0, 0, \alpha\}) \geq D_\delta(\{c_1, 0, 0\}, \{0, 0, 0\})$. Indeed, from Eq. (6.6) with $t \to \infty$ it can be seen that that $\Lambda_\infty^{AB}(\{c_1, -c_1c_3, c_3\}) = \{c_1, 0, 0\}$ and also $\Lambda_\infty^{AB}(\{0, 0, \alpha\}) = \{0, 0, 0\}$. Hence, the contractivity of D_δ gives

$$\begin{aligned} D_\delta(\{c_1, -c_1c_3, c_3\}, \{0, 0, \alpha\}) &\geq D_\delta(\Lambda_\infty^{AB}(\{c_1, -c_1c_3, c_3\}), \Lambda_\infty^{AB}(\{0, 0, \alpha\})) \\ &= D_\delta(\{c_1, 0, 0\}, \{0, 0, 0\}), \end{aligned} \tag{6.10}$$

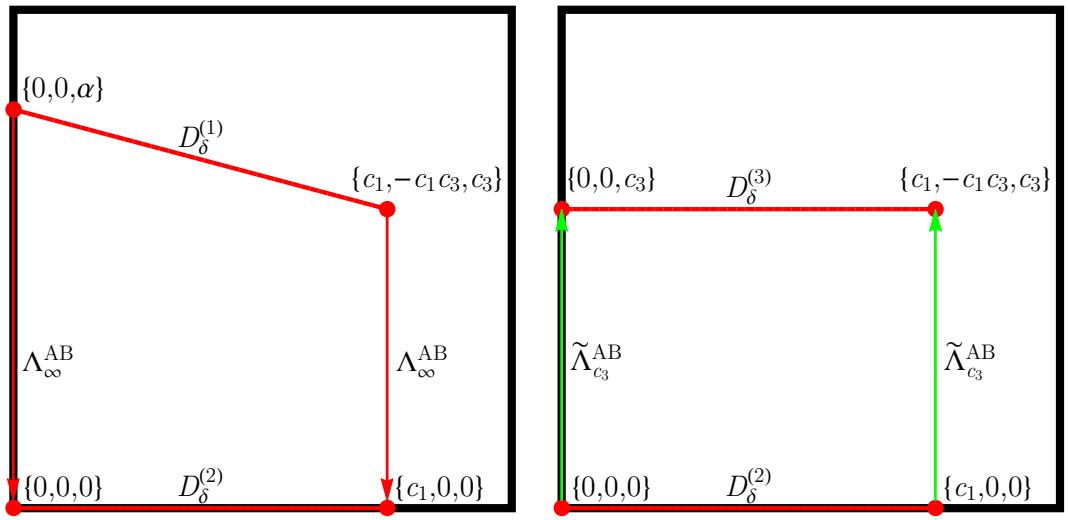

Figure 6.4: A pictorial representation of the arguments used to identify the closest incoherent BD state to any BD state on the freezing surface. Both squares represent the flattening of one quadrant of the freezing surface so that the c_1 axis is horizontal and the c_3 axis is vertical. In the first square, $D_\delta^{(1)}$ represents the distance between $\{c_1, -c_1c_3, c_3\}$ and $\{0, 0, \alpha\}$ for some $\alpha \in [-1, 1]$, while $D_\delta^{(2)}$ represents the distance between $\{c_1, 0, 0\}$ and $\{0, 0, 0\}$, which are the result of Λ_∞^{AB} on $\{c_1, -c_1c_3, c_3\}$ and $\{0, 0, \alpha\}$, respectively. We then have from contractivity of the distance that $D_\delta^{(1)} \geq D_\delta^{(2)}$. In the second square, $D_\delta^{(3)}$ represents the distance between $\{c_1, -c_1c_3, c_3\}$ and $\{0, 0, c_3\}$, while $D_\delta^{(2)}$ is the same as for the first square. We can use the quantum operation $\tilde{\Lambda}_{c_3}^{AB}$ to transform from $\{c_1, 0, 0\}$ and $\{0, 0, 0\}$ to $\{c_1, -c_1c_3, c_3\}$ and $\{0, 0, c_3\}$, respectively, so that $D_\delta^{(2)} \geq D_\delta^{(3)}$. Overall, we have that $D_\delta^{(1)} \geq D_\delta^{(2)} = D_\delta^{(3)}$ for any α, thus identifying $\{0, 0, c_3\}$ as the closest incoherent BD state to a BD state $\{c_1, -c_1c_3, c_3\}$ on the freezing surface.

see the first square of Fig. 6.4.

On the other hand, there exists a quantum operation $\tilde{\Lambda}_{c_3}^{AB}$ such that

$$\tilde{\Lambda}_{c_3}^{AB}(\{c_1, 0, 0\}) = \{c_1, -c_1c_3, c_3\} \qquad \tilde{\Lambda}_{c_3}^{AB}(\{0, 0, 0\}) = \{0, 0, c_3\}. \quad (6.11)$$

The quantum operation $\tilde{\Lambda}_{c_3}^{AB}$ acts globally on both qubits and is given explicitly in Ref. [TRB9], where it was derived using the method outlined in Ref. [244]. The contractivity of D_δ then gives

$$\begin{aligned} D_\delta(\{c_1, 0, 0\}, \{0, 0, 0\}) &\geq D_\delta(\tilde{\Lambda}_{c_3}^{AB}(\{c_1, 0, 0\}), \tilde{\Lambda}_{c_3}^{AB}(\{0, 0, 0\})) \\ &= D_\delta(\{c_1, -c_1c_3, c_3\}, \{0, 0, c_3\}), \end{aligned} \quad (6.12)$$

refer to the second square of Fig. 6.4. The above inequality and (6.10) together imply

$$\begin{aligned} D_\delta(\{c_1, -c_1c_3, c_3\}, \{0, 0, \alpha\}) &\geq D_\delta(\{c_1, 0, 0\}, \{0, 0, 0\}) \\ &\geq D_\delta(\{c_1, -c_1c_3, c_3\}, \{0, 0, c_3\}), \end{aligned} \tag{6.13}$$

which is the desired inequality in (6.9). Furthermore, it can be seen that the chain of inequalities in (6.13) reduces to an equality when $\alpha = c_3$, i.e. so that

$$D_\delta(\{c_1, -c_1c_3, c_3\}, \{0, 0, c_3\}) = D_\delta(\{c_1, 0, 0\}, \{0, 0, 0\}). \tag{6.14}$$

Combined with (6.9), this means that the BD states on the freezing surface with a fixed value of c_1 are all equally distant from the c_3 axis. This is a crucial property for the freezing of quantum coherence since the qubit bit flip noise maintains BD states on the freezing surface but does not alter the c_1 value, as can be seen in Fig. (6.2).

The quantum coherence of a BD state $\{c_1, -c_1c_3, c_3\}$ on the freezing surface is then

$$\begin{aligned} C^{D_\delta}(\{c_1, -c_1c_3, c_3\}) &= \inf_{\alpha\in[-1,1]} D_\delta(\{c_1, -c_1c_3, c_3\}, \{0, 0, \alpha\}) \\ &= D_\delta(\{c_1, -c_1c_3, c_3\}, \{0, 0, c_3\}). \end{aligned} \tag{6.15}$$

From Eq. (6.14) and the joint convexity of D_δ, we find that $C^{D_\delta}(\{c_1, -c_1c_3, c_3\})$ is simply a monotonic function $h_{D_\delta}(|c_1|)$ of $|c_1|$. Particular instances of $h_{D_\delta}(|c_1|)$, for each distance D_δ given in Table 1.1, are shown in Table 6.1. Now we can consider the quantum coherence for the time evolution of a BD state on the freezing surface according to Eq. (6.6) with triple $\{c_1(0), -e^{-2\gamma t}c_1(0)c_3(0), e^{-2\gamma t}c_3(0)\}$. It holds that

$$C^{D_\delta}(\{c_1(0), -e^{-2\gamma t}c_1(0)c_3(0), e^{-2\gamma t}c_3(0)\}) = h_{D_\delta}(|c_1(0)|), \tag{6.16}$$

which is not a function of t and thus constant for all time. Hence, we have permanent frozen quantum coherence for any choice of distance D_δ (satisfying the required properties of contractivity and joint convexity).

D_δ	$h_{D_\delta}(\lvert c_1\rvert)$
Trace	$\frac{\lvert c_1\rvert}{2}$
Hellinger (squared)	$2-\sqrt{1-\lvert c_1\rvert}-\sqrt{1+\lvert c_1\rvert}$
Bures (squared)	$2-\sqrt{1-\lvert c_1\rvert}-\sqrt{1+\lvert c_1\rvert}$
Infidelity	$\frac{1}{2}\left(1-\sqrt{1-\lvert c_1\rvert^2}\right)$
Relative entropy	$\frac{1}{2}\Big[(1-\lvert c_1\rvert)\log_2(1-\lvert c_1\rvert) + (1+\lvert c_1\rvert)\log_2(1+\lvert c_1\rvert)\Big]$

Table 6.1: The multiqubit coherence $C^{D_\delta}(\varpi^{AB})$ of a two qubit BD state $\varpi^{AB} \in \mathcal{BD}$ on the freezing surface with triple $\{c_1, -c_1c_3, c_3\}$ is a monotonic function $h_{D_\delta}(|c_1|)$ of $|c_1|$ set by the choice of distance D_δ.

6.1.4 Frozen Quantum Correlations

Just like for quantum coherence, we want to evaluate $Q_{AB}^{D_\delta}(\{c_1, -c_1c_3, c_3\})$ so that we can find $Q_{AB}^{D_\delta}(\Lambda_t^{AB}(\varpi^{AB}))$ for any time t and any $\varpi^{AB} \in \mathcal{BD}$ on the freezing surface. For quantum coherence, we used the discussion in Section 4.3 to see that the closest incoherent state to any BD state is itself a BD state. This relies on the fact that $\mathcal{M}_N^3$-fication, which for $N = 2$ projects every two qubit state onto the BD states, is an incoherent operation (as proved in Theorem 9). To find an analogous result for quantum correlations, i.e. that the closest CC state to any BD state is itself a BD state, $\mathcal{M}_N^3$-fication would need to be a type of quantum operation unable to create quantum correlations. However, it is not yet known whether this is the case. Nevertheless, it was shown using an alternative approach in Refs. [33, TRB10] that the closest CC state to any BD state is itself a BD state, provided that the distance D_δ is contractive, jointly convex, and also transposition invariant with respect to any basis, i.e.

$$D_\delta(\rho^\intercal, \sigma^\intercal) = D_\delta(\rho, \sigma) \tag{6.17}$$

for any two states ρ and σ. For a qubit state with a vector $\mathbf{n} := \{n_1, n_2, n_3\}$ in the Bloch ball representation discussed in Section 1.2.4, it can be seen that transposition with respect to the computational basis corresponds to a reflection of the vector $\mathbf{n}$ in the plane defined by the n_1 and n_3 axes. More generally, for d-dimensional quantum systems it can be understood that Eq. (6.17) corresponds to invariance of the distance D_δ under reflections in a $(d(d+1)/2-1)$-dimensional hyperplane of the (d^2-1)-dimensional state space of the system [TRB10], which is a natural property that is satisfied by all of the distances given in Table 1.1.

The BD states that are CC have the triple $\{s,0,0\}$, $\{0,s,0\}$ or $\{0,0,s\}$ for any $s \in [-1,1]$ [33, TRB10], corresponding in the $\{c_1,c_2,c_3\}$ space to the axes of the BD tetrahedron $\mathcal{T}_{-1}$, as can be seen in Fig. 6.2. Hence, we have for a general BD state (not necessarily on the freezing surface)

$$Q_{AB}^{D_\delta}(\{c_1,c_2,c_3\}) = \min\Bigg\{\inf_{s\in[-1,1]} D_\delta(\{c_1,c_2,c_3\},\{s,0,0\}),$$
$$\inf_{s\in[-1,1]} D_\delta(\{c_1,c_2,c_3\},\{0,s,0\}), \inf_{s\in[-1,1]} D_\delta(\{c_1,c_2,c_3\},\{0,0,s\})\Bigg\}. \quad (6.18)$$

This quantity can be evaluated analytically for certain D_δ. For the trace distance D_{Tr}, we have

$$Q_{AB}^{D_\delta}(\{c_1,c_2,c_3\}) = \frac{1}{2}\text{int}\{|c_1|,|c_2|,|c_3|\}, \quad (6.19)$$

where $\text{int}\{|c_1|,|c_2|,|c_3|\}$ denotes the intermediate value of $\{|c_1|,|c_2|,|c_3|\}$ [112, 144, 245, 246]. Nevertheless, for other D_δ it can be difficult to evaluate Eq. (6.18).

However, by restricting to BD states $\{c_1,-c_1c_3,c_3\}$ on the freezing surface, Eq. (6.18) can be evaluated for any distance (satisfying the established properties). We know that $\inf_{s\in[-1,1]} D_\delta(\{c_1,-c_1c_3,c_3\},\{0,0,s\}) = h_{D_\delta}(|c_1|)$ from the previous section, which is just the quantum coherence with respect to the two qubit computational basis. Furthermore,

$$\begin{aligned} D_\delta(\{c_1,-c_1c_3,c_3\},\{s,0,0\}) &= D_\delta(U\{c_1,-c_1c_3,c_3\}U^\dagger, U\{s,0,0\}U^\dagger) \\ &= D_\delta(\{c_3,-c_1c_3,c_1\},\{0,0,s\}) \\ &\geq D_\delta(\{c_3,-c_1c_3,c_1\},\{0,0,c_1\}) \\ &= h_{D_\delta}(|c_3|), \end{aligned} \quad (6.20)$$

where in the first equality we use the invariance of any D_δ under unitary transformations U, which is imposed by the contractivity of the distance. Then, in the second equality we set U to be the local unitary $U := \frac{1}{2}(\mathbb{I} + i\sigma_2) \otimes (\mathbb{I} + i\sigma_2)$ whose action is

$$U\{c_1, -c_1c_3, c_3\}U^\dagger = \{c_3, -c_1c_3, c_1\}\,, \qquad U\{s, 0, 0\}U^\dagger = \{0, 0, s\}. \quad (6.21)$$

In the inequality we use the result from Eq. (6.9), and in final equality we use Eq. (6.14) and joint convexity of D_δ to give the monotonic functions h_{D_δ} given in Table 6.1. The result is that $\inf_{s\in[-1,1]} D_\delta(\{c_1, -c_1c_3, c_3\}, \{s, 0, 0\}) = h_{D_\delta}(|c_3|)$. Finally, we see that

$$\begin{aligned} D_\delta(\{c_1, -c_1c_3, c_3\}, \{0, s, 0\}) &\geq D_\delta(\Lambda_\infty^{AB}(\{c_1, -c_1c_3, c_3\}), \Lambda_\infty^{AB}(\{0, s, 0\})) \\ &= D_\delta(\{c_1, 0, 0\}, \{0, 0, 0\}) \\ &= h_{D_\delta}(|c_1|), \end{aligned} \quad (6.22)$$

where in the final equality we again use the joint convexity of D_δ to rewrite $D_\delta(\{c_1, 0, 0\}, \{0, 0, 0\})$ as the monotonic function $h_{D_\delta}(|c_1|)$.

The result of these calculations is that

$$Q_{AB}^{D_\delta}(\{c_1, -c_1c_3, c_3\}) = \min\left\{h_{D_\delta}(|c_1|), h_{D_\delta}(|c_3|)\right\}. \quad (6.23)$$

Now we again consider the time evolution of a BD state on the freezing surface with triple $\{c_1(0), -e^{-2\gamma t}c_1(0)c_3(0), e^{-2\gamma t}c_3(0)\}$. Indeed,

$$\begin{aligned} &Q_{AB}^{D_\delta}(\{c_1(0), -e^{-2\gamma t}c_1(0)c_3(0), e^{-2\gamma t}c_3(0)\}) \\ &\qquad = \min\left\{h_{D_\delta}(|c_1(0)|), h_{D_\delta}(|c_3(0)|e^{-2\gamma t})\right\}. \end{aligned} \quad (6.24)$$

Following from the monotonicity of h_{D_δ}, there are here two scenarios: (i) $|c_3(0)| > |c_1(0)|$ and (ii) $|c_3(0)| \leq |c_1(0)|$. In the first scenario, we have that

$$Q_{AB}^{D_\delta}(\{c_1(0), -e^{-2\gamma t}c_1(0)c_3(0), e^{-2\gamma t}c_3(0)\}) = \begin{cases} h_{D_\delta}(|c_1(0)|) & 0 \leq t < t^\star; \\ h_{D_\delta}(|c_3(0)|e^{-2\gamma t}) & t \geq t^\star. \end{cases} \quad (6.25)$$

Hence, the quantum correlations are frozen at a value of $h_{D_\delta}(|c_1(0)|)$ for a finite time period until the threshold time $t^\star$ given in Eq. (6.7), while after $t^\star$ the

quantum correlations decay asymptotically. On the other hand, in the second scenario we have that for all t,

$$Q_{AB}^{D_\delta}(\{c_1(0), -e^{-2\gamma t}c_1(0)c_3(0), e^{-2\gamma t}c_3(0)\}) = h_{D_\delta}(|c_3(0)|e^{-2\gamma t}), \tag{6.26}$$

meaning that the quantum correlations are never frozen and simply decay asymptotically. We thus conclude that frozen quantum correlations occur with any choice of distance D_δ (satisfying the established properties) for a BD state on the freezing surface for a finite time, provided that the initial condition $|c_3(0)| > |c_1(0)|$ is satisfied.

6.1.5 Freezing Example

Here we study the freezing effect for a particular initial BD state ϖ^{AB} on the freezing surface with triple $\{\frac{3}{5}, -\frac{3}{5}, 1\}$, that evolves under qubit bit flip noise so that at time $t \in [0, \infty]$ the state is $\varpi^{AB}(t)$ with triple $\{\frac{3}{5}, -\frac{3}{5}e^{-2\gamma t}, e^{-2\gamma t}\}$. This evolution corresponds in the $\{c_1, c_2, c_3\}$ space to the blue line in Fig. 6.2. Focussing in particular on using the squared Bures distance to quantify our quantum resources, we have

$$\begin{aligned} C^{D_{Bu}}(\varpi^{AB}(t)) &= 2 - 3\sqrt{\frac{2}{5}}, \\ Q_{AB}^{D_{Bu}}(\varpi^{AB}(t)) &= \begin{cases} 2 - 3\sqrt{\frac{2}{5}} & 0 \leq t < t^\star; \\ 2 - \sqrt{1 - e^{-2\gamma t}} - \sqrt{1 + e^{-2\gamma t}} & t \geq t^\star, \end{cases} \end{aligned} \tag{6.27}$$

where $t^\star = -\frac{1}{2\gamma}\ln\frac{3}{5}$. Note that the quantum correlations according to the squared Bures distance have also been calculated for any BD state in Refs. [33, 247, 248]. We can also compare with the two qubit entanglement given in Eq. (4.22),

$$E^{D_{Bu}}(\varpi^{AB}(t)) = \begin{cases} 2 - \sqrt{\frac{6-4e^{-2\gamma t}}{5}} - \sqrt{\frac{4}{5}(1 + e^{-2\gamma t})} & 0 \leq t < \tilde{t}^\star; \\ 0 & t \geq \tilde{t}^\star, \end{cases} \tag{6.28}$$

where $\tilde{t}^\star = \frac{1}{\gamma}\ln 2$.

Furthermore, in Ref. [TRB11] the distance-based total and classical correlations according to Eq. (3.68) and Eq. (3.69), respectively, of any BD state were

evaluated using the squared Bures distance. Although the explicit form of the classical correlations for any BD state is too cumbersome to report here, we have in particular for any BD state $\{c_1, -c_1c_3, c_3\}$ on the freezing surface

$$CC_{AB}^{D_{Bu}}(\{c_1, -c_1c_3, c_3\}) = \max\{h_{D_{Bu}}(|c_1|), h_{D_{Bu}}(|c_3|)\}, \tag{6.29}$$

with $h_{D_{Bu}}$ the monotonic function of the squared Bures distance in Table 6.1. For the time evolved BD state $\varpi^{AB}(t)$ on the freezing surface, we then have

$$CC_{AB}^{D_{Bu}}(\varpi^{AB}(t)) = \begin{cases} 2 - \sqrt{1 - e^{-2\gamma t}} - \sqrt{1 + e^{-2\gamma t}} & 0 \leq t < t^\star; \\ 2 - 3\sqrt{\frac{2}{5}} & t \geq t^\star. \end{cases} \tag{6.30}$$

The total correlations for any BD state were evaluated in Ref. [TRB11] using a numerically supported ansatz. The result is too detailed to report explicitly here.

Figure 6.5 plots all of the above quantities for a bit flip noise strength of $\gamma = 1$. We then see an interesting interplay between the quantum and classical correlations: the quantum correlations are frozen until time $t^\star$ and then decay to zero asymptotically, while the classical correlations decay until time $t^\star$ and are then frozen forever afterwards. Instead, the quantum coherence is frozen for all times, and coincides with the quantum correlations until $t^\star$ and the classical correlations after $t^\star$.

The interplay between the quantum correlations, classical correlations and quantum coherence observed in Fig. 6.5 is not just a result of using the squared Bures distance to measure the resources, and can be observed for other choices of distance. In the following we highlight some of the other works identifying the freezing behaviour of these resources [31, 32, 34, 144, 234, 235, 237, 249]. This general interplay may be understood by identifying a so called pointer basis [215, 237, 249–252], which is the ONB in which states of the quantum system tend to become classical mixtures under the presence of noise: representing the emergence of a classical system. In the case of bit flip noise on two qubits, the pointer basis is the plus-minus product ONB $\{|{+}{+}\rangle, |{+}{-}\rangle, |{-}{+}\rangle, |{-}{-}\rangle\}$ corresponding to tensor products of the eigenbasis of σ_1, i.e. $|\pm\rangle = \frac{1}{\sqrt{2}}(|0\rangle \pm |1\rangle)$. The quantum coherence measured with respect to the pointer basis will decay with time asymptotically

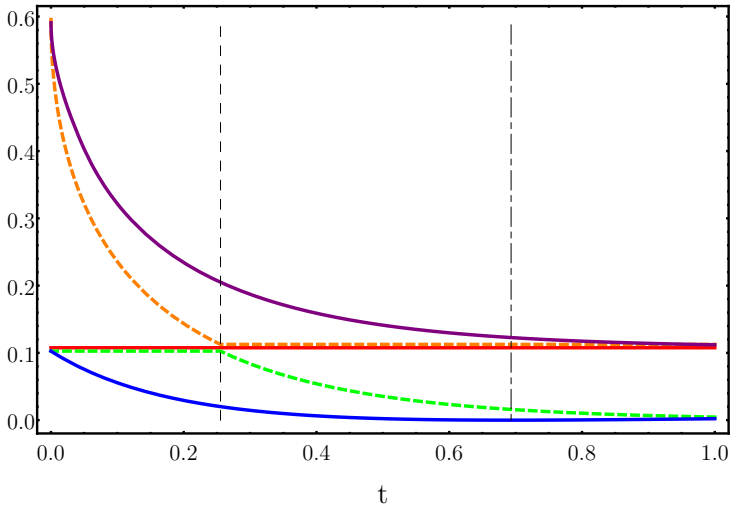

Figure 6.5: The time evolution of quantum coherence (red line), quantum correlations (dashed green line), entanglement (blue line), classical correlations (dashed orange line), and total correlations (purple line) of a two qubit BD state in initial triple $\{\frac{3}{5}, -\frac{3}{5}, 1\}$ undergoing qubit bit flip noise of strength $\gamma = 1$. The quantum coherence is frozen for all time, while the quantum correlations are frozen until time $t^\star = -\frac{1}{2}\ln\frac{3}{5}$ (dashed vertical black line) and then decay to zero asymptotically. The classical correlations begin decaying, but then freeze for all times after $t^\star$. Instead, the entanglement decays to zero in a finite time $\tilde{t}^\star = \ln 2$ (dot dashed vertical black line). Note that the quantum and classical correlations, when frozen, coincide with the quantum coherence, but have been drawn slightly offset so that all three lines are always visible.

to zero. However, we measure quantum coherence with respect to the two qubit computational basis. Since even the pointer basis states are coherent with respect to this basis, it is natural to expect some coherence of the initial two qubit system to be preserved under the bit flip noise. What we find is an initial state of the two qubit system so that distance-based quantum coherence is *exactly* frozen for all time.

On the other hand, as alluded to in Section 2.2.1, quantum correlations may be seen as the presence of coherence in all local product ONBs. Furthermore, we have discussed in Section 3.2.2 that measures of quantum correlations can be recast as measures of quantum coherence minimised over all local product ONBs [TRB12, 84, 141, 142], as noted in Ref. [TRB9]. The coincidence in Fig. 6.5 of the squared

Bures distance-based quantum correlations and quantum coherence for $0 \leq t \leq t^{\star}$ hence shows that a local product ONB minimising the quantum coherence is given by the two qubit computational basis. Since the quantum coherence is frozen with respect to this basis, the quantum correlations must be too. Then, after $t^{\star}$ it can be seen that a local product basis minimising the quantum coherence is the pointer basis, so that the quantum correlations coincide with the quantum coherence in this basis and decay asymptotically to zero.

Turning now to the classical correlations in the distance-based approach of Eq. (3.69), the BD state $\{0, 0, e^{-2\gamma t}c_3(0)\}$ is one of the closest classical states to the evolving BD state $\{c_1(0), -e^{-2\gamma t}c_1(0)c_3(0), e^{-2\gamma t}c_3(0)\}$ on the freezing surface before $t^{\star}$, while the BD state $\{c_1(0), 0, 0\}$ is one of the closest classical states after $t^{\star}$. If these two classical states before and after $t^{\star}$, respectively, satisfy the infimum in Eq. (3.69) over closest classical states for calculation of the classical correlations (as is the case for the Bures distance), then the observed behaviour of the classical correlations in Fig. 6.5 may be explained simply. Indeed, we may expect that the distance of the classical BD state $\{0, 0, e^{-2\gamma t}c_3(0)\}$ to the set of product states $\mathcal{P}^{AB}$ decays with time as this BD state approaches the uncorrelated maximally mixed state, hence giving the observed behaviour of the classical correlations before $t^{\star}$. On the other hand, it can be seen that the classical BD state $\{c_1(0), 0, 0\}$ is at a constant distance from the set of product states $\mathcal{P}^{AB}$, thus giving the observed freezing of classical correlations after $t^{\star}$.

6.1.6 Comparison to Other Results

Before proceeding to discuss the dynamical conditions for the preservation of quantum entanglement, we first discuss the body of works identifying and characterising frozen quantum coherence and quantum correlations, hence highlighting the exact contributions of Refs. [TRB9, TRB10]. A study of the evolution of quantum correlations and classical correlations using the conventional entropic approach [9, 10] was provided in Ref. [34], which spurred a series of works [TRB6, 31–33, TRB11, 144, 233–238] investigating frozen quantum and classical correla-

tions measured using both the entropic and distance-based approaches in various dynamical settings. The contribution of Ref. [TRB10] was to establish that the dynamical conditions discussed here lead to freezing universally for any distance-based measure of quantum correlations (whose distance satisfies the required properties of contractivity, joint convexity, and transposition invariance). Indeed, we do not rule out the existence of alternative dynamical conditions for freezing by focussing on particular distance-based measures.

The identification of frozen quantum correlations further led to the identification of frozen quantum coherence in Ref. [TRB9]. Again, while particular measures of coherence may exhibit freezing under a larger range of dynamical conditions, we show that two qubit BD states on the freezing surface subjected to qubit bit flip noise will universally have frozen quantum coherence for any distance-based measure (with a contractive and jointly convex distance). Furthermore, we have identified the universal freezing of distance-based measures of coherence for N qubit $\mathcal{M}_N^3$ states, of any even N, by finding the corresponding freezing surface in the $\mathcal{M}_N^3$ tetrahedron $\mathcal{T}_{(-1)^{N/2}}$ for bit flip noise on each qubit. In this thesis we restricted to BD states ($\mathcal{M}_2^3$ states) to allow for a simple comparison with quantum correlations. The interested reader may refer to Refs. [236, 238] for a discussion of the freezing conditions of quantum correlations beyond $N = 2$.

Subsequently, there have been theoretical findings on frozen quantum coherence [239–241] and also the demonstration of its occurrence in experimental systems using a nuclear magnetic resonance (NMR) setup involving two and four qubits [TRB6]. We note that the distance-based freezing of quantum coherence and quantum correlations occurs universally also if the system is instead subjected to qubit bit-phase flip or phase flip noise [7]. In this case, for the freezing effect to manifest, one can measure quantum coherence with respect to the plus-minus product ONB $\{|{+}{+}\rangle, |{+}{-}\rangle, |{-}{+}\rangle, |{-}{-}\rangle\}$ and choose initial two qubit BD states in a correspondingly rotated freezing surface of the tetrahedron $\mathcal{T}_{-1}$ [TRB9, TRB10]. Phase flip noise is equivalent to phase damping, which is one of the two dominant sources of noise in an NMR system along with amplitude damping [253]. The experiment in Ref. [TRB6] hence investigated freezing under phase damping,

and thus illustrated its occurrence under a natural and experimentally relevant type of noise.

6.2 Quantum Entanglement

It has long been accepted that quantum entanglement is more fragile than general quantum correlations in the presence of noise [34, 105, 116, 217, 243, 254, 255]: quantum entanglement tends to decay to zero at finite times while quantum correlations can survive for asymptotically large times, as can be seen for example in Fig. 6.5. However, some recent findings [35, 36] have identified a type of noise called collective dephasing, for which entanglement can show a strong resistance towards. Collective dephasing arises physically when a collection of spins are placed in a spatially homogeneous electromagnetic field that has imperfect fluctuations in the field strength, a situation typically encountered in the trapped ion experimental setup [256–258].

In Refs. [35, 36], it was shown that two qubit BD states can exhibit frozen entanglement for all times under the action of collective dephasing. Again, since BD states are $\mathcal{M}_N^3$ states with $N = 2$, Section 4.2.1 tells us that the entangled BD states are given by the four corners of the tetrahedron $\mathcal{T}_{-1}$ not contained within the octahedron $\mathcal{O}_1$ in the $\{c_1, c_2, c_3\}$ space, see Fig. 4.3 [152]. Then, the action of collective dephasing (for a set electromagnetic field direction) on any entangled BD state ϖ^{AB} with triple $\{c_1, c_2, c_3\}$ in a corner of the tetrahedron is to transform the BD state along a path with constant plane height $h_{\varpi^{AB}} := \frac{1}{2}(\sum_{i=1}^{3} |c_i| - 1)$. From Eq. (4.22), we know that any distance-based measure of entanglement is just a monotonic function $f_{D_\delta}(h_{\varpi^{AB}})$ of the plane height $h_{\varpi^{AB}}$ for any contractive and jointly convex distance D_δ, and is hence frozen for any time under collective dephasing. The freezing of an entanglement measure for collective dephasing was first noticed in Refs. [35, 36] in particular for the two qubit concurrence, given by the square root of the tangle in Eq. (5.27), which for BD states is exactly the plane height $h_{\varpi^{AB}}$.

Given such findings for two qubits, it is then natural to consider the possibility

of frozen multiqubit entanglement in an N qubit system, as has been investigated in Refs. [35, 36, 259]. Focussing on the results presented in this thesis, we may consider the freezing of multiqubit entanglement in $\mathcal{M}_N^3$ states, being the natural extension of BD states to N qubits. Indeed, we know for even N that the $\mathcal{M}_N^3$ states with plane height $h_\varpi := \frac{1}{2}(\sum_{i=1}^3 |c_i| - 1)$ all have the same distance-based multiqubit entanglement $E_M^{D_\delta}$ for any contractive and jointly convex distance D_δ and all $M > N/2$. Hence, any noise source whose action is to preserve the plane height of the $\mathcal{M}_N^3$ states will lead to frozen multiqubit entanglement. Whether this is the case for collective dephasing on the N qubits is left as a topic for further investigation. On the other hand, in Ref. [TRB4] we have identified two quantum operations that preserve h_ϖ, i.e. Λ_{in} and Λ_{out}, as described in the third step of Section 4.2.1. However, Λ_{in} is a convex combination of local unitaries and thus a type of LOCC, while Λ_{out} is a collective operation on each of the N qubits. It is then not clear whether either quantum operation corresponds to a physically relevant source of noise. Hence, the identification of frozen multiqubit entanglement within $\mathcal{M}_N^3$ states of N qubits in the presence of physically realistic sources of noise remains an open question.

Chapter 7

Discussion

The quantum mechanical world has become a major focus of modern scientific research. Its interest stems primarily from the potential to impact substantially upon the present development of technologies. Findings in quantum mechanics can also have interdisciplinary relevance: informing young evolving fields such as quantum biology [260–263], as well as more traditional fields like thermodynamics [264–266]. At the heart of its importance is *the quantum*: properties of quantum systems that do not emerge from the principles of classical mechanics. This thesis has focused upon the characterisation of some well established types of *the quantum*: quantum coherence, quantum correlations, and quantum entanglement. We began in Chapter 1 by comparing finite dimensional classical systems with finite dimensional quantum systems. From there, each type of *the quantum* was highlighted in Chapter 2 as a property arising only from the quantum formalism. We then set out to investigate three questions often posed by the scientific community:

1. How much of *the quantum* is there?

2. What can *the quantum* be used for?

3. Can *the quantum* be preserved in the presence of noise?

These questions were investigated in Chapters 3 to 6. A summary of the findings presented in this thesis can be found in Fig. I.2. We now discuss our findings.

Question 1

The objective of Chapter 3 was to describe methods to answer Question 1. Types of *the quantum* may be quantified by using the rigorous formalism provided by quantum resource theories [13–15], which motivate requirements for measures of quantum resources based on the restrictions imposed, leading to the sets of free states and free operations. We outlined the resource theories of quantum coherence [1], quantum correlations [11, TRB12, TRB13], and quantum entanglement [2], specifying the requirements typically imposed upon measures of these quantities. However, one issue at present is that the free operations of quantum coherence and quantum correlations have not yet been fully agreed upon by the scientific community [1], although there appears to be an increasing consensus for the so-called strictly incoherent operations [84, 85] as the free operations of quantum coherence. It is hoped that this issue can be resolved conclusively in the near future.

Another important aspect of quantum resource theories that we have not discussed is the characterisation of the intraconversion between resource states using free operations. For bipartite entanglement, such a characterisation is achieved for pure inseparable states in terms of majorisation of Schmidt coefficients [7, 267]. However, for mixed states the characterisation is not as clear [268]. It could be of interest to extend this analysis to quantum coherence and quantum correlations (some results exist already for quantum coherence [85, 87, 269]). The interconversion between different quantum resources is also worthy of further investigation and has been recently considered in Refs. [53, 137, 141, 270, 271].

In the second part of Chapter 3, we introduced two general approaches to measuring a resource. It is important to emphasise that there exist many alternative ways to measure a quantum resource and the interested reader is directed to the reviews in Refs. [1, 2, 11, TRB12, 57, 58, TRB13] for further information. We considered first the robustness of a resource, which is the minimum amount of classical mixing needed to recover a free state from a resource state. We showed that the robustness of a resource satisfies the minimal requirements of a resource

measure, and furthermore can be evaluated as the solution to an SDP if the corresponding resource theory is equipped with a resource destroying quantum operation. When the resource destroying quantum operation is self-dual, then it is simple to see that the robustness can be quantitatively witnessed by a class of experimentally accessible observables. It is hence of future interest to identify which quantum resources have a resource destroying quantum operation [128].

We also defined and partially characterised the robustness of coherence and the robustness of k coherence [TRB1, TRB2, TRB3]. Evaluation of the robustness of k coherence for all pure states is left as a line of future investigation. Instead, the robustness of quantum correlations has never been defined and it remains an interesting question to investigate the implications of measuring the robustness when the resource theory has a non-convex set of free states. Finally, we then explained the well established distance-based approach [18, 19] to quantifying a resource and showed its adherence to the minimal set of requirements. As an addition to this, we provided a well defined expression for the classical correlations.

Chapter 4 was also aimed at helping to answer Question 1. It can be difficult to evaluate a measure of a quantum resource for a given state of the quantum system, and instead it may be more reasonable to look for an informative lower bound. We constructed a general framework to provide lower bounds on measures of quantum resources [TRB4, TRB5, TRB6]. This framework relies on the identification of a resource non-increasing projection, which is a free operation that projects the set of states onto a restricted class of resource guarantor states with necessarily a non-increased amount of resource. Using this construct, one can employ a number of simplifications to evaluate measures of the resources for the resource guarantor states, and thus find lower bounds on the resources present in general states. We illustrated the application of this framework with the $\mathcal{M}_N^3$-fication resource non-increasing projection, which can provide lower bounds to multiqubit entanglement and coherence by focussing on the resource guarantor states given by the simple set of three parameter $\mathcal{M}_N^3$ states. The lower bounds for multiqubit entanglement are of particular relevance experimentally, being accessible with

only three local measurement settings and thus faring well in comparison with other approaches such as quantitative entanglement witnesses [129, 176]. We further hope to investigate whether $\mathcal{M}_N^3$ states can be used to provide lower bounds also for quantum correlations.

The most important question raised by our framework is the existence and identification of other resource non-increasing projections. Here it may be useful to develop a clear recipe to formulate other resource non-increasing projections. For multiqubit entanglement, we plan to study the various projections that can be given by performing convex combinations of local unitary transformations composed of tensor products of Pauli matrices, following the particular case in Eq. (4.16) for the $\mathcal{M}_N^3$-fication. It is clear that each resource non-increasing projection must make a compromise between the simplicity of the resource guarantor states and the amount of resources remaining in the resource guarantor states. Indeed, we know that $\mathcal{M}_N^3$-fication destroys all genuine and some partial multiqubit entanglement, so that one may need to use other less strong entanglement non-increasing projections such as GHZ-diagonalisation to provide non-trivial lower bounds on stronger forms of multiqubit entanglement. It will also be of interest to investigate the resource non-increasing projections of other types of quantum resources not discussed here, such as steering and Bell nonlocality.

Question 2

In Chapter 5, we considered Question 2 by identifying two operational tasks in quantum metrology for which *the quantum* plays an advantageous role. We first outlined a phase discrimination game, where the objective is to infer which of a set of phases is applied to a quantum probe by a unitary with a Hamiltonian that has a fixed eigenbasis. Here, the aim is to achieve the highest probability of successfully guessing the phase. One option is to simply guess the phase based on the maximum value of the known prior probability distribution describing the likelihood that the phases are applied. Alternatively, one can use coherence in the probe, with respect to the ONB given by the eigenbasis of the Hamiltonian,

to improve the probability of success. It was then shown that the robustness of coherence of the quantum probe exactly quantifies the optimum advantage of using coherence [TRB1, TRB2]. On the other hand, the performance of the phase discrimination game can also be used to quantitatively benchmark the robustness of k coherence [TRB3]. Future work will aim to clarify the exact role of k coherence in the phase discrimination game, as well as looking at the role of other quantum resources, such as entanglement by adding a correlated ancilla [272].

We proceeded to investigate the objective of precise phase estimation within quantum metrology, which can be understood in terms of the quantum Fisher information that gives the maximum possible precision on an estimator of the phase. The roles of quantum coherence and quantum entanglement in phase estimation were examined. Then, focussing on phase estimation in quantum interferometry, we also compared the roles of quantum correlations and quantum entanglement. A worst-case scenario interferometer was considered, consisting of an imprinting of the phase by a local unitary acting on one arm of the interferometer with a least informative Hamiltonian that has a fixed spectrum but variable eigenbasis. It is already established that the interferometric power represents one possible figure of merit in this setup [30, 114], which is thought to represent a measure of quantum correlations. We added weight to this notion by proving that the interferometric power is monotonically non-increasing under all local commutativity preserving operations acting on a qubit subsystem passing through the phase imprinting arm of the interferometer [TRB7]. A monotonicity under a subset of local commutativity preserving operations acting on higher dimensional subsystems was also shown. Furthermore, the interferometric entanglement was introduced as an alternative figure of merit in this setting. Shown to satisfy the requirements for a measure of quantum entanglement, we established a formal hierarchy between the interferometric entanglement and interferometric power [TRB7]. The next steps will be to consider the roles of quantum correlations and quantum entanglement for interferometers using other types of phase imprinting operations besides worst-case scenario local unitaries, such as using

the noisy phase-covariant operations [222]. Furthermore, it may be of interest to consider phase imprinting operations acting on both arms of the interferometer.

We stress that the two operational tasks highlighted here by no means represent the exhaustive knowledge of operational roles of *the quantum*. As before, the interested reader is directed to the reviews in Refs. [1, 2, 11, TRB12, TRB13] for further details. It is hoped that additional developments can be made in this area, given the drive to develop quantum technologies. However, it can be difficult to identify the operational role of a given measure of *the quantum*. Prime examples of this problem are the distance-based measures of a resource, which are well motivated geometrically but often lacking an operational perspective, aside from the more abstract concept of state distinguishability. Perhaps the more natural approach is to instead begin from an operational perspective and construct a quantity that may then be shown to be a measure of *the quantum*, as has been done for example in the interferometric setting [30, 273].

Question 3

The dynamical behaviour of *the quantum* in the presence of noise was considered in Chapter 6 [TRB8]. We investigated Question 3 by showing that types of *the quantum* may be constant, or frozen, in the presence of noise under certain dynamical conditions. These dynamical conditions are given in terms of initial states and the type of noise applied to the system. For quantum coherence and quantum correlations, measured using the distance-based approach, we identified a class of two qubit Bell diagonal states that lead to freezing when subjected to qubit bit flip noise. Here, quantum coherence with respect to the two qubit computational basis is frozen indefinitely, while quantum correlations are frozen until a finite threshold time and then decay [TRB9, TRB10]. Although the freezing effect was already identified for quantum correlations [31–33, TRB11, 34, 144, 233–237], our analysis shows that freezing of both quantum coherence and quantum correlations occurs under these dynamical conditions *universally* for any distance-based measure of the resource. We then proceeded to compare the behaviour of quantum

coherence, quantum correlations, quantum entanglement, total correlations, and classical correlations under a particular example of these dynamical conditions, with all quantities measured using the squared Bures distance. Here, we used the refined definition of classical correlations given in Ref. [TRB11]. The comparison highlighted an interplay between quantum correlations, classical correlations and quantum coherence, which can be physically justified by referring to the concept of a classical pointer basis [215, 249–252]. Furthermore, the freezing of classical correlations after a threshold time has been observed for a variety of measures [31, 32, TRB11, 34, 144, 233–236], and it is worthy of further investigation to establish whether this freezing may be understood from a universal perspective using the properties of contractivity and joint convexity in the distance-based approach.

It is of interest to investigate when dynamical conditions for freezing are relevant in real experimental setups. In Ref. [TRB6] we experimentally observed frozen quantum coherence in a two qubit and four qubit nuclear magnetic resonance system experiencing naturally occurring phase damping noise. Nevertheless, the ideal scenario would be to harness freezing to preserve the figure of merit of an operational task powered by a quantum resource when the task is carried out in the presence of noise. We remark that for N qubit $\mathcal{M}_N^3$ states, the robustness of coherence is twice the trace distance-based measure of coherence according to Eq. (4.44), so that the robustness of coherence is also frozen under the same dynamical conditions as for the distance-based measures (i.e. with N qubit $\mathcal{M}_N^3$ states on the freezing surface subjected to qubit bit flip noise). Furthermore, in Chapter 5 we identified the robustness of coherence as a figure of merit in the phase discrimination task. We have therefore found an operational task that can run in the presence of noise without deterioration of the figure of merit, and it may be of interest to investigate further the effects of noise in the phase discrimination game.

Given the prevalence of N qubit $\mathcal{M}_N^3$ states in this thesis, it will also be interesting to investigate the behaviour of these states, and their corresponding quantum resources, under more general sources of noise with potentially non-Markovian environments [32, TRB11, 144, 233–237, 242]. For entanglement, we

have already identified a freezing surface of constant M-inseparable multiqubit entanglement, given by the N even $\mathcal{M}_N^3$ states with $M > N/2$ that are, in the $\{c_1, c_2, c_3\}$ space, at a constant plane height $\frac{1}{2}(\sum_{i=1}^3 |c_i| - 1)$, see Eq. (4.22) [TRB4]. What is not clear is whether there is any realistic type of noise encountered in physical systems that maintains $\mathcal{M}_N^3$ states on this freezing surface for $N > 2$ (for $N = 2$, collective dephasing satisfies this requirement [35, 36]).

7.1 Conclusions and Outlook

We have identified three important questions for the present development of quantum science and investigated approaches to resolving them, highlighting the contributions of the author in Refs. [TRB1-TRB13]. These questions are related, and together form a relevant line of inquiry to help navigate the quantum-classical frontier. Indeed, quantification of *the quantum* allows for a comparison of the resources present in quantum systems and thus informs us on which systems carry the most resources for a given scenario. We can then attempt to address the usefulness of *the quantum* in an operational setting and associate the figure of merit quantifying the advantage of an operational task with a measure of the quantum resource. However, typical quantum systems are subjected to noise. It is then necessary to consider ways to combat the negative effects of this noise and identify conditions for which *the quantum* can be preserved.

Having discussed these questions in this thesis, it is natural to ask: what next? Of course, there are still many interesting open questions in the study of the quantification of quantum resources, their operational roles, and their behaviour in open quantum systems. We have given a non-extensive collection of possibilities for further research, arising from this work, in the discussion above. More generally, one of the most exciting prospects for the author is the current evolution of quantum resource theories and the rigorous framework that they impose upon measures of the resource. Understanding the interconversion between different quantum resources may benefit in particular from developments in quantum resource theories. It will also be worthwhile to study further other

types of *the quantum*, such as steering and Bell nonlocality, from the perspective of resource theories [80, 274]. Maybe even entirely new types of *the quantum* can be identified from the resource theoretic approach.

Outside of the familiar realm of quantum information theory, experimentalists and engineers are now busy attempting to fabricate quantum technologies [275–279]. The expectation is that these technologies will be commercially viable over the next few years, and one might argue that the only remaining obstacles are experimental and engineering rather than theoretical. While this may be true in some settings, we will always rely on theoretical breakthroughs to bring fresh new concepts and prevent stagnation of ideas. Nevertheless, it could be argued that quantum science might be served better by theoreticians tailoring their research more closely to experiments (however daunting this may at times sound). One area where theoreticians can play a key role is establishing the supremacy of quantum technologies over those currently available [187], which often relies on the field of computational complexity theory [280]. On the other hand, perhaps the continued study of quantum foundations [281–283] can also change our perspective over the years to come. What is clear is that we are in very exciting times for quantum science, there is a lot more to explore and discover. Let's see what's out there!

Appendix A

Isotropic Operations

Here we provide an operator sum representation of the isotropic operations, taken from Ref. [TRB7]. The isotropic operations acting on a d-dimensional system in the state ρ are written as [107]

$$\Lambda(\rho) = t\Phi(\rho) + (1-t)\frac{\mathbb{I}}{d}, \tag{A.1}$$

where Φ is either unitary, $\Phi(\rho) = U\rho U^\dagger$, or antiunitary, $\Phi(\rho) = U\rho^\intercal U^\dagger$, for some unitary U with $\rho^\intercal$ denoting the transposition of ρ in the standard basis. In particular, we provide the Kraus operators $\{K_i\}_i$ when $U = \mathbb{I}$. To find the Kraus operators for a general U, one simply needs to transform the Kraus operators by $K_i \to UK_i$. Note that quantum correlations are invariant under local unitary transformations, and so here when one considers the local isotropic operations as a subtype of the LCPO, it is sufficient to work with just the case $U = \mathbb{I}$.

The operator sum representation of Λ is

$$\Lambda(\rho) = \sum_i K_i \rho K_i^\dagger, \tag{A.2}$$

where $\{K_i\}_i$ are a set of Kraus operators obeying the condition $\sum_i K_i^\dagger K_i = \mathbb{I}$. In the following we first determine the allowed range of t for the isotropic operation Λ to be CPTP by imposing that the corresponding Choi state is positive semidefinite [284]. The Choi state is given by [242]

$$\tau := \Lambda \otimes \mathbb{I}(|\Psi_+\rangle\langle\Psi_+|) \tag{A.3}$$

where $|\Psi_+\rangle := \frac{1}{\sqrt{d}} \sum_{i=1}^{d} |i\rangle \otimes |i\rangle$ is a pure $(d \times d)$-dimensional state and $\mathbb{I}$ is the d-dimensional identity quantum operation, with $\{|i\rangle\}_{i=1}^{d}$ the standard basis.

The unitary case

First we consider the unitary Φ case. Considering only $U = \mathbb{I}$, for any $(d \times d)$-dimensional state ρ it holds that $\Lambda \otimes \mathbb{I}(\rho) = t\rho + (1-t)\frac{\mathbb{I}}{d} \otimes \mathrm{Tr}_1(\rho)$, with $\mathrm{Tr}_1(\rho)$ the partial trace of ρ over the first d-dimensions. The corresponding Choi state is

$$\tau = t\,|\Psi_+\rangle\langle\Psi_+| + \frac{1-t}{d^2}\mathbb{I}. \tag{A.4}$$

It is simple to see that the unique eigenvalues of τ are $\{t + (1-t)/d^2, (1-t)/d^2\}$. By imposing both unique eigenvalues to be non-negative we obtain the allowed range

$$-\frac{1}{d^2-1} \leq t \leq 1, \tag{A.5}$$

which is tighter than what was reported in [107]. We now provide the operator sum representation of Λ. Consider the d^2-1 generalised Gell-Mann matrices $\{\gamma_i\}_{i=1}^{d^2-1}$ [285], and fix the d-dimensional identity matrix as $\gamma_0 := \mathbb{I}$. The d^2 Kraus operators $\{K_i\}_{i=0}^{d^2-1}$ of Λ are then

$$\begin{aligned} K_0 &= \sqrt{\frac{1+(d^2-1)t}{d^2}}\gamma_0, \\ K_i &= \sqrt{\frac{1-t}{2d}}\gamma_i \qquad\qquad \forall i \in \{1,2,\ldots,d^2-1\}. \end{aligned} \tag{A.6}$$

We can now verify the condition $\sum_{i=0}^{d^2-1} K_i^\dagger K_i = \mathbb{I}$. Since the Kraus operators are self-adjoint, and since $\gamma_0^2 = \mathbb{I}$ and $\sum_{i=1}^{d^2-1}\gamma_i^2 = \frac{2(d^2-1)}{d}\mathbb{I}$, we have

$$\begin{aligned} \sum_{i=0}^{d^2-1} K_i^\dagger K_i &= \left(\left|\frac{1+(d^2-1)t}{d^2}\right| + \frac{2(d^2-1)}{d} \times \left|\frac{1-t}{2d}\right|\right)\mathbb{I} \\ &= \frac{1}{d^2}\left(\left|1+(d^2-1)t\right| + (d^2-1)\,|(1-t)|\right)\mathbb{I}. \end{aligned} \tag{A.7}$$

By exploiting Eq. (A.5), we can simplify $|1+(d^2-1)t| = 1+(d^2-1)t$ and

$|1-t| = 1-t$, hence

$$\begin{aligned}\sum_{i=0}^{d^2-1} K_i^\dagger K_i &= \frac{1}{d^2}\left(1+(d^2-1)t+(d^2-1)(1-t)\right)\mathbb{I} \\ &= \mathbb{I}. \end{aligned} \tag{A.8}$$

Antiunitary case

Now we treat the more complicated case of Φ being antiunitary (again, fixing $U = \mathbb{I}$). For any $(d\times d)$-dimensional state ρ, we have $\Lambda\otimes\mathbb{I}(\rho) = t\rho^{\mathsf{T}_1} + (1-t)\frac{\mathbb{I}}{d}\otimes \mathrm{Tr}_1(\rho)$, where ρ^{T_1} indicates partial transposition of ρ in the standard basis with respect to the first d-dimensions [20]. The corresponding Choi state is

$$\tau = \frac{t}{d}\sum_{i,j=1}^{d} |i\rangle\langle j| \otimes |j\rangle\langle i| + \frac{1-t}{d^2}\mathbb{I}. \tag{A.9}$$

By inspection the d^2 eigenvectors of τ can be found to be $|k\rangle\otimes|k\rangle$ with $k \in \{1,2,\ldots,d\}$, and $\frac{1}{\sqrt{2}}(|k\rangle\otimes|l\rangle \pm |l\rangle\otimes|k\rangle)$ for all pairs $k<l$. The unique eigenvalues of τ are then $\{(1-t)/d^2, t/d+(1-t)/d^2, -t/d+(1-t)/d^2\}$, which are all non-negative when

$$-\frac{1}{d-1} \le t \le \frac{1}{d+1}. \tag{A.10}$$

As before, to write down the operator sum representation of Λ, we can use the generalised Gell-Mann matrices $\{\gamma_i\}_{i=1}^{d^2-1}$ with the identity $\gamma_0 := \mathbb{I}$. Now, consider the set of vectorisations of the generalised Gell-Mann matrices, $\{\vec{v}_i\}_{i=1}^{d^2-1}$ with $\vec{v}_i = \mathrm{vec}(\gamma_i)$, where

$$\mathrm{vec}(X) := \{\langle 1|X|1\rangle, \langle 1|X|2\rangle, \ldots, \langle 1|X|d\rangle, \langle 2|X|1\rangle, \langle 2|X|2\rangle, \ldots, \langle d|X|d\rangle\} \tag{A.11}$$

is the vectorisation of X. We can split the generalised Gell-Mann matrices into two categories based on their corresponding vectorisations: (1) $\mathrm{sign}(\vec{v}_i.\vec{v}_i) = 1$, and (2) $\mathrm{sign}(\vec{v}_i.\vec{v}_i) = -1$. There are $(d+2)(d-1)/2$ generalised Gell-Mann of type (1) and $d(d-1)/2$ of type (2). We call the generalised Gell-Mann matrices of type (1): $\{\gamma_i^{(1)}\}_{i=1}^{(d+2)(d-1)/2}$, and of type (2): $\{\gamma_i^{(2)}\}_{i=1}^{d(d-1)/2}$. Now we can give

the d^2 Kraus operators $\{K_i\}_{i=0}^{d^2-1}$ of Λ as

$$\begin{aligned} K_0 &= \sqrt{\frac{1+(d-1)t}{d^2}}\gamma_0, \\ K_i &= \sqrt{\frac{1+(d-1)t}{2d}}\gamma_i^{(1)} \quad \forall i \in \{1,2,\ldots,(d+2)(d-1)/2\}, \\ K_{i+(d+2)(d-1)/2} &= \sqrt{\frac{1-(d+1)t}{2d}}\gamma_i^{(2)} \quad \forall i \in \{1,2,\ldots,d(d-1)/2\}. \end{aligned} \tag{A.12}$$

We can also consider the condition $\sum_{i=0}^{d^2-1} K_i^\dagger K_i = \mathbb{I}$. Since the Kraus operators are self-adjoint, and since $\gamma_0^2 = \mathbb{I}$, $\sum_{i=1}^{(d+2)(d-1)/2}(\gamma_i^{(1)})^2 = \frac{d^2+d-2}{d}\mathbb{I}$ and $\sum_{i=1}^{d(d-1)/2}(\gamma_i^{(2)})^2 = (d-1)\mathbb{I}$, we have

$$\begin{aligned} \sum_{i=0}^{d^2-1} K_i^\dagger K_i &= \left(\left|\frac{1+(d-1)t}{d^2}\right| + \frac{d^2+d-2}{d} \times \left|\frac{1+(d-1)t}{2d}\right| \right. \\ &\qquad \left. + (d-1)\left|\frac{1-(d+1)t}{2d}\right|\right)\mathbb{I} \\ &= \frac{1}{d^2}\left(|1+(d-1)t| + \frac{(d^2+d-2)}{2}|1+(d-1)t| \right. \\ &\qquad \left. + \frac{d^2-d}{2}|1-(d+1)t|\right)\mathbb{I} \\ &= \frac{1}{2d^2}\left((d^2+d)|1+(d-1)t| + (d^2-d)|1-(d+1)t|\right). \end{aligned} \tag{A.13}$$

Then, we may use Eq. (A.10) to simplify $|1+(d-1)t| = 1+(d-1)t$ and $|1-(d+1)t| = 1-(d+1)t$, yielding $\sum_{i=0}^{d^2-1} K_i^\dagger K_i = \mathbb{I}$.

Appendix B

Robustness and Semidefinite Programming

Consider a resource theory with a convex and compact set of free states $\mathcal{F}$ equipped with a resource destroying quantum operation Φ such that Eq. (3.40) holds. Here we show that the optimisation problem in Eq. (3.42), whose solution is the robustness of a resource, is a semidefinite program (SDP). Following the general description of an SDP in Refs. [TRB2, 117, 125], consider two d-dimensional self-adjoint operators X and C and two d'-dimensional self-adjoint operators Y and D, along with a linear map Ψ that maps d-dimensional operators to d'-dimensional operators such that the self-adjoint property is preserved. The following optimisation problem is the primal problem of an SDP

$$\begin{aligned} \text{minimise} \quad & \operatorname{Tr}(CX) \\ \text{subject to} \quad & \Psi(X) \geq D, \\ & X \geq 0. \end{aligned} \tag{B.1}$$

Every SDP has a dual problem, given by

$$\begin{aligned} \text{maximise} \quad & \operatorname{Tr}(DY) \\ \text{subject to} \quad & \Psi^{\dagger}(Y) \leq C, \\ & Y \geq 0, \end{aligned} \tag{B.2}$$

where $\Psi^\dagger$ is the dual map of Ψ, transforming from d'-dimensional operators to d-dimensional operators. The dual of a map Ψ is the unique linear map $\Psi^\dagger$ satisfying [20, 46]

$$\mathrm{Tr}(B^\dagger \Psi(A)) = \mathrm{Tr}(\Psi^\dagger(B^\dagger)A) \tag{B.3}$$

for any operators A and B. The solution to the dual problem of an SDP is generally a lower bound to the solution of the primal problem. Strong duality is said to hold when the solutions to both problems coincide [117, 125, 127]. A sufficient condition for this is when the primal problem is feasible and the dual problem is strictly feasible. The primal problem is feasible when there exists an $X \geq 0$ such that $\Psi(X) \geq D$, while the dual problem is strictly feasible if there exists a $Y > 0$ such that $\Psi^\dagger(Y) < C$.

The robustness of a resource (plus 1) is given from Eq. (3.42) as the optimisation problem

$$\begin{aligned} R^R(\rho) + 1 \;=\; & \text{minimise} && \mathrm{Tr}(\tilde{\sigma}) \\ & \text{subject to} && \Phi(\tilde{\sigma}) = \tilde{\sigma}, \\ & && \rho \leq \tilde{\sigma}. \end{aligned} \tag{B.4}$$

Following the strategy of Ref. [TRB2], to see that this problem may be written in the general form of the primal SDP in (B.1), first set $C = \mathbb{I}$ and $X = \tilde{\sigma}$ so that

$$\mathrm{Tr}(CX) = \mathrm{Tr}(\tilde{\sigma}). \tag{B.5}$$

Now set the following operators, represented as $(3d \times 3d)$-dimensional block diagonal matrices, as

$$\begin{aligned} \Psi(X) &= \begin{pmatrix} \tilde{\sigma} & 0 & 0 \\ 0 & \Phi(\tilde{\sigma}) - \tilde{\sigma} & 0 \\ 0 & 0 & -\Phi(\tilde{\sigma}) + \tilde{\sigma} \end{pmatrix} \\ D &= \begin{pmatrix} \rho & 0 & 0 \\ 0 & 0 & 0 \\ 0 & 0 & 0 \end{pmatrix}, \end{aligned} \tag{B.6}$$

with the 0 denoting $(d \times d)$-dimensional zero matrix. We have that $\Psi(X) \geq D$ is equivalent to $\tilde{\sigma} \geq \rho$ and $\Phi(\tilde{\sigma}) = \tilde{\sigma}$. Then, since $\tilde{\sigma} \geq \rho \geq 0$ implies $X \geq 0$, we have shown that Eq. (B.4) may be written in the standard SDP form of (B.1).

To find the dual of this problem, we set Y to be the $(3d \times 3d)$-dimensional matrix

$$Y = \begin{pmatrix} Y_1 & * & * \\ * & Y_2 & * \\ * & * & Y_3 \end{pmatrix}, \tag{B.7}$$

where Y_1, Y_2 and Y_3 are $(d \times d)$-dimensional matrices and $*$ denotes matrices that are irrelevant since we are generally dealing with the trace of a product of Y with a diagonal matrix. We also need to find $\Psi^\dagger(Y)$, which may be found using Eq. (B.3). Indeed,

$$\begin{aligned} \mathrm{Tr}(Y\Psi(X)) &= \mathrm{Tr}\left(Y_1\tilde{\sigma} + Y_2\left(\Phi(\tilde{\sigma}) - \tilde{\sigma}\right) + Y_3\left(-\Phi(\tilde{\sigma}) + \tilde{\sigma}\right)\right) \\ &= \mathrm{Tr}\left(Y_1\tilde{\sigma} + (\Phi^\dagger(Y_2) - Y_2)\tilde{\sigma} + (-\Phi^\dagger(Y_3) + Y_3)\tilde{\sigma}\right) \\ &= \mathrm{Tr}\left(\Psi^\dagger(Y)X\right), \end{aligned} \tag{B.8}$$

where

$$\begin{aligned} \Psi^\dagger(Y) &= Y_1 + \Phi^\dagger(Y_2) - Y_2 - \Phi^\dagger(Y_3) + Y_3 \\ &= Y_1 + \Phi^\dagger(Y_2 - Y_3) - (Y_2 - Y_3) \end{aligned} \tag{B.9}$$

and $\Phi^\dagger$ is the dual of the resource destroying quantum operation Φ. Hence, we can write the dual problem in (B.2) as

$$\begin{aligned} &\text{maximise} && \mathrm{Tr}(\rho Y_1) \\ &\text{subject to} && Y_1 + \Phi^\dagger(Y_2 - Y_3) - (Y_2 - Y_3) \leq \mathbb{I}, \\ & && Y_1 \geq 0, \;\; Y_2 \geq 0, \;\; Y_3 \geq 0, \end{aligned} \tag{B.10}$$

since $Y \geq 0$ implies $Y_1 \geq 0$, $Y_2 \geq 0$ and $Y_3 \geq 0$.

Now we see that (B.10) may be rewritten into the form given in Eq. (3.43) (plus 1) when the resource destroying quantum operation Φ is self dual, again following the strategy of Ref. [TRB2]. First, it holds that $\mathrm{Tr}(\rho Y_1)$ is maximised

by having equality in the first constraint, i.e. $Y_1 + \Phi^\dagger(Y_2 - Y_3) - (Y_2 - Y_3) = \mathbb{I}$. By imposing this and noting that any self-adjoint operator $\tilde{Y}$ may be written as $\tilde{Y} := Y_2 - Y_3$ for some $Y_2 \geq 0$ and $Y_3 \geq 0$, the dual problem becomes a constrained optimisation over self-adjoint $\tilde{Y}$,

$$\begin{aligned} \text{maximise} \quad & 1 - \mathrm{Tr}\left(\rho(\Phi^\dagger(\tilde{Y}) - \tilde{Y})\right) \\ \text{subject to} \quad & \Phi^\dagger(\tilde{Y}) - \tilde{Y} \leq \mathbb{I}, \end{aligned} \tag{B.11}$$

where we impose the constraint $\Phi^\dagger(\tilde{Y}) - \tilde{Y} = \Phi^\dagger(Y_2 - Y_3) - (Y_2 - Y_3) = \mathbb{I} - Y_1 \leq \mathbb{I}$ from above since $Y_1 \geq 0$.

Now, if the resource destroying quantum operation is self-dual, i.e. $\Phi^\dagger = \Phi$, then we can simplify the dual problem further to a constrained optimisation over self-adjoint W, i.e.

$$\begin{aligned} \text{maximise} \quad & 1 - \mathrm{Tr}\,(W\rho) \\ \text{subject to} \quad & W \leq \mathbb{I}, \\ & \Phi(W) = 0. \end{aligned} \tag{B.12}$$

To see this, we first note that Φ is idempotent on all self-adjoint operators, i.e. $\Phi(\Phi(\tilde{Y})) = \Phi(\tilde{Y})$ for all self-adjoint $\tilde{Y}$. This can be shown from Eq. (3.40) by using the linearity of Φ and the fact that $\tilde{Y} = Y_2 - Y_3$ for some $Y_2 \geq 0$ and $Y_3 \geq 0$. Now, choose any $\tilde{Y}$ such that $\Phi(\tilde{Y}) - \tilde{Y} \leq \mathbb{I}$ and set $W = \Phi(\tilde{Y}) - \tilde{Y}$. From the fact that Φ is idempotent, we have $\Phi(W) = 0$. This means that the range of values in the optimisation of (B.12) includes the range of values in. (B.11), so that the solution of (B.11) must lower bound (B.12). On the other hand, pick any $W \leq \mathbb{I}$ such that $\Phi(W) = 0$ and set $\tilde{Y} = -W$. This gives $\Phi(\tilde{Y}) - \tilde{Y} = W \leq \mathbb{I}$. Hence, the solution of (B.12) is a lower bound to the solution of (B.11), which completes the proof of their equivalence.

Finally, we rewrite (B.12) as

$$\begin{aligned} \text{maximise} \quad & 1 - \mathrm{Tr}\,(W\rho) \\ \text{subject to} \quad & W \leq \mathbb{I}, \\ & \Phi(W) \geq 0. \end{aligned} \tag{B.13}$$

Indeed, it is clear that the solution of (B.12) lower bounds the solution of (B.13). However, it also holds that the solution of (B.13) lower bounds the solution of (B.12). To see this, consider any $W \leq \mathbb{I}$ such that $\Phi(W) \geq 0$ and set $W' = W - \Phi(W)$ so that $\Phi(W') = 0$. We have that $W' \leq W \leq \mathbb{I}$ and so for any valid W satisfying the constraints of (B.13) there is a valid W' satisfying the constraints of (B.12) such that

$$1 - \mathrm{Tr}(W'\rho) = 1 - \mathrm{Tr}(W\rho) + \mathrm{Tr}(\Phi(W)\rho) \geq 1 - \mathrm{Tr}(W\rho), \tag{B.14}$$

since $\Phi(W) \geq 0$ implies $\mathrm{Tr}(\Phi(W)\rho) \geq 0$.

It is simple to see that strong duality holds if the resource destroying quantum operation is unital. A feasible solution to the primal problem is to choose $X = (1+\epsilon)\mathbb{I}$ for some $\epsilon \geq 0$ so that $X \geq 0$ and

$$\Psi(X) = \begin{pmatrix} (1+\epsilon)\mathbb{I} & 0 & 0 \\ 0 & 0 & 0 \\ 0 & 0 & 0 \end{pmatrix} \geq \begin{pmatrix} \rho & 0 & 0 \\ 0 & 0 & 0 \\ 0 & 0 & 0 \end{pmatrix} = D \tag{B.15}$$

for any ρ, where we use the use the unitality of Φ to see that $\Phi((1+\epsilon)\mathbb{I}) - (1+\epsilon)\mathbb{I} = 0$. Furthermore, the dual problem is strictly feasible since one may pick

$$Y = \begin{pmatrix} (1-\zeta)\mathbb{I} & 0 & 0 \\ 0 & \mathbb{I} & 0 \\ 0 & 0 & \mathbb{I} \end{pmatrix} \tag{B.16}$$

with $0 < \zeta < 1$ so that $Y > 0$ and

$$\Psi^\dagger(Y) = (1-\zeta)\mathbb{I} < \mathbb{I} = C, \tag{B.17}$$

which follows from the unitality of $\Phi^\dagger$ since the dual of any quantum operation is unital [20]. Strong duality holds in particular when Φ is self-dual (and hence unital). The self duality of Φ holds if and only if an operator sum representation of Φ may be found with a set of self-adjoint Kraus operators [286].

To summarise these results, if we consider a resource theory with a convex and compact set of free states and equipped with a self-dual resource destroying quantum operation Φ, then the robustness of the resource is given by the solution

of two equivalent optimisation problems in Eq. (3.42) and Eq. (3.43), that are the primal and dual problems of an SDP. Quantum coherence is an example of a resource for which the robustness can be posed in such a way [TRB1, TRB2]. Indeed, the set of incoherent states with respect to the ONB $\{|e_i\rangle\}_{i=1}^d$ is convex and compact, while a resource destroying quantum operation can be given by

$$\Delta(\rho) := \sum_{i=1}^{d} |e_i\rangle \langle e_i|\rho|e_i\rangle \langle e_i| . \tag{B.18}$$

Since the $|e_i\rangle \langle e_i|$ are self-adjoint Kraus operators, we know that $\Delta(\rho)$ is self dual.

We finally report on the robustness of k coherence given in Eq. (3.53). So far, the existence of a resource destroying quantum operation identifying the set $\mathcal{I}^{(k)}$ of free states with coherence number less than k has not yet been investigated (for $k > 2$). However, it is still possible to pose the robustness of k coherence as the solution to the primal problem of an SDP. We consider the problem

$$\begin{aligned} C_k^R(\rho) \;=\; & \text{minimise} && \mathrm{Tr}(\tilde{\sigma}) - 1 \\ & \text{subject to} && \frac{\tilde{\sigma}}{\mathrm{Tr}(\tilde{\sigma})} \in \mathcal{I}^{(k)}, \\ & && \rho \leq \tilde{\sigma}, \end{aligned} \tag{B.19}$$

and provide a characterisation of all $\tilde{\sigma}$ such that $\tilde{\sigma}/\mathrm{Tr}(\tilde{\sigma}) \in \mathcal{I}^{(k)}$ with respect to the ONB $\{|e_i\rangle\}_{i=1}^d$, proceeding to then show that (B.19) may be posed as an SDP.

Take the set $\mathcal{C}(k)$ of all combinations of k indices chosen from $\{1, 2, \ldots, d\}$ with cardinality $|\mathcal{C}(k)| = \binom{d}{k}$, where $\binom{d}{k}$ is the binomial coefficient, along with the set of projectors $\{P_{\mathcal{J}}\}_{\mathcal{J}\in\mathcal{C}(k)}$ given by

$$P_{\mathcal{J}} := \sum_{i\in\mathcal{J}} |e_i\rangle \langle e_i| , \tag{B.20}$$

where $\mathcal{J} \in \mathcal{C}(k)$ is one combination of k indices from $\{1, 2, \ldots, d\}$. Here it will be useful to write any pure state $|\psi\rangle$ as

$$|\psi\rangle = \sum_{i\in\mathcal{J}_{|\psi\rangle}} \psi_i |e_i\rangle , \tag{B.21}$$

with $\sum_{i\in\mathcal{J}_{|\psi\rangle}} |\psi_i|^2 = 1$, where the set $\mathcal{J}_{|\psi\rangle} \subseteq \{1, 2, \ldots, d\}$ denotes the indices i such that $\psi_i \neq 0$. If $k = \left|\mathcal{J}_{|\psi\rangle}\right|$ is the cardinality of $\mathcal{J}_{|\psi\rangle}$, then $|\psi\rangle$ has a coherence

number of k and $\mathcal{J}_{|\psi\rangle} \in \mathcal{C}(k)$. This notation is useful since it allows us to identify which of the $|e_i\rangle$ the state $|\psi\rangle$ is coherent with respect to.

We now prove the following relation

$$\begin{aligned} \tilde{\sigma} \geq 0\,,\ \frac{\tilde{\sigma}}{\mathrm{Tr}(\tilde{\sigma})} \in \mathcal{I}^{(k)} \quad \Leftrightarrow \quad \tilde{\sigma} = \sum_{\mathcal{J}\in\mathcal{C}(k-1)} \tilde{\sigma}_{\mathcal{J}} \\ \text{such that } \ \forall\ \mathcal{J} \in \mathcal{C}(k-1) \\ P_{\mathcal{J}}\tilde{\sigma}_{\mathcal{J}}P_{\mathcal{J}} = \tilde{\sigma}_{\mathcal{J}} \\ \tilde{\sigma}_{\mathcal{J}} \geq 0. \end{aligned} \tag{B.22}$$

First, suppose that we have a $\tilde{\sigma} \geq 0$ such that $\tilde{\sigma}/\mathrm{Tr}(\tilde{\sigma}) =: \sigma \in \mathcal{I}^{(k)}$. Using the definition of $\mathcal{I}^{(k)}$ in Section 2.1.1, we can always write

$$\sigma = \sum_i q_i \left|\psi_i^{(k)}\right\rangle \left\langle\psi_i^{(k)}\right| \tag{B.23}$$

with $\{q_i\}_i$ a probability distribution and $\left|\psi_i^{(k)}\right\rangle \left\langle\psi_i^{(k)}\right| \in \mathcal{I}^{(k)}$, so that

$$\tilde{\sigma} = \sum_i t q_i \left|\psi_i^{(k)}\right\rangle \left\langle\psi_i^{(k)}\right| \tag{B.24}$$

where $t := \mathrm{Tr}(\tilde{\sigma}) \geq 0$ since $\tilde{\sigma} \geq 0$. Now, consider one of the pure states $\left|\psi_i^{(k)}\right\rangle = \sum_{j\in\mathcal{J}_{\left|\psi_i^{(k)}\right\rangle}} \psi_{ij}^{(k)} |e_j\rangle$ with $\sum_{j\in\mathcal{J}_{\left|\psi_i^{(k)}\right\rangle}} \left|\psi_{ij}^{(k)}\right|^2 = 1$ and $\left|\mathcal{J}_{\left|\psi_i^{(k)}\right\rangle}\right| < k$. The action of any $P_{\mathcal{J}}$ for $\mathcal{J} \in \mathcal{C}(k-1)$ is given by

$$P_{\mathcal{J}} \left|\psi_i^{(k)}\right\rangle = \sum_{j\in\mathcal{J}\cap\mathcal{J}_{\left|\psi_i^{(k)}\right\rangle}} \psi_{ij}^{(k)} |e_i\rangle \tag{B.25}$$

so that $P_{\mathcal{J}} \left|\psi_i^{(k)}\right\rangle = \left|\psi_i^{(k)}\right\rangle$ if and only if $\mathcal{J}_{\left|\psi_i^{(k)}\right\rangle} \subseteq \mathcal{J}$. Furthermore, there is always a (not necessarily unique) $\mathcal{J} \in \mathcal{C}(k-1)$ such that for any i we have $\mathcal{J}_{\left|\psi_i^{(k)}\right\rangle} \subseteq \mathcal{J}$. Hence, we can distribute each $\left|\psi_i^{(k)}\right\rangle$ to one choice of $\mathcal{J} \in \mathcal{C}(k-1)$ so that $\mathcal{J}_{\left|\psi_i^{(k)}\right\rangle} \subseteq \mathcal{J}$, giving the corresponding set $\mathcal{N}_{\mathcal{J}} \subseteq \{1, 2, \ldots, i\}$ for each $\mathcal{J} \in \mathcal{C}(k-1)$ and allowing us to define

$$\tilde{\sigma}_{\mathcal{J}} = \sum_{i\in\mathcal{N}_{\mathcal{J}}} t q_i \left|\psi_i^{(k)}\right\rangle \left\langle\psi_i^{(k)}\right|. \tag{B.26}$$

By construction, we know that $\tilde{\sigma} = \sum_{\mathcal{J}\in\mathcal{C}(k-1)} \tilde{\sigma}_{\mathcal{J}}$, and for all $\mathcal{J} \in \mathcal{C}(k-1)$ it holds that $P_{\mathcal{J}}\tilde{\sigma}_{\mathcal{J}}P_{\mathcal{J}} = \tilde{\sigma}_{\mathcal{J}}$. Finally, since each $\left|\psi_i^{(k)}\right\rangle \left\langle\psi_i^{(k)}\right| \geq 0$, $q_i \geq 0$ and $t \geq 0$ we know

that $\tilde{\sigma}_{\mathcal{J}} \geq 0$. This means that we have proved the right-hand direction of the equivalence in (B.22).

On the other hand, suppose we have a $\tilde{\sigma}$ satisfying the conditions on the right-hand side of (B.22). It is immediate to see that $\tilde{\sigma} \geq 0$ since it is a sum of positive operators, so it just needs to be shown that $\tilde{\sigma}/\mathrm{Tr}(\tilde{\sigma}) \in \mathcal{I}^{(k)}$. We can always write

$$\frac{\tilde{\sigma}}{\mathrm{Tr}(\tilde{\sigma})} = \sum_{\mathcal{J} \in \mathcal{C}(k-1)} \frac{\mathrm{Tr}(\tilde{\sigma}_{\mathcal{J}})}{\mathrm{Tr}(\tilde{\sigma})} \frac{\tilde{\sigma}_{\mathcal{J}}}{\mathrm{Tr}(\tilde{\sigma}_{\mathcal{J}})}. \tag{B.27}$$

Since $\mathrm{Tr}(\tilde{\sigma}_{\mathcal{J}})/\mathrm{Tr}(\tilde{\sigma}) \geq 0$ with $\sum_{\mathcal{J} \in \mathcal{C}(k-1)} \mathrm{Tr}(\tilde{\sigma}_{\mathcal{J}})/\mathrm{Tr}(\tilde{\sigma}) = 1$, we have therefore written $\tilde{\sigma}/\mathrm{Tr}(\tilde{\sigma})$ as a convex combination of the states $\tilde{\sigma}_{\mathcal{J}}/\mathrm{Tr}(\tilde{\sigma}_{\mathcal{J}})$. Hence, if $\tilde{\sigma}_{\mathcal{J}}/\mathrm{Tr}(\tilde{\sigma}_{\mathcal{J}}) \in \mathcal{I}^{(k)}$ for all $\mathcal{J} \in \mathcal{C}(k-1)$, then we know from the convexity of $\mathcal{I}^{(k)}$ that $\tilde{\sigma}/\mathrm{Tr}(\tilde{\sigma}) \in \mathcal{I}^{(k)}$. To see that this is so, we write $\tilde{\sigma}_{\mathcal{J}}/\mathrm{Tr}(\tilde{\sigma}_{\mathcal{J}})$ as a convex combination of pure state projectors, i.e.

$$\frac{\tilde{\sigma}_{\mathcal{J}}}{\mathrm{Tr}(\tilde{\sigma}_{\mathcal{J}})} = \sum_i q_i^{\mathcal{J}} \left|\psi_i^{\mathcal{J}}\right\rangle \left\langle\psi_i^{\mathcal{J}}\right| \tag{B.28}$$

for some probability distribution $\{q_i^{\mathcal{J}}\}_i$ and an arbitrary set of pure state projectors $\{\left|\psi_i^{\mathcal{J}}\right\rangle \left\langle\psi_i^{\mathcal{J}}\right|\}_i$ (with no prior constraint on their coherence number). Now we consider the projection

$$\begin{aligned} \frac{P_{\mathcal{J}} \tilde{\sigma}_{\mathcal{J}} P_{\mathcal{J}}}{\mathrm{Tr}\left(P_{\mathcal{J}} \tilde{\sigma}_{\mathcal{J}} P_{\mathcal{J}}\right)} = \frac{P_{\mathcal{J}} \frac{\tilde{\sigma}_{\mathcal{J}}}{\mathrm{Tr}(\tilde{\sigma}_{\mathcal{J}})} P_{\mathcal{J}}}{\mathrm{Tr}\left(P_{\mathcal{J}} \frac{\tilde{\sigma}_{\mathcal{J}}}{\mathrm{Tr}(\tilde{\sigma}_{\mathcal{J}})} P_{\mathcal{J}}\right)} &= \frac{\sum_i q_i^{\mathcal{J}} P_{\mathcal{J}} \left|\psi_i^{\mathcal{J}}\right\rangle \left\langle\psi_i^{\mathcal{J}}\right| P_{\mathcal{J}}}{\mathrm{Tr}\left(\sum_i q_i^{\mathcal{J}} P_{\mathcal{J}} \left|\psi_i^{\mathcal{J}}\right\rangle \left\langle\psi_i^{\mathcal{J}}\right| P_{\mathcal{J}}\right)} \\ &= \sum_i \chi_i^{\mathcal{J}} \left|\chi_i^{\mathcal{J}}\right\rangle \left\langle\chi_i^{\mathcal{J}}\right|, \end{aligned} \tag{B.29}$$

where

$$\begin{aligned} \chi_i^{\mathcal{J}} &= \frac{q_i^{\mathcal{J}} \mathrm{Tr}\left(P_{\mathcal{J}} \left|\psi_i^{\mathcal{J}}\right\rangle \left\langle\psi_i^{\mathcal{J}}\right| P_{\mathcal{J}}\right)}{\mathrm{Tr}\left(\sum_i q_i^{\mathcal{J}} P_{\mathcal{J}} \left|\psi_i^{\mathcal{J}}\right\rangle \left\langle\psi_i^{\mathcal{J}}\right| P_{\mathcal{J}}\right)}, \\ \left|\chi_i^{\mathcal{J}}\right\rangle \left\langle\chi_i^{\mathcal{J}}\right| &= \frac{P_{\mathcal{J}} \left|\psi_i^{\mathcal{J}}\right\rangle \left\langle\psi_i^{\mathcal{J}}\right| P_{\mathcal{J}}}{\mathrm{Tr}\left(P_{\mathcal{J}} \left|\psi_i^{\mathcal{J}}\right\rangle \left\langle\psi_i^{\mathcal{J}}\right| P_{\mathcal{J}}\right)}, \end{aligned} \tag{B.30}$$

with $\{\chi_i^{\mathcal{J}}\}_i$ a probability distribution. It holds that $\left|\chi_i^{\mathcal{J}}\right\rangle \left\langle\chi_i^{\mathcal{J}}\right| \in \mathcal{I}^{(k)}$. Indeed, if $\left|\psi_i^{\mathcal{J}}\right\rangle = \sum_{j \in \mathcal{J}_{\left|\psi_i^{\mathcal{J}}\right\rangle}} \psi_{ij}^{\mathcal{J}} \left|e_j\right\rangle$ with $\sum_{j \in \mathcal{J}_{\left|\psi_i^{\mathcal{J}}\right\rangle}} \left|\psi_{ij}^{\mathcal{J}}\right|^2$ then

$$P_{\mathcal{J}} \left|\psi_i^{\mathcal{J}}\right\rangle = \sum_{j \in \mathcal{J} \cap \mathcal{J}_{\left|\psi_i^{\mathcal{J}}\right\rangle}} \psi_{ij}^{\mathcal{J}} \left|e_i\right\rangle \tag{B.31}$$

which is a pure state with $\left|\mathcal{J} \cap \mathcal{J}_{|\psi_i^{\mathcal{J}}\rangle}\right| < k$ non-zero terms. We therefore know that

$$\frac{P_{\mathcal{J}}\tilde{\sigma}_{\mathcal{J}}P_{\mathcal{J}}}{\mathrm{Tr}\left(P_{\mathcal{J}}\tilde{\sigma}_{\mathcal{J}}P_{\mathcal{J}}\right)} \in \mathcal{I}^{(k)} \tag{B.32}$$

since it can be written as a convex combination of pure state projectors $\{|\chi_i^{\mathcal{J}}\rangle\langle\chi_i^{\mathcal{J}}|\}$ that have coherence number of less than k. Furthermore, the condition $P_{\mathcal{J}}\tilde{\sigma}_{\mathcal{J}}P_{\mathcal{J}} = \tilde{\sigma}_{\mathcal{J}}$ in (B.22) requires that

$$\frac{\tilde{\sigma}_{\mathcal{J}}}{\mathrm{Tr}(\tilde{\sigma}_{\mathcal{J}})} = \frac{P_{\mathcal{J}}\tilde{\sigma}_{\mathcal{J}}P_{\mathcal{J}}}{\mathrm{Tr}\left(P_{\mathcal{J}}\tilde{\sigma}_{\mathcal{J}}P_{\mathcal{J}}\right)} \in \mathcal{I}^{(k)}. \tag{B.33}$$

As we have already discussed, this implies that $\tilde{\sigma}/\mathrm{Tr}(\tilde{\sigma}) \in \mathcal{I}^{(k)}$. We have thus shown the equivalence in (B.22).

We may then use the equivalence in (B.22) to rewrite Eq. (B.19) as

$$\begin{aligned} C_k^R(\rho) \;=\; & \text{minimise} && \mathrm{Tr}(\tilde{\sigma}) - 1 \\ & \text{subject to} && \tilde{\sigma} = \sum_{\mathcal{J}\in\mathcal{C}(k-1)} \tilde{\sigma}_{\mathcal{J}}, \\ & && P_{\mathcal{J}}\tilde{\sigma}_{\mathcal{J}}P_{\mathcal{J}} = \tilde{\sigma}_{\mathcal{J}} \;\forall\; \mathcal{J} \in \mathcal{C}(k-1), \\ & && \tilde{\sigma}_{\mathcal{J}} \geq 0 \;\forall\; \mathcal{J} \in \mathcal{C}(k-1), \\ & && \rho \leq \tilde{\sigma}. \end{aligned} \tag{B.34}$$

To see that $C_k^R(\rho) + 1$ may be written as an SDP in the standard form of (B.1) we first label the set $\mathcal{C}(k-1)$ with indices $\{1, 2, \ldots, n\}$, where $n := \binom{d}{k-1}$, such that $i \in \{1, 2, \ldots, n\}$ corresponds to one of the $\mathcal{J} \in \mathcal{C}(k-1)$. We then fix X to be an $(n \times d)$-dimensional self-adjoint operator and define the projectors $\{Q_i\}_{i=1}^n$ that project onto the i-th d-dimensional block of X so that $\sum_{i=1}^n Q_i X Q_i$ is block diagonal. Each $Q_i X Q_i$ will represent the corresponding $\sigma_{\mathcal{J}}$. Now, by defining C as the $(n \times d)$-dimensional identity operator and

$$\begin{aligned} \Psi(X) \;=\; & \left(\sum_{i=1}^d \mathrm{Tr}_{\setminus i} Q_i X Q_i\right) \oplus \left(\sum_{i=1}^d Q_i X Q_i - X\right) \oplus \left(X - \sum_{i=1}^d Q_i X Q_i\right) \\ & \oplus \left(\sum_{i=1}^d P_i Q_i X Q_i P_i - Q_i X Q_i\right) \oplus \left(\sum_{i=1}^d Q_i X Q_i - P_i Q_i X Q_i P_i\right), \\ D \;=\; & \rho \oplus 0 \oplus 0 \oplus 0 \oplus 0, \end{aligned} \tag{B.35}$$

with $\mathrm{Tr}_{\setminus i}$ the partial trace over all but block i, $\oplus$ the direct sum operation, P_i a projection onto the i-th block corresponding to $P_{\mathcal{J}}$, and 0 the $(n \times d)$-dimensional

zero operator. By requiring $\Psi(X) \geq D$, the first term of $\Psi(X)$ imposes $\tilde{\sigma} \geq \rho$, the next two terms impose that X is block diagonal with blocks of $\sigma_{\mathcal{J}}$ for $\mathcal{J} \in \mathcal{C}(k-1)$, while the final two terms impose that $P_{\mathcal{J}}\tilde{\sigma}_{\mathcal{J}}P_{\mathcal{J}} = \tilde{\sigma}_{\mathcal{J}}$ for all $\mathcal{J} \in \mathcal{C}(k-1)$. Furthermore, $X \geq 0$ implies that $\tilde{\sigma}_{\mathcal{J}} \geq 0$ for all $\mathcal{J} \in \mathcal{C}(k-1)$. Finally, $\mathrm{Tr}(CX) = \sum_{\mathcal{J}\in\mathcal{C}(k-1)} \mathrm{Tr}\left(\tilde{\sigma}_{\mathcal{J}}\right) = \mathrm{Tr}\left(\sum_{\mathcal{J}\in\mathcal{C}(k-1)} \tilde{\sigma}_{\mathcal{J}}\right) = \mathrm{Tr}(\tilde{\sigma})$ with $\tilde{\sigma} = \sum_{\mathcal{J}\in\mathcal{C}(k-1)} \tilde{\sigma}_{\mathcal{J}}$. To see that this SDP is feasible, one only needs to consider the case $\tilde{\sigma} = \mathbb{I}$, with $\mathbb{I}/d \in \mathcal{I}^{(k)}$ for any k.

Appendix C

Theorems

List of theorems **Page**

We now provide the theorems and corresponding proofs of any unproven theorems in the main text. These theorems and proofs are taken from Refs. [TRB3, TRB4, TRB6, TRB7].

Theorem 3 *For any pure state* $|\psi\rangle = \sum_{i=1}^{d} \psi_i |e_i\rangle$ *with* $\sum_{i=1}^{d} |\psi_i|^2 = 1$*, it holds that* [TRB3]

$$C_k^R(|\psi\rangle\langle\psi|) \geq \max\left\{\frac{C^{l_1}(|\psi\rangle\langle\psi|)+1}{k-1} - 1\,,\, 0\right\}. \tag{C.1}$$

Proof. Here we use the notation discussed in Eq. (B.21) and consider a pure state $|\psi\rangle = \sum_{i\in\mathcal{J}_{|\psi\rangle}} \psi_i |e_i\rangle$ such that $\sum_{i\in\mathcal{J}_{|\psi\rangle}} |\psi_i|^2 = 1$, with coherence number $k' = \left|\mathcal{J}_{|\psi\rangle}\right|$. If $k' < k \leq d$ then $|\psi\rangle\langle\psi| \in \mathcal{I}^{(k)}$ and $C_k^R(|\psi\rangle\langle\psi|) = 0$. Furthermore, it can be seen that $C^{l_1}(|\psi\rangle\langle\psi|) \leq k' - 1$ since $|\psi\rangle$ can be thought of a k'-dimensional pure state embedded in a d-dimensional space. Hence,

$$\frac{C^{l_1}(|\psi\rangle\langle\psi|) + 1}{k-1} - 1 \leq 0, \tag{C.2}$$

so that the right hand side of Eq. (C.1) is also zero.

Now consider a pure state $|\psi\rangle$ with $k' \geq k$. Let us write the optimal pseudo-mixture of $|\psi\rangle$ satisfying the infimum in Eq. (3.53) as

$$|\psi\rangle\langle\psi| \leq (1 + C_k^R(|\psi\rangle\langle\psi|))\delta_\star^{(k)} \tag{C.3}$$

for some optimal $\delta_\star^{(k)} \in \mathcal{I}^{(k)}$. This implies that

$$\langle\phi|\psi\rangle\langle\psi|\phi\rangle \leq (1 + C_k^R(|\psi\rangle\langle\psi|))\langle\phi|\delta_\star^{(k)}|\phi\rangle \tag{C.4}$$

for any pure state $|\phi\rangle$, which can be chosen in particular to be

$$|\phi\rangle = \frac{1}{\sqrt{k'}} \sum_{j\in\mathcal{J}_{|\psi\rangle}} e^{i\theta_j} |e_j\rangle \tag{C.5}$$

where $\psi_j = |\psi_j|e^{i\theta_j}$ with $\theta_j \in [0, 2\pi]$ for any $j \in \mathcal{J}_{|\psi\rangle}$. It can then be seen that

$$\langle\phi|\psi\rangle\langle\psi|\phi\rangle = \frac{1}{k'}\left(\sum_{j\in\mathcal{J}_{|\psi\rangle}} |\psi_j|\right)^2. \tag{C.6}$$

On the other hand,

$$\begin{aligned}
\langle\phi|\delta_\star^{(k)}|\phi\rangle &\leq \sup_{\delta^{(k)}\in\mathcal{I}^{(k)}} \langle\phi|\delta^{(k)}|\phi\rangle \\
&= \sup_{\substack{\{q_i\}_i, \{|\psi_i^{(k)}\rangle\}_i \\ |\psi_i^{(k)}\rangle\langle\psi_i^{(k)}|\in\mathcal{I}^{(k)}\ \forall\ i}} \sum_i q_i \left|\langle\phi|\psi_i^{(k)}\rangle\right|^2 \\
&= \sup_{|\psi^{(k)}\rangle\langle\psi^{(k)}|\in\mathcal{I}^{(k)}} \left|\langle\phi|\psi^{(k)}\rangle\right|^2,
\end{aligned} \tag{C.7}$$

where in the first equality we use the fact that any state $\delta_\star^{(k)} \in \mathcal{I}^{(k)}$ with coherence number less than k can be written as a convex combination of pure states projectors $|\psi_i^{(k)}\rangle \langle\psi_i^{(k)}| \in \mathcal{I}^{(k)}$.

To achieve the above supremum, we write a general pure state with a coherence number of less than k as

$$|\psi^{(k)}\rangle = \sum_{j \in \mathcal{J}_{|\psi^{(k)}\rangle}} d_j |e_j\rangle \tag{C.8}$$

with $\left|\mathcal{J}_{|\psi^{(k)}\rangle}\right| < k$ and $\sum_{j \in \mathcal{J}_{|\psi^{(k)}\rangle}} |d_j|^2 = 1$. Now,

$$\begin{aligned}
\left|\langle\phi|\psi^{(k)}\rangle\right|^2 &= \frac{1}{k'} \left| \sum_{j \in \mathcal{J}_{|\psi\rangle} \cap \mathcal{J}_{|\psi^{(k)}\rangle}} d_j e^{-i\theta_j} \right|^2 \\
&\leq \frac{1}{k'} \sum_{j \in \mathcal{J}_{|\psi\rangle} \cap \mathcal{J}_{|\psi^{(k)}\rangle}} |d_j|^2 \sum_{j \in \mathcal{J}_{|\psi\rangle} \cap \mathcal{J}_{|\psi^{(k)}\rangle}} \left|e^{i\theta_j}\right|^2 \\
&\leq \frac{\left|\mathcal{J}_{|\psi\rangle} \cap \mathcal{J}_{|\psi^{(k)}\rangle}\right|}{k'} \\
&\leq \frac{\left|\mathcal{J}_{|\psi^{(k)}\rangle}\right|}{k'} \\
&\leq \frac{k-1}{k'},
\end{aligned} \tag{C.9}$$

where in the first inequality we use the Cauchy-Schwarz inequality and in the final two inequalities we use the fact that $|\psi^{(k)}\rangle$ has a coherence number of less than k while $|\psi\rangle$ has a coherence number of $k' \geq k$. Equality is achieved in (C.9) by picking the pure state

$$|\psi^{(k)}\rangle = \frac{1}{\sqrt{k-1}} \sum_{j \in \mathcal{J}_{|\psi^{(k)}\rangle}} e^{i\theta_j} |e_j\rangle \tag{C.10}$$

such that $\mathcal{J}_{|\psi^{(k)}\rangle} \subset \mathcal{J}_{|\psi\rangle}$ and $\left|\mathcal{J}_{|\psi^{(k)}\rangle}\right| = k-1$. We therefore have that

$$\langle\phi|\delta_\star^{(k)}|\phi\rangle \leq \sup_{|\psi^{(k)}\rangle\langle\psi^{(k)}| \in \mathcal{I}^{(k)}} \left|\langle\phi|\psi^{(k)}\rangle\right|^2 = \frac{k-1}{k'}. \tag{C.11}$$

Putting everything together, Eq. (C.4) implies that

$$\frac{1}{k'} \left(\sum_{j \in \mathcal{J}_{|\psi\rangle}} |\psi_j| \right)^2 \leq (1 + C_k^R(|\psi\rangle\langle\psi|)) \frac{k-1}{k'}, \tag{C.12}$$

which may be rearranged to

$$\begin{aligned} C_k^R(|\psi\rangle\langle\psi|) &\geq \frac{1}{k-1}\left(\sum_{j\in\mathcal{J}_{|\psi\rangle}}|\psi_j|\right)^2 - 1, \\ &= \frac{C^{l_1}(|\psi\rangle\langle\psi|)+1}{k-1} - 1, \end{aligned} \tag{C.13}$$

where in the equality we use the explicit form of the l_1 norm of coherence for pure states in Eq. (3.50). The right-hand side of this inequality can be negative for some $|\psi\rangle$, while the robustness is always a non-negative quantity. Hence, we include the max in (C.1). The saturability of (C.1) is dealt with by Theorem 4. □

Theorem 4 *For any* $x \in \left[\frac{1}{\sqrt{j}}, \frac{1}{\sqrt{j-1}}\right]$ *and* $j \in \{2, 3, \ldots, d\}$ [TRB3],

$$C_k^R(|\psi(x,j)\rangle\langle\psi(x,j)|) = \max\left\{\frac{C^{l_1}(|\psi(x,j)\rangle\langle\psi(x,j)|)+1}{k-1} - 1, 0\right\}. \tag{C.14}$$

Proof. For $j < k$ it is clear that $|\psi(x,j)\rangle$ has a coherence number of less than k and therefore $C_k^R(|\psi(x,j)\rangle\langle\psi(x,j)|) = 0$. Furthermore, it can be seen that from Eq. (3.50) and Eq. (3.56) that

$$C^{l_1}(|\psi(x,j)\rangle\langle\psi(x,j)|) = \left((j-1)x + \sqrt{1-(j-1)x^2}\right)^2 - 1, \tag{C.15}$$

so that the range of the l_1 norm of coherence for $x \in \left[\frac{1}{\sqrt{j}}, \frac{1}{\sqrt{j-1}}\right]$ is $[j-2, j-1]$. Hence, for $j < k$

$$\frac{C^{l_1}(|\psi(x,j)\rangle\langle\psi(x,j)|)+1}{k-1} - 1 \leq 0 \tag{C.16}$$

so that the right hand side of Eq. (C.14) is also zero.

We now restrict to $j \geq k$. From the range of the l_1 norm of coherence for $x \in \left[\frac{1}{\sqrt{j}}, \frac{1}{\sqrt{j-1}}\right]$ we know that

$$\frac{C^{l_1}(|\psi(x,j)\rangle\langle\psi(x,j)|)+1}{k-1} - 1 \geq 0. \tag{C.17}$$

Hence, we need to show for $j \geq k$ and $x \in \left[\frac{1}{\sqrt{j}}, \frac{1}{\sqrt{j-1}}\right]$ that

$$\begin{aligned} C_k^R(|\psi(x,j)\rangle\langle\psi(x,j)|) &= \frac{C^{l_1}(|\psi(x,j)\rangle\langle\psi(x,j)|)+1}{k-1} - 1 \\ &= \frac{\left((j-1)x + \sqrt{1-(j-1)x^2}\right)^2}{k-1} - 1. \end{aligned} \tag{C.18}$$

Theorem 3 tells us that the right-hand side of this equation lower bounds the left-hand side, and so we can prove the equality by showing that the right-hand side of this equation also upper bounds the left-hand side. To do this, we provide an operator $\tilde{\sigma}$ that satisfies the constraints

$$\begin{aligned} \tilde{\sigma} &= \sum_{\mathcal{J}\in\mathcal{C}(k-1)} \tilde{\sigma}_{\mathcal{J}}, && \text{(C.19)} \\ P_{\mathcal{J}}\tilde{\sigma}_{\mathcal{J}}P_{\mathcal{J}} &= \tilde{\sigma}_{\mathcal{J}} \qquad \forall\ \mathcal{J}\in\mathcal{C}(k-1), && \text{(C.20)} \\ \tilde{\sigma}_{\mathcal{J}} &\geq 0 \qquad \forall\ \mathcal{J}\in\mathcal{C}(k-1), && \text{(C.21)} \\ |\psi(x,j)\rangle\langle\psi(x,j)| &\leq \tilde{\sigma}, && \text{(C.22)} \end{aligned}$$

with $P_{\mathcal{J}}$ given in Eq. (B.20), and where

$$\mathrm{Tr}(\tilde{\sigma}) = \frac{\left((j-1)x+\sqrt{1-(j-1)x^2}\right)^2}{k-1}, \tag{C.23}$$

so that $\mathrm{Tr}(\tilde{\sigma})-1 \geq C_k^R(|\psi(x,j)\rangle\langle\psi(x,j)|)$, since $C_k^R(|\psi(x,j)\rangle\langle\psi(x,j)|)$ is the minimum of $\mathrm{Tr}(\tilde{\sigma})-1$ over all $\tilde{\sigma}$ satisfying the constraints (C.19)–(C.22), see Eq. (B.34).

First consider the set $\mathcal{C}_1 \subset \mathcal{C}(k-1)$ of all combinations of $k-1$ indices from $\{1,2,\ldots,j-1\}$, the set $\mathcal{C}_2 \subset \mathcal{C}(k-1)$ of all combinations of $k-1$ indices from $\{1,2,\ldots,j\}$ that are not included in $\mathcal{C}_1$, and the set $\mathcal{C}_3 \subset \mathcal{C}(k-1)$ of all the remaining combinations of $k-1$ indices from $\{1,2,\ldots,d\}$. We have that

$$\begin{aligned} \mathcal{C}_1\cap\mathcal{C}_2=\emptyset, \qquad \mathcal{C}_1\cap\mathcal{C}_3 &= \emptyset, \qquad \mathcal{C}_2\cap\mathcal{C}_3=\emptyset, \\ \mathcal{C}_1\cup\mathcal{C}_2\cup\mathcal{C}_3 &= \mathcal{C}(k-1). \end{aligned} \tag{C.24}$$

Now, for $\mathcal{J}\in\mathcal{C}(k-1)$ we define

$$\tilde{\sigma}_{\mathcal{J}} = \begin{cases} P_{\mathcal{J}}M_1P_{\mathcal{J}} & \forall \mathcal{J}\in\mathcal{C}_1; \\ P_{\mathcal{J}}M_2P_{\mathcal{J}} & \forall \mathcal{J}\in\mathcal{C}_2; \\ 0 & \forall \mathcal{J}\in\mathcal{C}_3, \end{cases} \tag{C.25}$$

where M_1 and M_2 are $(d\times d)$-dimensional constant matrices with entries a and b, respectively, and 0 is the $(d\times d)$-dimensional zero matrix. The entries of M_1

and M_2 are given by

$$\begin{aligned} a &= \frac{-(k-2)+(j-1)(j+k-3)x^2-(k-3)(j-1)x\sqrt{1-(j-1)x^2}}{(k-1)(j-k+1)\binom{j-1}{k-2}}, \\ b &= \frac{1+(j-1)x\left(-x+\sqrt{1-(j-1)x^2}\right)}{(k-1)\binom{j-1}{k-2}}, \end{aligned} \tag{C.26}$$

where $\binom{j-1}{k-2}$ is the binomial coefficient.

It is clear that each $\tilde{\sigma}_{\mathcal{J}}$ satisfies constraint (C.20) by construction. Furthermore, since for $x \in \left[\frac{1}{\sqrt{j}}, \frac{1}{\sqrt{j-1}}\right]$ we have $a \geq 0$ and $b \geq 0$, it holds that each $\tilde{\sigma}_{\mathcal{J}}$ satisfies constraint (C.21). Now we set

$$\tilde{\sigma} = \sum_{\mathcal{J} \in \mathcal{C}(k-1)} \tilde{\sigma}_{\mathcal{J}}, \tag{C.27}$$

so that by construction $\tilde{\sigma}$ satisfies constraint (C.19). It can be found that the eigenvalues of $\tilde{\sigma} - |\psi(x,j)\rangle\langle\psi(x,j)|$ are all non-negative: there are $j-2$ eigenvalues equal to $\binom{j-3}{k-2}a + \binom{j-3}{k-3}b$, whose non-negativity follows from the non-negativity of a and b; $d-j+1$ eigenvalues that are zero; and a final non-negative eigenvalue. Hence, $\tilde{\sigma}$ satisfies constraint (C.22). We therefore know that $\mathrm{Tr}(\tilde{\sigma}) - 1 \geq C_k^R(|\psi(x,j)\rangle\langle\psi(x,j)|)$.

To calculate the trace of $\tilde{\sigma}$, we use the fact that

$$\tilde{\sigma} = \tilde{M}_1 + \tilde{M}_2, \tag{C.28}$$

where

$$\begin{aligned} \tilde{M}_1 &:= \sum_{\mathcal{J} \in \mathcal{C}_1} \tilde{\sigma}_{\mathcal{J}} \qquad\qquad (C.29) \\ &= \begin{pmatrix} \left[\binom{j-1}{k-2} - \binom{j-2}{k-3}\right]a & \left[\binom{j-2}{k-3} - \binom{j-3}{k-4}\right]a & \cdots & \left[\binom{j-2}{k-3} - \binom{j-3}{k-4}\right]a \\ \left[\binom{j-2}{k-3} - \binom{j-3}{k-4}\right]a & \left[\binom{j-1}{k-2} - \binom{j-2}{k-3}\right]a & \cdots & \left[\binom{j-2}{k-3} - \binom{j-3}{k-4}\right]a \\ \vdots & \vdots & \ddots & \vdots \\ \left[\binom{j-2}{k-3} - \binom{j-3}{k-4}\right]a & \left[\binom{j-2}{k-3} - \binom{j-3}{k-4}\right]a & \cdots & \left[\binom{j-1}{k-2} - \binom{j-2}{k-3}\right]a \end{pmatrix} \oplus 0, \end{aligned}$$

where we consider a matrix of dimension $j-1$ along with the zero matrix of

dimension $d-j+1$. Furthermore,

$$\begin{aligned}\tilde{M}_2 &:= \sum_{\mathcal{J}\in\mathcal{C}_2}\tilde{\sigma}_{\mathcal{J}} \qquad\qquad (C.30)\\ &= \begin{pmatrix} \binom{j-2}{k-3}b & \binom{j-3}{k-4}b & \cdots & \binom{j-3}{k-4}b & \binom{j-2}{k-3}b \\ \binom{j-3}{k-4}b & \binom{j-2}{k-3}b & \cdots & \binom{j-3}{k-4}b & \binom{j-2}{k-3}b \\ \vdots & \vdots & \ddots & \vdots & \vdots \\ \binom{j-3}{k-4}b & \binom{j-3}{k-4}b & \cdots & \binom{j-2}{k-3}b & \binom{j-2}{k-3}b \\ \binom{j-2}{k-3}b & \binom{j-2}{k-3}b & \cdots & \binom{j-2}{k-3}b & \binom{j-1}{k-2}b \end{pmatrix} \oplus 0,\end{aligned}$$

where we consider a matrix of dimension j along with the zero matrix of dimension $d-j$. We then find that

$$\begin{aligned}\mathrm{Tr}(\tilde{\sigma}) &= \mathrm{Tr}(\tilde{M}_1)+\mathrm{Tr}(\tilde{M}_2)\\ &= (j-1)\left[\binom{j-1}{k-2}-\binom{j-2}{k-3}\right]a+(j-1)\binom{j-2}{k-3}b+\binom{j-1}{k-2}b\\ &= \frac{\left((j-1)x+\sqrt{1-(j-1)x^2}\right)^2}{k-1}, \qquad\qquad (C.31)\end{aligned}$$

as given by Eq. (C.23) and hence showing that showing that the right-hand side of (C.18) upper bounds the left-hand side, thus giving the desired equality and concluding the proof. Finally, it is interesting to note that as a result of this theorem, the $\tilde{\sigma}$ in Eq. (C.27) is actually (one of) the optimal operators satisfying the optimisation in (B.19). □

Theorem 7 *For any N qubit state ρ and $\Pi(\rho)$ as in Eq.* (4.16)*,*

$$\Pi(\rho)=\frac{1}{2^N}\left(\mathbb{I}^{\otimes N}+\sum_{i=1}^{3}c_i\sigma_i^{\otimes N}\right) \qquad (C.32)$$

where $c_i=\mathrm{Tr}(\rho\sigma_i^{\otimes N})\in[-1,1]$ [TRB4].

Proof. We fix a sequence of states $\{\rho_0,\rho_1,\ldots\rho_{2(N-1)}\}$ defined by

$$\rho_j := \frac{1}{2}\left(\rho_{j-1}+U_j\rho_{j-1}U_j^\dagger\right) \qquad (C.33)$$

for $j\in\{1,2,\ldots 2(N-1)\}$. By setting $\rho_0=\rho$ it can be seen that $\rho_{2(N-1)}=\Pi(\rho)$.

Consider the arbitrary N-qubit state ρ written in the form

$$\rho = \frac{1}{2^N} \sum_{i_1 i_2 \ldots i_N = 0}^{3} R^{\rho}_{i_1 i_2 \ldots i_N} \sigma_{i_1} \otimes \sigma_{i_2} \ldots \otimes \sigma_{i_N}, \tag{C.34}$$

where the $R^{\rho}_{i_1, i_2, \ldots i_N} = \mathrm{Tr}\left(\rho\ \sigma_{i_1} \otimes \sigma_{i_2} \ldots \otimes \sigma_{i_N}\right) \in [-1, 1]$ with $\sigma_0 := \mathbb{I}$ as discussed in Section 1.3. Convex combination of two arbitrary N-qubit states ρ and ρ' with weighting $q \in [0, 1]$ gives

$$q\rho + (1-q)\rho' = \frac{1}{2^N} \sum_{i_1 i_2 \ldots i_N = 0}^{3} R^{q\rho + (1-q)\rho'}_{i_1 i_2 \ldots i_N} \sigma_{i_1} \otimes \sigma_{i_2} \ldots \otimes \sigma_{i_N} \tag{C.35}$$

where $R^{q\rho+(1-q)\rho'}_{i_1 i_2 \ldots i_N} = q R^{\rho}_{i_1 i_2 \ldots i_N} + (1-q) R^{\rho'}_{i_1 i_2 \ldots i_N}$.

We now understand the evolution of the $R^{\rho_j}_{i_1 i_2 \ldots i_N}$ for each step j in Eq. (C.33). The action of U_1 on ρ is

$$U_1 \rho U_1^{\dagger} = \frac{1}{2^N} \sum_{i_1 i_2 \ldots i_N = 0}^{3} R^{\rho}_{i_1 i_2 \ldots i_N} \sigma_1 \sigma_{i_1} \sigma_1 \otimes \sigma_1 \sigma_{i_2} \sigma_1 \otimes \sigma_{i_3} \ldots \otimes \sigma_{i_N}. \tag{C.36}$$

From $\sigma_1 \sigma_i \sigma_1 = -(-1)^{\delta_{0i} + \delta_{1i}} \sigma_i$, we have that the correlation tensor elements of $U_1 \rho U_1^{\dagger}$ are $R^{U_1 \rho U_1^{\dagger}}_{i_1 i_2 \ldots i_N} = (-1)^{\delta_{0 i_1} + \delta_{1 i_1} + \delta_{0 i_2} + \delta_{1 i_2}} R^{\rho}_{i_1 i_2 \ldots i_N}$. By using Eq. (C.33) and Eq. (C.35), it is clear that the $R^{\rho_1}_{i_1 i_2 \ldots i_N}$ of ρ_1 are $R^{\rho}_{i_1 i_2 \ldots i_N}$ if i_1 and i_2 are (i) any combination of only 1 and 0 or (ii) any combination of only 2 and 3, and zero otherwise.

Generally, for $j \in [1, N-1]$, the $R^{\rho_j}_{i_1 i_2 \ldots i_N}$ of ρ_j are $R^{\rho_{j-1}}_{i_1 i_2 \ldots i_N}$ if i_j and i_{j+1} are (i) any combination of only 1 and 0 or (ii) any combination of only 2 and 3, and zero otherwise. For $j \in [N, 2(N-1)]$ the conditions are analogous, where the $R^{\rho_j}_{i_1 i_2 \ldots i_N}$ of ρ_j are $R^{\rho_{j-1}}_{i_1 i_2 \ldots i_N}$ if i_j and i_{j+1} are (i) any combination of only 2 and 0 or (ii) any combination of only 1 and 3, and zero otherwise. For the final state $\rho_{2(N-1)}$, the only non-zero $R^{\rho_{2(N-1)}}_{i_1 i_2 \ldots i_N}$ are those for which $\{i_1 i_2 \ldots i_N\}$ consists of only 0, 1, 2, or 3, and that for these elements $R^{\rho_{2(N-1)}}_{i_1 i_2 \ldots i_N} = R^{\rho}_{i_1 i_2 \ldots i_N}$. Therefore,

$$\begin{aligned} \Pi(\rho) = \rho_{2(N-1)} &= \frac{1}{2^N} \sum_{i=0}^{3} R^{\rho}_{ii \ldots i} \sigma_i \otimes \sigma_i \ldots \otimes \sigma_i \\ &= \frac{1}{2^N} \left(\mathbb{I}^{\otimes N} + \sum_{i=1}^{3} c_i \sigma_i^{\otimes N} \right), \end{aligned} \tag{C.37}$$

where we use $R^{\rho}_{ii \ldots i} = \mathrm{Tr}(\rho \sigma_i^{\otimes N}) =: c_i$ for $i \in \{1, 2, 3\}$ and $R^{\rho}_{00 \ldots 0} = \mathrm{Tr}(\rho) = 1$. $\square$

Theorem 8 *For any N, the set of M-separable $\mathcal{M}_N^3$ states $\mathcal{S}_M^{\mathcal{M}_N^3}$ is either* [TRB4]*:*

- *the set of all $\mathcal{M}_N^3$ states, for any $M \leq \lceil N/2 \rceil$;*
- *the set of $\mathcal{M}_N^3$ states represented in the $\{c_1, c_2, c_3\}$ space by the unit octahedron $\mathcal{O}_1$ with vertices $\{\pm 1, 0, 0\}$, $\{0, \pm 1, 0\}$ and $\{0, 0, \pm 1\}$, for any $M > \lceil N/2 \rceil$.*

Proof. We begin by working in the partition dependent setting and note that the $\mathcal{M}_N^3$ states are invariant under any permutation of the N qubits. Hence, for $\mathcal{M}_N^3$ states it does not matter *which* qubits belong to each subsystem of a given M-partition $\{Q_\alpha\}_{\alpha=1}^M$ and it is sufficient to specify a partition only with the cardinalities $\{K_\alpha\}_{\alpha=1}^M$ of the M subsystems. This means that the set of $\{Q_\alpha\}_{\alpha=1}^M$-separable $\mathcal{M}_N^3$ states $\mathcal{S}_{\{Q_\alpha\}_{\alpha=1}^M}^{\mathcal{M}_N^3}$ can be specified by the set $\mathcal{S}_{\{K_\alpha\}_{\alpha=1}^M}^{\mathcal{M}_N^3}$ describing only the cardinalities $\{K_\alpha\}_{\alpha=1}^M$ of the M-partition. We now identify $\mathcal{S}_{\{K_\alpha\}_{\alpha=1}^M}^{\mathcal{M}_N^3}$. In order to characterise this set, we simply need to identify its representation in the $\{c_1, c_2, c_3\}$ space. We know from Eq. (4.2) that

$$\mathcal{S}_{\{K_\alpha\}_{\alpha=1}^M}^{\mathcal{M}_N^3} = \left\{ \Pi(\varsigma) \mid \varsigma \in \mathcal{S}_{\{Q_\alpha\}_{\alpha=1}^M} \right\} \tag{C.38}$$

for any M-partition $\{Q_\alpha\}_{\alpha=1}^M$, and so we just need to find the possible values of $\{c_1, c_2, c_3\}$ for any $\varsigma \in \mathcal{S}_{\{Q_\alpha\}_{\alpha=1}^M}$ with $c_j = \mathrm{Tr}(\varsigma \sigma_j^{\otimes N})$. Using Eq. (2.21), the vector $\vec{c} = \{c_1, c_2, c_3\}$ of any $\varsigma \in \mathcal{S}_{\{Q_\alpha\}_{\alpha=1}^M}$ is given by

$$\begin{aligned} c_j &= \mathrm{Tr}\left(\varsigma \sigma_j^{\otimes N}\right) = \mathrm{Tr}\left[\left(\sum_i p_i \rho_i^{(1)} \otimes \rho_i^{(2)} \otimes \ldots \otimes \rho_i^{(M)}\right) \sigma_j^{\otimes N}\right] \\ &= \sum_i p_i \mathrm{Tr}\left[\rho_i^{(1)} \sigma_j^{\otimes K_1} \otimes \rho_i^{(2)} \sigma_j^{\otimes K_2} \otimes \ldots \otimes \rho_i^{(M)} \sigma_j^{\otimes K_M}\right] \\ &= \sum_i p_i \prod_{\alpha=1}^M \mathrm{Tr}\left(\rho_i^{(\alpha)} \sigma_j^{\otimes K_\alpha}\right) = \sum_i p_i \prod_{\alpha=1}^M c_{i,j}^{(\alpha)}, \end{aligned} \tag{C.39}$$

where in the final equality we denote $c_{i,j}^{(\alpha)} = \mathrm{Tr}\left(\rho_i^{(\alpha)} \sigma_j^{\otimes K_\alpha}\right)$ as the j-th component of the vector $\vec{c}_i^{(\alpha)} = \{c_{i,1}^{(\alpha)}, c_{i,2}^{(\alpha)}, c_{i,3}^{(\alpha)}\}$ corresponding to the arbitrary state $\rho_i^{(\alpha)}$ of subsystem α. Eq. (C.39) can be simplified further by introducing the Hadamard product as the componentwise multiplication of vectors, i.e. for $\vec{u} = \{u_1, u_2, u_3\}$ and $\vec{v} = \{v_1, v_2, v_3\}$ the Hadamard product is $\vec{u} \circ \vec{v} = \{u_1 v_1, u_2 v_2, u_3 v_3\}$. Using

the Hadamard product simplifies Eq. (C.39) to

$$\vec{c} = \sum_i p_i \vec{c}_i^{(1)} \circ \vec{c}_i^{(2)} \circ \ldots \circ \vec{c}_i^{(M)}. \tag{C.40}$$

Hence, the $\vec{c}$ vector of any $\{Q_\alpha\}_{\alpha=1}^M$-separable state is a convex combination of Hadamard products of $\vec{c}_i^{(\alpha)}$ vectors corresponding to states $\rho_i^{(\alpha)}$ of subsystem α. Since $\vec{c}_i^{(\alpha)}$ describes a K_α qubit $\mathcal{M}_N^3$ state, we know from the discussion in step one of Section 4.2.1 that $\vec{c}_i^{(\alpha)} \in \mathcal{B}_1$ when K_α is odd and $\vec{c}_i^{(\alpha)} \in \mathcal{T}_{(-1)^{K_\alpha/2}}$ when K_α is even, and so $\mathcal{S}^{\mathcal{M}_N^3}_{\{K_\alpha\}_{\alpha=1}^M}$ is represented by the following set

$$\mathcal{S}^{\mathcal{M}_N^3}_{\{K_\alpha\}_{\alpha=1}^M} = conv\left(A^{(1)} \circ A^{(2)} \circ \ldots \circ A^{(M)}\right), \tag{C.41}$$

with

$$A^{(\alpha)} = \begin{cases} \mathcal{B}_1 & \text{if } K_\alpha \text{ is odd,} \\ \mathcal{T}_{(-1)^{K_\alpha/2}} & \text{if } K_\alpha \text{ is even,} \end{cases} \tag{C.42}$$

where we define the Hadamard product between any two sets A and B as $A \circ B = \{\vec{a} \circ \vec{b} \,|\, \vec{a} \in A\,, \vec{b} \in B\}$ and the convex hull $conv(A)$ is the set of all possible convex combinations of elements in A. The commutativity and associativity of the Hadamard product allow us to rearrange the ordering in Eq. (C.41) in the following way

$$\mathcal{S}^{\mathcal{M}_N^3}_{\{K_\alpha\}_{\alpha=1}^M} = conv\left[\left(\bigcirc_{\mu:K_\mu even} \mathcal{T}_{(-1)^{K_\mu/2}}\right) \circ \left(\bigcirc_{\nu:K_\nu odd} \mathcal{B}_1\right)\right], \tag{C.43}$$

where $\bigcirc_{\alpha=1}^n A^{(\alpha)} := A^{(1)} \circ A^{(2)} \circ \ldots \circ A^{(n)}$.

By writing any vector in $\mathcal{T}_{\pm 1}$ as a convex combination of the vertices of $\mathcal{T}_{\pm 1}$, one can easily show that

$$\begin{aligned} \mathcal{T}_{-1} \circ \mathcal{T}_{-1} &= \mathcal{T}_1, \\ \mathcal{T}_1 \circ \mathcal{T}_1 &= \mathcal{T}_1, \\ \mathcal{T}_1 \circ \mathcal{T}_{-1} &= \mathcal{T}_{-1}, \end{aligned} \tag{C.44}$$

so that

$$\bigcirc_{\mu:K_\mu even} \mathcal{T}_{(-1)^{K_\mu/2}} = \mathcal{T}_{(-1)^{\mathcal{M}_-}}, \tag{C.45}$$

where $\mathcal{M}_-$ is the number of K_μ with odd $K_\mu/2$. Similarly, one can see that

$$\mathcal{T}_{\pm 1} \circ \mathcal{B}_1 = \mathcal{B}_1. \tag{C.46}$$

Finally, we have that

$$conv\left(\bigcirc_{i=1}^{n}\mathcal{B}_1\right)=\mathcal{O}_1 \quad \forall n\geq 2. \tag{C.47}$$

Indeed, since

$$\begin{aligned}\{\{\pm1,0,0\},\{0,\pm1,0\},\{0,0,\pm1\}\} &\subset \bigcirc_{i=1}^{n}\mathcal{B}_1,\\ conv\{\{\pm1,0,0\},\{0,\pm1,0\},\{0,0,\pm1\}\} &= \mathcal{O}_1,\end{aligned} \tag{C.48}$$

we know that $\mathcal{O}_1\subseteq conv\left(\bigcirc_{i=1}^{n}\mathcal{B}_1\right)$. Now we will show that $\mathcal{O}_1\supseteq conv\left(\bigcirc_{i=1}^{n}\mathcal{B}_1\right)$. To do so, it is sufficient to see that

$$\vec{b}\circ\vec{b}'\in\mathcal{O}_1 \tag{C.49}$$

for any $\vec{b},\vec{b}'\in\mathcal{B}_1$, which trivially implies that $\bigcirc_{i=1}^{n}\mathcal{B}_1\subseteq\mathcal{O}_1$, and therefore $conv\left(\bigcirc_{i=1}^{n}\mathcal{B}_1\right)\subseteq conv\left(\mathcal{O}_1\right)=\mathcal{O}_1$. Equation (C.49) holds since

$$\begin{aligned}|b_1b_1'|+|b_2b_2'|+|b_3b_3'| &= |b_1|\,|b_1'|+|b_2|\,|b_2'|+|b_3|\,|b_3'|\\ &= \vec{n}\cdot\vec{n}'=||\vec{n}||\,||\vec{n}'||\cos\theta\leq 1,\end{aligned} \tag{C.50}$$

where we define $\vec{n}=\{|b_1|,|b_2|,|b_3|\}$ and $\vec{n}'=\{|b_1'|,|b_2'|,|b_3'|\}$, respectively, as the vectors corresponding to $\vec{b}$ and $\vec{b}'$ in the positive octant of the unit ball $\mathcal{B}_1$, and θ as the angle between these vectors.

Now, due to Eqs. (C.43), (C.45), (C.46) and (C.47), and also the fact that $conv(A)=A$ for any convex set A, we identify four cases:

1. if K_α is even for all values of α then

$$\begin{aligned}\mathcal{S}^{\mathcal{M}_N^3}_{\{K_\alpha\}_{\alpha=1}^{M}} &= conv\left(\bigcirc_{\mu:K_\mu even}\mathcal{T}_{(-1)^{K_\mu/2}}\right)\\ &= conv\left(\mathcal{T}_{(-1)^{\mathcal{M}_-}}\right)\\ &= \mathcal{T}_{(-1)^{\mathcal{M}_-}},\end{aligned} \tag{C.51}$$

   where $\mathcal{M}_-$ is the number of K_μ with odd $K_\mu/2$;

2. if K_α is odd for just one value of α then

$$\begin{aligned} \mathcal{S}^{\mathcal{M}_N^3}_{\{K_\alpha\}_{\alpha=1}^M} &= conv\left[\left(\bigcirc_{\mu:K_\mu even} \mathcal{T}_{(-1)^{K_\mu/2}}\right)\circ\mathcal{B}_1\right] \\ &= conv\left(\mathcal{T}_{\pm 1}\circ\mathcal{B}_1\right) \\ &= \mathcal{B}_1; \end{aligned} \tag{C.52}$$

3. if K_α is odd for all values of α then

$$\begin{aligned} \mathcal{S}^{\mathcal{M}_N^3}_{\{K_\alpha\}_{\alpha=1}^M} &= conv\left(\bigcirc_{\nu:K_\nu odd}\mathcal{B}_1\right) \\ &= \mathcal{O}_1; \end{aligned} \tag{C.53}$$

4. otherwise,

$$\begin{aligned} \mathcal{S}^{\mathcal{M}_N^3}_{\{K_\alpha\}_{\alpha=1}^M} &= conv\left[\left(\bigcirc_{\mu:K_\mu even} \mathcal{T}_{(-1)^{K_\mu/2}}\right)\circ\left(\bigcirc_{\nu:K_\nu odd}\mathcal{B}_1\right)\right] \\ &= conv\left[\mathcal{T}_{\pm 1}\circ\left(\bigcirc_{\nu:K_\nu odd}\mathcal{B}_1\right)\right] \\ &= conv\left[\mathcal{T}_{\pm 1}\circ\mathcal{B}_1\circ\ldots\circ\mathcal{B}_1\right] \\ &= conv\left(\bigcirc_{\nu:K_\nu odd}\mathcal{B}_1\right) \\ &= \mathcal{O}_1. \end{aligned} \tag{C.54}$$

For any even N-qubit system, only a $\{K_\alpha\}_{\alpha=1}^M$-partitioning within cases 1, 3 and 4 may be realised. In case 1, i.e. when K_α is even for any α, we have $\mathcal{S}^{\mathcal{M}_N^3}_{\{K_\alpha\}_{\alpha=1}^M} = \mathcal{T}_{(-1)^{\mathcal{M}_-}}$, where $\mathcal{M}_-$ is the number of K_α with odd $K_\alpha/2$. However, one can simply see that $(-1)^{\mathcal{M}_-} = (-1)^{N/2}$, and thus $\mathcal{S}^{\mathcal{M}_N^3}_{\{K_\alpha\}_{\alpha=1}^M}$ is the set $\mathcal{T}_{(-1)^{N/2}}$ of all $\mathcal{M}_N^3$ states. Otherwise, in cases 3 and 4, we have $\mathcal{S}^{\mathcal{M}_N^3}_{\{K_\alpha\}_{\alpha=1}^M} = \mathcal{O}_1$. For any odd N-qubit system, only a $\{K_\alpha\}_{\alpha=1}^M$-partitioning within cases 2, 3 and 4 may be realised. In case 2, i.e. when K_α is odd for only one α, we have $\mathcal{S}^{\mathcal{M}_N^3}_{\{K_\alpha\}_{\alpha=1}^M} = \mathcal{B}_1$, and thus $\mathcal{S}^{\mathcal{M}_N^3}_{\{K_\alpha\}_{\alpha=1}^M}$ is the set $\mathcal{B}_1$ of all $\mathcal{M}_N^3$ states. Otherwise, in cases 3 and 4, we have $\mathcal{S}^{\mathcal{M}_N^3}_{\{K_\alpha\}_{\alpha=1}^M} = \mathcal{O}_1$.

In summary, for any N, the set of $\{K_\alpha\}_{\alpha=1}^M$ separable $\mathcal{M}_N^3$ states $\mathcal{S}_{\{K_\alpha\}_{\alpha=1}^M}^{\mathcal{M}_N^3}$ is either:

- the set of all $\mathcal{M}_N^3$ states, for any allowed $\{K_\alpha\}_{\alpha=1}^M$-partition such that K_α is odd for at most one value of α;
- the set of $\mathcal{M}_N^3$ states represented in the $\{c_1, c_2, c_3\}$ space by the unit octahedron $\mathcal{O}_1$ with vertices $\{\pm 1, 0, 0\}$, $\{0, \pm 1, 0\}$ and $\{0, 0, \pm 1\}$, for any allowed $\{K_\alpha\}_{\alpha=1}^M$-partition such that K_α is odd for more than one value of α.

Now we are ready to characterise the set of M-separable $\mathcal{M}_N^3$ states $\mathcal{S}_M^{\mathcal{M}_N^3}$. Indeed, Eq. (2.24) and Eq. (4.2) together imply that $\mathcal{S}_M^{\mathcal{M}_N^3}$ is just the convex hull of the union of all the sets of $\{K_\alpha\}_{\alpha=1}^M$-separable $\mathcal{M}_N^3$ states $\mathcal{S}_{\{K_\alpha\}_{\alpha=1}^M}^{\mathcal{M}_N^3}$ obtained by considering all the possible M-partitions $\{K_\alpha\}_{\alpha=1}^M$. Furthermore, one can easily see that for any $M \leq \lceil N/2 \rceil$ one can always find an M-partition $\{K_\alpha\}_{\alpha=1}^M$ such that K_α is odd for at most one value of α and thus $\mathcal{S}_M^{\mathcal{M}_N^3} = \mathcal{M}_N^3$, whereas for any $M > \lceil N/2 \rceil$ this is impossible and thus $\mathcal{S}_M^{\mathcal{M}_N^3}$ is described in the $\{c_1, c_2, c_3\}$ space by the unit octahedron $\mathcal{O}_1$ with vertices $\{\pm 1, 0, 0\}$, $\{0, \pm 1, 0\}$ and $\{0, 0, \pm 1\}$. □

Theorem 9 *The projection* Π *of* $\mathcal{M}_N^3$*-fication in Eq.* (4.16) *is an incoherent operation with respect to the reference ONB* $\{|i_1 i_2 \dots i_N\rangle\}_{i_1, i_2, \dots, i_N = 0}^1$*, i.e. there exists an operator sum representation of* Π *with Kraus operators* $\{K_i\}_i$ *such that* (3.1) *holds* [TRB6].

Proof. Consider an operator sum representation of Π with $2^{2(N-1)}$ Kraus operators $\{K_i\}_{i=1}^{2^{2(N-1)}}$ given by

$$K_i = \frac{1}{2^{N-1}} U_i' \tag{C.55}$$

with U_i' from Eq. (4.17), so that for a given state ρ

$$\sum_{i=1}^{2^{2(N-1)}} K_i \rho K_i^\dagger = \frac{1}{2^{2(N-1)}} \sum_{i=1}^{2^{2(N-1)}} U_i' \rho U_i'^\dagger = \Pi(\rho). \tag{C.56}$$

It is clear that

$$\sum_{i=1}^{2^{2(N-1)}} K_i^\dagger K_i = \frac{1}{2^{2(N-1)}} \sum_{i=1}^{2^{2(N-1)}} \mathbb{I}^{\otimes N} = \mathbb{I}^{\otimes N}, \tag{C.57}$$

so that we have a valid set of Kraus operators.

The condition of (3.1) specialised to coherence is $K_i\delta K_i^\dagger/\mathrm{Tr}(K_i\delta K_i^\dagger) \in \mathcal{I}$ for all $\delta \in \mathcal{I}$ and for any i. It is clear that this holds for the above set of Kraus operators if and only if $U_i'\delta U_i'^\dagger \in \mathcal{I}$ for all $\delta \in \mathcal{I}$ and for any i. Furthermore, we know from Eq. (4.17) that any U_i' can be written as a product of unitaries from the set $\{U_j\}_{j=1}^{2(N-1)}$ given in Eq. (4.15). Hence, it holds that $U_i'\delta U_i'^\dagger \in \mathcal{I}$ for all $\delta \in \mathcal{I}$ and for any i if $U_j\delta U_j^\dagger \in \mathcal{I}$ for all $\delta \in \mathcal{I}$ and all $j \in \{1, 2, \ldots, 2(N-1)\}$. This is now shown to be the case.

Consider any incoherent state $\delta \in \mathcal{I}$ with respect to the reference ONB $\{|i_1 i_2 \ldots i_N\rangle\}_{i_1,i_2,\ldots,i_N=0}^{1}$, given by

$$\delta = \sum_{i_1,i_2,\ldots,i_N=0}^{1} p_{i_1 i_2 \ldots i_N} |i_1 i_2 \ldots i_N\rangle \langle i_1 i_2 \ldots i_N|, \tag{C.58}$$

with $\{p_{i_1 i_2 \ldots i_N}\}_{i_1,i_2,\ldots,i_N=0}^{1}$ a probability distribution. Then, using the definition of $\{U_j\}_{j=1}^{2(N-1)}$ in Eq. (4.15), it can be seen that

$$U_1\delta U_1^\dagger = \sum_{i_1,i_2,\ldots,i_N=0}^{1} p_{i_1 i_2 \ldots i_N} |\pi(i_1)\pi(i_2) \ldots i_N\rangle \langle \pi(i_1)\pi(i_2) \ldots i_N|, \tag{C.59}$$

where $|\pi(0)\rangle = |1\rangle$ and $|\pi(1)\rangle = |0\rangle$, i.e. that the action of U_1 is just to perform a bit flip on the first two qubits. It is then clear that $U_1\delta U_1^\dagger \in \mathcal{I}$. Similarly, the action of U_j for $j \in \{1, 2, \ldots, N-1\}$ is just to perform a bit flip on the j-th and $(j+1)$-th qubit so that $U_j\delta U_j^\dagger \in \mathcal{I}$. Now, when $j = N$ we also have

$$U_N\delta U_N^\dagger = \sum_{i_1,i_2,\ldots,i_N=0}^{1} p_{i_1 i_2 \ldots i_N} |\pi(i_1)\pi(i_2) \ldots i_N\rangle \langle \pi(i_1)\pi(i_2) \ldots i_N|, \tag{C.60}$$

so that $U_N\delta U_N^\dagger \in \mathcal{I}$. Moreover, the action of U_j for $j \in \{N, N+1, \ldots, 2(N-1)\}$ is to perform a bit flip on the $(j-N+1)$-th and $(j-N+2)$-th qubit so that $U_j\delta U_j^\dagger \in \mathcal{I}$. Overall then, it holds that $U_j\delta U_j^\dagger \in \mathcal{I}$ for any $\delta \in \mathcal{I}$ and all $j \in \{1, 2, \ldots, 2(N-1)\}$. □

Theorem 10 *For a $(2 \times d_B)$-dimensional bipartite system it holds for all LCPO Λ_{CPO}^A acting on subsystem A that*

$$P_A^\Gamma(\Lambda_{CPO}^A \otimes \mathbb{I}^B(\rho^{AB})) \leq P_A^\Gamma(\rho^{AB}) \tag{C.61}$$

for any state ρ^{AB} and any d_B [TRB7].

Proof. As discussed in Section 3.1.2, the CPOs acting on a qubit are either completely decohering or unital. When Λ^A_{CPO} is completely decohering, we know from Eq. (3.13) that $\Lambda^A_{CPO} \otimes \mathbb{I}^B(\rho^{AB}) \in \mathcal{C}^{AB}_{CQ}$ so that

$$0 = P^\Gamma_A(\Lambda^A_{CPO} \otimes \mathbb{I}^B(\rho^{AB})) \leq P^\Gamma_A(\rho^{AB}). \tag{C.62}$$

Hence, to establish (C.61) we only need to consider the case when Λ^A_{CPO} is unital, i.e. $\Lambda^A_{CPO}(\mathbb{I}^A) = \mathbb{I}^A$.

Consider the dilation τ^{ABC} of $\Lambda^A_{CPO} \otimes \mathbb{I}^B(\rho^{AB})$ into a larger space including an extra ancillary system C, such that $\mathrm{Tr}_C[\tau^{ABC}] = \Lambda^A_{CPO} \otimes \mathbb{I}^B(\rho^{AB})$ [287]. The following inequality holds

$$P^\Gamma_A(\tau^{ABC}) \geq P^\Gamma_A(\mathrm{Tr}_C[\tau^{ABC}]) = P^\Gamma_A(\Lambda^A_{CPO} \otimes \mathbb{I}^B(\rho^{AB})) \ , \tag{C.63}$$

since we know that the interferometric power never increases under any operation on subsystems other than A [30]. It is then sufficient to prove that $P^\Gamma_A(\rho^{AB}) \geq P^\Gamma_A(\tau^{ABC})$ to arrive at the desired inequality. To do this, we use the fact that any unital qubit operation can be equivalently written as a convex combination of unitaries [288], i.e.

$$\Lambda^A_{CPO}(\rho^A) = \sum_i p_i U^A_i \rho^A (U^A_i)^\dagger \tag{C.64}$$

for some mixture of unitaries $\{U^A_i\}_i$ with probabilities $\{p_i\}_i$ acting on subsystem A in the state ρ^A. This can be used to explicitly write the dilated state as

$$\tau^{ABC} = U^{ABC}(\rho^{AB} \otimes |\alpha^C\rangle \langle\alpha^C|)(U^{ABC})^\dagger, \tag{C.65}$$

with

$$\begin{aligned} U^{ABC} &= \sum_i U^A_i \otimes \mathbb{I}^B \otimes |i^C\rangle \langle i^C| \, , \\ |\alpha^C\rangle &= \sum_i \sqrt{p_i} \, |i^C\rangle \, , \end{aligned} \tag{C.66}$$

where $\{|i^C\rangle\}_i$ is an ONB of the ancilla C.

We now make use of the explicit form of the interferometric power for states of a $(2 \times d_B)$-dimensional bipartite system given in Ref. [30], i.e. $P^\Gamma_A(\rho^{AB}) =$

$\alpha^2 \min\{\lambda_i\}_{i=1}^3$, where $\{\lambda_i\}_{i=1}^3$ are the eigenvalues of the real and symmetric 3×3 matrix

$$M := \frac{1}{2} \sum_{\substack{m,n \\ q_m+q_n\neq 0}} \frac{(q_m-q_n)^2}{q_m+q_n} \langle \phi_m^{AB}|\vec{\sigma}^A \otimes \mathbb{I}^B|\phi_n^{AB}\rangle \langle \phi_n^{AB}|(\vec{\sigma}^A)^T \otimes \mathbb{I}^B|\phi_m^{AB}\rangle , \quad \text{(C.67)}$$

with $\rho^{AB} = \sum_m q_m |\phi_m^{AB}\rangle \langle \phi_m^{AB}|$ written in its spectral decomposition, and $\vec{\sigma}^A$ the vector of the three Pauli matrices. We also write any 2-dimensional spectrum as $\Gamma = \{\beta-\alpha, \beta+\alpha\}$ with $\alpha, \beta \in \mathbb{R}$. For convenience, in the following we set $\alpha = 1$ and $\beta = 0$ and consider the standard equispaced spectrum $\{-1, 1\}$, but this proof can hold for any α and β.

The task is then to calculate the matrix M' corresponding to τ^{ABC}. The eigenvalues of τ^{ABC} are the same as those of ρ^{AB}, while the normalised eigenvectors of τ^{ABC} are given by

$$|\Phi_m^{ABC}\rangle = U^{ABC} |\phi_m^{AB}\rangle \otimes |\alpha^C\rangle . \quad \text{(C.68)}$$

We can then write

$$\begin{aligned} M' &= \frac{1}{2} \sum_{\substack{m,n \\ q_m+q_n\neq 0}} \frac{(q_m-q_n)^2}{q_m+q_n} \langle \Phi_m^{ABC}|\vec{\sigma}^A \otimes \mathbb{I}^{BC}|\Phi_n^{ABC}\rangle \langle \Phi_n^{ABC}|(\vec{\sigma}^A)^T \otimes \mathbb{I}^{BC}|\Phi_m^{ABC}\rangle \\ &= \frac{1}{2} \sum_{\substack{m,n \\ q_m+q_n\neq 0}} \frac{(q_m-q_n)^2}{q_m+q_n} \langle \phi_m^{AB}| \otimes \langle \alpha^C| (U^{ABC})^\dagger \vec{\sigma}^A \otimes \mathbb{I}^{BC} U^{ABC} |\phi_n^{AB}\rangle \otimes |\alpha^C\rangle \\ &\qquad \langle \phi_n^{AB}| \otimes \langle \alpha^C| (U^{ABC})^\dagger (\vec{\sigma}^A)^T \otimes \mathbb{I}^{BC} U^{ABC} |\phi_m^{AB}\rangle \otimes |\alpha^C\rangle \\ &= \frac{1}{2} \sum_{\substack{m,n \\ q_m+q_n\neq 0}} \frac{(q_m-q_n)^2}{q_m+q_n} \langle \phi_m^{AB}| \sum_i p_i (U_i^A)^\dagger \vec{\sigma}^A U_i^A \otimes \mathbb{I}^B |\phi_n^{AB}\rangle \\ &\qquad \langle \phi_n^{AB}| \sum_j p_j (U_j^A)^\dagger (\vec{\sigma}^A)^T U_j^A \otimes \mathbb{I}^B |\phi_m^{AB}\rangle , \end{aligned} \quad \text{(C.69)}$$

where we have used the fact that $U^{ABC}|\alpha^C\rangle = \sum_i \sqrt{p_i} U_i^A \otimes \mathbb{I}^B |i^C\rangle$. From the correspondence between the special unitary group $\mathsf{SU}(2)$ and special orthogonal group $\mathsf{SO}(3)$, we can see that for each i there exists an orthogonal matrix R_i such that $(U_i^A)^\dagger \vec{\sigma}^A U_i^A = R_i \vec{\sigma}^A$. We thus obtain

$$M' = LML^T, \quad \text{(C.70)}$$

where $L = \sum_i p_i R_i$ is a real matrix such that $L^T L \leq \mathbb{I}$.

Finally, let us consider the eigenvalues of M'. If L is non-invertible we know that M' has a zero eigenvalue, and hence $P_A^\Gamma(\rho^{AB}) \geq P_A^\Gamma(\tau^{ABC}) = 0$. Instead, if M' is invertible, consider the unit vector $|v\rangle$ constructed by

$$|v\rangle = \frac{(L^T)^{-1}|v_0\rangle}{\sqrt{||(L^T)^{-1}|v_0\rangle||}}, \tag{C.71}$$

where $|v_0\rangle$ is the eigenvector of M corresponding to the smallest eigenvalue $\lambda_{\min} \equiv \min\{\lambda_i\}_{i=1}^3$ of M. It is then simple to see that

$$\lambda'_{\min} \leq \langle v|M'|v\rangle = \frac{\lambda_{\min}}{||(L^T)^{-1}|v_0\rangle||} \leq \lambda_{\min}, \tag{C.72}$$

where $\lambda'_{\min}$ is the minimum eigenvalue of M' and we have used the fact that $\left|\left|(L^T)^{-1}|v_0\rangle\right|\right| \geq 1$ since $L^T L \leq \mathbb{I}$. Combined with Eq. (C.63), we then have that

$$P_A^\Gamma(\rho^{AB}) = \lambda_{\min} \geq \lambda'_{\min} = P_A^\Gamma(\tau^{ABC}) \geq P_A^\Gamma(\Lambda_{CPO}^A \otimes \mathbb{I}^B(\rho^{AB})), \tag{C.73}$$

establishing the monotonicity of the interferometric power under unital operations on a qubit subsystem A. The above inequality and (C.62), together imply (C.61).

□

Theorem 11 *For a $(d_A \times d_B)$-dimensional bipartite system, it holds for all LCPO Λ_{CPO}^A acting on subsystem A of the form $\Lambda_{CPO}^A(\rho^A) = t\Phi^A(\rho^A) + (1-t)\frac{\mathbb{I}^A}{d_A}$, with $t \in [0,1]$ and $\Phi^A(\rho^A)$ a unitary transformation acting on any state ρ^A of subsystem A, that*

$$P_A^\Gamma(\Lambda_{CPO}^A \otimes \mathbb{I}^B(\rho^{AB})) \leq P_A^\Gamma(\rho^{AB}) \tag{C.74}$$

for any state ρ^{AB} of the bipartite system and any d_A and d_B [TRB7].

Proof. It can be seen that

$$\Lambda_{CPO}^A \otimes \mathbb{I}^B(\rho^{AB}) = t\Phi^A \otimes \mathbb{I}^B(\rho^{AB}) + (1-t)\frac{\mathbb{I}^A}{d_A} \otimes \mathrm{Tr}_A(\rho^{AB}). \tag{C.75}$$

When Φ^A is a unitary transformation, i.e. $\Phi^A(\rho^A) = U^A\rho^A(U^A)^\dagger$ for any local unitary U^A, and $t \in [0,1]$, we have that $\Lambda_{CPO}^A \otimes \mathbb{I}^B(\rho^{AB})$ is just a convex combination between $U^A \otimes \mathbb{I}^B \rho^{AB}(U^A \otimes \mathbb{I}^B)^\dagger$ and $\mathbb{I}^A/d_A \otimes \mathrm{Tr}_A(\rho^{AB})$. From the convexity

of the quantum Fisher information [199], it holds that

$$\begin{aligned} & F_{H_\Gamma^A}\left(\Lambda_{CPO}^A \otimes \mathbb{I}^B(\rho^{AB})\right) \\ = \; & F_{H_\Gamma^A}\left(tU^A \otimes \mathbb{I}^B \rho^{AB}(U^A \otimes \mathbb{I}^B)^\dagger + (1-t)\frac{\mathbb{I}^A}{d_A} \otimes \mathrm{Tr}_A(\rho^{AB})\right) \\ \leq \; & tF_{H_\Gamma^A}\left(U^A \otimes \mathbb{I}^B \rho^{AB}(U^A \otimes \mathbb{I}^B)^\dagger\right) + (1-t)F_{H_\Gamma^A}\left(\frac{\mathbb{I}^A}{d_A} \otimes \mathrm{Tr}_A(\rho^{AB})\right) \\ = \; & tF_{H_\Gamma^A}\left(U^A \otimes \mathbb{I}^B \rho^{AB}(U^A \otimes \mathbb{I}^B)^\dagger\right) \\ \leq \; & F_{H_\Gamma^A}\left(U^A \otimes \mathbb{I}^B \rho^{AB}(U^A \otimes \mathbb{I}^B)^\dagger\right), \end{aligned} \tag{C.76}$$

where in the second equality we use the fact that $F_{H_\Gamma^A}\left(\frac{\mathbb{I}^A}{d_A} \otimes \mathrm{Tr}_A(\rho^{AB})\right) = 0$, which follows by noting that $\left[\frac{\mathbb{I}^A}{d_A} \otimes \mathrm{Tr}_A(\rho^{AB}), H_\Gamma^A \otimes \mathbb{I}^B\right] = 0$. Using the above inequality, we arrive at the monotonicity of the interferometric power,

$$\begin{aligned} P_A^\Gamma(\Lambda_{CPO}^A \otimes \mathbb{I}^B(\rho^{AB})) &= \frac{1}{4}\inf_{\{H_A^\Gamma\}} F_{H_\Gamma^A}\left(\Lambda_{CPO}^A \otimes \mathbb{I}^B(\rho^{AB})\right) \\ &\leq \frac{1}{4}\inf_{\{H_A^\Gamma\}} F_{H_\Gamma^A}\left(U^A \otimes \mathbb{I}^B \rho^{AB}(U^A \otimes \mathbb{I}^B)^\dagger\right) \\ &= P_A^\Gamma(U^A \otimes \mathbb{I}^B \rho^{AB}(U^A \otimes \mathbb{I}^B)^\dagger) \\ &= P_A^\Gamma(\rho^{AB}), \end{aligned} \tag{C.77}$$

where in the third equality we use the invariance of the interferometric power under local unitary transformations [30]. □

Theorem 12 *For any state ρ^{AB} of any $(d_A \times d_B)$-dimensional bipartite system* [TRB7]*,*

$$E^\Gamma(\rho^{AB}) \leq P_A^\Gamma(\rho^{AB}). \tag{C.78}$$

Proof. The proof of this theorem relies on the recently proved fact that the quantum Fisher information is (four times) the convex roof of the variance [209, 210], i.e.

$$F_{H_\Gamma^A}(\rho^{AB}) = 4 \inf_{\substack{\{q_i\}_i, \{|\psi_i^{AB}\rangle\langle\psi_i^{AB}|\}_i \\ \rho^{AB} = \sum_i q_i |\psi_i^{AB}\rangle\langle\psi_i^{AB}|}} \sum_i q_i V_{H_\Gamma^A}(|\psi_i^{AB}\rangle\langle\psi_i^{AB}|). \tag{C.79}$$

It then holds that

$$\begin{aligned} F_{H_\Gamma^A}(\rho^{AB}) &= 4 \inf_{\substack{\{q_i\}_i,\{|\psi_i^{AB}\rangle\langle\psi_i^{AB}|\}_i \\ \rho^{AB}=\sum_i q_i|\psi_i^{AB}\rangle\langle\psi_i^{AB}|}} \sum_i q_i V_{H_\Gamma^A}(|\psi_i^{AB}\rangle\langle\psi_i^{AB}|) \\ &\geq 4 \inf_{\substack{\{q_i\}_i,\{|\psi_i^{AB}\rangle\langle\psi_i^{AB}|\}_i \\ \rho^{AB}=\sum_i q_i|\psi_i^{AB}\rangle\langle\psi_i^{AB}|}} \sum_i q_i \inf_{\{H_\Gamma^A\}} V_{H_\Gamma^A}(|\psi_i^{AB}\rangle\langle\psi_i^{AB}|) \\ &= 4 \inf_{\substack{\{q_i\}_i,\{|\psi_i^{AB}\rangle\langle\psi_i^{AB}|\}_i \\ \rho^{AB}=\sum_i q_i|\psi_i^{AB}\rangle\langle\psi_i^{AB}|}} \sum_i q_i E^\Gamma(|\psi_i^{AB}\rangle\langle\psi_i^{AB}|) \\ &= 4E^\Gamma(\rho^{AB}), \end{aligned} \tag{C.80}$$

where in the second equality we use the definition of the interferometric entanglement for pure states in Eq. (5.23), while in the final equality we use the fact that the interferometric entanglement is defined for mixed states through the convex roof construction, see Eq. (5.25). From (C.80) and the definition of the interferometric power in Eq. (5.18), we arrive at the desired inequality,

$$\begin{aligned} P_A^\Gamma(\rho^{AB}) &= \frac{1}{4} \inf_{\{H_\Gamma^A\}} F_{H_\Gamma^A}(\rho^{AB}) \\ &\geq \inf_{\{H_\Gamma^A\}} E^\Gamma(\rho^{AB}) \\ &= E^\Gamma(\rho^{AB}). \end{aligned} \tag{C.81}$$

□

List of Figures

List of Tables

Author's Works

[TRB1] C. Napoli, T. R. Bromley, M. Cianciaruso, M. Piani, N. Johnston and G. Adesso, 'Robustness of Coherence: An Operational and Observable Measure of Quantum Coherence', Physical Review Letters **116**, 150502 (2016) (cit. on pp. 5, 6, 33, 45, 51, 57, 58, 63, 67, 69, 107, 108, 110, 143, 145, 159).

[TRB2] M. Piani, M. Cianciaruso, T. R. Bromley, C. Napoli, N. Johnston and G. Adesso, 'Robustness of asymmetry and coherence of quantum states', Physical Review A **93**, 042107 (2016) (cit. on pp. 5, 6, 45, 50, 57, 61–63, 66–68, 104, 107, 108, 110, 143, 145, 154–156, 159).

[TRB3] M. Ringbauer, T. R. Bromley, M. Cianciaruso et al., 'Quasi-device independent witnessing of genuine multilevel quantum coherence' (cit. on pp. 5, 32, 45, 57, 63, 69, 70, 107, 110, 143, 145, 164, 167).

[TRB4] M. Cianciaruso, T. R. Bromley and G. Adesso, 'Accessible quantification of multiparticle entanglement', npj Quantum Information **2**, 16030 (2016) (cit. on pp. 5, 6, 51, 52, 74, 78, 80, 86, 87, 89–91, 93, 96, 98, 122, 140, 143, 148, 164, 170, 172).

[TRB5] T. Bromley, M. Cianciaruso and G. Adesso, 'A framework for the accessible quantification of multiqubit entanglement', in preparation (cit. on pp. 5, 78, 80, 143).

[TRB6] I. A. Silva, A. M. Souza, T. R. Bromley et al., 'Observation of Time-Invariant Coherence in a Nuclear Magnetic Resonance Quantum Sim-

ulator', Physical Review Letters **117**, 160402 (2016) (cit. on pp. 5, 6, 78, 103, 104, 137, 138, 143, 147, 164, 176).

[TRB7] T. R. Bromley, I. A. Silva, C. O. Oncebay-Segura et al., 'There is more to quantum interferometry than entanglement', Physical Review A **95**, 052313 (2017) (cit. on pp. 6, 54, 55, 107, 116, 117, 120, 145, 150, 164, 177, 180, 181).

[TRB8] R. Nichols, T. R. Bromley, L. A. Correa and G. Adesso, 'Practical quantum metrology in noisy environments', Physical Review A **94**, 042101 (2016) (cit. on pp. 6, 122, 123, 146).

[TRB9] T. R. Bromley, M. Cianciaruso and G. Adesso, 'Frozen Quantum Coherence', Physical Review Letters **114**, 210401 (2015) (cit. on pp. 6, 74–76, 104, 122, 127–129, 136–138, 146).

[TRB10] M. Cianciaruso, T. R. Bromley, W. Roga, R. L. Franco and G. Adesso, 'Universal freezing of quantum correlations within the geometric approach', Scientific Reports **5**, 10177 (2015) (cit. on pp. 6, 55, 56, 122, 127, 131, 132, 137, 138, 146).

[TRB11] T. R. Bromley, M. Cianciaruso, R. L. Franco and G. Adesso, 'Unifying approach to the quantification of bipartite correlations by bures distance', Journal of Physics A: Mathematical and Theoretical **47**, 405302 (2014) (cit. on pp. 6, 76, 124, 134, 135, 137, 146, 147).

[TRB12] G. Adesso, T. R. Bromley and M. Cianciaruso, 'Measures and applications of quantum correlations', Journal of Physics A: Mathematical and Theoretical **49**, 473001 (2016) (cit. on pp. 22, 34, 36, 55–57, 74–76, 136, 142, 146).

[TRB13] G. Adesso, M. Cianciaruso and T. R. Bromley, 'An introduction to quantum discord and non-classical correlations beyond entanglement', arXiv:1611.01959 (2016) (cit. on pp. 34, 36, 53, 142, 146).

References

[1] A. Streltsov, G. Adesso and M. B. Plenio, arXiv:1609.02439 (2016) (cit. on pp. 1, 31, 33, 49, 50, 58, 68, 74, 75, 85, 105, 114, 142, 146).

[2] R. Horodecki, P. Horodecki, M. Horodecki and K. Horodecki, Reviews of Modern Physics **81**, 865 (2009) (cit. on pp. 1, 39, 40, 51, 52, 64, 74, 75, 88, 118, 119, 125, 142, 146).

[3] A. Rae, *Quantum Mechanics* (Taylor & Francis, Abingdon, 2008) (cit. on p. 2).

[4] E. Schrödinger, Naturwissenschaften **23**, 823–828 (1935) (cit. on p. 2).

[5] J. D. Trimmer, Proceedings of the American Philosophical Society **124**, 323–338 (1980) (cit. on p. 2).

[6] C. H. Bennett, G. Brassard, C. Crépeau, R. Jozsa, A. Peres and W. K. Wootters, Physical Review Letters **70**, 1895 (1993) (cit. on p. 2).

[7] M. Nielsen and I. Chuang, *Quantum Computation and Quantum Information* (Cambridge University Press, Cambridge, 2010) (cit. on pp. 2, 7, 9, 12, 17–19, 74, 80, 124, 138, 142).

[8] C. H. Bennett and S. J. Wiesner, Physical Review Letters **69**, 2881 (1992) (cit. on p. 2).

[9] H. Ollivier and W. H. Zurek, Physical Review Letters **88**, 017901 (2001) (cit. on pp. 2, 34, 36, 76, 137).

[10] L. Henderson and V. Vedral, Journal of Physics A: Mathematical and General **34**, 6899 (2001) (cit. on pp. 2, 34, 36, 76, 137).

[11] K. Modi, A. Brodutch, H. Cable, T. Paterek and V. Vedral, Reviews of Modern Physics **84**, 1655 (2012) (cit. on pp. 2, 34, 36, 57, 75, 142, 146).

[12] W. H. Zurek, Physics Today **44**, 36–44 (1991) (cit. on pp. 2, 122).

[13] M. Horodecki and J. Oppenheim, International Journal of Modern Physics B **27**, 1345019 (2013) (cit. on pp. 3, 49, 142).

[14] B. Coecke, T. Fritz and R. W. Spekkens, Information and Computation **250**, 59–86 (2016) (cit. on pp. 3, 46, 49, 142).

[15] F. G. Brandão and G. Gour, Physical Review Letters **115**, 070503 (2015) (cit. on pp. 3, 46, 49, 63, 142).

[16] G. Vidal and R. Tarrach, Physical Review A **59**, 141 (1999) (cit. on pp. 5, 45, 58, 61–63).

[17] M. Steiner, Physical Review A **67**, 054305 (2003) (cit. on pp. 5, 45, 61–63).

[18] V. Vedral, M. B. Plenio, M. A. Rippin and P. L. Knight, Physical Review Letters **78**, 2275 (1997) (cit. on pp. 5, 45, 51, 73, 74, 143).

[19] V. Vedral and M. B. Plenio, Physical Review A **57**, 1619 (1998) (cit. on pp. 5, 45, 51, 52, 73, 74, 143).

[20] I. Bengtsson and K. Życzkowski, *Geometry of Quantum States: An Introduction to Quantum Entanglement* (Cambridge University Press, Cambridge, 2007) (cit. on pp. 5, 7, 9, 11, 18, 20, 23, 39, 52, 64, 66, 69, 71, 72, 74, 94, 95, 111, 118, 121, 152, 155, 158).

[21] A. Acín, Physical Review Letters **87**, 177901 (2001) (cit. on pp. 5, 106).

[22] M. F. Sacchi, Physical Review A **71**, 062340 (2005) (cit. on pp. 5, 106).

[23] R. Duan, Y. Feng and M. Ying, Physical Review Letters **103**, 210501 (2009) (cit. on pp. 5, 106).

[24] M. Piani and J. Watrous, Physical Review Letters **102**, 250501 (2009) (cit. on pp. 5, 106).

[25] V. Giovannetti, S. Lloyd and L. Maccone, Science **306**, 1330–1336 (2004) (cit. on pp. 6, 106, 112).

[26] V. Giovannetti, S. Lloyd and L. Maccone, Physical Review Letters **96**, 010401 (2006) (cit. on pp. 6, 106, 112, 114, 115).

[27] V. Giovannetti, S. Lloyd and L. Maccone, Nature Photonics **5**, 222–229 (2011) (cit. on pp. 6, 106, 112, 114, 115).

[28] M. G. Paris, International Journal of Quantum Information **7**, 125–137 (2009) (cit. on pp. 6, 106, 112, 113).

[29] A. M. Childs, J. Preskill and J. Renes, Journal of Modern Optics **47**, 155–176 (2000) (cit. on pp. 6, 106, 112).

[30] D. Girolami, A. M. Souza, V. Giovannetti et al., Physical Review Letters **112**, 210401 (2014) (cit. on pp. 6, 107, 116, 118, 120, 145, 146, 178, 181).

[31] L. Mazzola, J. Piilo and S. Maniscalco, Physical Review Letters **104**, 200401 (2010) (cit. on pp. 6, 124, 125, 127, 135, 137, 146, 147).

[32] L. Mazzola, J. Piilo and S. Maniscalco, International Journal of Quantum Information **9**, 981–991 (2011) (cit. on pp. 6, 124, 135, 137, 146, 147).

[33] B. Aaronson, R. L. Franco and G. Adesso, Physical Review A **88**, 012120 (2013) (cit. on pp. 6, 56, 124, 131, 132, 134, 137, 146).

[34] J. Maziero, L. C. Celeri, R. Serra and V. Vedral, Physical Review A **80**, 044102 (2009) (cit. on pp. 6, 124, 125, 127, 135, 137, 139, 146, 147).

[35] E. G. Carnio, A. Buchleitner and M. Gessner, Physical Review Letters **115**, 010404 (2015) (cit. on pp. 6, 122, 139, 140, 148).

[36] E. G. Carnio, A. Buchleitner and M. Gessner, New Journal of Physics **18**, 073010 (2016) (cit. on pp. 6, 122, 139, 140, 148).

[37] C. E. Shannon, The Bell System Technical Journal **27**, 379–423 (1948) (cit. on p. 8).

[38] T. M. Cover and J. A. Thomas, *Elements of Information Theory* (John Wiley & Sons, Hoboken, 2006) (cit. on p. 9).

[39] G. H. Hardy, J. E. Littlewood and G. Pólya, Messenger Math **58**, 310 (1929) (cit. on p. 12).

[40] C. E. Mackenzie, *Coded-Character Sets: History and Development* (Addison-Wesley, Boston, 1980) (cit. on p. 13).

[41] J. Von Neumann, *Mathematical Foundations of Quantum Mechanics* (Princeton University Press, Princeton, 1955) (cit. on p. 18).

[42] C. A. Fuchs, 'Distinguishability & Accessible Information in Quantum Theory', PhD thesis (University of New Mexico, Albuquerque, New Mexico, USA, Dec. 1995) (cit. on pp. 18, 74).

[43] K. Kraus, Annals of Physics **64**, 311–335 (1971) (cit. on p. 19).

[44] S. Luo and Q. Zhang, Physical Review A **69**, 032106 (2004) (cit. on pp. 20, 72, 74).

[45] E. B. Davies and J. T. Lewis, Communications in Mathematical Physics **17**, 239–260 (1970) (cit. on p. 22).

[46] J.-P. Pellonpää, Journal of Physics A: Mathematical and Theoretical **46**, 025302 (2012) (cit. on pp. 23, 66, 155).

[47] T. Baumgratz, M. Cramer and M. Plenio, Physical Review Letters **113**, 140401 (2014) (cit. on pp. 31, 49, 68, 74, 127).

[48] J. Åberg, arXiv:quant-ph/0612146 (2006) (cit. on pp. 31, 49).

[49] F. Levi and F. Mintert, New Journal of Physics **16**, 033007 (2014) (cit. on pp. 32, 50).

[50] B. Witt and F. Mintert, New Journal of Physics **15**, 093020 (2013) (cit. on p. 32).

[51] S. Chin, arXiv:1702.06061 (2017) (cit. on p. 32).

[52] S. Chin, arXiv:1702.03219 (2017) (cit. on p. 32).

[53] N. Killoran, F. E. Steinhoff and M. B. Plenio, Physical Review Letters **116**, 080402 (2016) (cit. on pp. 32, 142).

[54] A. Streltsov, *Quantum Correlations Beyond Entanglement and Their Role in Quantum Information Theory* (Springer, Berlin, 2014) (cit. on pp. 34, 36).

[55] K. Modi, Open Systems & Information Dynamics **21**, 1440006 (2014) (cit. on pp. 34, 36).

[56] D. Spehner, Journal of Mathematical Physics **55**, 075211 (2014) (cit. on pp. 34, 36, 56, 57).

[57] A. Bera, T. Das, D. Sadhukhan, S. Singha Roy, A. Sen De and U. Sen, arXiv:1703.10542 (2017) (cit. on pp. 34, 36, 142).

[58] V. Vedral, arXiv:1702.01327 (2017) (cit. on pp. 34, 36, 142).

[59] D. Cavalcanti and P. Skrzypczyk, Reports on Progress in Physics **80**, 024001 (2017) (cit. on p. 40).

[60] N. Brunner, D. Cavalcanti, S. Pironio, V. Scarani and S. Wehner, Reviews of Modern Physics **86**, 419 (2014) (cit. on p. 40).

[61] M. Blasone, F. Dell'Anno, S. De Siena and F. Illuminati, Physical Review A **77**, 062304 (2008) (cit. on pp. 40, 44).

[62] W. Dür and J. I. Cirac, Physical Review A **61**, 042314 (2000) (cit. on pp. 41, 97).

[63] G. Andrews, *The Theory of Partitions* (Cambridge University Press, Cambridge, 1998) (cit. on p. 41).

[64] O. Gühne, G. Tóth and H. J. Briegel, New Journal of Physics **7**, 229 (2005) (cit. on p. 43).

[65] O. Gühne and G. Toth, Physical Review A **73**, 052319 (2006) (cit. on p. 43).

[66] T.-C. Wei, D. Das, S. Mukhopadyay, S. Vishveshwara and P. M. Goldbart, Physical Review A **71**, 060305 (2005) (cit. on p. 44).

[67] A. Acin, D. Bruß, M. Lewenstein and A. Sanpera, Physical Review Letters **87**, 040401 (2001) (cit. on p. 44).

[68] O. Gühne and M. Seevinck, New Journal of Physics **12**, 053002 (2010) (cit. on pp. 44, 97, 100, 101).

[69] B. Jungnitsch, T. Moroder and O. Gühne, Physical Review Letters **106**, 190502 (2011) (cit. on p. 44).

[70] F. Levi and F. Mintert, Physical Review Letters **110**, 150402 (2013) (cit. on pp. 44, 97).

[71] J. P. Dowling and G. J. Milburn, Philosophical Transactions of the Royal Society of London A: Mathematical, Physical and Engineering Sciences **361**, 1655–1674 (2003) (cit. on p. 45).

[72] L. del Rio, L. Kraemer and R. Renner, arXiv:1511.08818 (2015) (cit. on p. 46).

[73] W. Dür, G. Vidal and J. I. Cirac, Physical Review A **62**, 062314 (2000) (cit. on pp. 46, 68, 95).

[74] F. G. Brandão, M. Horodecki, J. Oppenheim, J. M. Renes and R. W. Spekkens, Physical Review Letters **111**, 250404 (2013) (cit. on p. 49).

[75] F. G. S. L. Brandão, M. Horodecki, N. Ng, J. Oppenheim and S. Wehner, Proceedings of the National Academy of Sciences **112**, 3275–3279 (2015) (cit. on p. 49).

[76] G. Gour, M. P. Müller, V. Narasimhachar, R. W. Spekkens and N. Y. Halpern, Physics Reports **583**, 1–58 (2015) (cit. on p. 49).

[77] V. Veitch, S. H. Mousavian, D. Gottesman and J. Emerson, New Journal of Physics **16**, 013009 (2014) (cit. on p. 49).

[78] N. Schuch, F. Verstraete and J. I. Cirac, Physical Review Letters **92**, 087904 (2004) (cit. on p. 49).

[79] G. Gour and R. W. Spekkens, New Journal of Physics **10**, 033023 (2008) (cit. on pp. 49, 50).

[80] J. I. De Vicente, Journal of Physics A: Mathematical and Theoretical **47**, 424017 (2014) (cit. on pp. 49, 149).

[81] Z.-W. Liu, X. Hu and S. Lloyd, Physical Review Letters **118**, 060502 (2017) (cit. on pp. 49, 65).

[82] I. Devetak, A. W. Harrow and A. J. Winter, IEEE Transactions on Information Theory **54**, 4587–4618 (2008) (cit. on p. 49).

[83] T. Theurer, N. Killoran, D. Egloff and M. B. Plenio, arXiv:1703.10943 (2017) (cit. on p. 49).

[84] B. Yadin, J. Ma, D. Girolami, M. Gu and V. Vedral, Physical Review X **6**, 041028 (2016) (cit. on pp. 49, 50, 55, 76, 136, 142).

[85] A. Winter and D. Yang, Physical Review Letters **116**, 120404 (2016) (cit. on pp. 49, 74, 142).

[86] I. Marvian, R. W. Spekkens and P. Zanardi, Physical Review A **93**, 052331 (2016) (cit. on pp. 49–51, 114).

[87] E. Chitambar and G. Gour, Physical Review Letters **117**, 030401 (2016) (cit. on pp. 49, 142).

[88] I. Marvian and R. W. Spekkens, Physical Review A **94**, 052324 (2016) (cit. on pp. 49, 50).

[89] J. I. de Vicente and A. Streltsov, Journal of Physics A: Mathematical and Theoretical **50**, 045301 (2016) (cit. on p. 49).

[90] J. A. Vaccaro, F. Anselmi and H. M. Wiseman, International Journal of Quantum Information **1**, 427–441 (2003) (cit. on p. 50).

[91] S. D. Bartlett, T. Rudolph and R. W. Spekkens, Reviews of Modern Physics **79**, 555 (2007) (cit. on p. 50).

[92] J. A. Vaccaro, F. Anselmi, H. M. Wiseman and K. Jacobs, Physical Review A **77**, 032114 (2008) (cit. on p. 50).

[93] G. Gour, I. Marvian and R. W. Spekkens, Physical Review A **80**, 012307 (2009) (cit. on p. 50).

[94] I. Marvian and R. W. Spekkens, New Journal of Physics **15**, 033001 (2013) (cit. on pp. 50, 51).

[95] I. Marvian and R. W. Spekkens, Nature Communications **5** (2014) (cit. on p. 50).

[96] M. B. Plenio and S. Virmani, Quantum Information & Computation **7**, 1 (2007) (cit. on pp. 51, 52).

[97] C. H. Bennett, H. J. Bernstein, S. Popescu and B. Schumacher, Physical Review A **53**, 2046 (1996) (cit. on p. 51).

[98] F. G. Brandão and M. B. Plenio, Nature Physics **4**, 873–877 (2008) (cit. on p. 51).

[99] E. M. Rains, arXiv:quant-ph/9707002 (1997) (cit. on p. 51).

[100] C. H. Bennett, D. P. DiVincenzo, C. A. Fuchs et al., Physical Review A **59**, 1070 (1999) (cit. on p. 51).

[101] M. J. Donald, M. Horodecki and O. Rudolph, Journal of Mathematical Physics **43**, 4252–4272 (2002) (cit. on p. 51).

[102] G. Vidal, Journal of Modern Optics **47**, 355–376 (2000) (cit. on pp. 52, 119).

[103] M. B. Plenio, Physical Review Letters **95**, 090503 (2005) (cit. on p. 52).

[104] M. Horodecki, Quantum Information & Computation **1**, 3 (2001) (cit. on p. 52).

[105] F. Ciccarello and V. Giovannetti, Physical Review A **85**, 010102 (2012) (cit. on pp. 53, 139).

[106] A. Streltsov, H. Kampermann and D. Bruß, Physical Review Letters **107**, 170502 (2011) (cit. on pp. 53, 54).

[107] X. Hu, H. Fan, D. Zhou and W.-M. Liu, Physical Review A **85**, 032102 (2012) (cit. on pp. 53, 54, 117, 150, 151).

[108] Y. Guo and J. Hou, Journal of Physics A: Mathematical and Theoretical **46**, 155301 (2013) (cit. on pp. 54, 55, 117).

[109] A. Streltsov, H. Kampermann and D. Bruß, Physical Review Letters **106**, 160401 (2011) (cit. on pp. 55, 74).

[110] W. Roga, D. Spehner and F. Illuminati, Journal of Physics A: Mathematical and Theoretical **49**, 235301 (2016) (cit. on pp. 56, 57).

[111] W. Roga, S. Giampaolo and F. Illuminati, Journal of Physics A: Mathematical and Theoretical **47**, 365301 (2014) (cit. on p. 56).

[112] F. Ciccarello, T. Tufarelli and V. Giovannetti, New Journal of Physics **16**, 013038 (2014) (cit. on pp. 56, 132).

[113] A. Farace, A. De Pasquale, L. Rigovacca and V. Giovannetti, New Journal of Physics **16**, 073010 (2014) (cit. on p. 56).

[114] D. Girolami, T. Tufarelli and G. Adesso, Physical Review Letters **110**, 240402 (2013) (cit. on pp. 56, 116, 118, 145).

[115] A. Brodutch and K. Modi, Quantum Information & Computation **12**, 0721 (2012) (cit. on p. 57).

[116] A. Ferraro, L. Aolita, D. Cavalcanti, F. Cucchietti and A. Acin, Physical Review A **81**, 052318 (2010) (cit. on pp. 58, 139).

[117] M. Piani and J. Watrous, Physical Review Letters **114**, 060404 (2015) (cit. on pp. 63, 66, 154, 155).

[118] J. Geller and M. Piani, Journal of Physics A: Mathematical and Theoretical **47**, 424030 (2014) (cit. on p. 63).

[119] A. W. Harrow and M. A. Nielsen, Physical Review A **68**, 012308 (2003) (cit. on p. 63).

[120] F. G. Brandão, Physical Review A **72**, 022310 (2005) (cit. on pp. 63, 67).

[121] F. G. Brandão and R. O. Vianna, International Journal of Quantum Information **4**, 331–340 (2006) (cit. on pp. 63, 64).

[122] K. Bu, N. Anand and U. Singh, arXiv:1703.01266 (2017) (cit. on p. 63).

[123] M. Horodecki, P. Horodecki and R. Horodecki, Physics Letters A **223**, 1–8 (1996) (cit. on p. 64).

[124] B. M. Terhal, Physics Letters A **271**, 319–326 (2000) (cit. on p. 64).

[125] J. Watrous, arXiv:0901.4709 (2009) (cit. on pp. 64, 66, 109, 154, 155).

[126] L. Vandenberghe and S. Boyd, SIAM Review **38**, 49–95 (1996) (cit. on p. 64).

[127] S. Boyd and L. Vandenberghe, *Convex Optimization* (Cambridge University Press, Cambridge, 2004) (cit. on pp. 64, 155).

[128] G. Gour, arXiv:1610.04247 (2016) (cit. on pp. 65, 143).

[129] J. Eisert, F. G. Brandão and K. M. Audenaert, New Journal of Physics **9**, 46 (2007) (cit. on pp. 67, 98, 144).

[130] Y. Peng, Y. Jiang and H. Fan, Physical Review A **93**, 032326 (2016) (cit. on p. 68).

[131] K. Życzkowski and H.-J. Sommers, Physical Review A **71**, 032313 (2005) (cit. on pp. 69, 111, 121).

[132] J. Eisert, K. Audenaert and M. Plenio, Journal of Physics A: Mathematical and General **36**, 5605 (2003) (cit. on p. 74).

[133] C. Witte and M. Trucks, Physics Letters A **257**, 14–20 (1999) (cit. on p. 74).

[134] M. Ozawa, Physics Letters A **268**, 158–160 (2000) (cit. on p. 74).

[135] A. Streltsov, H. Kampermann and D. Bruß, New Journal of Physics **12**, 123004 (2010) (cit. on p. 74).

[136] S. Rana, P. Parashar and M. Lewenstein, Physical Review A **93**, 012110 (2016) (cit. on p. 74).

[137] A. Streltsov, U. Singh, H. S. Dhar, M. N. Bera and G. Adesso, Physical Review Letters **115**, 020403 (2015) (cit. on pp. 74, 75, 142).

[138] Y. Huang, New Journal of Physics **16**, 033027 (2014) (cit. on p. 75).

[139] K. Modi, T. Paterek, W. Son, V. Vedral and M. Williamson, Physical Review Letters **104**, 080501 (2010) (cit. on pp. 75, 76).

[140] B. Bellomo, G. L. Giorgi, F. Galve, R. L. Franco, G. Compagno and R. Zambrini, Physical Review A **85**, 032104 (2012) (cit. on pp. 75, 76).

[141] J. Ma, B. Yadin, D. Girolami, V. Vedral and M. Gu, Physical Review Letters **116**, 160407 (2016) (cit. on pp. 76, 136, 142).

[142] Y. Yao, X. Xiao, L. Ge and C. Sun, Physical Review A **92**, 022112 (2015) (cit. on pp. 76, 136).

[143] F. Paula, A. Saguia, T. R. de Oliveira and M. Sarandy, EPL (Europhysics Letters) **108**, 10003 (2014) (cit. on p. 76).

[144] B. Aaronson, R. L. Franco, G. Compagno and G. Adesso, New Journal of Physics **15**, 093022 (2013) (cit. on pp. 76, 124, 132, 135, 137, 146, 147).

[145] L. E. Buchholz, T. Moroder and O. Gühne, Annalen der Physik (2015) (cit. on pp. 80, 98).

[146] M. Hofmann, T. Moroder and O. Gühne, Journal of Physics A: Mathematical and Theoretical **47**, 155301 (2014) (cit. on pp. 80, 98, 100, 101).

[147] J. Siewert and C. Eltschka, Physical Review Letters **108**, 230502 (2012) (cit. on pp. 80, 98).

[148] C. Eltschka and J. Siewert, Scientific Reports **2**, 942 (2012) (cit. on pp. 80, 98).

[149] D. F. James, P. G. Kwiat, W. J. Munro and A. G. White, Physical Review A **64**, 052312 (2001) (cit. on p. 80).

[150] R. Thew, K. Nemoto, A. G. White and W. J. Munro, Physical Review A **66**, 012303 (2002) (cit. on p. 80).

[151] B. Hiesmayr, F. Hipp, M. Huber, P. Krammer and C. Spengler, Physical Review A **78**, 042327 (2008) (cit. on pp. 87, 98).

[152] R. Horodecki et al., Physical Review A **54**, 1838 (1996) (cit. on pp. 88, 125, 139).

[153] P. Comon and M. Sorensen, 'Tensor Diagonalization by Orthogonal Transforms', Report ISRN I3S-RR-2007-06-FR, `http://www.i3s.unice.fr/~mh/RR/2007/RR-07.06-P.COMON.pdf` (2007) (cit. on pp. 94, 95).

[154] D. M. Greenberger, M. Horne and A. Zeilinger, 'Going Beyond Bell's Theorem', in *Bell's Theorem, Quantum Theory, and Conceptions of the Universe*, edited by M. Kafatos (Springer, Dordrecht, 1989), pp. 69–72 (cit. on p. 95).

[155] D. M. Greenberger, M. A. Horne, A. Shimony and A. Zeilinger, American Journal of Physics **58**, 1131–1143 (1990) (cit. on p. 95).

[156] N. D. Mermin, Physical Review Letters **65**, 1838 (1990) (cit. on p. 95).

[157] D. Bouwmeester, J. Pan, M. Daniell, H. Weinfurter and A. Zeilinger, Physical Review Letters **82**, 1345 (1999) (cit. on p. 95).

[158] C. F. Roos, M. Riebe, H. Häffner et al., Science **304**, 1478–1480 (2004) (cit. on p. 95).

[159] P. Agrawal and A. Pati, Physical Review A **74**, 062320 (2006) (cit. on p. 95).

[160] S.-B. Zheng, Physical Review A **74**, 054303 (2006) (cit. on p. 95).

[161] A. Cabello, Physical Review A **65**, 032108 (2002) (cit. on p. 95).

[162] T.-C. Wei, J. B. Altepeter, P. M. Goldbart and W. J. Munro, Physical Review A **70**, 022322 (2004) (cit. on p. 96).

[163] T.-C. Wei, Physical Review A **78**, 012327 (2008) (cit. on p. 96).

[164] X.-y. Chen, L.-z. Jiang, P. Yu and M. Tian, arXiv:1204.5511 (2012) (cit. on pp. 96, 101).

[165] O. Gühne and G. Tóth, Physics Reports **474**, 1–75 (2009) (cit. on p. 97).

[166] T. Gao, F. Yan and S. van Enk, Physical Review Letters **112**, 180501 (2014) (cit. on p. 97).

[167] M. Huber, F. Mintert, A. Gabriel and B. C. Hiesmayr, Physical Review Letters **104**, 210501 (2010) (cit. on p. 97).

[168] A. Gabriel, B. C. Hiesmayr and M. Huber, Quantum Information & Computation **10**, 829 (2010) (cit. on p. 97).

[169] C. Klöckl and M. Huber, Physical Review A **91**, 042339 (2015) (cit. on p. 97).

[170] P. Badziag, Č. Brukner, W. Laskowski, T. Paterek and M. Żukowski, Physical Review Letters **100**, 140403 (2008) (cit. on p. 97).

[171] J.-Y. Wu, H. Kampermann, D. Bruß, C. Klöckl and M. Huber, Physical Review A **86**, 022319 (2012) (cit. on p. 98).

[172] S. H. Rafsanjani, M. Huber, C. Broadbent and J. Eberly, Physical Review A **86**, 062303 (2012) (cit. on pp. 98, 100).

[173] K. Audenaert and M. Plenio, New Journal of Physics **8**, 266 (2006) (cit. on p. 98).

[174] H. Wunderlich and M. B. Plenio, Journal of Modern Optics **56**, 2100–2105 (2009) (cit. on p. 98).

[175] Z.-H. Ma, Z.-H. Chen, J.-L. Chen, C. Spengler, A. Gabriel and M. Huber, Physical Review A **83**, 062325 (2011) (cit. on p. 98).

[176] O. Gühne, M. Reimpell and R. Werner, Physical Review Letters **98**, 110502 (2007) (cit. on pp. 98, 144).

[177] J. A. Smolin, Physical Review A **63**, 032306 (2001) (cit. on p. 98).

[178] R. Augusiak and P. Horodecki, Physical Review A **73**, 012318 (2006) (cit. on p. 98).

[179] J. Lavoie, R. Kaltenbaek, M. Piani and K. J. Resch, Physical Review Letters **105**, 130501 (2010) (cit. on pp. 98, 100).

[180] R. H. Dicke, Physical Review **93**, 99 (1954) (cit. on p. 98).

[181] J. Tura, R. Augusiak, A. B. Sainz, T. Vértesi, M. Lewenstein and A. Acín, Science **344**, 1256–1258 (2014) (cit. on pp. 98, 99).

[182] R. Prevedel, G. Cronenberg, M. S. Tame et al., Physical Review Letters **103**, 020503 (2009) (cit. on pp. 99, 100).

[183] W. Wieczorek, R. Krischek, N. Kiesel, P. Michelberger, G. Tóth and H. Weinfurter, Physical Review Letters **103**, 020504 (2009) (cit. on pp. 99, 100).

[184] T. Monz, P. Schindler, J. T. Barreiro et al., Physical Review Letters **106**, 130506 (2011) (cit. on p. 99).

[185] T. Monz, 'Quantum information processing beyond ten ion-qubits', PhD thesis (University of Innsbruck, Innsbruck, Austria, Aug. 2011) (cit. on pp. 99, 100).

[186] O. Gühne, C.-Y. Lu, W.-B. Gao and J.-W. Pan, Physical Review A **76**, 030305 (2007) (cit. on p. 103).

[187] J. Preskill, arXiv:1203.5813 (2012) (cit. on pp. 106, 149).

[188] A. K. Bewoor and V. A. Kulkarni, *Metrology and Measurement* (McGraw Hill Education, New York, 2009) (cit. on p. 106).

[189] C. W. Helstrom, Journal of Statistical Physics **1**, 231–252 (1969) (cit. on pp. 106, 112, 113).

[190] A. S. Holevo, *Probabilistic and Statistical Aspects of Quantum Theory*, Vol. 1 (Springer, Berlin, 2011) (cit. on pp. 106, 112, 113).

[191] E. O. Göbel and U. Siegner, *Quantum Metrology: Foundation of Units and Measurements* (John Wiley & Sons, Hoboken, 2015) (cit. on p. 106).

[192] J. Kolodynski, 'Precision bounds in noisy quantum metrology', PhD thesis (University of Warsaw, Warsaw, Poland, Sept. 2014) (cit. on pp. 112, 113).

[193] S. Ragy, 'Resources in Quantum Imaging, Detection and Estimation', PhD thesis (University of Nottingham, Nottingham, United Kingdom, Apr. 2015) (cit. on p. 112).

[194] S. L. Braunstein and C. M. Caves, Physical Review Letters **72**, 3439 (1994) (cit. on pp. 112, 113).

[195] D. Girolami, Physical Review Letters **113**, 170401 (2014) (cit. on p. 114).

[196] B. Yadin and V. Vedral, Physical Review A **92**, 022356 (2015) (cit. on p. 114).

[197] B. Yadin and V. Vedral, Physical Review A **93**, 022122 (2016) (cit. on p. 114).

[198] L. Pezzé and A. Smerzi, Physical Review Letters **102**, 100401 (2009) (cit. on p. 114).

[199] G. Tóth and I. Apellaniz, Journal of Physics A: Mathematical and Theoretical **47**, 424006 (2014) (cit. on pp. 114, 115, 118, 181).

[200] P. Hyllus, W. Laskowski, R. Krischek et al., Physical Review A **85**, 022321 (2012) (cit. on pp. 114, 115).

[201] G. Tóth, Physical Review A **85**, 022322 (2012) (cit. on pp. 114, 115).

[202] A. Przysiężna, M. Horodecki, P. Horodecki et al., Physical Review A **92**, 062303 (2015) (cit. on p. 115).

[203] P. Hyllus, O. Gühne and A. Smerzi, Physical Review A **82**, 012337 (2010) (cit. on p. 115).

[204] G. Adesso, Physical Review A **90**, 022321 (2014) (cit. on p. 116).

[205] A. Farace, A. De Pasquale, G. Adesso and V. Giovannetti, New Journal of Physics **18**, 013049 (2016) (cit. on p. 116).

[206] A. Uhlmann, Open Systems and Information Dynamics **5**, 209–228 (1998) (cit. on p. 118).

[207] A. Uhlmann, International Journal of Theoretical Physics **42**, 983–999 (2003) (cit. on p. 118).

[208] A. Uhlmann, Entropy **12**, 1799–1832 (2010) (cit. on pp. 118, 119).

[209] G. Tóth and D. Petz, Physical Review A **87**, 032324 (2013) (cit. on pp. 120, 181).

[210] S. Yu, arXiv:1302.5311 (2013) (cit. on pp. 120, 181).

[211] P. Rungta, V. Bužek, C. M. Caves, M. Hillery and G. J. Milburn, Physical Review A **64**, 042315 (2001) (cit. on p. 120).

[212] P. Rungta and C. M. Caves, Physical Review A **67**, 012307 (2003) (cit. on p. 120).

[213] V. Coffman, J. Kundu and W. K. Wootters, Physical Review A **61**, 052306 (2000) (cit. on p. 121).

[214] S. Hill and W. K. Wootters, Physical Review Letters **78**, 5022 (1997) (cit. on p. 121).

[215] W. H. Zurek, Reviews of Modern Physics **75**, 715 (2003) (cit. on pp. 122, 135, 147).

[216] T. Yu and J. Eberly, Science **323**, 598–601 (2009) (cit. on p. 122).

[217] M. P. Almeida, F. de Melo, M. Hor-Meyll et al., Science **316**, 579–582 (2007) (cit. on pp. 122, 139).

[218] R. Demkowicz-Dobrzanski, J. Kolodynski and M. Guta, Nature Communications **3** (2012) (cit. on pp. 122, 123).

[219] E. M. Kessler, I. Lovchinsky, A. O. Sushkov and M. D. Lukin, Physical Review Letters **112**, 150802 (2014) (cit. on pp. 122, 123).

[220] W. Dür, M. Skotiniotis, F. Froewis and B. Kraus, Physical Review Letters **112**, 080801 (2014) (cit. on pp. 122, 123).

[221] Y. Matsuzaki, S. C. Benjamin and J. Fitzsimons, Physical Review A **84**, 012103 (2011) (cit. on pp. 122, 123).

[222] A. Smirne, J. Kołodyński, S. F. Huelga and R. Demkowicz-Dobrzański, Physical Review Letters **116**, 120801 (2016) (cit. on pp. 122, 123, 146).

[223] R. Chaves, J. Brask, M. Markiewicz, J. Kołodyński and A. Acín, Physical Review Letters **111**, 120401 (2013) (cit. on pp. 122, 123).

[224] P. Sekatski, M. Skotiniotis, J. Kołodyński and W. Dür, arXiv:1603.08944 (2016) (cit. on pp. 122, 123).

[225] B. Escher, R. de Matos Filho and L. Davidovich, Nature Physics **7**, 406–411 (2011) (cit. on pp. 122, 123).

[226] S. F. Huelga, C. Macchiavello, T. Pellizzari, A. Ekert, M. B. Plenio and J. I. Cirac, Physical Review Letters **79**, 3865 (1997) (cit. on pp. 122, 123).

[227] S. J. Glaser, U. Boscain, T. Calarco et al., The European Physical Journal D **69**, 279 (2015) (cit. on p. 122).

[228] L. Viola, E. Knill and S. Lloyd, Physical Review Letters **82**, 2417 (1999) (cit. on p. 122).

[229] A. M. Souza, G. A. Álvarez and D. Suter, Physical Review Letters **106**, 240501 (2011) (cit. on p. 122).

[230] H. Rabitz, R. de Vivie-Riedle, M. Motzkus and K. Kompa, Science **288**, 824–828 (2000) (cit. on p. 122).

[231] D. A. Lidar, I. L. Chuang and K. B. Whaley, Physical Review Letters **81**, 2594 (1998) (cit. on p. 122).

[232] R. Fisher, Proceedings of the Royal Society of London A: Mathematical, Physical and Engineering Sciences **217**, 295–305 (1953) (cit. on p. 123).

[233] B. You and L.-X. Cen, Physical Review A **86**, 012102 (2012) (cit. on pp. 124, 137, 146, 147).

[234] R. L. Franco, B. Bellomo, E. Andersson and G. Compagno, Physical Review A **85**, 032318 (2012) (cit. on pp. 124, 135, 137, 146, 147).

[235] P. Haikka, T. Johnson and S. Maniscalco, Physical Review A **87**, 010103 (2013) (cit. on pp. 124, 135, 137, 146, 147).

[236] T. Chanda, A. K. Pal, A. Biswas, A. Sen, U. Sen et al., Physical Review A **91**, 062119 (2015) (cit. on pp. 124, 137, 138, 146, 147).

[237] P. C. Obando, F. M. Paula and M. S. Sarandy, Physical Review A **92**, 032307 (2015) (cit. on pp. 124, 135, 137, 146, 147).

[238] J. Xu, Physics Letters A **377**, 238–242 (2013) (cit. on pp. 124, 137, 138).

[239] X.-D. Yu, D.-J. Zhang, C. Liu and D. Tong, Physical Review A **93**, 060303 (2016) (cit. on pp. 124, 138).

[240] S. Bhattacharya, S. Banerjee and A. K. Pati, arXiv:1601.04742 (2016) (cit. on pp. 124, 138).

[241] D.-J. Zhang, X.-D. Yu, H.-L. Huang and D. Tong, Physical Review A **95**, 022323 (2017) (cit. on pp. 124, 138).

[242] H.-P. Breuer and F. Petruccione, *The Theory of Open Quantum Systems* (Oxford University Press, Oxford, 2002) (cit. on pp. 124, 147, 150).

[243] T. Yu and J. Eberly, Physical Review Letters **97**, 140403 (2006) (cit. on pp. 124, 139).

[244] E. Andersson, J. D. Cresser and M. J. Hall, Journal of Modern Optics **54**, 1695–1716 (2007) (cit. on p. 129).

[245] T. Nakano, M. Piani and G. Adesso, Physical Review A **88**, 012117 (2013) (cit. on p. 132).

[246] F. Paula, J. Montealegre, A. Saguia, T. R. de Oliveira and M. Sarandy, EPL (Europhysics Letters) **103**, 50008 (2013) (cit. on p. 132).

[247] D. Spehner and M. Orszag, New Journal of Physics **15**, 103001 (2013) (cit. on p. 134).

[248] D. Spehner and M. Orszag, Journal of Physics A: Mathematical and Theoretical **47**, 035302 (2013) (cit. on p. 134).

[249] M. Cornelio, O. J. Farías, F. F. Fanchini et al., Physical Review Letters **109**, 190402 (2012) (cit. on pp. 135, 147).

[250] W. H. Zurek, Physical Review D **24**, 1516 (1981) (cit. on pp. 135, 147).

[251] J. P. Paz and W. H. Zurek, Physical Review Letters **82**, 5181 (1999) (cit. on pp. 135, 147).

[252] J. P. Paz, S. Habib and W. H. Zurek, Physical Review D **47**, 488 (1993) (cit. on pp. 135, 147).

[253] I. Oliveira, R. Sarthour Jr, T. Bonagamba, E. Azevedo and J. C. Freitas, *NMR Quantum Information Processing* (Elsevier, Amsterdam, 2011) (cit. on p. 138).

[254] Z. Ma, Z. Chen and F. F. Fanchini, New Journal of Physics **15**, 043023 (2013) (cit. on p. 139).

[255] B. Bellomo, G. Compagno, R. Lo Franco, A. Ridolfo and S. Savasta, International Journal of Quantum Information **9**, 1665–1676 (2011) (cit. on p. 139).

[256] J. I. Cirac and P. Zoller, Physical Review Letters **74**, 4091 (1995) (cit. on p. 139).

[257] H. Häffner, C. F. Roos and R. Blatt, Physics Reports **469**, 155–203 (2008) (cit. on p. 139).

[258] P. Schindler, D. Nigg, T. Monz et al., New Journal of Physics **15**, 123012 (2013) (cit. on p. 139).

[259] M. Ali, arXiv:1703.09932 (2017) (cit. on p. 140).

[260] P. Ball, Nature **474**, 272 (2011) (cit. on p. 141).

[261] N. Lambert, Y.-N. Chen, Y.-C. Cheng, C.-M. Li, G.-Y. Chen and F. Nori, Nature Physics **9**, 10–18 (2013) (cit. on p. 141).

[262] M. B. Plenio and S. F. Huelga, New Journal of Physics **10**, 113019 (2008) (cit. on p. 141).

[263] P. Rebentrost, M. Mohseni and A. Aspuru-Guzik, The Journal of Physical Chemistry B **113**, 9942–9947 (2009) (cit. on p. 141).

[264] J. Goold, M. Huber, A. Riera, L. del Rio and P. Skrzypczyk, Journal of Physics A: Mathematical and Theoretical **49**, 143001 (2016) (cit. on p. 141).

[265] J. Millen and A. Xuereb, New Journal of Physics **18**, 011002 (2016) (cit. on p. 141).

[266] J. Oppenheim, M. Horodecki, P. Horodecki and R. Horodecki, Physical Review Letters **89**, 180402 (2002) (cit. on p. 141).

[267] M. A. Nielsen, Physical Review Letters **83**, 436 (1999) (cit. on p. 142).

[268] P. Hayden, B. M. Terhal and A. Uhlmann, arXiv:quant-ph/0011095 (2000) (cit. on p. 142).

[269] S. Du, Z. Bai and Y. Guo, Physical Review A **91**, 052120 (2015) (cit. on p. 142).

[270] M. Piani, S. Gharibian, G. Adesso, J. Calsamiglia, P. Horodecki and A. Winter, Physical Review Letters **106**, 220403 (2011) (cit. on p. 142).

[271] H. Zhu, Z. Ma, Z. Cao, S.-M. Fei and V. Vedral, arXiv:1704.01935 (2017) (cit. on p. 142).

[272] E. Chitambar, A. Streltsov, S. Rana, M. Bera, G. Adesso and M. Lewenstein, Physical Review Letters **116**, 070402 (2016) (cit. on p. 145).

[273] T. Biswas, M. G. Díaz and A. Winter, arXiv:1701.05051 (2017) (cit. on p. 146).

[274] R. Gallego and L. Aolita, Physical Review X **5**, 041008 (2015) (cit. on p. 149).

[275] J. L. O'Brien, A. Furusawa and J. Vučković, Nature Photonics **3**, 687–695 (2009) (cit. on p. 149).

[276] R. Ursin, F. Tiefenbacher, T. Schmitt-Manderbach et al., Nature Physics **3**, 481–486 (2007) (cit. on p. 149).

[277] D. Bouwmeester, J.-W. Pan, K. Mattle, M. Eibl, H. Weinfurter and A. Zeilinger, Nature **390**, 575–579 (1997) (cit. on p. 149).

[278] G. Brida, M. Genovese and I. R. Berchera, Nature Photonics **4**, 227–230 (2010) (cit. on p. 149).

[279] T. D. Ladd, F. Jelezko, R. Laflamme, Y. Nakamura, C. Monroe and J. L. O'Brien, Nature **464**, 45–53 (2010) (cit. on p. 149).

[280] C. H. Papadimitriou, *Computational Complexity* (John Wiley & Sons, Hoboken, 2003) (cit. on p. 149).

[281] C. J. Isham, *Lectures on Quantum Theory* (World Scientific, Singapore, 2001) (cit. on p. 149).

[282] C. A. Fuchs et al., NATO Science Series, III: Computer and Systems Sciences **182**, 38–82 (2001) (cit. on p. 149).

[283] M. Navascués, Y. Guryanova, M. J. Hoban and A. Acín, Nature Communications **6** (2015) (cit. on p. 149).

[284] M.-D. Choi, Linear Algebra and its Applications **10**, 285–290 (1975) (cit. on p. 150).

[285] R. A. Bertlmann and P. Krammer, Journal of Physics A: Mathematical and Theoretical **41**, 235303 (2008) (cit. on p. 151).

[286] M. M. Wolf, 'Quantum Channels & Operations Guided Tour', `http://www-m5.ma.tum.de/foswiki/pub/M5/Allgemeines/MichaelWolf/QChannelLecture.pdf` (2012) (cit. on p. 158).

[287] M. Keyl, Physics Reports **369**, 431–548 (2002) (cit. on p. 178).

[288] C. B. Mendl and M. M. Wolf, Communications in Mathematical Physics **289**, 1057–1086 (2009) (cit. on p. 178).